FERNANDA MENDES DE REZENDE

Chemical analysis of color change and transcriptional profile in flavonoids biosynthesis during flower development of *Tibouchina pulchra* (Cham.) Cogn.

Análises químicas da mudança de cor e perfil transcricional da biossíntese de flavonoides durante o desenvolvimento floral de *Tibouchina pulchra* (Cham.) Cogn.

São Paulo

2018

FERNANDA MENDES DE REZENDE

Chemical analysis of color change and transcriptional profile in flavonoids biosynthesis during flower development of *Tibouchina pulchra* (Cham.) Cogn.

Análises químicas da mudança de cor e perfil transcricional da biossíntese de flavonoides durante o desenvolvimento floral de *Tibouchina pulchra* (Cham.) Cogn.

Tese apresentada ao Instituto de Biociências da Universidade de São Paulo, para a obtenção de Título de Doutor em Botânica, na Área de Recursos Econômicos vegetais.

Orientadora: Dra. Cláudia Maria Furlan
Co-orientadora: Dra. Maria Magdalena Rossi

São Paulo

2018

Rezende, Fernanda Mendes
Análises químicas da mudança de cor e perfil transcricional da biossíntese de flavonoides durante o desenvolvimento floral de *Tibouchina pulchra* (Cham.) Cogn.
165 páginas.

Tese (Doutorado) – Instituto de Biociências da Universidade de São Paulo. Departamento de Botânica.

Palavra-Chave: 1. antocianinas; 2. Ácidos fenólicos; 3. CHS, 4. FLS, 5. ANS.

Universidade de São Paulo. Instituto de Biociências. Departamento de Botânica.

Banca Examinadora

_____ _____

Prof(a). Dr(a) Prof(a). Dr(a)

_____ _____

Prof(a). Dr(a) Prof(a). Dr(a)

_____

Profa. Dra. Claudia M. Furlan

Dedico à minha família e a todos

que de alguma forma contribuíram

para a realização deste trabalho.

Agradecimentos

Ao fim de quatro anos tenho muito o que agradecer. Foram anos de aprendizado, dedicação e mudanças. Muitas pessoas participaram deste processo.

Primeiramente gostaria de agradecer à Claudia, minha orientadora, por toda paciência, incentivo e suporte em minha formação. Desde a iniciação científica até aqui passaram-se dez anos, meu amadurecimento científico deve-se em grande parte ao seu apoio. Obrigada.

À Magda, minha co-orientadora, agradeço por me inserir no mundo da biologia molecular e por todo aprendizado acadêmico compartilhado. Também sou muito grata pelo grande apoio à ida ao exterior. Não poderia deixar de mencionar que as pausas para um cigarro foram sempre produtivas, seja para falar da vida ou para ter insights sobre o trabalho.

Aos professores da Fitoquímica por todos os anos em que aprendi muito com vocês, tanto numa conversa informal, quanto em nossos seminários. Ao Marcelo, agradeço por toda a ajuda nas identificações químicas e paciência diante dos meus questionamentos.

Ao Eduardo Leal da Sistemática Vegetal que me auxiliou com os nomes de espécies da grande tabela do capítulo 1. Ao Erismaldo, jardineiro do IB, que muito me ajudou para que as mudas de *Tibouchina* ficassem bem.

Ao Mads que me recebeu em seu laboratório na Dinamarca e ao Thomas, além de todos os técnicos dos laboratórios e amigos que fiz por lá. Em especial Irene, Christou e Jorge.

Aos meus colegas da Fitoquímica, agradeço pelos anos em que discutíamos resultados entre pausas de almoço e café. Aqui vai um agradecimento especial à Priscila, Alice, Fernanda, Dalila e Kátia que me ajudaram nas coletas ou regando plantas quando eu estava ausente. Falando em almoço, não posso deixar de agradecer às amigas que almoçam comigo, quase que diariamente, nos últimos anos: Aline, Kátia e Mourisa. Apesar de hoje em dia estar ausente, agradeço à Carol, pois muito trocamos nos anos de convivência.

Às técnicas do laboratório, agradeço por tantas vezes que passamos almoços falando sobre cromatografias e afins. Obrigada por serem sempre prestativas e por todas as risadas compartilhadas.

Ao pessoal do lab de Biologia Celular e Biologia Molecular de plantas, agradeço pelas trocas de experiências e bons momentos. Agradecimento especial à Dani, Paula e Bruno que me ajudaram muito nos procedimentos no laboratório.

À minha família agradeço por serem os pilares que sustentam meus sonhos. Obrigada mãe, pai, amo vocês! Não posso deixar de fora aquela família que a gente escolhe, nossos amigos. Agradeço aos meus por me levarem para me descontrair, afinal não é só de um doutorado que se vive.

Por fim, aos órgãos financiadores: CAPES, FAPESP (2013/10413-0) e Instituto de Biociências.

Gosto das cores, das flores, das estrelas, do verde das árvores, gosto de observar. A beleza da vida se esconde por ali, e por mais uma infinidade de lugares, basta saber, e principalmente, basta querer enxergar.

Clarice Lispector

Rezende, F.M. Análises químicas da mudança de cor e perfil transcricional da biossíntese de flavonoides durante o desenvolvimento floral de *Tibouchina pulchra* (Cham.) Cogn. [tese]. São Paulo: Instituto de Biociências, Universidade de São Paulo; 2018.

Resumo

A mudança de cor em flores é um fenômeno generalizado entre as angiospermas, mas pouco compreendido do ponto de vista genético e químico. Este estudo teve como objetivo investigar esse fenômeno em *Tibouchina pulcha,* uma espécie nativa brasileira, cujas flores mudam do branco para rosa escuro. Para alcançar o objetivo, os perfis dos compostos e de expressão de genes da via de biossíntese de flavonoides foram estudados. Utilizando técnicas hifenadas (UPLC-HRMS and NMR), trinta compostos foram quantificados e identificados, sendo: dezesseis descritos pela promeira vez em *T. pulchra*. Além idsso, um composto inédito foi identificado. Cinco genes que codificam para enzimas chaves da via foram parcialmente clonados, sequenciados, e os níveis de mRNA foram analisados (RT-qPCR) durante o desenvolvimento das flores. Coletivamente, os dados obtidos demonstram que a mudança de cor em flores de *T. pulchra* é regulada transcricionalmente. Além disso, quantificações de metais sugerem que o ion Fe^{3+} esteja relacionado a saturação da cor no estágio rosa escuro.

Palavras-chave: antocianina, ácidos fenólicos, CHS, FLS, ANS

Rezende, F.M. Chemical analysis of color change and transcriptional profile in flavonoids biosynthesis during flower development of *Tibouchina pulchra* (Cham.) Cogn. [thesis]. São Paulo: Instituto de Biociências, Universidade de São Paulo; 2018.

Abstract

Floral color change is a widespread phenomenon in angiosperms, but poorly understood from the genetic and chemical point of view. This thesis aimed to investigate this phenomenon in *Tibouchina pulcha*, a native species whose flowers change from white to dark pink. To reach this goal, flavonoid biosynthetic gene expression and compounds were profiled. By using hyphenated techiniques (UPLC-HRMS and NMR), thirty phenolic compounds were quantified and identified, being sixteen described for the first time in *T. pulchra*. Moreover, an inedite compound was also identified. Five key genes of the flavonoid biosynthetic pathway were partially cloned, sequenced, and the mRNA levels were analyzed (RT-qPCR) along flower development. Collectively, the obtained results demonstrated that the flower color change in *T. pulchra* is regulated at transcriptional level. Additionally, a metal quantification suggests that Fe^{3+} ion might influence the saturation of the color at dark pink stage.

Key words: anthocyanin, phenolic acids, CHS, FLS, ANS

List of Abreviations

[M+H]: molecular ion

2-ODD: 2-oxoglutarate/Fe(Ii)-dependent dioxygenase

4CL: 4-coumarate:CoA-ligase

aa: amino acids

AACT: anthocyanidin acyl transferase

ACT: acyl transferase

amu: atomic mass unit

ANS: anthocyanidin synthase

AT: *Arabdopsis thaliana*

B5GT: betanidin-5-*O*-glucosyltransferase

bbCID: broadband collision Induced dissociation

bHLH: basic helix–loop–helix

BLAST: basic local alignment search tool

Bp: base pair

Brara: *Brassica rapa*

C3H: coumarate 3-hydroxylase

C4H: cinnamate 4-Hydroxylase

CCD: carotenoid cleavage dioxygenase

CD: carotene desaturase

CD_3OD: deuterated methanol

cD5G2′GlcUT: cyclo-DOPA-5-glucose-2′-*O*-glucuronyl- transferase

cD5GT: cyclo-DOPA-5-*O*-glucosyltransferase

CDNA: complementary DNA

cDOPA: cyclo: DOPA

CHI: chalcone isomerase

CHS: chalcone synthase

CI: carotene isomerase

Co-A: Coenzyma A

Ct: treshold cycle

CTAB: cetyl trimethylammonium bromide

d: dublet

DAD: diode array detector

dd: double dublet

DEPC: dietilpirocarbonato

DFR: dihydroflavanol 4-reductase

DMAPP: dimethylallyl diphosphate

DMSO-d6: deuterated dimethyl sulfoxide

DNA: desoxyribonucleic acid

DNAse: desoxyribonuclease

Dntp: riphosphate desoribonucleotides

DO: diphenol oxidase (DO)

DOD: DOPA dioxygenase

DOPA: dihydrophenylalanine

DW: dried weight

DXP: 1-deoxy-D-xylulose-5-phosphate

DXR: DXP reductoisomerase

DXS: deoxy-D-xylulose synthase

DXS: DXP synthase

E4P: erythrose 4-phosphate

EDTA: ethylenediaminetetraacetic acid

ESI: electrospray Ionization

Eucgr: *Eucalyptus grandis*

F3′5′: flavonoid 3′5′-hydroxylase

F3′H: flavonoid 3′-hydroxylase

F3H: flavonoid 3-hydroxylase

FDP: farnesyl diphosphate synthase

FGT flavonoid glucosyltransferase

FLS: flavonol synthase

FPP: farnesyl diphosphate

FS: flavone synthase

GA3P: glyceraldehyde 3-P

GDS: GPP synthase reaction

GGDS: geranylgeranyl diphosphate synthase

GGPP: geranylgeranyl diphosphate

GPP: geranyl diphosphate

HCl: hydrocloric acid

HMBC: heteronuclear multiple bond correlation

HPLC: high performance liquid chromatography

HRMS: high-resolution mass spectrometry

HSQC: heteronuclear single quantum coherence

IFS: isoflavone synthase

IPP: isopentenyl diphosphate

IPPI: isopentenyl diphosphate isomerase

IPTG: isopropil β-D-1-tiogalactopiranosida

IspH: 4-hydroxy-3-methylbut-2-enyl diphosphate reductase

J: coupling constant

LB: Luria Bertani growth medium
LCYB: Lycopene B-Cyclase
LCYE: Lycopene B-Cyclase
m: multiplet
MAL: malonate pathway
Me: methyl group
Medtr: *Mendicago trunculata*
MeOH: methanol
MEP: 2-C-methyl-D-erythritol 4- phosphate
MEP: methylerythritol phosphate pathway
MEV: mevalonate pathway
miRNA: micro RNA
mRNA: messenger RNA
MS: mass spectrometry
MYB: myeloblastosis
n: nucleotide
NMR: nuclear magnetic resonance
NS: neoxanthin synthase
OMT: *O*-methyl transferase
P450: Cytochrome P450 Monooxygenase
PAD: photodiode array detector
PAL: phenylalanine ammonia lyase
PCR: polymerase chain reaction
PD: phytoene desaturase
PEP: phosphoenolpyruvate
ppm: parts per million
PS: phytoene synthase
QTOF: quadrupole time-of-flight
RNA: ribonucleic acid
RNAi: RNA interference
RT: retention time
RT-Qpcr: reverse transcriptase quantitative polymerase chain reaction
s: singlet
S1: stage one of *T. pulchra* flower
S2: stage two of *T. pulchra* flower
S3: stage three of *T. pulchra* flower
S4: stage four of *T. pulchra* flower
SKM: shikimate pathway
sl: large singlet
SOC: super optimal broth
Soly: *Solanum lycopersicum*
tasiRNA: trans-acting short-interfering RNA
TOH: tyrosine hydroxylase
Tp: *Trifolium pratense*
UPLC: ultra performance liquid chromatography
UV/Vis: ultraviolet/visible
WDRs: tryptophan-aspartic acid dipeptide repeat
X-Gal: 5-bromo-4-chloro-3-indoxyl-β-D-galactopyranoside
ZE: zeaxanthin epoxidase
β-CO: β-carotene oxygenase
B-RH: B-Ring Hydroxylase
δ: chemical shift
E-RH: E-ring hydroxylase

List of Figures

Chapter 1

Chapter 2

Chapter 3

List of Tables

Chapter 1

Chapter 2

Chapter 3

Sumary

Chapter 1- Plant pigments involved in floral color.

1. INTRODUCTION

Flower colors are important in the interaction between plants and their pollinators. Since Darwin evolutionary theory, biologists have studied the role of floral variation in plant reproductive fitness and its influence in pollination. Flower colors define pollination syndromes, which are associated with pollinator groups such as bees, moths, butterflies, bats, birds, beetles, flies, and others (Fenster *et al*. 2004; Yan *et al*. 2016). The coevolution of pollinators and angiosperm drives the floral diversity (*e.g*. flower morphology, color, scent, nectar quantity and nectar quality) (Van der Niet *et al*. 2014), and this resulted in reproductive isolation and plant speciation (Kay & Sargent 2009).

Interestingly, pollinators have different color vision spectra and, due to the diverse chemical nature of molecules, the differential accumulation of specific metabolites leads to changes in pollinator preferences, which may not appear evident to the human eye (Grotewold 2006). For example, bee-pollinated flowers are often blue or yellow but rarely red, which may appear black to bees (Grotewold 2016; Papiorek *et al*. 2016).

Furthermore, flower coloring is an important aesthetic factor for the ornamental plant market since it directly influences the commercial value of flowers (Zhao & Tao 2015). Gregor Mendel, who established the fundamental laws of genetics, was interested in plant breeding and succeeded in obtaining a new variety of *Fuchsia* (Onagraceae, Myrtales) with a novel color, which rendered him a prize for his agronomic research (Freire-Maia 1995). The advent of genetic engineering tools brings new insights to basic research and breeding, aiming to obtain different coloring patterns (*i.e.* more lasting or vibrant), or completely different colors from those of the wild type genotype. This is the case of the first genetically modified commercial flower species, *Dianthus* (Caryophyllaceae, Caryophyllales), which display a wide variation of colors ranging from white to red (Tanaka *et al*. 2005).

According to the European Commission, in 2012, the European Union assumed 42.6% of the total world flower and ornamental plant production, followed by China, USA and Japan with 15.5%, 11.1% and 9.5%, respectively. Brazil is the ninth in the ranking with 1.71% of the world market (Neves & Pinto 2015). In Brazil, there is increasing investment and attention to flower and ornamental plant production market. Since 1970, the floriculture has a commercial

and professional character, promoted mainly by Japanese and Dutch immigrants. The creation of the Brazilian Institute of Floriculture (IBRAFLOR) in 1994, was an important enterprise to integrate and politically represent the Brazilian`s interests at national and international levels. In 2010, a strategic agenda was created focused on encouraging and supporting the development and growth of the flower and ornamental plant domestic market (AEFP 2011). Since 2012, the increasing of this sector, with 6.17% per year, exposes the success of these strategies (Neves & Pinto 2015). Brazilian flora provides an invaluable diversity of native ornamental species to be exploited highlighting the economic potential of this market for the country's development.

The color of the flowers is one of the best-studied floral traits in terms of its genetic and chemical bases, as well as its ecological significance. Regardless the chlorophyll, there are three types of pigments present in vegetal tissues and all confers color to flowers: carotenoids, betalains and flavonoids (specially anthocyanins). These secondary metabolites are originated from products of the primary metabolism by the plastidial shikimate (SKM) and methylerythritol phosphate (MEP) pathways, and the cytosolic malonate (MAL) pathway. Carotenoids are produced by MEP, SKM originates betalains, while intermediates of SKM and MAL condensate to produce flavonoids. In this chapter, we review the biosynthesis of these compounds and the current knowledge about spatial and temporal flower color change, an unusual, but widespread phenomenon in angiosperms.

1.1. Carotenoids

Carotenoids, also known as tetraterpenoids (C_{40}), belong to terpenoid class of secondary metabolites. They are lipid soluble substances produced by all photosynthetic organisms (plants, algae and bacteria), likewise some non-photosynthetic bacteria and fungi (Hirschberg *et al*. 1997; Li *et al*. 2001). In green tissues, carotenoids act as components of the light harvesting machinery and photo-protectants from oxidative damage, being essential players for photosynthetic activity (Bartley & Scolnik 1995; Ronen *et al*. 1999; Davies 2004). Yet, in many flowers and fruits, after chloroplasts to chromoplast transition, carotenoids act as pollinator and seed dispersal attractants (Ronen *et al*. 1999; Niyogi *et al*. 2001; Lao *et al*. 2011).

Since 19th century, carotenoids, together with other natural pigments, attracted the attention of organic chemists. β-carotene was the first carotenoid isolated in 1817 and, in 1937, xanthophylls were identified as the pigments involved in autumnal leaf color (Isler 1971).

Furthermore, carotenoids are essential components of human diets, providing precursors for the biosynthesis of vitamin A (Krinsky & Johnson 2005). They also serve as antioxidants, reducing age related degeneration of the eye and lowering the risk of cancer and cardiovascular diseases (Sandmann *et al*. 2006; Johnson & Krinsky 2009; Ford & Erdman 2012).

In general, yellow and orange tones shown by tissue/organ plants are conferred by carotenoids (Tanaka 2010), especially in flowers. Carotenoids can also coexist with anthocyanins resulting in brown and bronze tones despite of their contribution for red colors (Forkmann 1991; Nisar *et al*. 2015).

The building blocks of all terpenoids are isopentenyl diphosphate (IPP) and its isomer dimethylallyl diphosphate (DMAPP) (Chappell *et al*. 1995), being synthetized by two distinct pathways: mevalonate (MEV) and MEP, cytosolic and plastidial localized, respectively (Lichtenthaler 1999; Eisenreich *et al*. 2001; Rodriguez-Concepcion & Boronat 2002). However, the exchange of intermediates between the pathways is well documented (Dudavera *et al*. 2006).

MEV pathway supplies most of the C_5 units for the biosynthesis of C_{15} (sesquiterpenes), C_{30} (triterpenes and sterols), and larger compounds (dolichols), substances whose later biosynthetic steps take place in cytosol. However, plastidial localized terpenoids, such as C_5 (isoprene), C_{10} (monoterpenes), C_{20} (diterpenes), C_{30} (triterpenes) and C_{40} carotenoids are synthesized *via* MEP (Lichtenthaler *et al*. 1997; Milborrow & Lee 1998; Matusova *et al*. 2005; Rodriguez-Concepcion 2010; Buchanan *et al*. 2015). The MEP pathway (Figure 1.1) initiates with glyceraldehyde 3-phosphate (GA3P) and pyruvic acid that by the action of the DEOXY-D-XYLULOSE SYNTHASE (DXS) form deoxy-D-xylulose 5-phosphate (DXP). Subsequently intramolecular rearrangement and reduction of DXP by the DXP REDUCTOISOMERASE (DXR) leads MEP formation. After some steps IPP and DMAPP are formed, and undergo sequential condensation reactions to form C_{20} geranylgeranyl diphosphate (GGPP), precursor of carotenoid biosynthesis. The condensation of two molecules of GGPP, tail-to-tail, results in phytoene, which is further converted in lycopene by a series of desaturations and isomerizations by the action of PHYTOENE DESATURASE (PD), CAROTENE DESATURASE (CD) and CAROTENE ISOMERASE (CI). Lycopene represents a branch point in carotenoid pathway that is enzyme-mediated cyclized by LYCOPENE CYCLASES (LCYε, LCYβ), to produce α-carotene or β-carotene (Nisar *et al*. 2015). These two compounds are precursors of the oxygenated carotenoids, xanthophylls (*e.g.* lutein, violaxanthin and zeaxanthin), which are produced by the

action of β-RING HYDROXYLASE (β-RH) and ε-RING HYDROXYLASE (ε-RH) (Finkelstein 2013; Nisar *et al*. 2015).

The enzyme encoding genes involved in carotenogenesis have been identified in many plant species, while its regulation has been addressed by several studies (Fraser & Bramley 2004; Tanaka *et al*. 2008; Li & Yuan, 2013; Liu *et al*. 2015a). Some steps are regulated by light and chloroplast redox status (Jahns & Holzwarth 2012; Llorente *et al*. 2016). In Solanaceae crop species (*e.g*. tomato fruit) and *Arabidopsis thaliana* (L.) Heynh model plant, transcription factors of carotenoid biosynthetic genes were well characterized (*e.g*. PHYTOCHROME INTERACTING FACTOR 1a, RIPENING INHIBITOR, etc) (Toledo-Ortiz *et al*. 2010; Martel *et al*. 2011), demonstrating that the accumulation of carotenoids is transcriptionally regulated. Red-colored flowers due to the accumulation of carotenoids are rare among angiosperms and even scarcer are the studies about their biosynthetic regulation (Ohmiya 2011).

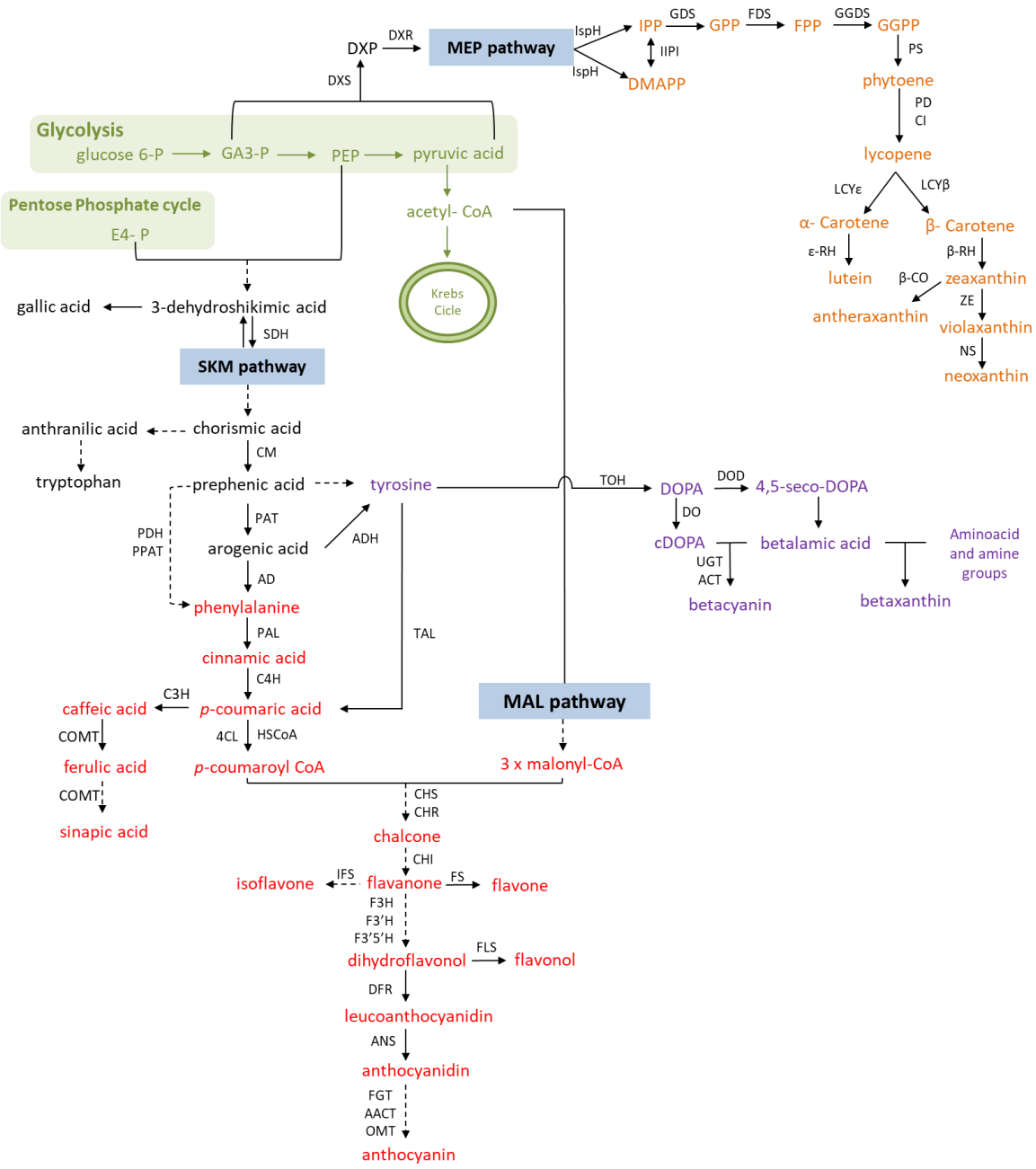

Figure 1.1. Simplified schematic representation of plant pigment biosynthetic pathways. Primary metabolism, **carotenoid**, **flavonoid** and **betalain** pathways are highlighted in green, orange, red, and purple, respectively. In blue boxes are the names of the main intermediate for each pathway: SKM (shikimate), MEP (methyl-D-erythritol 4-P), and MAL (malonate). Abbreviations indicate the following metabolites and enzymes: 1-deoxy-D-xylulose-5-P (**DXP**), 4-HYDROXY-3-METHYLBUT-2-ENYL DIPHOSPHATE REDUCTASE (**IspH**), ACYL TRANSFERASE (**ACT**), ANTHOCYANIDIN ACYL TRANSFERASE (**AACT**), ANTHOCYANIDIN SYNTHASE (**ANS**), AROGENATE DEHYDRATASE (**AD**), AROGENATE DEHYDROGENASE (**ADH**), CAFFEIC ACID *O*-METHYLTRANSFERASE (**COMT**), CAROTENE ISOMERASE (**CI**), CHALCONE SYNTHASE (**CHS**), CHALCONE ISOMERASE (**CHI**), CHALCONE REDUCTASE (**CHR**), CHORISMATE MUTASE (**CM**), CINNAMATE 4-HYDROXYLASE (**C4H**), Coenzyma A (**CoA**), COUMARATE 3-HYDROXYLASE (**C3H**), cyclo-DOPA (**cDOPA**), DIHYDROFLAVANOL 4-REDUCTASE (**DFR**), dihydrophenylalanine (**DOPA**), dimethylallyl diphosphate (**DMAPP**), DIPHENOL OXIDASE (**DO**), DOPA DIOXYGENASE (**DOD**), DXP REDUCTOISOMERASE (**DXR**), DXP SYNTHASE (**DXS**), erythrose 4-phosphate (**E4P**), farnesyl diphosphate (**FPP**), FARNESYL DIPHOSPHATE SYNTHASE (**FDS**), FLAVANONE 3'5'-HYDROXYLASE (**F3'5'H**), FLAVANONE 3'-HYDROXYLASE (**F3'H**), FLAVANONE 3-HYDROXYLASE (**F3H**), FLAVONE SYNTHASE (**FS**), FLAVONOID GLYCOSYL TRANSFERASE (**FGT**), FLAVONOL SYNTHASE (**FLS**), geranyl diphosphate (**GPP**), geranylgeranyl diphosphate (**GGPP**), GERANYLGERANYL DIPHOSPHATE SYNTHASE (**GGDS**), glyceraldehyde 3- phosphate (**GA3P**), GPP SYNTHASE (**GDS**), Coenzyme A (**HSCoA**) ISOFLAVONE SYNTHASE (**IFS**), ISOPENTENYL DIPHOSPHATE ISOMERASE (**IPPI**), isopentenyl

diphosphate (**IPP**), LYCOPENE β-CYCLASE (**LCYβ**), LYCOPENE ε-CYCLASE (**LCYε**), NEOXANTHIN SYNTHASE (**NS**), *O*-METHYLTRANSFERASE (OMT), PHENYLALANINE AMMONIA LYASE (**PAL**), PHENYLPYRUVATE AMINOTRANSFERASE (**PPAT**) phosphoenolpyruvate (**PEP**), PHYTOENE DESATURASE (**PD**), PHYTOENE SYNTHASE (**PS**), PREPHENATE AMINOTRANSFERASE (**PAT**) PREPHENATE DEHYDROGENASE (**PDH**), SHIKIMATE DEHYDROGENASE (**SDH**), TYROSINE AMMONIA LYASE (**TAL**)**,** TYROSINE OXYDASE HYDROXYLASE (**TOH**), UDP-GLUCOSYLTRANSFERASE (**UGT**), ZEAXANTHIN EPOXIDASE (**ZE**), B-CAROTENE OXYGENASE (**β-CO**), β-RING HYDROXYLASE (**β-RH**), ε-RING HYDROXYLASE (**ε-RH**). Adapted from Andersen & Markham (2005), Dewick (2009), Khan & Giridhar (2015), and Nisar *et al* (2015).

1.2. Betalains

Betalains are pigments possessing a nitrogenous core structure. They confer colors from red to violet (betacyanins) or yellow to orange (betaxanthins) and are exclusively present in members of some families of Caryophyllales order. This well-defined clade comprises 38 families being 17 betalain accumulators (Strack *et al*. 2003; Grotewold 2006; APG 2016). Betalains are considered chemosystematics markers of the core Caryophyllales (Slimen *et al.* 2017), where approximately 75 distinct compounds were identified (Khan & Giridhar 2015). Interestingly, within core Caryophyllales, only two families (*i.e*. Caryophyllaceae and Molluginaceae) are known to produce anthocyanin as the noncore Caryophyllales (Brockington *et al*. 2011).

As well as many other naturally occurring compounds, betalains present chemical instability related to several factors, such as light, temperature, oxygen, pH value, water content, and storage conditions (Gonçalves *et al*. 2012; Fernández-Lopez *et al*. 2013; Molina *et al*. 2014; Otálora *et al*. 2016).

Betalains are derived from the amino acid L-tyrosine, an aromatic amino acid synthetized by the SKM plastidial pathway (Figure 1.1). The primary substrates for this pathway are the phosphoenolpyruvate (PEP- a glycolytic intermediate) and the erythrose 4-phosphate (E4P- from the pentose phosphate cycle). Chorismic and prephenic acids are key intermediates that lead to the synthesis of the aromatic amino acids: phenylalanine, tryptophan, and tyrosine. These amino acids are involved in aromatic alkaloids and phenolic compounds pathways. In monocots, tyrosine is the precursor for phenolic compounds synthesis, while in eudicots, the universal precursor of numerous phenolic compounds (*e.g.* phenylpropanoids, lignans, lignins, stilbenes and flavonoids) is the phenylalanine (Maeda & Dudavera 2012).

Betalain synthesis starts with dihydrophenylalanine (DOPA) formation catalyzed by the TYROSINE OXYDASE HYDROXYLASE (TOH). DOPA is an important precursor not only of betalains but also of other secondary metabolites in plants (Tanaka 2008). The cleavage of

DOPA mediated by DOPA 4,5-DIOXYGENASE (DOD) followed by non-enzymatical rearrangements result in the formation of betalamic acid, the core structure of betalains (Khan & Giridhar 2015). Betalamic acid is the chromophore molecule of both betacyanins (violet) and betaxanthins (yellow) (Tanaka 2008). Its condensation with cyclo-DOPA (cDOPA) and glucosyl derivatives, amino acids, and amine groups leads to the formation of these two categories of betalains: betacyanins and betaxanthins (Khan & Giridhar 2015) (Figure 1.1).

Betaxanthins were structurally identified in *Beta vulgaris* L. (Amaranthaceae), *Portulaca grandiflora* Hook. (Portulacaceae), *Mirabilis jalapa* L. (Nyctaginaceae), *Glottiphyllum longum* (Haw.) N.E.Br. (Aizoaceae), *Rivina humilis* L. (Phytolacaceae), *Amaranthus tricolor* L. (Amaranthaceae), among other species. Moreover, betacyanins were found in *Celosia argentea* L. (Amaranthaceae), *Iresine herbstii* Hook. (Amaranthaceae), *Bougainvilea glabra* Choisy (Nyctaginaceae), and *Gomphrena globose* L. (Amaranthaceae) (Khan & Giridhar 2015).

Betalains and anthocyanins seem to be mutually exclusive pigments because there are no evidences of the occurrence of these two pigments in the same plant. This two classes of compounds play equal biological function, since both confer similar color to flowers and fruits, and accumulate in response to stress signals. The functional and biochemical similarities among betalains and anthocyanins suggest similar biosynthetic regulatory mechanisms (Stafford 1994; Brockington *et al*. 2011). Studies with *Phytolacca americana* Z. (Phytolacaceae) (Takahashi *et al*. 2009) demonstrated that DOD encoding gene is transcriptional regulated. The identification of MYELOBLASTOSIS (MYB) and BASIC HELIX–LOOP–HELIX (bHLH) transcription factor responsive elements in *P. americana* DOD promoter region suggest that these proteins regulate betalain biosynthesis (Takahashi *et al*. 2009). Interestingly, MYB and bHLH, together with TRYPTOPHAN-ASPARTIC ACID DIPEPTIDE REPEAT proteins (WDRs) are transcription factors that interact among each other to form the MBW complex, which has been extensively demonstrated to regulate flavonoid biosynthesis (Hichri *et al*. 2011). Recently, the first *MYB*-like regulatory gene for betalain pathway, *BvMYB1*, has been identified in *Beta vulgaris*, however, unlike anthocyanin-related MYBs, the product of this gene does not interact with bHLH members of the MBW complex. Phylogenetic analyses indicated that *BvMYB1* and anthocyanin MYBs of *Antirrhinum majus* L. (Plantaginaceae, Lamilaes) (*AmROSEA*) and *A. thaliana* (*AtPAP1*) (Solanaceae, Solanales) probably derive from a common ancestor gene (Hatlestad *et al*. 2014).

Recent studies on comparative genetics of betalain producing taxa revealed another possible explanation for the mutual exclusion between anthocyanins and betalains. The promoter region of *DIHYDROFLAVONOL 4-REDUCTASE* (*DFR*) and *ANTHOCYANIDIN SYNTHASE* (*ANS*) are different in anthocyanin and betalain producing species. Both genes are expressed in betalain producing taxa, but they do not lead to anthocyanin production (Shimada *et al*. 2005, 2007). It has been proposed that, even when the putative MYB and bHLH transcriptional factors for anthocyanin biosynthesis are present and bind to the *DFR* and *ANS* promoters of the Caryophyllales, other factors involved in the activation of these genes might be missing in anthocyanin non-producing plants (Broun 2005; Ramsay *et al*. 2005; Shimada *et al*. 2007). The other possible explanation is the presence of a repressor-binding site in Caryophyllales promoters (Shimada *et al*. 2007). Despite of advances in this understanding, the evolution of this pathway and the mechanism behind the mutual exclusivity of betalains and anthocyanins has not been resolved (Sakuta 2014).

1.3. Anthocyanins

Among angiosperms, flavonoids, specially anthocyanins, are the predominant floral pigments (Winkel-Shirley 2001; Tanaka *et al*. 2010). These pigments are responsible for the red/orange to violet/blue coloration of fruits and flowers according to the vacuole pH (Katsumoto *et al*. 2007). Similar to carotenoids, anthocyanins act as photoprotectants, due to their UV absorption spectra and high antioxidant activity. In general, in non-reproductive tissues, anthocyanins are accumulated in response to biotic and abiotic stresses, such as pathogens, high/low temperatures, high light, UV-B radiation, drought, nutrient deficiencies, high ozone concentration, etc. (Chalker-Scott 1999; Feild *et al*. 2001; Neill *et al*. 2002; Oberbaueri & Starr 2002; Steyn *et al*. 2002; Takos *et al*. 2006; Gould *et al*. 2008; Rezende & Furlan 2009).

Anthocyanins are synthesized by the combination of precursors from the SKM and MAL pathways, being the terminal branch of the highly conserved flavonoid pathway (Holton & Cornish 1995). Flavonoids constitute a relatively diverse family of aromatic molecules derived from L-phenylalanine (Winkel-Shirley 2001). Flavonoid synthesis is initiated by the action of the CHALCONE SYNTHASE (CHS) that catalyzes the condensation of *p*-coumaroyl-CoA (SKM) with three molecules of malonyl-CoA (MAL- fatty acid pathway), resulting in the formation of a tetrahydroxylalcohol. This compound is cyclized producing chalcone, precursor of all classes of

flavonoids including flavonols, flavones, flavandiols, dihydroflavonols, proanthocyanidins, isoflavonoids and anthocyanins (Dewick 2009).

Flavones are formed from the C-ring dehydrogenation of flavanones, a class of flavonoids formed by chalcone isomerization mediated by the enzyme CHALCONE ISOMERASE (CHI), which forms a third ring, characteristic in the $C_6C_3C_6$ flavonoid basic structure (Dewick 2009).

Dihydroflavonol is the branching point for the synthesis of flavonols and anthocyanins by FLAVONOL SYNTHASE (FLS) and DFR, respectively (Cooper-Driver 2001; Saito & Yamazaki 2002; Dewick 2009; Buchanan *et al*. 2015). Anthocyanin synthesis further requires the activity of ANS, FLAVONOID GLYCOSYL TRANSFERASE (FGT), ANTHOCYANIDIN ACYL TRANSFERASE (ACT) and O-METHYL TRANSFERASE (OMT). Anthocyanidins are the aglycones and chromophores of anthocyanins (glycosylated compounds), probably the best-known and most studied group of flavonoids.

In nature, anthocyanins provide a wide range of colors. Out of the twenty-three described anthocyanidins, six are particularly abundant: cyanidin, delphinidin, malvidin, pelargonidin, peonidin, and petunidin. The difference in color tones is determined by the substitution patterns in the core structure of the B-ring (*e.g.* hydroxyl and methoxyl) and in the A and C-ring (*e.g.* glycosylations and acylations) (Castañeda-Ovando *et al*. 2009, Trouwillas *et al*. 2016).

When considering their structures, studies on anthocyanins have demonstrated that they can exist in various colored and colorless forms; the predominant form is largely determined by pH. At acidic pH (< pH 2.5), the dominant form is the colored flavylium cation form, however, about pH 3 most anthocyanins undergo nucleophilic attack by water with subsequent loss of a proton resulting in the colorless or pale-yellow hemiacetal (or hemiketal) form. The hemiacetal form can then undergo ring-opening tautomerization to the *cis*-hydroxychalcone or (*Z*)-hydroxychalcone, which can isomerize thermally or photochemically to the *trans*-chalcone or (*E*)-chalcone, both of which are also colorless or pale-yellow (Silva *et al*. 2016). Additionally, anthocyanins with two or more *ortho*-hydroxyl groups in the B-ring form complexes with divalent and trivalent metal cations, such as Al^{3+}, Fe^{2+}/Fe^{3+}, and Mg^{2+}, which results in color changes (Buchweitz *et al*. 2001; Yoshida *et al*. 2009; Soumille *et al*., 2013; Sigurdson *et al*. 2014).

Two categories of genes are involved in the biosynthesis of anthocyanins (Martin *et al*. 1991; Jackson *et al*. 1992): structural enzyme encoding genes, such as *PHENILALANINE AMONIA LIASE* (*PAL*), *CINNAMATE 4-HYDROXYLASE (C4H*), *CHS*, *FLAVANONE 3-HYDROXYLASE*

(*F3H*), *DFR*, *ANS*, and *FGT*; and regulatory transcription factor encoding genes, basically MYB, bHLH, and WDR proteins, which coregulate the expression of the structural genes (Uematsu *et al*. 2014). Maize (*Zea mays* L., Poaceae, Poales), snapdragon (*A. majus*) and petunia (*Petunia hybrid* Vilm., Solanaceae, Solanales) are the major model species for the study of flavonoid biosynthesis, from which several structural and regulatory genes have been characterized (Holton & Cornish 1995; Mol *et al*. 1998; Whinkel-Shirley 2001; Dhar *et al*. 2014). Moreover, anthocyanin biosynthesis and regulation have also been studied in other plants, such as *Solanum tuberosum* L. (potato) and *S. melongena* L. (eggplant), Solanaceae (Solanales), and *A. thaliana*, etc. (Jeon *et al*. 1996; Holton & Cornish 1997; Quattrocchio *et al*. 1999; Noda *et al*. 2000; Jung *et al*. 2005; Katsumoto *et al*. 2007; Chaudhary & Mukhopadhyay 2012).

Over the past 150 years, flavonoids have featured in major scientific breakthroughs, from Mendel's elucidation of genetic bases, where seed coat color was one of the major characters followed in his experiments with peas (*Pisum sativum* L., Fabaceae, Fabales), to McClintock's discovery of transposable elements, which move in and out of flavonoid biosynthetic genes expressed in colored maize kernels (Whinkel-Shirley 2001). Flavonoid pathway also helped to clarify the phenomenon of transgene co-suppression. Aiming to intensify the violet pigmentation, an extra copy of *CHS* was introduced in *P. hybrida* resulting in totally white flowers. Expression profile analysis showed that in these transgenic plants neither the transgene nor the endogenous copy of the gene were expressed (Napoli *et al*. 1990).

Few studies regarding RNAi-based regulation of flavonoid biosynthetic pathway can be found, but certainly it will be a research focus of interest in the future. In *A. thaliana*, it was reported the regulation of MYB anthocyanin regulators by miRNAs and tasiRNA (Rajagopalan *et al*. 2006; Hsieh *et al*. 2009; Gou *et al*. 2011).

Recently, additional levels of regulation have been reported to modulate the production of anthocyanins. These include the post-translational modifications of anthocyanin transcription factors (Xie *et al*. 2012; Ye *et al*. 2012; Maier *et al*. 2013; Patra *et al*. 2013), chromatin remodeling (Hernandez *et al*. 2007), and the identification of repressor proteins that limit expression of the anthocyanin biosynthetic genes (Aharoni *et al*. 2001; Dubos *et al*. 2008; Matsui *et al*. 2008; Yuan *et al*. 2013).

Despite vacuolar pH, metal complexation and biosynthetic regulations, copigmentation influence the color of plant organs (Tanaka 2010). Copigmentation can be defined as the formation of noncovalent complexes involving an anthocyanin or anthocyanin derived pigment

and a copigment (in the presence or absence of metal ions), and the subsequent changes in optical properties of the pigment. There are over ten-thousand compounds that could potentially serve as copigments but, in any case, they should have (i) sufficiently extended π-conjugated systems, which are supposed to favor π−π stacking interactions and (ii) hydrogen bond donor/acceptor groups such as OH and C=O groups (Trouwillas *et al*. 2016). The major natural copigments are hydrolyzable tannins, flavonoids, and phenolic acids. Some flavonoid classes are copigments (flavonols, flavones, flavanols, and even dihydroflavonols), which appear to be the most efficient due to extension of their π-conjugation over their entire tricyclic core structure (rings A, B, and C), being the flavones and flavonols (*e.g.* quercetin, kaempferol, isoquercitrin, and rutin) the most efficient among them. Hydroxycinnamic acids and derivatives such as caffeic, *p*-coumaric, ferulic, sinapic, chlorogenic, and caftaric acids are commonly described as relatively efficient copigments as well (Trouwillas *et al*. 2016). Some non-phenolic copigments have also been described, including alkaloids, amino acids, organic acids, nucleotides, and polysaccharides (He *et al*. 2012), but their efficiency is usually lower than polyphenols. It remains unclear whether these compounds can significantly contribute to color expression provided by anthocyanins (Trouwillas *et al*. 2016).

1.4. Spatial distribution of flower pigments

Petal tissue and leaf blade structure are similar, both can be divided into four parts: upper epidermis, palisade tissue, sponge tissue, and lower epidermis. Petal pigments are mainly distributed in the upper epidermal cells, but they can also be found in the palisade tissue and the lower epidermis. For example, in pale blue grape hyacinth (*Muscari latifolium* J.Kirk, Asparagaceae, Asparagales) pigments were found in the palisade tissue (Qi *et al*. 2013), while in *Tulipa* (Liliaceae, Liliales) cv. murasakizuisho (Shoji *et al*. 2007), *Ipomoea tricolor* Cav. (Convolvulaceae, Solanales) cv. heavenly blue (Yoshida *et al*. 2009) and *Meconopsis grandis* Prain. (Papaveraceae, Ranunculales) (Yoshida *et al*. 2006), pigments occur in the petal lower epidermis. Typically, no pigment is deposited in the sponge tissue, but the thickness and density of this layer is related to the brightness of flower color. As thicker and denser the sponge tissue is, the brighter is the color (An, 1989).

The shape of petal epidermal cells also impacts on flower color. Conical cells enhance pigment light absorption, by increasing the amount of incident light on epithelial cells, thereby leading to darker flower color and enhanced color saturation. Flat cells reflect more light,

leading to lighter flower color. Protruding papillae in epidermal cells generate a velvet shine on the petals (Zhao & Thao 2015). The deposition subcellular localization depends on the nature of the pigment. In general, carotenoids are deposited in the plastids, while flavonoids and betalains are deposited into the vacuoles.

The wide variation in flower color and color patterning is indicative of the diversity in the regulatory mechanisms of pigment biosynthetic pathways (Saito *et al*. 2006). Studies of gene expression regulation with flavonoid producing species, such as petunia and snapdragon, have clarified the genetic control of different coloring patterns, such as pigmented venation (stripes) (Schwinn *et al*. 2006; Shang *et al*. 2011), picotee (segments) (Saito *et al*. 2006), as well as distinct pigmentation/intensity among the corolla (Jackson *et al*. 1992; Schwinn *et al*. 2006; Albert *et al*. 2011; Martins *et al*. 2013).

The mechanism for vein associated pigmentation (venation) patterning is the result of anthocyanin accumulation in the epidermal cells overlaying the vasculature, in accordance to the expression domain of the MYB (transcript gradient from vasculature) and bHLH (epidermal) transcriptional factors, which control the expression of the structural genes (Shang *et al*. 2011; Davies *et al*. 2012). Some petunia cultivars have corollas with white margins and red/purple cores; or the opposite, pigmented margins and white central regions. In these cultivars, color is determined by differential accumulation of anthocyanins (petunidin, cyanidin and peonidin) and flavonols (quercetin and kaempferol) among the corolla regions. Gene expression studies showed that white margins have low levels of *CHS* mRNA, while flowers with white center accumulate a high amount of *FLS* transcripts. Thus, the white color may either be the result of the lack of flavonoid production or the deviation of the metabolic flux towards the production of the white-colored flavonol (Saito *et al*. 2006).

Parakeelya mirabilis Hershk. (Montiaceae, Caryophyllales) petals display violet, red, and yellow regions separated by a colorless white zone. These colored sectors accumulate different amounts of betacyanins and betaxanthins, suggesting that their biosynthesis is regulated both, spatially and temporally, by a still unknown regulatory mechanism (Chung *et al*. 2015).

1.5. Temporal distribution of pigments in flowers

Color change is not a simple degeneration phenomenon, instead it includes the gain or loss of pigments (*e.g*. such as anthocyanins, carotenoids, flavonols and betalains), metal complexation or changes in pH (Weiss 1995).

In *Viola cornuta* L. (cv Yesterday, Today and Tomorrow- Violaceae, Malpighiales), a model system for flower color change studies, the flowers change from white to purple. Fazard *et al.* (2002) studied the physiological and biochemical mechanisms involved in flower color change by the investigation of environmental signals that would influence the accumulation of anthocyanins. They verified that this change is related to the presence of pollen in the stigma and to the incidence of light, and suggested that anthocyanin biosynthesis would be regulated at the transcriptional level. This agrees with previous studies where it was observed that in some species, pollination triggers biosynthesis of anthocyanins, produced in less than 24h (Weiss 1991). Additionally, the transcriptional induction of anthocyanin biosynthetic enzyme encoding genes by light has been described in several systems (Koes *et al*. 1989; Procissi *et al*. 1997; Shin *et al*. 2007; Liu *et* al. 2015b; Kim *et al*. 2017).

Brunfelsia calycina Benth. (Solanaceae, Solanales), is a model for anthocyanin degradation mechanism, the petals turn from dark-purple to completely white within three days after anthesis, due to the reduction of anthocyanin concentration and increase of phenolic acid contents during flower development (Vaknin *et al*. 2005; Bar-Akiva *et al*. 2010). Zipor *et al*. (2014) showed a novel BASIC VACUOLAR PEROXIDASE as the responsible for the *in planta* degradation of anthocyanins in *B. calycina*.

Regarding carotenoid pathway, in marigold petals (*Tagetes* spp., Asteraceae, Asterales), Moehs *et al*. (2001) reported DXS and PS as the enzymes responsible for the color development from pale-yellow to deep yellow. In *Sandersonia aurantiaca* Hook. (Colchicaceae, Liliales), petals of pale-yellow flowered cultivars showed a lower expression of *PD* than those of yellow flowered cultivars, and the expression level of this gene showed to be proportional to the carotenoid accumulation level (Nielsen *et al*. 2003). Kishimoto & Ohmiya (2006) reported that the white colored chrysanthemum petals (Asterales) are the result of the up-regulation of the *CAROTENOID CLEAVAGE DIOXYGENASE* (*CCD*) gene, which degrades carotenoids into colorless compounds. *CCD* genes are also responsible for the differences in carotenoid levels between yellow and white tissues in melon, peach, potato, and saffron (Campbell *et al*. 2010; Brandi *et al*. 2011; Ibdah *et al*. 2006; Rubio *et al*. 2008).

Flower color change during anthesis is a natural phenomenon, widespread in angiosperms, and already reported in at least 33 orders, 78 families, and 253 genera; but it is an uncommon strategy regarding the few number of species into each genus (Weiss 1995; Weiss & Lamont 1997). It has been reported that color change is often triggered in response

to pollination. This may involve the whole flower, only the center, the corolla tube, the nectary/hypanthium, the nectar guide/banner petal spot, selected petals, the petal appendages, the androecium or the gynoecium (Weiss 1995). Otherwise, maintaining post-color flower change is an enhanced of floral display advantage, as it increases the attractiveness of individual plants and, consequently, the approximation frequency of pollinators since they become showy at long distances (Weiss 1995; Niesenbaum *et al*. 1999; Oberrath & Böhning-Gaese 1999; Sun *et al*. 2005). From the ecological point of view, flower color change can reflect the reward for pollination. For example, some flowers (*e.g. Weigela middendorffiana* C. Koch*, W. japonica* Thunb. – Caprifoliaceae, Dipsacales - and *Pedicularis monbeigiana* Bonati – Orobanchaceae, Lamiales) have a large amount of nectar, as well as high pollen viability and stigma receptivity, but all these characteristics decline after the floral color change (Ida & Kudo 2003, 2010; Sun *et al*. 2005; Zhang *et al*. 2012). In other cases, including *Leucojum vernum* L. (Amaryllidaceae, Asparagales), *Nicotiana rustica* L. (Solanaceae, Solanales), and *Pulmonaria officinalis* L. (Boraginaceae, Boraginales), floral color change 'advertises' nectar rewards and successfully attracts pollinators (Lunau 1996).

Bellow, Table 1.1 describes species with whole flower color change. Weiss reviewed in 1995 by using Cronquist classification, here we updated species names, families, and orders following the APG IV, Taxonomic Name Resoltion (http://tnrs.iplantcollaborative.org), and Leal, E. (personal communication). After Weiss (1995), only 17 new species were described regarding floral color change. Whole flower color change was reported for 48 families, representing 23 orders and 138 species in APG IV classification (Figure 1.2). However, only for a few species the mechanism of color change has been studied: *Viola* cornuta (white to purple), *Brunfelsia calycina* (purple to white), *Nicotiana mutabilis* Stehmann & Semir (white to pink, Solanaceae, Solanales) and *Paeonia ostii* Hong & Zhang (white to pink, Paeoniaceae, Saxifragales) (Farzad 2003; Vaknin *et al*. 2005; Macnish *et al*. 2010; Gao *et al*. 2016).

Within the species where the corolla changes the color during flower development, only for few of them, the molecular mechanism underneath this process has been explored (Farzad *et al*. 2002; Macnish *et al*. 2010; Gao *et al*. 2016; Ruxton & Schaefer 2016). Color change has been described for at least eight Brazilian native species, and in any case the mechanism that determines it has been addressed. The flower color development is predominantly mediated by anthocyanins (Table 1.1), whose biosynthesis is regulated by physical (temperature, light, water, pollinators, ion-beam radiation, and gamma rays) and chemical (pH, mineral nutrients,

and hormones) factors. The identification and characterization of genes encoding key enzymes or transcription factors involved in plant anthocyanin biosynthesis are powerful tools to develop metabolic engineering approaches aiming to manipulate flower color (Zhao & Tao 2015).

As discussed above, the color change of the flowers can be determined by the transcriptional or post-transcriptional control of the enzymes of flavonoid pathway, the presence of accessory pigments, the association of pigments with metals, or even a combination of these factors.

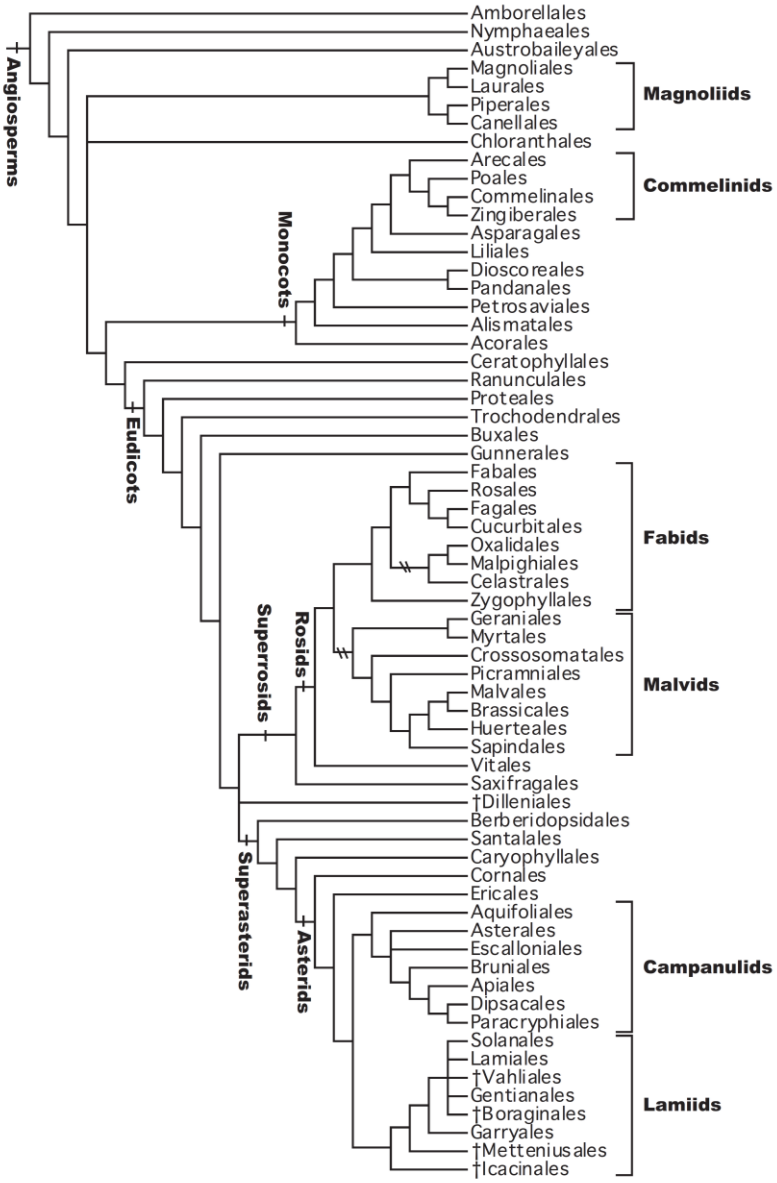

Figure 1.2. Angiosperm orders with color change during flower development according to APG IV classification. Asterisks indicate the presence of at least one family with floral color change reported (adapted from APG IV).

Table 1.1. Angiosperms that display color change along floral development. Adapted and updated from Weiss 1995.

Taxon[1]			Color change[2]	Pigment involved[3]	Native habitat[4]	Reference
Order	Family	Species				
Apiales						
	Pittosporaceae					
		Billardiera ringens (Harv.) E.M.Benn.	Yellow-orange to red	(+) A	Australia	Erickson *et al.* 1973
		Pittosporum rhombifolium A. Cunn. ex Hook.	White to orange-yellow	(+) C	Australia	Bailey 1949
		Pittosporum undulatum Vent.	White to yellow	(+) C*	Australia	Weiss 1995
Asparagales						
	Asparagaceae					
		Beschorneria yuccoides K.Koch	Green to pink	(+) A*	Chiapas, Mexico	Weiss 1995
	Orchidaceae					
		Cyrtorchis arcuata (Lindl.) Schltr.	White to yellow	(+) C	E. Africa	Blundell 1987
		Epidendrum ciliare L.	White to pale yellow	(+) C	Tropical America	Weiss 1995
		Epidendrum paniculatum Ruiz & Pav.	White to yellow	(+) C	Tropical America	Weiss 1995
		Epidendrum stamfordianum Bateman	White to pale yellow	(+) C	Tropical America	Weiss 1995
		Malaxis seychellarum (Kraenzl.) Summerh.	Green to brown	(+) A, (+) C	Seychelles	Friedmann 1986
		Vanda sp.	Lavender to white	(-) A*	Old World	Burg & Dulkman 1967
		Ypsilopus longifolius (Kraenzl.) Summerh.	White to yellow-green	(+) C	E. Africa	Blundell 1987
Asterales						
	Campanulaceae					
		Lobelia excelsa Bonpl.	Orange to red	(+)A	Chile	Weiss 1995
Brassicales						
	Brassicaceae					
		Erysimum bicolor (Hornem.) DC.	White to purple	(+) A	Canary Islands	Weiss 1995
		Erysimum scoparium (Brouss. ex Willd.) Wettst.	White to purple	(+) A	Canary Islands	Weiss 1995
		Erysimum mutabile Boiss. & Heldr.	White to lavender	(+) A	Canary Islands	Bramwell & Bramwell 1984
		Iberis linifolia L.	White to lavender	(+) A	Spain	Weiss 1995
		Lobularia maritima (L.) Desv.	White to purple	(+) A*	Medit.	Weiss 1995

Table 1.1. *(Continued)*

Taxon[1]			Color change[2]	Pigment involved[3]	Native habitat[4]	Reference
Order	Family	Species				
Caryophyllales						
	Aizoaceae					
		Carpobrotus edulis (L.) N.E.Br.	Pale yellow to pink	(+) B*	S. Africa	Weiss 1995
	Cactaceae					
		Opuntia phaeacantha Engelm.	Yellow to orange	(+) B	Arizona	Weiss 1995
	Polygonaceae					
		Polygonum emondi Meisn.	Red to whitish	(-) B	Himalayas	Weiss 1995
Dipsacales						
	Caprifoliaceae					
		Diervilla lonicera Mill.	Yellow to orange	(+)A, (+) C*	E. North America	Schoen 1977
		Lonicera hildebrandiana Collett & Hemsl.	White to yellow-orange	(+)A, (+) C	Burma	Weiss 1995
		*Lonicera japonica T*hunb.	White to yellow	(+)A, (+) C	Japan	Weiss 1995
		Lonicera tatarica var. *morrowii* (A. Gray) Q. E. Yang, Landrein, Borosova & J. Osborne	White to yellow	(+)A, (+) C	Japan	Niering & Olmstead 1979
		Lonicera periclymenum L.	White to yellow	(+)A, (+) C	Europe and Medit.	Weiss 1995
		Lonicera tatarica L.	White to yellow	(+)A, (+) C	Europe	Niering & Olmstead 1979
		Patrinia villosa Juss.	Yellow to white	(+)A, (-) C	Old World	Weiss 1995
		Weigela decora (Nakai) Nakai	Pale yellow to pink	(+)A, (+) C	Japan	Weiss 1995
Ericales						
	Ericaceae					
		Brachyloma preissii Sond.	White to red	(+) A	Australia	Erickson *et al*. 1973
	Polemoniaceae					
		Cobaea scandens Cav.	Whitish to purple	(+) A	Tropical America	Proctor & Proctor 1978
Fabales						
	Fabaceae					
		Argyrolobium fischeri Taub.	Bright yellow to red	(+) A	E. Africa	Blundell 1987
		Bauhinia bidentata Jack	Yellow to red	(+)A, (+) C	Thailand	Larsen *et al*. 1984
		Cadia purpúrea (G.Piccioli) Aiton	White to dark pink	(+) A	Saudi Arabia	Collenette 1985

Table 1.1. *(Continued)*

Taxon[1]			Color change[2]	Pigment involved[3]	Native habitat[4]	Reference
Order	Family	Species				
	Fabaceae					
		Castanospermum australe A.Cunn & C.Fraser ex Hook	Yellow to red	(+) A	Australia	Macoboy 1979
		Colutea multiflora Ali	Yellow to pink-red	(+) A	Nepal	Polunin & Stainton 1984
		Dichrostachys cinerea (L.) Wight & Arn.	Pink to white	(-) A	S. Africa	Van & Malan 1988
		Intsia bijuga (Colebr.) Kuntze	White to pink	(+)A, (+) C	Seychelles	Friedmann 1986
		Lotononis eriantha Benth.	Yellow to orange-red	(+) A, (+) C	South Africa	Van & Malan 1988
		Lotononis laxa Eckl. & Zeyh	Yellow to orange	(+) C	South Africa	Van & Malan 1988
		Lotus corniculatus L.	Yellow to deep orange	(+) A, (+) C	Europe, Asia	Jones & Cruzan 1982
		Syrmatium tomentosum (Hook. & Arn.) Vogel	Yellow to red-orange	(+) A, (+) C	California	Weiss 1995
		*Syrmatium glabrum*Vogel	Yellow to deep orange	(+) C	California	Weiss 1995
		Lotus pedunculatus	Yellow to red	(+) A	California	Weiss 1995
		Mimosa rubicaulis Lam.	Pink to white	(-) A	Himalayas	Polunin & Stainton 1984
		Pearsonia sessilifolia (Harv.) Dummer	Yellow to red	(+) A	South Africa	Van & Malan 1988
		Psoralea esculenta Pursh	Lavender to pale yellow	(-) C	South Africa	Freeman & Schofield 1991
		Saraca declinata Miq.	Pale yellow to red	(+)A, (+) C	Thailand	Larsen *et al*. 1984
		Saraca indica L.	Pale orange to red	(+)A, (+) C	India, Malaysia	Macaboy 1982
		Saraca thaipingensis Prain	Yellow to deep orange-red	(+)A, (+) C	Malaysia	Polunin 1987
		Trifolium stellatum L.	White to deep pink	(+) A	Europe	Weiss 1995
	Polygalaceae					
		Polygala cruciata L.	White to pink		SE. United States	Duncan & Foote 1975
		Polygala curtissii A. Gray	White and yellow to pink		SE. United States	Duncan & Foote 1975
Gentianales						
	Rubiaceae					
		Canthium lucidum R.Br.	White to yellow	(+) C	Australia	Brock 1988
		Glionnetia sericea (Baker) Tirveng.	White to dark red	(+) A	Seychelles	Friedmann 1986
		Hamelia patens Jacq.	Orange to red	(+) A	Costa Rica	Lackie *et al*. 1986
		Ixora javanica (Blume) DC.	Yellow-orange to red	(+) A	SE. Asia	Polunin 1987

Table 1.1. *(Continued)*

Taxon[1]			Color change[2]	Pigment involved[3]	Native habitat[4]	Reference
Order	Family	Species				
	Apocynaceae					
		Glossonema revoilii Franch.	White to yellow-bronze	(+) C, pH	E. Africa	Blundell 1987
		Oxypetalum coeruleum (D. Don ex Sweet) Decne.	Pale blue to pink	(+) C, pH	Brazil, Uruguay	Weiss 1995
Lamiales						
	Acanthaceae					
		Asystasia gangetica (L.) T.Anderson	Pale yellow to lavender	(+)A	India	Gracie 1993
		Avicennia marina (Forssk.) Vierh.	Yellow to orange	(+)A, (-) C*	Australia	Brock 1988
		Crossandra johanninae Fiori	White to lavender	(+)A	Saudi Arabia	Collenette 1985
	Bignoniaceae					
		Mansoa hymenaea (DC.) A.H.Gentry	Purple to white	(-) A	Central America	Barrows 1977
	Boraginaceae					
		Arnebia euchroma (Royle) I.M.Johnst.	Pink to deep purple	(+) A, pH	Himalayas	Weiss 1995
		Cryptantha flava (A.Nelson) Payson	White to yellow	(+) C	SW. United States	Welsh & Ratcliffe 1986
		Heliotropium arbainense Fresen.	Pale cream to deep yellow	(+) C	Saudi Arabia	Collenette 1985
		Pulmonaria officinalis L.	Red to blue	pH	Europe	Müller 1883
	Scrophulariaceae					
		Buddleja marrubiifolia Benth.	Yellow to red	(+) A	Chihuahuan desert	Weiss 1995
	Plantaginaceae					
		Hebe townsonii Cheeseman	Purple to white	(-) A	New Zealand	Weiss 1995
	Verbenaceae					
		Lantana camara L.	Yellow to red	(+)A, (-) C*	W. Indies	Mathur & Mohan Ram 1978
		Lantana viburnoides (Forssk.) Vahl	Yellow to deep pink	(+)A, (-) C*	Saudi Arabia	Collenette 1985
Liliales						
	Colchicaceae					
		*Sandersonia aurantiaca*Hook.	Pale yellow to deep yellow	(+) C*	S. Africa	Nilsen *et al* 2003
	Liliaceae					
		Lilium brownii F.E.Br. ex Miellez	Yellow to white	(-) C*	China	Hai *et al* 2012

Table 1.1. *(Continued)*

Taxon[1]			Color change[2]	Pigment involved[3]	Native habitat[4]	Reference
Order	Family	Species				
	Melanthiaceae					
		Trillium ovatum Pursh	White to deep pink	(+) A	W. United States	Weiss 1995
		Zigadenus glaberrimus Michx.	White to pale yellow	(+) C	Mississippi	Timme 1989
Malphighialies						
	Malpighiaceae					
		Byrsonima crassifolia (L.) Kunth	Yellow to orange	(+) A	Costa Rica	Weiss 1995
		Byrsonima microphylla A.Juss.	Yellow to red	(+) A	Brazil	Costa *et al*. 2006
		Byrsonima gardnerana A.Juss.	Yellow to red	(+) A	Brazil	Costa *et al*. 2006
		Heteropterys alternifolia W.R. Anderson	Yellow to red	(+) A	Brazil	Costa *et al*. 2006
		Tetrapterys phlomoides (Spreng.) Nied.	Yellow to orange	(+) A	Brazil	Weiss 1995
	Passifloraceae					
		Passiflora sp.	White to yellow	(+) C	New Zealand	Weiss 1995
	Rhizophoraceae					
		Ceriops tagal (Perr.) C.B.Rob.	White to orange	(+) A	N. Australia	Brock 1988
	Violaceae					
		*Viola cornuta*L.	White to purple	(+)A*		Farzad et al. 2002
Malvales						
	Malvaceae					
		Brachychiton discolor F.Muell.	White to purple	(+) A	Australia	Macaboy 1982
		Gossypium barbadense L.	Cream to pink	(+) A*		Tan *et al*. 2013
		Gossypium hirsutum L.	Cream to pink	(+) A*		Weiss 1995; Tan *et al*. 2013
		Hibiscus mutabilis L.	Yellow to orange-red	(+) A *	China	Chin 1977; Shanker & Vankar 2007
		Hibiscus tilliaceous L.	Yellow to orange-red	(+) A	Pantropical	Weiss 1995
		Lasiopetalum behrii	Pale yellow to pink	(+) A	Australia	Costermans 1981
		Malvaviscus arboreus Cav.	Red to pink	(-) A*	America	Gottsberger 1971

Table 1.1. *(Continued)*

Taxon[1]			Color change[2]	Pigment involved[3]	Native habitat[4]	Reference
Order	Family	Species				
	Malvaceae					
		Thespesia populnea (L.) Sol. ex Corrêa	Yellow to purple	(+) A*	Pantropical	Mabberley 1987; Lowry 1976
	Thymelaeaceae					
		Edgeworthia tomentosa (Thunb.) Nakai	Yellow to white	(-) A, (-) C	China	Macoboy 1984
		Pimelea ferruginea Labill.	Pink to white	(-) A, (-) C	W. Australia	Weiss 1995
Myrtales						
	Combretaceae					
		Combretum farinosum Kunth	Green to orange	(+) A	S. and C. America	Schemske 1980
		Combretum indicum (L.) DeFilipps	White to deep red	(+) A	Burma	Weiss 1995
	Melastomataceae					
		Tibouchina lepidota (Bonpl.) Baill.	Magenta to purple	(+) A*	Ecuador	Weiss 1995; Hendra & Keller, 2016
		Tibouchina pulchra (Cham.) Cogn.	White to dark pink	(+) A	Brazil	Brito *et al.* 2015
		Tibouchina sellowiana (Cham.) Cong.	White to red	(+) A	Brazil	Ludwing 1886
	Myrtaceae					
		Chamelaucium megalopetalum F.Muell. ex Benth.	White to red	(+) A	Australia	Erickson *et al*. 1973
		Darwinia citriodora (Endl.) Benth.	Yellow to red	(+) A	Australia	Lamont 1985
		Darwinia fascicularis Rudge	White to red	(+) A	Australia	Lamont 1985
		Hypocalymma angustifolium (Endl.) Schauer	White to deep pink	(+) A	Australia	Lamont 1985
		Myrtella sp.	White to pink	(+) A	Australia	Brock 1988
		Verticordia acerosa Lindl.	Yellow to orange-red	(+) A	Australia	Lamont 1985
		Verticordia chrysantha Endl.	Yellow to red	(+) A	Australia	Lamont 1985
		Verticordia grandiflora Endl.	Yellow to orange	(+) A	Australia	Erickson *et al*. 1973
		Verticordia huegelii Endl.	White to red	(+) A	Australia	Lamont 1985
	Onagraceae					
		Fuchsia excorticata (G.Forst.) L.f.	Green and black to deep red	(+) A*	New Zealand	Delph & Lively 1989; Webby & Bloor 2000

Table 1.1. *(Continued)*

Taxon[1]			Color change[2]	Pigment involved[3]	Native habitat[4]	Reference
Order	Family	Species				
	Onagraceae					
		Gaura coccinea Nutt. ex Pursh	White to maroon	(+) A	SW. United States	Welsh & Ratcliffe 1986
		Hauya sp.	White to deep pink	(+) A*	C. America	Averett & Raven 1984; Weiss 1995
		Oenothera epilobiifolia Kunth	Green to orange-red	(+) A	Venezuela	Weiss 1995
	Vochysiaceae					
		Qualea multiflora Mart.	White to pale yellow	(+) C	Brazil	Weiss 1995
Nymphaeales						
	Nymphaeaceae					
		Victoria amazonica (Poepp.) J.C. Sowerby	White to pale purple	(+) A	S. America	Weiss 1995
Oxialidales						
	Elaeocarpaceae					
		Aristotelia fruticosa Hook.f.	White to red	(+) A	New Zealand	Salmon 1968
		Aristotelia serrata (J.R.Forst. & G.Forst.) Oliv.	White to red	(+) A	New Zealand	Weiss 1995
Poales						
	Bromeliaceae					
		Aechmea sp.	Pink to blue	pH	Tropical America	Weiss 1995
Proteales						
	Proteaceae					
		Banksia ilicifolia R.Br.	Yellow to red	(+) A	Australia	Lamont & Collins 1988
		Leucospermum oleaefolium R. Br.	Yellow to orange-red	(+) A	S. Africa	Van Der Spuy 1971
Rosales						
	Rhamnaceae					
		Cryptandra amara Sm.	White to red	(+) A	Australia	Williams 1979
	Rosaceae					
		Rosa chinensis f. *mutabilis* (Correvon) Rehder	Yellow to deep pink	(+) A*	China	Weiss 1995; Cai *et al.* 2005

Table 1.1. *(Continued)*

Taxon[1]			Color change[2]	Pigment involved[3]	Native habitat[4]	Reference
Order	Family	Species				
Santalales						
	Loranthaceae					
		Phragmanthera dshallensis (Engl.) M.G.Gilbert	Yellow to red	(+) A	E. Africa	Gill & Wolf 1975
		Phragmanthera regularis (Steud. ex Sprague) M.G. Gilbert	Yellow to red	(+) A	E. Africa	Blundell 1987
	Santalaceae					
		Santalum freycinetianum F. Phil.	Greenish-yellow to red	(+) A*	Hawaii	Sohmer & Gustafson 1987
		Santalum haleakalae Hillebr.	White to red	(+) A	Hawaii	Sohmer & Gustafson 1987
		Santalum album L.	White to red	(+) A	Australia	Erickson *et al.* 1973; Harsha *et al.* 2013
	Schoepfiaceae					
		Quinchamalium chilense Molina	Yellow to orange	(+) A*	Andes	Riveros *et al.* 1987; Simirgiotis *et al.* 2012
Sapindales						
	Anacardiaceae					
		Anacardium occidentale L.	White to pink	(+) A	Tropical America	Weiss 1995
	Rutaceae					
		Boronia molloyae J.R.Drumm.	Magenta to deep red	(+) A	Old World	Weiss 1995
		Boronia polygalifolia Sm.	Pale yellow to pinkish	(+) A	Australia	Williams 1979.
Saxifragales						
	Paeoniaceae					
		Paeonia ostii T.Hong & J.X.Zhang	White to pink	(+) A*		Li *et al.* 2011
	Saxifragaceae					
		Tellima grandiflora (Pursh) Douglas ex Lindl.	White to red	(+) A	W. United States	Weiss 1995
Solanales						
	Solanaceae					
		Brugmansia versicolor Lagerh.	Cream to pink	(+) A	South America	Weiss 1995
		Brunfelsia calycina Benth.	Purple to white	(-) A*	Tropical America	Weiss 1995

Table 1.1. *(Continued)*

Taxon[1]			Color change[2]	Pigment involved[3]	Native habitat[4]	Reference
Order	Family	Species				
	Solanaceae					
		Solanum diploconos (Mart.) Bohs	Violet to yellow-ochre	(-) A, (+) C	Tropical America	Sazima *et al*. 1993
		Solanum endopogon (Bitter) Bohs	Lavender to greenish-white	(-) A	Tropical America	Gracie 1993
		Solanum sciadostylis (Sendtn.) Bohs	Violet to yellow-ochre	(-) A, (+) C	Tropical America	Sazima *et al*. 1993
		Nicotiana mutabilis Stehmann & Semir	White to pink	(+) A*	Australia	Stehmann *et al*. 2002
		Solandra sp.	White to yellow	(+) C	Tropical America	Van Der Spuy 1971
		Streptosolen jamesonii (Benth.) Miers	Yellow to deep orange	(+) C	Peru	Weiss 1995

[1] Taxa for which the mechanism of color change was reported

[2] Color change described for sepals, petals or both.

[3] Mechanism of flower color change, pH or pigments. (+) A: anthocyanin accumulation, (-) A: anthocyanin degradation; (+) C: carotenoid accumulation, (-) C: carotenoid degradation, (+) B: betalain accumulation, (-) B: betalain degradation, N.: North, S.: South, E: East, W: West, SE.: Southeast, SW.: Southwest., Medt.: Mediterranean. * Asterisks indicates that the pigment was experimentally addressed, in other cases, the mechanism was inferred by Weiss, 1995.

[4] N.: North, S.: South, E: East, W: West, SE.: Southeast, SW.: Southwest., Medt.: Mediterranean.

2. OBJECTIVES

The overall aim of this thesis was to explore the phenomenon of flower color change in *Tibouchina pulchra* by the chemical characterization of flower extracts and the study of the regulatory mechanisms involved in this temporal phenotypic change. Results were organized in the following to chapters:

Chapter 2: Chemical characterization of *Tibouchina Pulchra* (Cham.) Cogn. flowers.

Chapter two describes the chemical characterization of petal pigments by isolation procedures and spectroscopic analysis (UV-Vis absorption spectra, mass spectra and nuclear magnetic resonance).

Chapter 3: The Regulation of color change in *Tibouchina pulchra* flowers.

In this chapter, the goal was to investigate whether the color change is determined either by the differential accumulation of flavonoid derivatives and/or metals along the different stages of floral development. In order to investigate the putative transcriptional regulation of the biosynthetic enzyme encoding genes, key genes of the flavonoid biosynthesis were cloned and the transcript accumulation patterns profiled along floral development.

3. REFERENCES

AEFP-Agenda estratégica de Flores e Plantas Ornamentais. Ministério da Agricultura, Pecuária e Abastecimento Secretaria Executiva, Brasília. 2011.

Albert, N.W., Lewis, D.H., Zhang, H., Schwinn, K.E., Jameson, P.E. & Davies K.M. Members of an R2R3-MYB transcription factor family in *Petunia* are developmentally and environmentally regulated to control complex floral and vegetative pigmentation patterning. The Plant Journal. 2011, 65: 771–784.

An, T.Q. The mystery of flower color. Beijing: China Forestry Publishing House. 1989.

Andersen, O.M., & Markham, K.R. Flavonoids: chemistry, biochemistry and applications. CRC press. 2005.

APG IV - The Angiosperm Phylogeny Group. An update of the Angiosperm Phylogeny Group classification for the orders and families of flowering plants: APG IV. Botanical Journal of the Linnean Society. 2016, 181: 1-20.

Averett, J.E., & Raven, P.H. Flavonoids of Onagraceae. Annals of the Missouri Botanical Garden, 1984: 30-34. DOI: 10.2307/2399055.

Bailey, L.H. Manual of cultivated plants. Revised Edition. The MacMillan Company. New York, NY. 1949.

Bar-Akiva, A.; Ovadia, R.; Rogachev, I.; Bar-Or, C.; Bar, E.; Freiman, Z.; Nissim-Levi, A.; Gollop, N.; Lewinsohn, E.; Aharoni, A.; Weiss, D.; Koltai, H. & Oren-Shamir, M. Metabolic networking in *Brunfelsia calycina* petals after flower opening. Journal of Experimental Botany. 2010, 61 (5): 1393–1403. DOI: org/10.1093/jxb/erq008

Barrows, E.M. Floral maturation and insect visitors of *Pachyptera hymenaea* (Bignoniaceae). Biotropica. 1977, 9: 133-134 p.

Bartley, G.E. & Scolnik, P.A. Plant carotenoids: pigments for photoprotection, attraction, and human health. Plant Cell. 1995; 7: 1027–1038. DOI: 10.2307/3870055

Blundell, M. Collins guide to the wild flowers of East Africa. Collins and Gafton. London. 1987.

Bramwell D. & Bramwell, Z.I. Wild Flowers of the Canary Islands. Cabildo Insular de Tenerife, Santa Cruz de Tenerife, Spain. 1974, p. 190

Brandi, F.; Bar, E.; Mourgues, F.; Horváth, G.; Turcsi, E.; Giuliano, G.; Liverani, A.; Tartarini, S.; Lewinsohn, E. & Rosati, C. Study of 'Redhaven' peach and its white-fleshed mutant suggests a key role of CCD4 carotenoid dioxygenase in carotenoid and norisoprenoid volatile metabolism. BMC Plant Biology, 2011, 11(1), 24.

Brito, V.L.; Weynans, K.; Sazima, M. & Lunau, K. Trees as huge flowers and flowers as oversized floral guides: the role of floral color change and retention of old flowers in *Tibouchina pulchra*. Frontiers in plant science. 2015, 6: 1-6.

Brock, J. Top End native plants. John Brock, Darwin. Australia. 1988

Brockington, S.F.; Walker, R.H.; Glover, B.J.; Soltis, P.S. & Soltis, D.E. Complex pigment evolution in the Caryophyllales. New Phytologist. 2011; 190: 854–864.

Broun P. Transcriptional control of flavonoid biosynthesis: a complex network of conserved regulators involved in multiple aspects of differentiation in Arabidopsis. Current Opinion in Plant Biology. 2005, 8: 272–279.

Buchanan, B.B.; Gruissem, W. & Jones, R.L. Biochemistry and molecular biology of plants. John Wiley & Sons. 2ªedition, 1283p. 2015.

Buchweitz, M., Gudi, G., Carle, R., Kammerer, D. R., & Schulz, H. Systematic investigations of anthocyanin–metal interactions by Raman spectroscopy. Journal of Raman Spectroscopy. 2012, 43(12): 2001-2007. DOI: 10.1002/jrs.4123.

Burg, S.D. & Dijkman, M.J. Ethylene and auxin participation in pollen induced fading of Vanda orchid blossoms. Plant Physiology. 1967, 42(11): 1648-1650 p. DOI: 10.1104/pp.42.11.1648

Cai, Y.Z., Xing, J., Sun, M., Zhan, Z.Q., & Corke, H. Phenolic antioxidants (hydrolyzable tannins, flavonols, and anthocyanins) identified by LC-ESI-MS and MALDI-QIT-TOF MS from *Rosa chinensis* flowers. Journal of agricultural and food chemistry. 2005, 53(26): 9940-9948. DOI: 10.1021/jf052137k.

Campbell, R., Ducreux, L.J., Morris, W.L., Morris, J.A., Suttle, J.C., Ramsay, G., Bryan, G.J.; Hedley, P.E. & Taylor, M.A. The metabolic and developmental roles of carotenoid cleavage dioxygenase4 from potato. Plant Physiology. 2010, 154(2): 656-664. DOI: 10.1104/pp.110.158733

Castañeda-Ovando, A., Pacheco-Hernández, M.D.L., Páez-Hernández, M.E., Rodríguez, J.A., & Galán-Vidal, C.A. Chemical studies of anthocyanins: A review. Food Chemistry. 2009, 113(4): 859–871. DOI: 10.1016/j.foodchem.2008.09.001

Chalker-Scott, L. Environmental significance of anthocyanins in plant stress responses. Photochemistry and photobiology. 1999; 70: 1–9.

Chappell, J., Wolf, F., Proulx, J., Cuellar, R. & Saunders, C. Is the reaction catalyzed by 3-hydroxy-3-methylglutaryl coenzyme A reductase a rate-limiting step for isoprenoid biosynthesis in plants? Plant Physiol. 1995; 109: 1337–1343.

Chaudhary B. & Mukhopadhyay K. Induction of anthocyanin pigment in callus cultures of *Solanum melongena* L. in response to plant growth regulators and light. IOSR Journal of Pharmacy. 2012; 2:76–80.

Chin, H.F. Malaysian flowers in color. Tropical Press Sdn.Bhd. Kuala Lumpur, Malaysia. 1977, ISBN 967-73-0018-0.

Chung, H.H., Schwinn, K.E., Ngo, H.M., Lewis, D.H., Massey, B., Calcott, K. E., Joyce D.C.; Gould, KS., Davies, K.M. & Harrison, D.K. Characterization of betalain biosynthesis in Parakeelya flowers identifies the key biosynthetic gene DOD as belonging to an expanded LigB gene family that is conserved in betalain-producing species. Frontiers in Plant Science. 2015, 6: 499. DOI: 10.3389/fpls.2015.00499.

Collenette, S. An Illustrated Guide to the Flowers of Saudi Arabia. Flora Publication 1. Meteorological and Environmental Protection Administration, Jeddah, K. S. A.; Scorpion Publishing Ltd. London. 1985, 514 p.

Cooper-Driver, G.A. Contributions of Jeffrey Harborne and co-workers to the study of anthocyanins. Phytochemistry. 2001, 56(3): 229-236.

Costa, N.; Costa, C.B. & Ramalho, M. Biologia reprodutiva de espécies simpátricas de Malpighiaceae em dunas costeiras da Bahia, Brasil. Revista Brasileira de Botânica. São Paulo. 2006, 29 (1): 103-114, p. DOI: 10.1590/S0100-84042006000100010

Costermans, L.F. Native trees and shrubs of south-eastern Australia. Libraries Australia. Adelaide: Rigby. 1981, ISBN: 072701403X

Davies, K.M., Albert, N.W. & Schwinn, K.E. From landing lights to mimicry: The molecular regulation of flower colouration and mechanisms for pigmentation patterning. Functional and Plant Biology. 2012, 39:619-38. DOI: 10.1071/FP12195.

Delph, L.F. & Lively, C.M. The evolution of floral color change: pollinator attraction versus physiological constraints in *Fuchsia excorticata*. Evolution. 1989, 43(6): 1252-1 262. DOI: 10.1111/j.1558-5646.1989.tb02572.x

Dewick, P.M. Medicinal Natural Products – A biosynthetic approach. Third edition. John Wiley and Sons. West Sussex. UK. 2009, 546 p.

Dhar, M.K., Sharma, R., Koul, A., & Kaul, S. Development of fruit color in Solanaceae: a story of two biosynthetic pathways. Briefings in functional genomics. 2014, 14(3): 199-212.

Domonkos, I., Kis, M., Gombos, Z., & Ughy, B. Carotenoids, versatile components of oxygenic photosynthesis. Progress in lipid research. 2013, 52(4): 539-561.

Dudavera, N., Negre, F., Nagegowda, D.A. & Orlova, I. Plant Volaties: Recent Advances and Future Perspectives. Critical Reviews in Plant Science, 25:417-440.

Duncan, W.H., & Foote, L.E. Wildflowers of the Southeastern United States. Athens: University of Georgia Press. 1975, 296 p.

Eisenreich, W., Rohdich, F. & Bacher, A. Deoxyxylulose phosphate pathway to terpenoids. Trends in Plant Science. 2001, 6:78–84.

Erickson, R.A.S; George, N.; Marchant, G. & Morcombe, M.K. Flowers and plants of western Australia. Reed Books, Chatswood, NSW. Sydney. 1973.

Farzad, M., Griesbach, R. & Weiss, M.R. Floral color change in *Viola cornuta* L. (Violaceae): a model system to study regulation of anthocyanin production. Plant Science. 2002, 162: 225–231.

Farzad, M., Griesbach, R., Hammond, J., Weiss, M.R., & Elmendorf, H.G. Differential expression of three key anthocyanin biosynthetic genes in a color-changing flower, *Viola cornuta* cv. Yesterday, Today and Tomorrow. Plant Science. 2003, 165(6): 1333–1342. DOI: 10.1016 DOI:/j.plantsci.2003.08.001

Feild, T.S., Lee, D.W. & Holbrook, N.M. Why leaves turn red in autumn. the role of anthocyanins in senescing leaves of red-osier dog- wood. Plant Physiology. 2001, 127: 566–574. DOI: 10.1104/pp.010063.

Fenster, C.B.; Armbruster, W.S.; Wilson, P.; Dudash, M.R. & James, D. Pollination syndromes and floral specialization. Annual Review of Ecology, Evolution, and Systematics. 2004, 35: 375–403. DOI: 10.1146/annurev.ecolsys.34.011802.132347.

Fernández-López, J.A.; Angosto, J.M.; Giménez, P.J. & León, G. Thermal stability of selected natural red extracts used as food colorants. Plant Foods for Human Nutrition. 2013, 68,11–17. DOI: 10.1007/s11130-013-0337-1.

Finkelstein, R. Abscisic acid synthesis and response. The Arabidopsis Book. Abscisic acid synthesis and response. 2013, 11: e0166. DOI: 10.1199/tab.0166.

Ford, N.A., & Erdman Jr, J.W. Are lycopene metabolites metabolically active. Acta Biochimica Polonica. 2012, 59(1): 1-4.

Forkmann, G. Flavonoids as flower pigments: the formation of the natural spectrum and its extension by genetic engineering. Plant Breeding. 1991, 106: 1-26. DOI: 10.1111/j.1439-0523.1991.tb00474.x

Fraser, P.D. & Bramley, P.M. The biosynthesis and nutritional uses of carotenoids. Progress in Lipid Research, 2004, 43: 228–26. DOI 10.1016/j.plipres.2003.10.002

Freeman, C.C., & Schofield, E.K. Roadside wildflowers of the southern Great Plains. University Press of Kansas. Lawrence, KS. 1991, 280 p.

Freire-Maia, N. Gregor Mendel: Vida e Obra. T. A. Queiroz, São Paulo. 1995, 97 p.

Friedmann, F. Fleurs et arbres des Seychelles. Office de la Recherche Scientifique et Technique Outre-Mer, Paris. 1986.

Gao, L., Yang, H., Liu, H., Yang, J., & Hu, Y. Extensive Transcriptome Changes Underlying the Flower Color Intensity Variation in *Paeonia ostia*. Frontiers in Plant Science. 2016, 6: 1–16. DOI: 10.3389/fpls.2015.01205

Gill, F.B., & Wolf, L.L. Foraging strategies and energetics of east African sunbirds at mistletoe flowers. American Naturalist. 1975, 109: 491-510. DOI: 10.1086/283022

Gonçalves, L.C.P., Trassi, M.A.D.S., Lopes, N.B., Dorr, F.A., Dos Santos, M.T., Baader, W.J., Oliveira, V.X. & Bastos, E.L. A comparative study of the purification of betanin. Food Chemistry. 2012, 131: 231–238. DOI: 10.1016/j.foodchem.2011.08.067.

Gottsberger, G. Colour change of petals in Malvaviscus arboreus flowers. Acta Botanica Neerlandica. 1971, 20: 38 1-388. DOI: 10.1111/j.1438-8677.1971.tb00723.x

Gould, K., Davies, K. M. & Winefield, C. Anthocyanins: Biosynthesis, Functions, and Applications. Springer New York. 2008, 356 p.

Gracie, C. Pollination of *Cyphomandra endopogon* var *endopogon* (Solanaceae) by *Eufriesea* spp. (Euglossini) in French Guiana. Brittonia. 1993, 45:39-46. DOI: 10.2307/2806859

Grotewold, E. Flavonols drive plant microevolution. Nature Genetics. 2016, 48(2): 112–113. DOI: 10.1038/ng.3490.

Grotewold, E. The genetics and biochemistry of floral pigments. Annual Review of Plant Biology. 2006, 57: 761–80. DOI: 10.1146/annurev.arplant.57.032905.105248

Hatlestad, G.J., Akhavan, N.A., Sunnadeniya, R.M., Elam, L., Cargile, S., Hembd, A., Gonzalez, A., McGrath, J.M. & Lloyd, A. M. The beet Y locus encodes an anthocyanin MYB-like protein that activates the betalain red pigment pathway. Nature Genetics. 2014, 47(1): 92–96. DOI: 10.1038/ng.3163.

Harsha, P.S., Khan, M.I., Prabhakar, P., & Giridhar, P. Cyanidin-3-glucoside, nutritionally important constituents and in vitro antioxidant activities of *Santalum album* L. berries. Food research international. 2013, 50 (1): 275-281. DOI: 10.1016/j.foodres.2012.10.024.

Hichri, I., Barrieu, F., Bogs, J., Kappel, C., Delrot, S. & Lauvergeat, V. Recent advances in the transcriptional regulation of the flavonoid biosynthetic pathway. Journal of Experimental Botany. 2011, 62(8): 2465–2483. DOI: 10.1093/jxb/erq442.

Hirschberg, J., Cohen, M., Harker, M., Lotan, T., Mann, V. & Pecker, I. Molecular genetics of the carotenoid biosynthesis pathway in plants and algae. Pure and Applied Chemistry. 1997; 69: 2152–8. DOI: 10.1351/pac199769102151.

Holton, T.A. & Cornish E.C. Genetics and Biochemistry of Anthocyanin Biosynthesis. The Plant Cell Online. 1995; 7:1071–83. DOI: 10.1105/tpc.7.7.1071.

Ibdah, M., Azulay, Y., Portnoy V., Wasserman, B., Bar, E., Meir, A., Burger, Y., Hirschberg, J., Schaffer, A. A., Katzir, N., Tadmor, Y. & Lewinsohn, E.. Functional characterization of CmCCD1, a carotenoid cleavage dioxygenase from melon. Phytochemistry. 2006, 67: 1579–1589. DOI: 10.1016/j.phytochem.2006.02.009.

Ida, T.Y. & Kudo, G. Floral color change in *Weigela middendorffiana* (Caprifoliaceae): reduction of geitonogamous pollination by bumble bees. American Journal of Botany. 2003, 90: 1751–1757. DOI: 10.3732/ajb.90.12.1751.

Ida, T.Y. & Kudo, G. Modification of bumblebee behavior by floral color change and implications for pollen transfer in *Weigela middendorffiana*. Evolutionary Ecology. 2010, 24: 671–684. DOI: 10.1007/s10682-009-9324-2.

Isler, O. Carotenoids. 1971, 850p. DOI: 10.1007/978-3-0348-5831-1

Jackson, D., Roberts, K. & Martin, C. Temporal and spatial control of expression of anthocyanin biosynthetic genes in developing flowers of *Antirrhinum majus*. The Plant Journal. 1992, 2: 425–434. DOI: 10.1111/j.1365-313X.1992.00425.x.

Jahns, P. & Holzwarth, A.R. The role of the xanthophyll cycle and of lutein in photoprotection of photosystem II. Biochimica et Biophysica Acta. 2012, 1817(1):182–193. DOI: 10.1016/j.bbabio.2011.04.012.

Jeon, J.H., Joung, H. & Byun, S.M. Characterization of two members of the chalcone synthase gene family from *Solanum tuberosum* L. Plant Physiology. 1996; 111:348.

Johnson, E.J. & Krinsky, N.I. Carotenoids and coronary heart disease. Carotenoids. 2009, 287-300.

Jones, C.E., & Cruzan, M. Floral color changes in deenveed (*Lotus scoparius*): possible function. Crossosoma. 1982, 8: 1-6.

Jung, C.S., Griffiths, H.M., DeJong, D.M., Cheng, S., Bodis, M. & De Jong, W.S. The potato P locus codes for flavonoid 3′,5′-hydroxylase. Theoretical and Applied Genetics. 2005;190: 269–75. DOI: 10.1007/s00122-004-1829-z.

Katsumoto, Y., Fukuchi-Mizutani, M., Fukui, Y., Brugliera, F., Holton, T.A., Karan, M., Nakamura, N., Yonekura-Sakakibara, K., Togami, J., Pigeaire, A., Tao, G.Q., Nehra, N.S., Lu, C.Y., Dyson, B.K., Tsuda, S., Ashikari, T., Kusumi, T., Mason, J.G. & Tanaka, Y. Engineering of the rose flavonoid biosynthetic pathway successfully generated blue-hued flowers accumulating delphinidin. Plant and Cell Physiology. 2007, 48: 1589–600. DOI: 10.1093/pcp/pcm131.

Kay, K.M., & Sargent, R.D. The role of animal pollination in plant speciation: integrating ecology, geography, and genetics. Annual Review of Ecology, Evolution, and Systematics. 2009, 40: 637-656. DOI: 10.1146/annurev.ecolsys.110308.120310.

Khan, M I., & Giridhar, P. Plant betalains: Chemistry and biochemistry. Phytochemistry. 2015, 117: 267–295. DOI: 10.1016/j.phytochem.2015.06.008

Kim, S., Hwang, G., Lee, S., Zhu, J. Y., Paik, I., Nguyen, T. T., & Oh, E. High ambient temperature represses anthocyanin biosynthesis through degradation of HY5. Frontiers in plant science. 2017, 8: 1787. DOI: 10.3389/fpls.2017.01787.

Kirilovsky, D., & Kerfeld, C. A. The orange carotenoid protein: a blue-green light photoactive protein. Photochemical & Photobiological Sciences. 2013, 12(7): 1135-1143. DOI: 10.1039/c3pp25406b.

Krinsky, N.I., & Johnson, E.J. Carotenoid actions and their relation to health and disease. Molecular aspects of medicine. 2005, 26(6), 459-516. DOI: 10.1016/j.mam.2005.10.001.

Lacke, P.M., Thomas, C.D., Brisco, M.J. & Hepper, D.N. On the pollination ecology of Hamelia patens (Rubiaceae) at Monteverde, Costa Rica. Brenesia. 1986, 25-26: 203-213.

Lamont, B.B. & Collins, B.G. 1988. Flower colour change in *Banksia ilicifolia*: a signal for pollinators. Australian Journal of Ecology

Lamont, B.B. The significance of flower colour change in eight co-occurring shrub species. Botanical Journal of the Linnean Society. 1985, 90: 145-1 55.

Lao, Y.M., Xiao, L., Jiang, J.G. & Zhou, S.S. In silico analysis of phytoene synthase and its promoter reveals hints for regulation mechanisms of carotenogenesis in *Duanliella bardawil*. Bioinformatics. 2011, 27: 2201–8. DOI: 10.1093/bioinformatics/btr371.

Larsen, K., Larsen, S.S. & Vidal, J.E. Flora of Thailand, Leguminosae-Caesalpinoideae. The Forest Herbarium, Royal Forest Department, Bangkok. 1984, 4(1).

Li, J.J., Zhang, X.F. & Zhao, X.Q. Tree Peony of China. Beijing: Encyclopedia of China Publishing House. 2011: 10-11.

Li, L., & Yuan, H. Chromoplast biogenesis and carotenoid accumulation. Archives of Biochemistry and Biophysics. 2013, 539: 102–109. DOI: 10.1016/j.abb.2013.07.002.

Li, L., Paolillo, D.J., Parthasarathy, M.V., Dimuzio, E.M. & Garvin, D.F. A novel gene mutation that confers abnormal patterns of beta-carotene accumulation in cauliflower (*Brassica oleracea* var botrytis). The Plant Journal. 2001, 26: 59–67. DOI: 10.1046/j.1365-313x.2001.01008.x.

Lichtenthaler, H.K. The 1-deoxy-D-xylulose-5-phosphate pathway of isoprenoid biosynthesis in plants. Annual Review of Plant Biology. 1999, 50: 47–65. DOI: 10.1146/annurev.arplant.50.1.47

Lichtenthaler, H.K., Schwender, J., Disch, A., and Rohmer, M. (1997). Biosynthesis of isoprenoids in higher plant chloroplasts proceeds via a mevalonate-independent pathway. FEBS Lett. 400:271–274

Liu, L., Shao, Z., Zhang, M., & Wang, Q. Regulation of carotenoid metabolism in tomato. Molecular Plant. 2015a, 8(1), 28–39. DOI: 10.1016/j.molp.2014.11.006.

Liu, Z., Zhang, Y., Wang, J., Li, P., Zhao, C., Chen, Y., et al. Phytochrome-interacting factors PIF4 and PIF5 negatively regulate anthocyanin biosynthesis under red light in Arabidopsis seedlings. Plant Sci. 2015b, 238, 64–72. DOI: 10.1016/j.plantsci.2015.06.001

Llorente, B., D'Andrea, L., Ruiz-Sola, M. A., Botterweg, E., Pulido, P., Andilla, J., Loza-Alvarez, P. & Rodriguez-Concepcion, M. Tomato fruit carotenoid biosynthesis is adjusted to actual ripening progression by a light-dependent mechanism. The Plant Journal. 2016, 85: 107–119. doi: 10.1111/tpj.13094

Ludwig, F. Einige neue Falle von Farbenwechsel in verbliihenden Bliitenstanden. Biologisches Centralblatt.1886, 6: 1-3.

Lunau, K. Unidirectionality of floral colour changes. Plant Systematics and Evolution. 1996, 200: 125–140. DOI: 10.1007/BF00984753.

Mabberley, D.J. The plant-book. Cambridge University Press, Cambridge. 1987

Macaboy, S. Trees for Flower and fragrance, Lansdowne Press, Sydney.1982.

Macnish, A.J., Jiang, C.Z., Zakharov-Negre, F. & Reid, M. Physiological and molecular changes during opening and senescence of *Nicotiana mutabilis* flowers. Plant Science. 2010, 179: 267-272. DOI: 10.1016/j.plantsci.2010.05.011.

Macoboy, S. What tree is that? Tiger Books, London. 1979.

Macoboy, Stirling. Flowering shrubs. Lansdowne Press, Sydney. 1984.

Maeda, H & Dudavera, N. The Shikimate pathway and aromatic amino acid biosynthesis in plants. Annual reviews of plant biology. 2012, 63: 73-105. DOI: 10.1146/annurev-arplant-042811-105439.

Martel, C., Vrebalov, J., Tafelmeyer, P. & Giovannoni, J.J. The tomato MADS-box transcription factor RIPENING INHIBITOR interacts with promoters involved in numerous ripening processes in a COLORLESS NONRIPENING-dependent manner. Plant Physiology. 2011, 157: 1568–1579. DOI: 10.1104/pp.111.181107.

Martins, T.R., Berg, J.J., Blinka, S., Rausher, M.D. & Baum, D.A. Precise spatio-temporal regulation of the anthocyanin biosynthetic pathway leads to petal spot formation in *Clarkia gracilis* (Onagraceae). New Phytologist. 2013, 197: 958–969. DOI: 10.1111/nph.12062.

Mathur, G. & Mohanram, H. Y. Significance of petal colour in thrips-pollinated *Lantana camara* L. Annals of Botany. 1978, 42: 1473-1476.

Matusova, R., Rani, K., Verstappen, F.W.A., Franssen, M.C.R., Beale, M.H. & Bouwmeester, H.J. The strigolactone germination stimulants of the plant-parasitic Striga and *Orobanche* spp. are derived from the carotenoid pathway. Plant Physiol. 2005, 139:920–934. DOI: 10.1104/pp.105.061382.

Milborrow, B.V. & Lee, H.S. Endogenous biosynthetic precursors of (+)-abscisic acid. VI. Carotenoids and ABA are formed by the 'non-mevalonate' triose-pyruvate pathway in chloroplasts. Australian Journal of Plant Physiology. 1998, 25: 507–512. DOI: 10.1071/PP98006.

Moehs, C.P., Tian, L., Osteryoung, K.W. & Dellapenna, D. Analysis of carotenoid biosynthetic gene expression during marigold petal development. Plant Molecular Biology. 2001, 45: 281–293. DOI: 10.1023/A:1006417009203.

Mol, J., Grotewold, E., & Koes, R. How genes paint flowers and seeds. Trends in Plant Science. 1998, 3(6): 212-217. DOI: 10.1007/978-94-011-4661-6_134.

Molina, G.A., Hernández-Martínez, A.R., Cortez- Valadez, M., García-Hernández, F. & Estevez, M. Effects of tetraethyl orthosilicate (TEOS) on the light and temperature stability of a pigment from Beta vulgaris and its potential food industry applications. Molecules. 2014, 19: 17985–18002. DOI: 10.3390/molecules191117985.

Müller, H. The effect of the change of colour in the flowers of *Pulmonaria oficinalis* upon its pollinators. Nature. 1883, 28: 8 1.

Napoli, C., Lemieux, C. & Jorgensen, R. lntroduction of a Chimeric Chalcone Synthase Gene into Petunia Results in Reversible Co-Suppression of Homologous Genes Ín trans, 1990, 2: 279–289. DOI: 10.1105/tpc.2.4.279.

Neill, S.O., Gould, K.S., Kilmartin, P.A., Mitchell, K.A. & Markham, K.R. Antioxidant activities of red versus green leaves in *Elatostema rugosum*. Plant, Cell and Environment. 2002, 25: 539–547. DOI: 10.1046/j.1365-3040.2002.00837.x.

Nielsen, K. M., Lewis, D.H., & Morgan, E.R. Characterization of carotenoid pigments and their biosynthesis in two yellow flowered lines of *Sandersonia aurantiaca* (Hook). Euphytica, 2003, 130(1): 25-34. DOI: 10.1023/A:1022328828688.

Nielsen, K.M., Lewis, D.H., & Morgan, E.R. Characterization of carotenoid pigments and their biosynthesis in two yellow flowered lines of *Sandersonia aurantiaca* (Hook). Euphytica. 2003, 130(1), 25-34 p. DOI: 10.1023/A:1022328828688.

Niering, W.A. & Olmstead, N.C. The Audubon society field guide to North American wildflowers-eastern. Alfred A. Knopf, New York, NY. 1979.

Niesenbaum, R.A. The effects of pollen load size and donor diversity on pollen performance, selective abortion, and progeny vigor in *Mirabilis jalapa* (Nyctaginaceae). American Journal of Botany, 86(2): 261-268.

Nisar, N., Li, L., Lu, S., Khin, N.C. & Pogson, B.J. Carotenoid metabolism in plants. Molecular Plant, 2015, 8(1), 68–82. DOI: 10.1016/j.molp.2014.12.007.

Niyogi, K.K., Shih, C., Chow, W.S., Pogson, B.J., DellaPenna, D. & Björkman, O. Photoprotection in a zeaxanthin- and lutein-deficient double mutant of *Arabidopsis*. Photosynthesis Research. 2001, 67:139–45. DOI: 10.1023/A:101066110.

Noda, Y., Kneyuki, T., Igarashi, K., Morri, A. & Packer, L. Antioxidant activity of nasunin, an anthocyanin in eggplant peels. Toxicology 2000, 148: 119–23. DOI: 10.1016/S0300-483X(00)00202-X.

Oberbaueri, S.F. & Starr, G. The role of anthocyanins for photo- synthesis of Alaskan arctic evergreens during snowmelt. Advances in Botanical Research. 2002, 37: 129–145. DOI: 10.1016/S0065-2296(02)37047-2.

Oberrath, R., & Böhning-Gaese, K. Floral color change and the attraction of insect pollinators in lungwort (*Pulmonaria collina*). Oecologia, 1999, 121(3): 383-391. DOI: 10.1007/s004420050943.

Ohmiya A. Diversity of carotenoid composition in flower petals. Japan International Research Center for Agricultural Sciences. 2011, 45: 163–171. DOI: 10.6090/jarq.45.163.

Ohmiya, A., Kishimoto, S., Aida, R., Yoshioka, S. & Sumitomo, K. Carotenoid cleavage dioxygenase (CmCCD4a) contributes to white color formation in chrysanthemum petals. Plant Physiology. 2006, 142(3): 1193-1201.

Otálora, M.C., Carriazo, J.G., Iturriaga, L., Osorio, C. & Nazareno, M.A. Encapsulating betalains from *Opuntia* ficus-indica fruits by ionic gelation: Pigment chemical stability during storage of beads. Food chemistry. 2016, 202: 373-382. DOI: 10.1016/j.foodchem.2016.01.115.

Papiorek, S., Junker, R.R., Alves-Dos-Santos, I., Melo, G.A., Amaral-Neto, L.P., Sazima, M., Wolowski, M., Freitas, L. & Lunau, K. Bees, birds and yellow flowers: pollinator-dependent convergent evolution of UV patterns. Plant Biology. 2016, 18: 46–55. DOI: 10.1111/plb.12322.

Polunin, I. Plants and flowers of Singapore. Times editions, Singapore. 1987.

Polunin, O. & Stainton, A. Flowers of the Himalaya. Oxford University Press, Delhi. 1984

Proctor, J. & S. Proctor. Nature's use of colour in plants and their flowers. Peter Lowe, Eurobook Ltd., London. 1978.

Qi, Y., Lou, Q., Li, H., Yue, J., Liu, Y. & Wang, Y. Anatomic al and biochemical studies of bicolored flower development in *Muscari latifolium*. Protoplasma. 2013, 250: 1273–1281. DOI: 10.1007/s00709-013-0509-8.

Quattrocchio, F., Wing, J., Van der Woude, K., Souer, E., de Vetten, N., Mol, J. & Koes, R. Molecular analysis of the anthocyanin2 gene of *Petunia* and its role in the evolution of flower color. Plant Cell. 1999,11: 1433–44. DOI: 10.1105/tpc.11.8.1433.

Ramsay, N.A. & Glover, B.J. MYB–bHLH–WD40 protein complex and the evolution of cellular diversity. Trends in Plant Science. 2005, 10: 63–70. DOI: 10.1016/j.tplants.2004.12.011.

Rezende, F.M., & Furlan, C.M. Anthocyanins and tannins in ozone-fumigated guava trees. Chemosphere, 2009, 76 (10): 1445-1450. DOI: 10.1016/j.chemosphere.2009.05.028.

Riveros, M., Arroyo, M.T. K. & Humaña, A.M. An unusual kind of distyly in *Quinchamalium chilense* (Santalaceae) on Volcan Casablanca, Southern Chile. American Journal of Botany. 1987: 313-320.

Rodriguez-Concepcion, M. & Boronat, A. Elucidation of the methylerythritol phosphate pathway for isoprenoid biosynthesis in bacteria and plastids. A metabolic milestone achieved through genomics. Plant Physiology. 2002, 130: 1079–1089. DOI: 10.1104/pp.007138.

Rodriguez-Concepcion, M. Supply of precursors for carotenoid biosynthesis in plants. Archives of Biochemistry and Biophysics. 2010, 504: 118–122. DOI: 10.1016/j.abb.2010.06.016.

Ronen, G., Cohen, M., Zamir, D. & Hirschberg, J. Regulation of carotenoid biosynthesis during tomato fruit development: ex- pression of the gene for lycopene epsilon-cyclase is down- regulated during ripening and is elevated in the mutant delta. Plant Journal. 1999, 17: 341–351.

Rubio, A., Rambla, J.L., Santaella, M., Gomez, M.D., Orzaez, D., Granell, A. & Gomez-Gomez, L. Cytosolic and plastoglobule-targeted carotenoid dioxygenases from Crocus sativus are both involved in beta-ionone release. The Journal of Biological Chemistry. 2008, 283: 24816–24825. DOI: 10.1074/jbc.M804000200.

Ruxton, G.D., & Schaefer, H.M. (2016). Floral colour change as a potential signal to pollinators. Current Opinion in Plant Biology, 32, 96–100. DOI: 10.1016/j.pbi.2016.06.021

Saito, K. & Yamazaki, M. Biochemistry and molecular biology of the late-stage of biosynthesis of anthocyanin: lessons from *Perilla frutescens* as a model plant. New Phytologist. 2002, 155: 9–23. DOI: 10.1046/j.1469-8137.2002.00440.x.

Saito, R., Fukuta, N., Ohmiya, A., Itoh, Y., Ozeki, Y., Kuchitsu, K. & Nakayama, M. Regulation of anthocyanin biosynthesis involved in the formation of marginal picotee petals in *Petunia*. Plant Science. 2006, 170: 828–834. DOI: 10.1016/j.plantsci.2005.12.003.

Sakuta, M. Diversity in plant red pigments: Anthocyanins and betacyanins. Plant Biotechnology Reports. 2014, 8(1), 37–48. DOI: 10.1007/s11816-013-0294-z.

Salmon, J. Collins guide to the alpine plants of New Zealand. Collins, Auckland. 1968

Sazima, M., Vogel, S., Cocucci, A. & Hausner, G.. The perfume flowers of Cyphomandra (Solanaceae): pollination by euglossine bees, bellows mechanism, osmophores, and volatiles. Plant Systematics and Evolution. 1993, 187: 51-88.

Schemske, D.W. Floral Ecology and Hummingbird Pollination of *Combretum farinosum* in Costa Rica. Biotropica. 1980, 12(3): 169-81.

Schoen,D.J. Floral biology of *Diervilla lonicera* (Caprifoliaceae). Bulletin of the Torrey Botanical Club. 1977, 104: 234-240.

Schwinn, K., Venail, J., Shang, Y., Mackay, S., Alm, V., Butelli, E., Oyama, R., Bailey, P., Davies, K. & Martin, C.A small family of MYB-regulatory genes controls floral pigmentation intensity and patterning in the genus *Antirrhinum*. The Plant Cell. 2006, 18: 831–851.

Shanker, R. & Vankar, P.S. Dyeing cotton, wool and silk with *Hibiscus mutabilis* (Gulzuba). Dyes and pigments. 2007, 74(2): 464-469. DOI: 10.1016/j.dyepig.2006.03.007.

Shang, Y., Venail, J., Mackay, S., Bailey, P.C., Schwinn, K.E., Jameson, P.E., Martin, C.R. & Davies K.M. The molecular basis for venation patterning of pigmentation and its effect on pollinator attraction in flowers of *Antirrhinum*. New Phytologist. 2011, 189:602-15. DOI: 10.1111/j.1469-8137.2010.03498.x.

Shimada, S., Inoue, Y.T. & Sakuta, M. Anthocyanidin synthase in non- anthocyanin-producing Caryophyllales species. The Plant Journal. 2005, 44: 950–959. DOI: 10.1111/j.1365-313X.2005.02574.x.

Shimada, S., Otsuki, H., & Sakuta, M. Transcriptional control of anthocyanin biosynthetic genes in the Caryophyllales. Journal of Experimental Botany. 2007, 58(5): 957–967. DOI: 10.1093/jxb/erl256.

Shin, D.H., Choi, M.G., Kang, C.S., Park, C.S., Choi, S.B., & Park, Y.I. Overexpressing the wheat dihydroflavonol 4-reductase gene TaDFR increases anthocyanin accumulation in an Arabidopsis dfr mutant. Genes & Genomics, 2016, 38(4), 333-340. DOI: 10.1007/s13258-015-0373-3

Shoji, K., Miki, N., Nakajima, N., Momonoi, K., Kato, C., & Yoshida, K. Perianth bottom-specific blue color development in Tulip cv. murasak- izuisho requires ferric ions. Plant Cell Physiol. 2007, 48: 243–251. DOI: 10.1093/pcp/ pcl060

Silva, V.O., Freitas, A.A., Maçanita, A.L., & Quina, F.H. Chemistry and photochemistry of natural plant pigments: the anthocyanins. Journal of Physical Organic Chemistry. 2016, 29(11), 594–599. DOI: 10.1002/poc.3534.

Simirgiotis, M.J., Silva, M., Becerra, J., & Schmeda-Hirschmann, G. Direct characterisation of phenolic antioxidants in infusions from four Mapuche medicinal plants by liquid chromatography with diode array detection (HPLC-DAD) and electrospray ionisation tandem mass spectrometry (HPLC-ESI–MS*)*. Food chemistry. 2012, 131(1): 318-327. DOI: 10.1016/j.foodchem.2011.07.118.

Slimen, I.B., Najar, T. & Abderrabba, M. Chemical and antioxidant properties of betalains. Journal of Agricultural and Food Chemistry. 2017,65(4), 675–689. DOI: 10.1021/acs.jafc.6b04208.

Sohmer, S.H. & Gustafson, R. Plants and flowers of Hawai'i. University of Hawaii Press. 1987,159 p.

Stafford, H.A. Anthocyanins and betalains: evolution of the mutually exclusive pathways. Plant Science. 1994, 101: 91–98. DOI: 10.1016/0168-9452(94)90244-5.

Stehmann, J.R., Semir, J. & Ippolito, A. *Nicotiana mutabilis* (Solanaceae), a new species from southern Brazil, Kew Bull. 57 (2002) 639–646.

Steyn, W.J., Wand, S.J.E., Holcroft, D. M. & Jacobs, G. Anthocyanins in vegetative tissues: a pryamaoposed unified function in photoprotection. New Phytologist. 2002. 155: 349–361. DOI: 10.1046/j.1469-8137.2002.00482.x.

Sun, S.G., Liao, K., Xia, J. & Guo, Y.H. Floral colour change in *Pedicularis monbeigiana* (Orobanchaceae). Plant Systematics and Evolution. 2005, 255: 77–85. DOI: 10.1007/s00606-005-0348-y.

Takahashi, K., Takamura, E. & Sakuta, M. Isolation and expression analysis of two DOPA dioxygenases in *Phytolacca americana*. Zeitschrift Fur Naturforschung - Section C Journal of Biosciences. 2009, 6*4*(7-8): 564–573. DOI: 0939 – 5075/2009/0700 – 0564.

Takos, A.M., Jaffé, F., Jacob, S.R., Bogs, J., Robinson, S.P. & Walker, A.R. Light-induced expression of a MYB gene regulates anthocyanin biosynthesis in red apples. Plant Physiology. 2006, 142: 1216–1232. DOI: 10.1104/pp.106.088104.

Tan, J., Wang, M., Tu, L., Nie, Y., Lin, Y., & Zhang, X. The Flavonoid Pathway Regulates the Petal Colors of Cotton Flower. Plos One. 2013, *8*(8). DOI: 10.1371/journal.pone.0072364.

Tanaka, Y., Brugliera, F., Kalc, G., Senior, M., Dyson, B., Nakamura, N., Katsumoto, Y. & Chandler, S. Flower color modification by engineering of the flavonoid biosynthetic pathway: practical perspectives. Bioscience, Biotechnology, and Biochemistry. 2010, 74: 1760–1769.

Tanaka, Y., Katsumoto, Y., Brugliera, F. & Mason, J. Genetic engineering in floriculture. Plant Cell, Tissue and Organ Culture. 2005, 80: 1-24. DOI: 10.1007/s11240-004-0739-8.

Tanaka, Y., Sasaki, N., & Ohmiya, A. Biosynthesis of plant pigments: anthocyanins, betalains and carotenoids. The Plant Journal: For Cell and Molecular Biology. 2008, 54(4): 733–49. DOI: 10.1111/j.1365-313X.2008.03447.x

Timme, S.L. Wildflowers of Mississippi. University Press of Mississippi, Jackson, MS. 1989.

Toledo-Ortiz, G., Huq, E. & Rodríguez-Concepción, M. Direct regulation of phytoene synthase gene expression and carotenoid biosynthesis by phytochrome-interacting factors. Proceedings of the National Academy of Sciences. 2010, 107: 11626–31. DOI: 10.1073/pnas.0914428107.

Trouillas, P., Sancho-garc, J.C., Freitas, V. De, Gierschner, J., Otyepka, M. & Dangles, O. Stabilizing and Modulating Color by Copigmentation : Insights from Theory and Experiment. 2016, 116(9): 4937-82. DOI: 10.1021/acs.chemrev.5b00507.

Uematsu, C., Katayama, H., Makino, I., Inagaki, A., Arakawa, O., & Martin, C. Peace, a MYB-like transcription factor, regulates petal pigmentation in flowering peach "Genpei" bearing variegated and fully pigmented flowers. Journal of Experimental Botany, 2014, 65(4): 1081–94. DOI: 10.1093/jxb/ert456.

Vaknin, H., Bar-Akiva, A., Ovadia, R., Nissim-Levi, A., Forer, I., Weiss, D., & Oren-Shamir, M. (2005). Active anthocyanin degradation in Brunfelsia calycina (yesterday-today- tomorrow) flowers. *Planta*, *222*(1), 19–26. https://doi.org/10.1007/s00425-005-1509-5.

Van der Niet, T., Pirie, M.D., Shuttleworth, A., Johnson, S. D., & Midgely, J.J. Do pollinator distributions underlie the evolution of three pollination ecotypes in the Cape shrub *Erica plukenetii*? Annals of Botany. 2014, 113 (2): 301-316.

Van Der Spuy. South African trees and shurbs for the garden. Hugh Keartland, Johannesberg. 1971.

Van, W.Y.K. & Malan, B. S. Field guide to the wild flowers of the Witwatersrand and Pretoria region. Struik, Cape Town. 1988.

Webby, R., & Bloor, S. Pigments in the blue pollen and bee pollen of *Fuchsia excorticata*. Zeitschrift für Naturforschung C. 2000, 55(7-8): 503-505. DOI: 10.1515/znc-2000-7-803.

Weiss, M.R. & Lamont, B. Floral color change and insect pollination: a dynamic relationship. Israel Journal of Plant Sciences. 1997, 45: 185–199. DOI: 10.1080/07929978.1997.10676683.

Weiss, M.R. Floral color change: A widespread functional convergence. American Journal of Botany. 1995, 82(2), 167–185. DOI: 10.2307/2445525.

Weiss, M.R. Floral colour changes as cues for pollinators. Nature. 1991, 35: 227-229. DOI: 10.1038/354227a0.

Welsh, S.L., & Ratcliffe, B. Flowers of the Canyon Country. Canyonlands Natural History Association, Moab, UT. 1986.

Williams, K. A.W. Native plants-Queensland. Keith A. W. Williams, North Ipswich. 1979.

Winkel-shirley, B. Flavonoid Biosynthesis. A Colorful Model for Genetics, Biochemistry, Cell Biology, and Biotechnology. Plant Physiology. 2001, 126(2): 485-493. DOI: 10.1104/pp.126.2.485.

Yan, J., Wang, G., Sui, Y., Wang, M., & Zhang, L. Pollinator responses to floral colour change, nectar, and scent promote reproductive fitness in *Quisqualis indica* (Combretaceae). Scientific Reports. 2016, 6(1): 24408. DOI: 10.1038/srep24408.

Yoshida, K., Miki, N., Momonoi, K., Kawachi, M., Katou, K., Okazaki, Y., Uozumi, N., Meshima, M. & Kondo, T. Synchrony between flower opening and petal-color change from red to blue in morning glory *Ipomoea tricolor* cv. heavenly blue. Proceedings of the Japan Academy, Ser. B. 2009, 85: 187–197. DOI: 10.2183/pjab.85.187.

Zhang, Y. W., Zhao, X. N., Huang, S. J., Zhang, L. H. & Zhao, J. M. Temporal pattern of floral color change and time retention of post-change flowers in *Weigela japonica* var. sinica (Caprifoliaceae). Journal of Systematics and Evolution. 2012, 50: 519–526. DOI: 10.1111/j.1759-6831.2012.00218.x.

Zhao, D., & Tao, J. Recent advances on the development and regulation of flower color in ornamental plants. Frontiers in Plant Science. 2015, 6: 1–13, DOI: 10.3389/fpls.2015.00261.

Zipor, G., Shahar, L., Ovadia, R., Teper-bamnolker, P., Levin, Y., Doron-faigenboim, A., & Oren-shamir, M. In planta anthocyanin degradation by a vacuolar class III peroxidase in *Brunfelsia calycina* flowers. New Phytologist. 2014, 205: 653–665. DOI: 10.1111/nph.13038.

Chapter 2 – Chemical characterization of *Tibouchina pulchra* (Cham.) Cogn. flowers.

1. INTRODUCTION

Tibouchina Aubl. is one of the most representative genera within Melastomataceae A. Juss., the fifth largest angiosperm family in Brazil (BFG 2015). This family contains approximately 170 genera and 4,500 species with a pantropical distribution, but particularly rich and dominant in the Neotropics with about 3,000 species, being 1,367 Brazilian natives. Melastomataceae species can be easily recognized among eudicots by their leaves with characteristic acrodromous venation. It contains thirteen well differentiated tribes (APG 2016).

Recently, a study that addressed the reproductive strategies within three tribes (*i.e*. Miconieae, Microlicieae and Melastomeae) found that Miconieae encompasses pollinator independent and fleshy fruit bearing species, mainly bird dispersed. On the other hand, in Microlicieae and Melastomeae, although the dispersion is abiotic (dry fruit), the breeding strategy depends on pollinators, mainly bees (Brito *et al*. 2017). By means nuclear and plastid markers, a molecular phylogenetic analysis demonstrated that *Tibouchina*, the largest genus in Melastomeae, is polyphyletic once some species grouped together with other genera, such as *Brachyotum*, *Bucquetia*, *Castratella*, *Centradenia*, *Chaetolepis*, *Heterocentron*, *Itatiaia*, *Microlepis*, *Monochaetum*, *Pilocosta*, *Svitramia*, and *Tibouchinopsis*, which are all monophyletic (Michelangeli *et al*. 2013). Moreover, *Tibouchina* has several plesiomorphic characters as the core Melastomeae: tetramerous or pentamerous flowers that show anthers with developed pedoconnectives (*i.e.* the connective tissue below the anther locules) and short bilobed ventral anther appendages. These data clearly expose that *Tibouchina* phylogeny is unsolved and it has been proposed that either the genus is recognized as much-expanded, although no morphological synapomorphies for this clade were identified, or all the other genera could be maintained, while *Tibouchina* should be divided into smaller and diagnosable units (Michelangeli *et al*. 2013).

Tibouchina has approximately 460 species (Clausing & Renner 2001, Tropicos 2017, Guimarães 2014). High level of endemism was verified for Brazilian species, being 145 out of the 166 reported considered restricted to the country, occurring in Atlantic rainforest and Cerrado (BFG 2015, Guimarães 2016). Studies aiming to describe the biological activities of

Tibouchina species have shown promising results. Jiménez *et al.* (2015) reported the use of *Tibuchina kingii* Wurdack in traditional medicine due to its anti-inflammatory properties and demonstrated high antioxidant potential of the aqueous leaf extract. *T. pereirae* Brade & Markgr also exhibited antioxidant activity by free radical scavenging assay and antinociceptive effect of *n*-hexanic extract (Dias *et al.* 2016). Low antimicrobial activity was found in extracts of *Tibouchina candolleana* Cong. (Santos *et al.* 2012). Additionally, isolated compounds (*i.e.* 2,8-dihydroxy-7H-furo[2,3-f] chromen-7-one and isoquercitrin) from *Tibouchina paratropica* (Grised.) Cong. showed antibacterial and antifungal activity. Interestingly, 2,8-dihydroxy-7H-furo[2,3-f] chromen-7-one also displayed potent antiparasitic activity against *Leishmania donovani* (Tracanna 2015). Antifungal (Niño *et al*. 2003, Kuster *et al*. 2009), anticancer (Jones *et al*. 1981) and antiparasitic activities (Singha *et al*. 1992, Mpalantinos *et al*. 1998, Cunha *et al*. 2009) have also been reported for the genus.

Phytochemical studies in eleven species of *Tibouchina* (*T. candolleana, T. ciliares* (Vent.) Cong.*, T. grandiflora* Cong.*, T. lepidota* (Bonpl.) Baill.*, T. multiflora* Cong.*, T. paratropica, T. pereirae, T. pulchra, T. semidecantra* (Mart & Schrank ex DC.) Cong.*, T. urvilleana* (DC.) Cong.*, T. granulosa* (Desr.) Cong.) reported the presence of several natural products, such as flavonoids (flavonol glycosides and anthocyanins), isoflavonoids, phenolic derivatives, tannins and triterpenes (Table 2.1). Structural elucidation by Nuclear Magnetic Resonance (NMR) was performed for some triterpenoids, tannins, flavonols, and anthocyanins in *T. urvilleana* and *T. lepidota* (Terahara *et al*. 1993, Pérez-Castorena 2014, Hendra & Keller 2016). As reviewed above, few studies have addressed the chemical profile of *Tibouchina* species, which remains largely elusive.

Table 2.1- Natural products reported for *Tibouchina* species.

Species	Class of metabolite	Compound	Organ	Reference
T. candolleana	triterpene/ flavone/ isoflavoid	α- and β-amyrin, β- sitosterol, ursolic and oleanolic acids/ luteolin/ genistein	aerial parts	Dos Santos *et al*. 2012
T. ciliaris	flavonol	kaempferol 7-*O*-*p*-coumaroyl, quercetin 3-*O*-rhamnopyranoside, quercetin 3-*O*-arabnoside	leaves	Colorado *et al*. 2007
T. grandiflora	flavonol/ anthocyanin	quercetin 3-*O*-β-D-glucuronide, quercetin 3-*O*-β-D-glucopyranoside, quercetin 3-*O*-β-D-galactopyranoside, quercetin 3-*O*-α-L-rhamnopyranoside, quercetin 3-*O*-β-L-arabinopyranoside, quercetin 3-*O*-β-D-(6″-*p*-coumaroyl)-glucopyranoside/ peonidin 3-sophoroside, peonidin 3-sambubioside, malvidin 3,5-diglucose, malvidin 3-(*p*-coumaroyl)-sambubioside-5-glucoside	leaves/ flowers	Kuster *et al*. 2009, Bobbio *et al*. 1985
T. granulosa	flavonol/ flavone/ proanthocyanidin/ anthocyanin	Isorhamnetin 3-*O*-glucuronide, isorhamnetin 3-*O*-di-glucoside, isorhamnetin 3-*O*-rutinoside, quercetin 3-(*O*-galloyl)-hexoside/ hispidulin 7-*O*-glucoside/ B-type procyanidin monomer, dimer, trimer and pentamer/ petunidin, pelargonidin	flowers/ leaves	Okumura *et al*. 2002, Sobrinho *et al*. 2017
T. lepidota	tannin/ flavonol/ anthocyanin	gallic acid, 2,3,5-trihydroxybenzoic acid/ quercetin 3-*O*-arabnoside, quercetin, quercetin 3-glucoside, isorhamnetin 3-rutinoside/ malvidin 3-(*p*-coumaryl-glucoside)-5-(acetyl-xyloside)	flowers	Hendra & Keller 2016
T. multiflora	tannin	nobotanins O and P	leaves	Yoshida *et al*.1999,
T. paratropica	phenolic derivative/ flavonoL	2,8-dihydroxy-7H-furo (2,3-f)-chromen-7-one/ isoquercitrin	aerial parts	Tracanna *et al*. 2015
T. pereirae	flavonol	Isorhamnetin 3-*O*-galloyl-glucoside, isorhamnetin-3-*O*-glucoside, kaempferol 3-*O*-rutinoside, quercetin 3-*O*-(galloyl)-glucoside, rutin	aerial parts	Dias 2013
T. pulchra	flavonol/ tannin	kaempferol 3-*O*-galactoside, kaempferol 3-*O*-glucoside, myricetin 3-*O*-galactoside, myricetin 3-*O*-glucoside, quercetin, myricetin, kaempferol, luteolin/ gallic acid	leaves	Furlan 2004, Motta *et al*. 2005

Table 2.1. *(Continued)*

Species	Class of metabolite	Compound	Organ	Reference
T. semidecantra	tannin/ flavonol/ anthocyanin/ proanthocyanidin	1,2,6-tri-*O*-galloyl-β-D-glucose, 1,4,6-tri-O-galloyl-β-D-glucose, 1,2,3,6-tetra-*O*-galloyl-β-D-glucose, nobotanin A, B, C, D, E and F, casuarictin, pedunculagin, praecoxin A and B, casuarinin, 2,3-*O*-(S)-hexahydroxydiphenoyl-D-glucopyranose, castalagin, vescalagin, 1-*O*-methylvescalaginnobotanins A, B, F, 3,3'-*O*-dimethyl ellagic acid 4-*O*-α-L-rhamnopyranoside/ quercetin, myricetin, quercetin 3-*O*-(6''-*O*-galloyl) galactoside, quercetin 3-*O*-α-L-(2''-*O*-acetyl) arabinofuranoside, quercetin 3-*O*-arabnoside, quercetin 3-*O*-rhamnopyranoside/ malvidin 3-(*p*-coumaroylglucoside)-5-glucoside/ leucodelphinidin, leucocyanidin	aerial parts	Sirat *et al*. 2010, Yoshida *et al*. 1991, Harbone 1964, Lowry 1975
T. urvilleana	flavonol/ flavone/ anthocyanin/ triterpene	quercetin 3-*O*-arabnoside/ hispidulin 7-*O*-β-D-glucopyranoside / malvidin 3-*O*-(6-*O*-*p*-coumaryl-β-D-glucopyranoside)-5-*O*-(2-*O*-acetyl-β-D-xylopyranosyl)/ glutinol, taraxerol, α- and β-amyrin, β- sitosterol, ursolic and oleanolic acids	aerial parts	Perez-Castorena 2014, Terahara *et al*. 1993.

T. granulosa and *T. pulchra* have been characterized as possible biomonitors of air pollution, *i.e.* particulate matter and ozone (Klumpp *et al.* 2001, Furlan *et al*. 2004, Furlan *et al*. 2008, Santos & Furlan 2013, Zampieri *et al*. 2013, Espósito & Domingos 2014, Espósito & Domingos 2016, Pedroso *et al.* 2016). Moreover, as they occur mainly in open areas, such as forest edges and clearings, *Tibouchina* species are considered important for restoration/reforestation purposes (Ellison *et al*. 1993).

Tibouchina pulchra (Figure 2.1), popularly known as "manacá-da-serra", has been increasingly used for urban ornamentation and, nowadays several cultivars are available in the flower market. The beauty and fascinating feature of these flowers is the development-associated color change: the buds open as white flowers that the next day become pink, further, from the third day towards senescent, the flowers maintain a deep pink color. The well-determined stages of flower coloring in *T. pulchra* raise interesting questions about the genetic and chemical mechanisms involved in the regulation of this phenomenon, which has up to now been unexplored (see Chapter 3).

In this context, this chapter presents results of isolation and identification of the petal tissue pigments of *Tibouchina pulchra*.

Figure 2.1. *Tibouchina pulchra* tree and its flowers.

2. MATERIAL AND METHODS

2.1. Plant Material

Pink petals of *Tibouchina pulchra* (cv. "manacá-anão") flowers were sampled at Praça Carlos José Gíglio (Latitude: -23.57998, Longitude: -46.73403) in the most vigorous flowering period (May and June/2016) between 8 and 9 a.m. Petals were immediately frozen in liquid nitrogen and stored at -80°C until processing. Samples were freeze dried in a lyophilizer (K202, Liobras) and crushed in a ball mill (TissueLyser, Qiagen) for further analyses. An exsiccate was deposited on herbarium of Institute of Bioscience (SPF) of University of São Paulo (ID: Furlan73).

2.2. Extraction and analysis by UPLC-MS

Phenolic compounds were extracted from 100 mg of petal powder with two times of 1.5 mL of 0.2 % HCl in methanol (MeOH). The samples were sonicated for 10 min and centrifugated at 10,000 rpm for 10 min. The extract was filtered (PTFE 0.45 µm) and analyzed by Ultra Performance Liquid Chromatography (UPLC) system with Diode Array Detector (DAD) (Dionex Ultimate 3000) and Electrospray Ionization Quadrupole Time-of-Flight High-Resolution Mass Spectrometry (ESI-QTOF-HRMS) detector (Bruker Maxis), MS/MS analysis was performed with a Broadband Collision Induced Dissociation (bbCID) detector. Separation was achieved by using a C18 column (Waters Acquity UPLC 100 x 2.1 mm - 1.7 µm) at a flow rate of 0.3 mL min^{-1}, and 4 µL of injection volume, the column temperature was 45°C, and the solvent system composed of 1% formic acid in water (A) and 1% formic acid in acetonitrile (B). Gradient elution: 5 to 25% of B (0- 40 min), 25 to 100% of B (40- 42 min), 100% of B (42- 42.5 min), 100 to 5% of B (42.5- 43 min), 5% of B (43- 46 min). Separated compounds were first monitored using DAD (200 to 600 nm) and then MS scans were performed in positive ion mode (MS^+), in the range m/z 75−1250 m/z, in the following conditions: capillary voltage set to 4,500 V, end plate offset at -500 V, nebulizer at 2 Bar, dry gas 12 L min^{-1} and dry gas temperature at 200°C MS was calibrated using sodium formate. All data were processed using Data analysis software 4.2 (Bruker). This analysis was performed in the Department of Chemistry at Denmark Technical University under the supervision of Ph.D. Mads H. Clausen.

2.3. Isolation by preparative HPLC and identification by Nuclear Magnetic Resonance (NMR)

Also in partnership with Ph.D. Mads H. Clausen, flavonoids were isolated from 10 g of petal powder by extracting four times in 200 mL of hydrochloric acid 0.2% in MeOH. The samples were sonicated for 15 min, pillowed for 10 min, vacuum filtered and concentrated with a rotary evaporator. The crude extract was diluted to, approximately, 250 mg/mL and injected in a preparative High Performance Liquid Chromatography (HPLC- Waters) with Photodiode Array Detector (PAD). Separation was achieved on a C18 column (Waters X Bridge BEH ODB 30 x 150 mm, 5µm) at a flow rate of 20 mL min^{-1}, using 1 mL of injection volume, and a solvent system composed of 1% formic acid in water (A) and 1% formic acid in acetonitrile (B). Gradient elution: 10% of B (0- 3 min), 10 to 15% of B (3- 30 min), 15% of B (30- 50 min), 15 to 20% of B (50- 60 min), 20 to 25% of B (60- 80 min), 25 to 35% of B (80- 90 min), 35 to 45% of B (90- 95 min), 45 to 100% of B (95- 96 min), 100% of B (96- 98 min), 100 to 10% of B (98- 98.5 min), 10% of B (98.5- 102 min), and monitored using DAD (200 to 600 nm). Fractions were collected by time. All the fractions were concentrated by rotary evaporator. An aliquot was resuspended in 0.2% HCl in MeOH to check the purity by UPLC-MS. For the isolated compounds the dried sample was dissolved in deuterated dimethylsulfoxide (DMSO-d_6) for NMR analysis. ^{1}H and ^{13}C NMR spectra were obtained by using a AVANCE III HD spectrometer (Bruker) operating at frequency of 800 MHz and equipped with a 5 mm TCI CryoProbe (Bruker). Two-dimensional analysis (HSQC and HMBC) were also performed. All data were processed using MestreNova software 11.0 (Mestrelab Research). The identification of compounds was performed in collaboration with Ph.D. Marcelo José Pena Ferreira from Department of Botany, University of São Paulo.

3. RESULTS AND DISCUSSION

3.1. Analysis by UPLC-MS

HPLC analysis showed a high diversity of compounds in petal extract, being integrated 30 constituents (Figure 2.2). UV-Vis absorption spectra and mass fragmentation of each detected constituent allowed the identification of two phenolic classes: phenolic acids (constituents **1** to **6**) and flavonoids (constituents **7** to **30**). Flavonoid compounds showed glucosyl and acyl groups as substituents (Table 2.2 and Figures 2.3 to 2.8).

Since the chromatogram did not exhibit an accurate resolution of the phenolic acids, generating low-quality spectra (Supplemental Figures 2.1 and 2.2), the identification of these compounds was not properly performed.

Regarding flavonoids, the analysis revealed hexosyl, pentosyl, glucuronic acid, galloyl, acetylpentosyl, and *p*-coumaroyl as substituents. Kaempferol, quercetin and myricetin were the detected flavonol aglycones, while malvidin and petunidin were the base skeleton for the identified anthocyanins (Table 2.2).

In many of the obtained mass spectra, it was possible to observe adduct from $[M+Na]^+$. Sodium and potassium adduct ions are often detected in first-order mass spectra obtained with ESI in the positive ion mode. These alkali metals are generally extracted from glass during solution storage and are more easily formed in flavonoids substituted at the 3-position (Cuyckens & Claeys 2004).

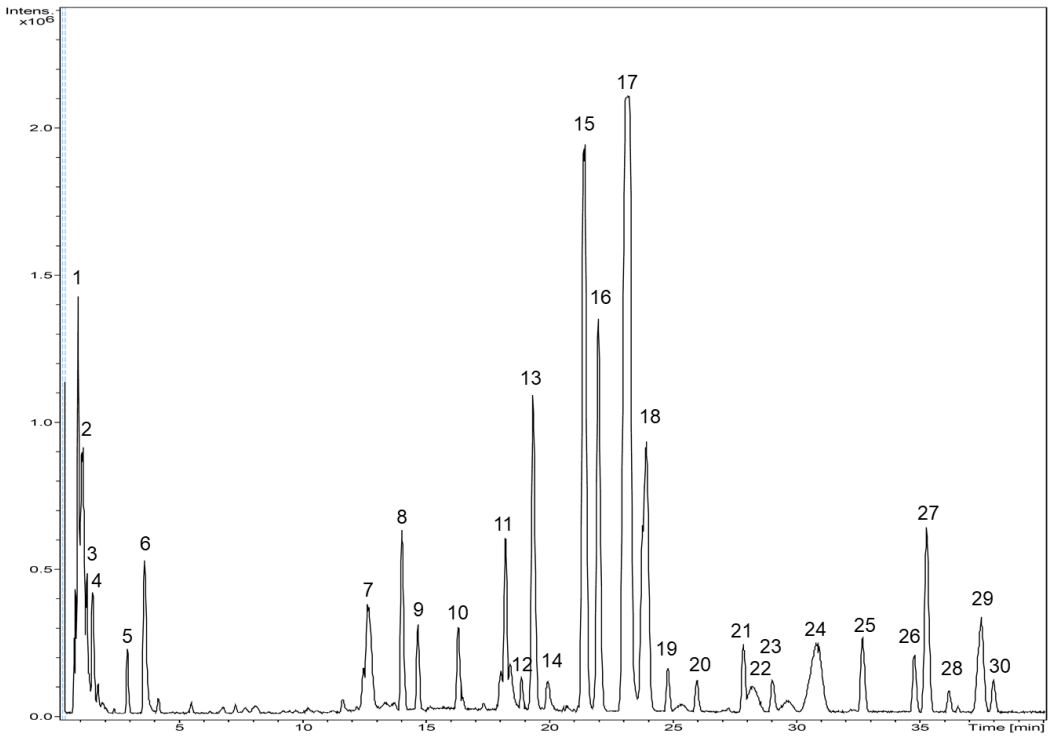

Figure 2.2. Chromatogram obtained by UPLC-ESI-QTOF-HRMS from *T. pulchra* petals extracted with acidified methanol. Separation was performed with a column Waters Acquity UPLC C18 (1.7 µm 100 x 2.1 mm) at a flow rate of 0.3 mL min^{-1}, using 4 µL of injection volume, column temperature of 45°C, and a solvent system composed by 1% formic acid in water (A) and 1% formic acid in acetonitrile (B). Gradient elution: 5 to 25% of B (0- 40 min), 25 to 100% of B (40- 42 min), 100% of B (42- 42.5 min), 100 to 5% of B (42.5- 43 min), 5% of B (43- 46 min). Numbers correspond to the identification presented in Table 2.2.

Table 2.2. Phenolic constituents from *T. pulchra* petals extracted with acidified methanol and analyzed by UPLC-DAD-ESI-QTOF-HRMS.

Compound	RT (min)	UV/ Vis (nm)	Mass spectrum HRMS-MS	Suggestion
1	0.97	278	L.Q.	Phenolic acid
2	1.13	278, (sh) 308	L.Q.	Cinnamic acid derivative
3	1.55	278	L.Q.	Phenolic acid
4	1.76	278	L.Q.	Phenolic acid
5	2.95	278, (sh) 308	L.Q.	Cinnamic acid derivative
6	3.65	278	L.Q.	Phenolic acid
7	12.69	270	453.0083 $[M+H]^+$, 303.0134 $[M-150]^+$	N.I.
8	14.05	268, 294 (sh), 354	481.0967 $[M+H]^+$, 319.0446 $[M-162]^+$	Myricetin hexoside
9	14.70	268, 294 (sh), 354	481.0964 $[M+H]^+$, 319.0445 $[M-162]^+$	Myricetin hexoside
10	16.33	269, 290 (sh), 354	639.0946 $[M+Na]^+$, 617.1121 $[M+H]^+$, 303.0498 $[M-314]^+$	Quercetin galloylhexoside
11	18.25	269, 290 (sh), 355	465.1020 $[M+H]^+$, 303.0499 $[M-162]^+$	Quercetin hexoside
12	18.89	269, 290 (sh), 355	479.0804 $[M+H]^+$, 303.0493 $[M-176]^+$	Quercetin glucuronide
13	19.36	266,290,350	601.1183 $[M+H]^+$, 287.0552 $[M-314]^+$	Kaempferol galloylhexoside
14	19.95	270	453.0083 $[M+H]^+$, 303.0134 $[M-150]^+$	N.I.
15	21.42	266, 346	471.0894 $[M+Na]^+$, 449.1073 $[M+H]^+$, 287.0549 $[M-162]^+$	Kaempferol hexoside
16	22.00	266,290,350	601.1184 $[M+H]^+$, 287.0551 $[M-314]^+$	Kaempferol galloylhexoside
17	23.18	266, 348	449.1079 $[M+H]^+$, 287.0551 $[M-162]^+$/ 463.0865 $[M+H]^+$, 287.0551 $[M-176]^+$	Mixture: Kaempferol 3-*O*-β-D-glucopyranoside (Astragalin)/ Kaempferol-(2''-*O*-methyl)-4'-*O*-α-D-glucopyranoside
18	23.93	266, 355	441.0790 $[M+Na]^+$, 419.0971 $[M+H]^+$, 287.0551 $[M-132]^+$	Kaempferol pentoside
19	24.81	266,290,350	623.1000 $[M+Na]^+$, 601.117 $[M+H]^+$, 287.0547 $[M-314]^+$	Kaempferol galloylhexoside
20	25.98	266, 355	441.0785 $[M+Na]^+$, 419.0959 $[M+H]^+$, 287.0545 $[M-132]^+$	Kaempferol pentoside
21	27.87	268, 314	595.1445 $[M+H]^+$, 287.0551 $[M-308]^+$	Kaempferol *p*-coumaroylhexoside

Table 2.2. *(Continued)*

Compound	RT (min)	UV/ Vis (nm)	Mass spectrum HRMS-MS	Suggestion
22	28.24	282, 305(om), 530	799.2077 $[M+H]^+$, 625.1552 {M-174}$^+$, 491.1176 [M-308]$^+$, 317.0655 [M-482]$^+$	Petunidin *p*-coumaroylhexoside acetylpentoside
23	29.04	268, 320, 530	499.0839 $[M+Na]^+$, 477.1031 $[M+H]^+$, 287.0547 [M-190]$^+$/ 771.2138 $[M+H]^+$, 317.0665 [M-454]$^+$	Mixture- Kaempferol 3-*O*-glucuronide-6''-*O*-methylester / Petunidin derivative
24	30.82	282, 310(om), 534	813.2243 $[M+H]^+$, 639.1716 [M-174]$^+$, 505.1336 [M-308]$^+$, 331.0812 [M-482]$^+$	Malvidin *p*-coumaroylhexoside acetylpentoside
25	32.68	271, 312	633.1203 $[M+Na]^+$, 611.1393 $[M+H]^+$, 303.0496 [M-308]$^+$	Quercetin 3-*O*-(6''-*O*-*p*-coumaroyl)-β-D-glucopyranoside (Helichrysoside)
26	34.78	266, 349	593.0892 $[M+H]^+$, 285.0603 [M-308]$^+$	N.I.
27	35.27	268, 314	617.1258 $[M+Na]^+$, 595.1437 $[M+H]^+$, 287.0546 [M-308]$^+$	Kaempferol 3-*O*-(6''-*O*-*p*-coumaroyl)-β-D-glucopyranoside (Tiliroside)
28	36.17	268, 314	617.1256 $[M+Na]^+$, 595.1418 $[M+H]^+$, 287.0545 [M-308]$^+$	Kaempferol *p*-coumaroylhexoside
29	37.48	270, 368	287.0546 $[M+H]^+$	Kaempferol
30	37.98	268, 314	617.1248 $[M+Na]^+$, 595.1455 $[M+H]^+$, 287.0549 [M-308]$^+$	Kaempferol *p*-coumaroylhexoside

*RT (min): retention time in minutes, sh: shoulder, N.I: not identified, L.Q: low quality. Numbers highlighted in bold indicate compounds reported for the first time in *Tibouchina*.

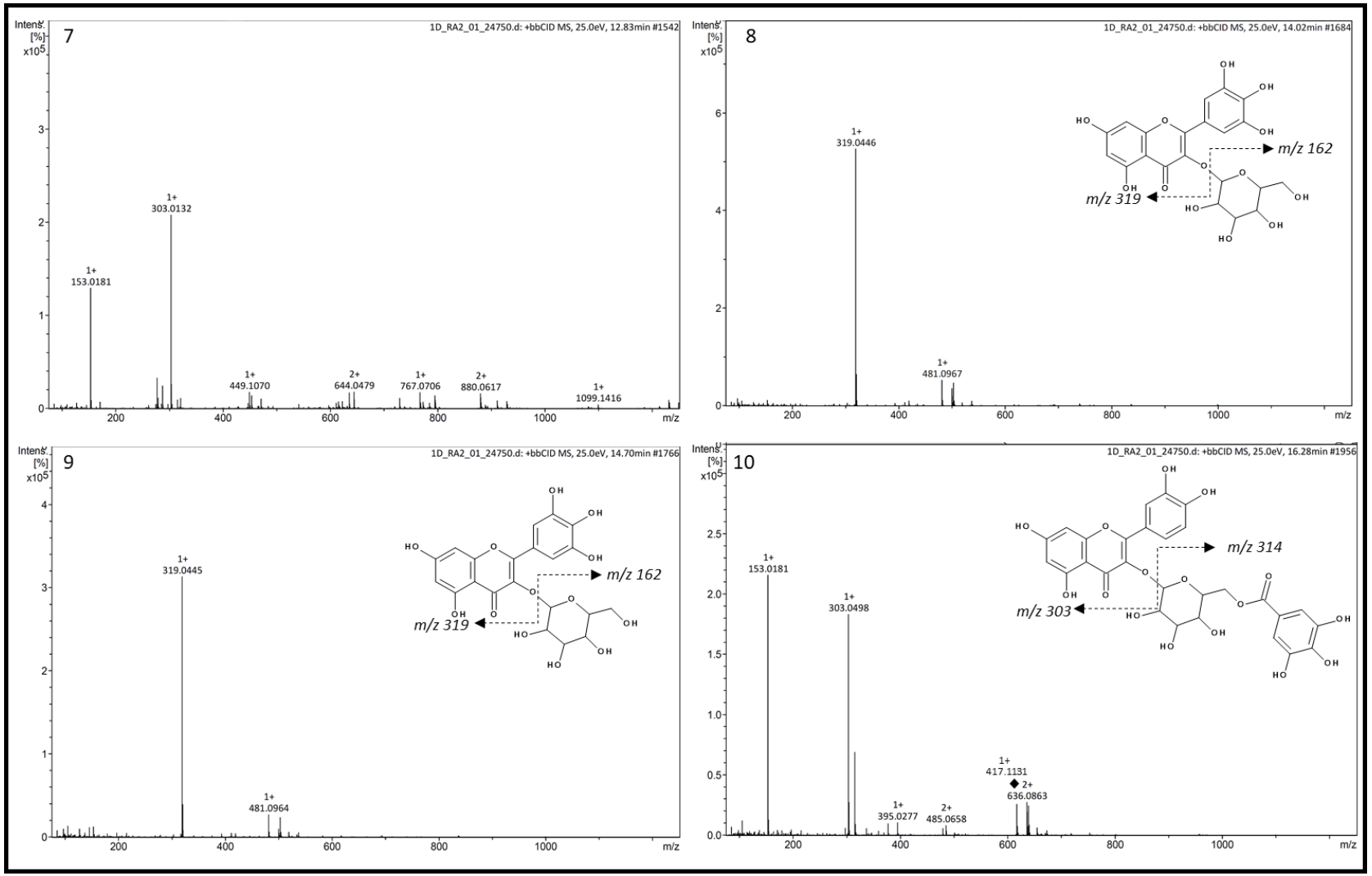

Figure 2.3. Mass spectra (MS^+) of compounds **7**, **8**, **9** and **10**. Structures represent the proposed compound and its main fragmentation.

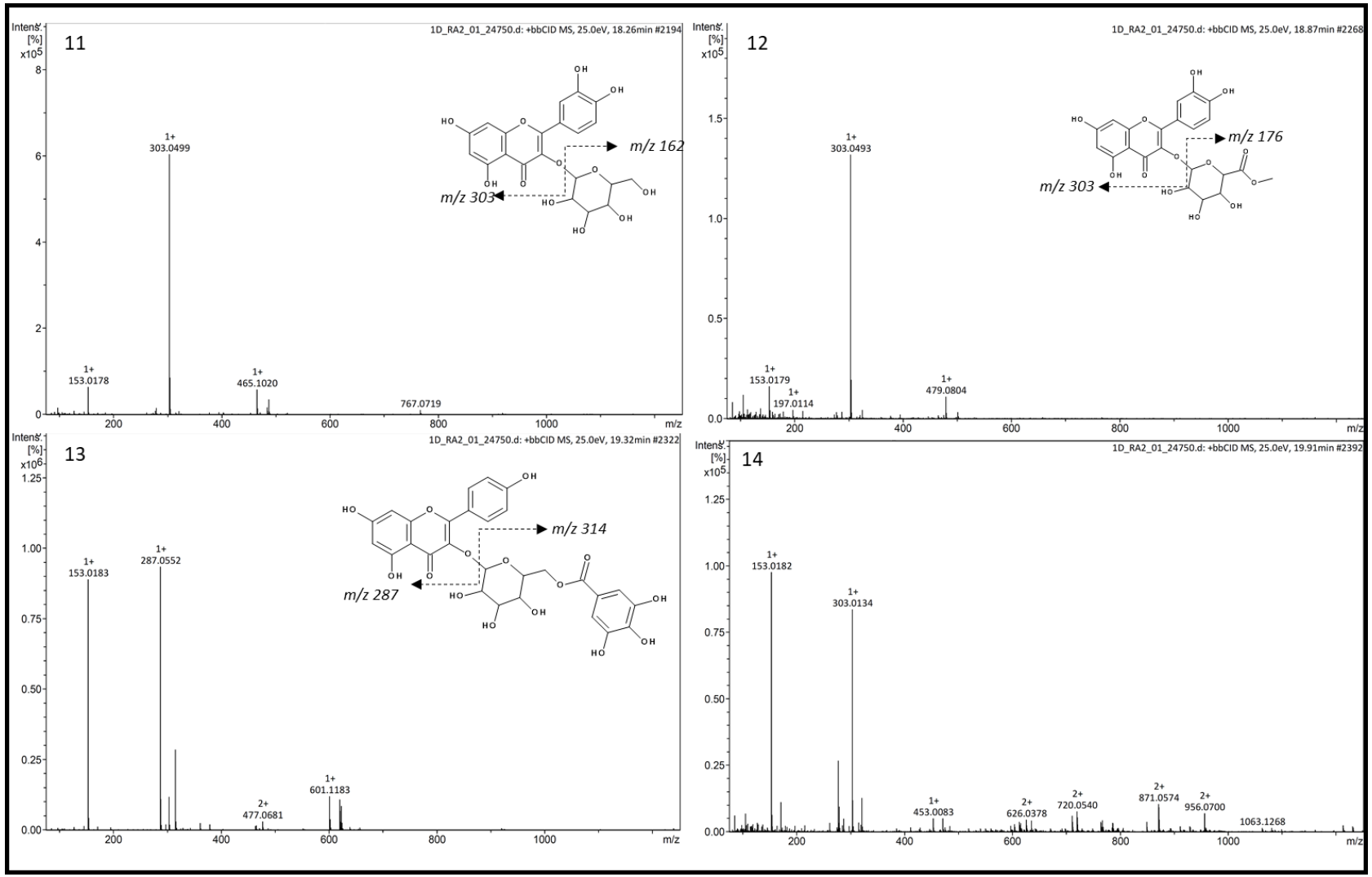

Figure 2.4. Mass spectra (MS^+) of compounds **11**, **12**, **13** and **14**. Structures represent the proposed compound and its main fragmentation.

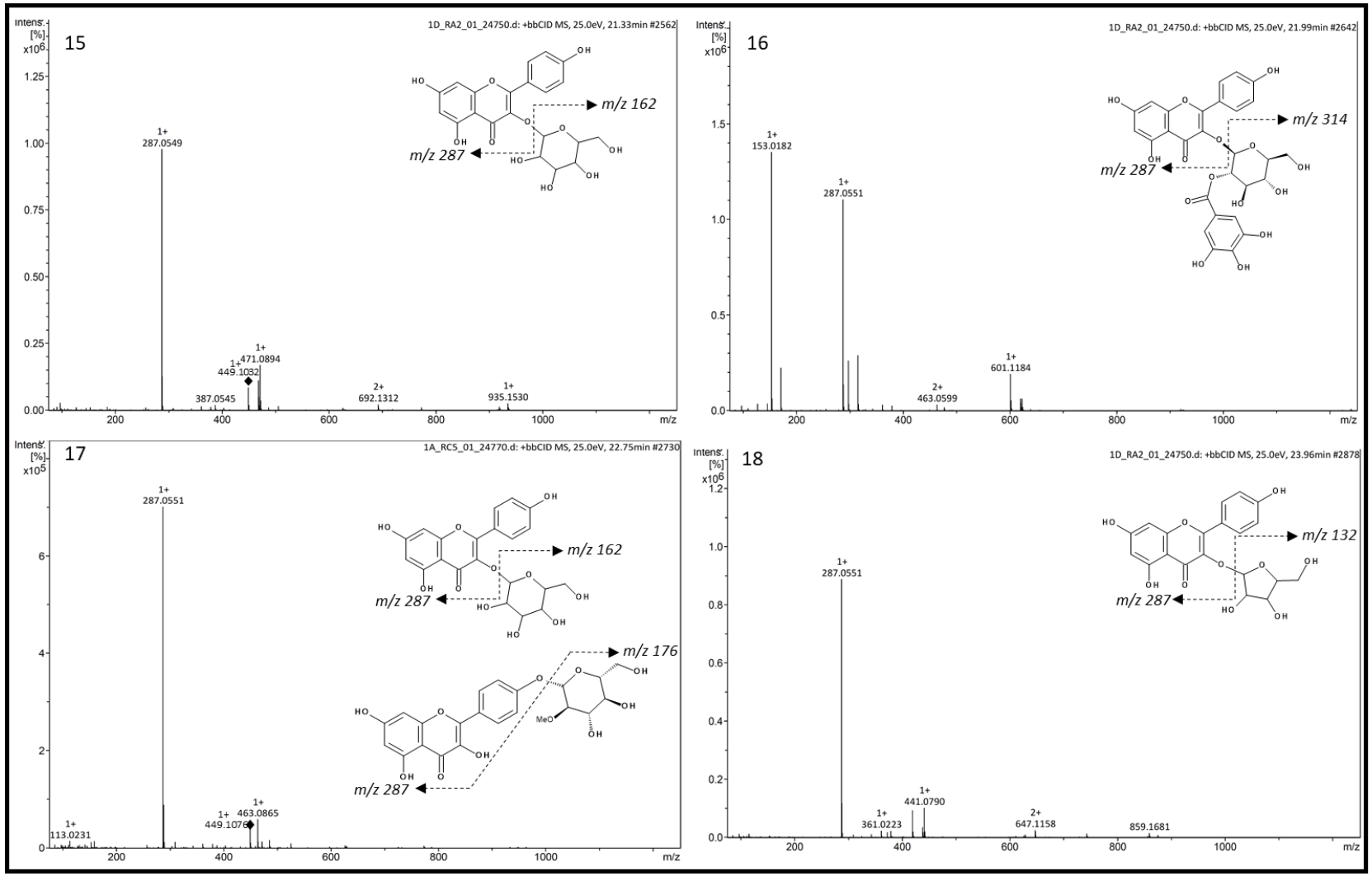

Figure 2.5. Mass spectra (MS^+) of compounds **15**, **16**, **17** and **18**. Structures represent the proposed compound and its main fragmentation.

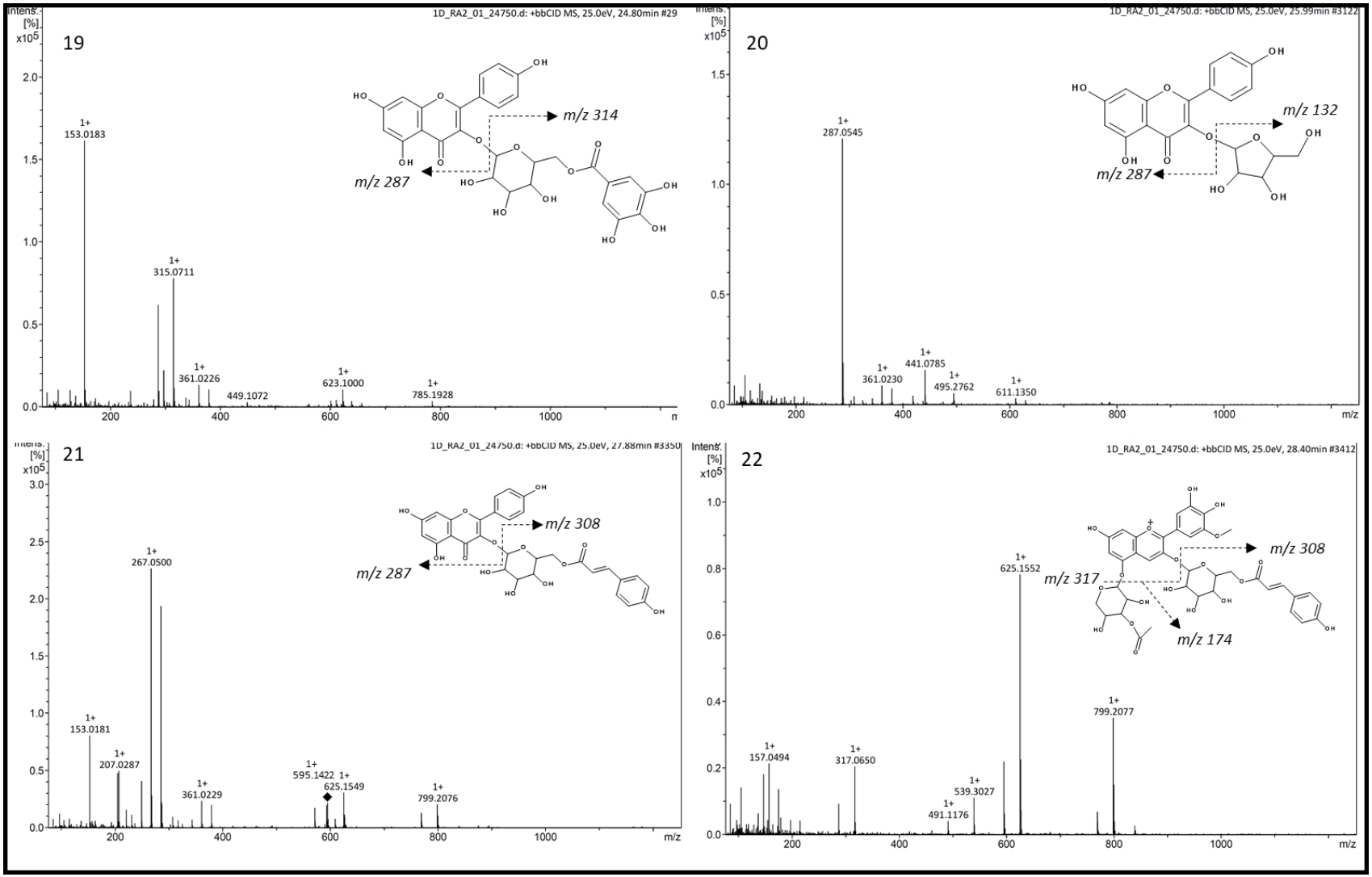

Figure 2.6. Mass spectra (MS^+) of compounds **19**, **20**, **21** and **22**. Structures represent the proposed compound and its main fragmentation.

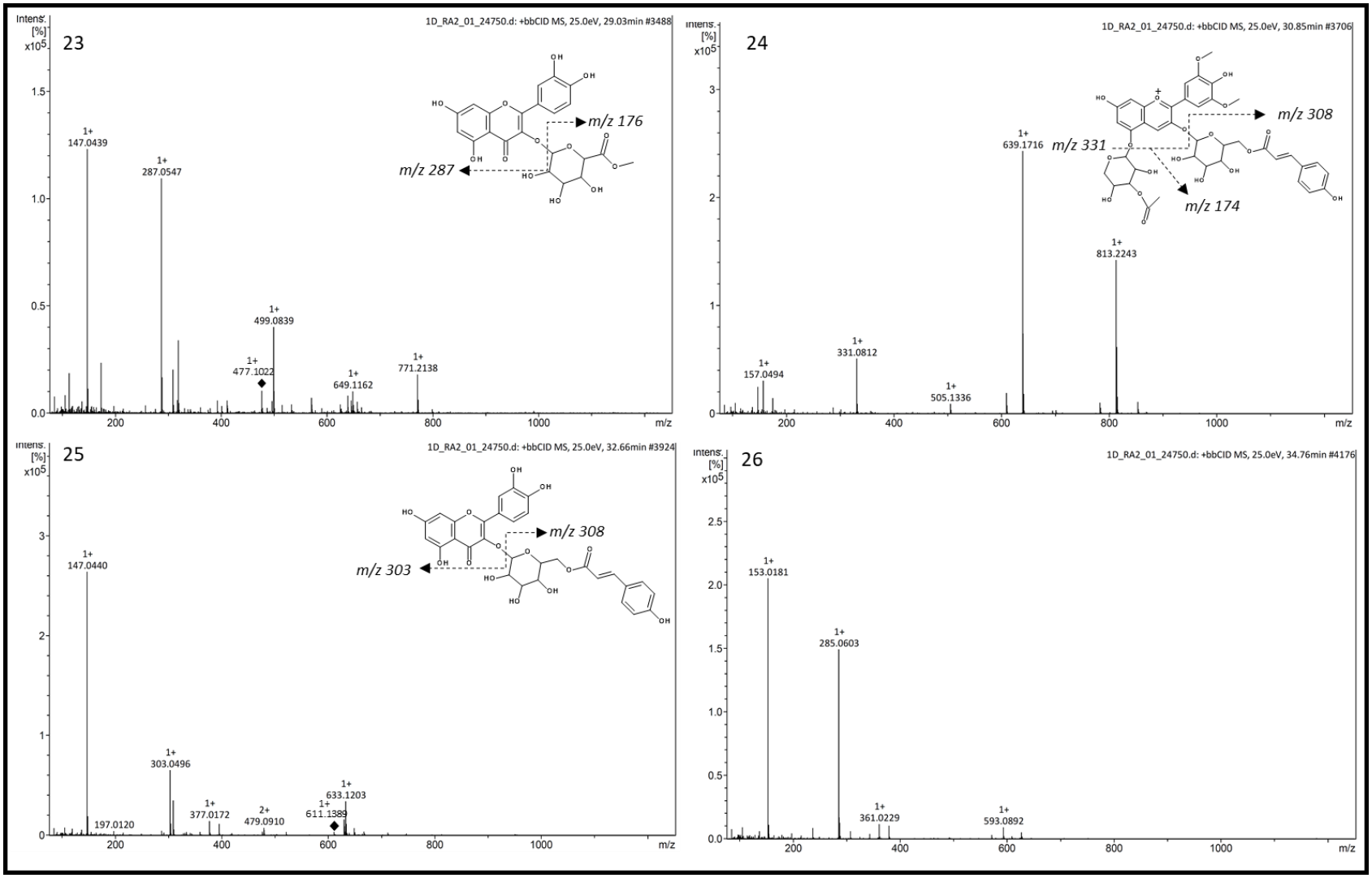

Figure 2.7. Mass spectra (MS^+) of compounds **23**, **24**, **25** and **26**. Structures represent the proposed compound and its main fragmentation.

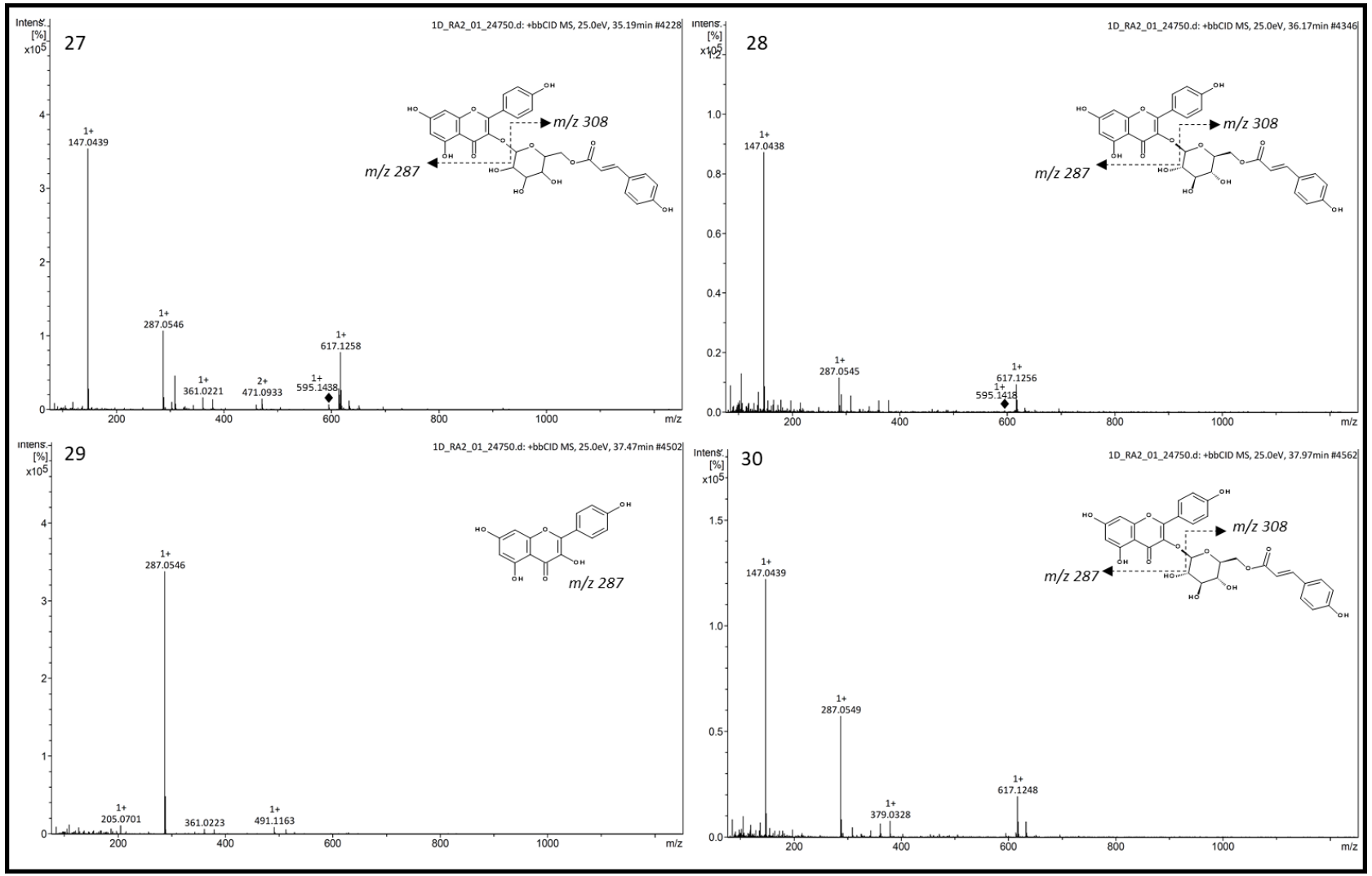

Figure 2.8. Mass spectra (MS^+) of compounds **27**, **28**, **29** and **30**. Structures represent the proposed compound and its main fragmentation

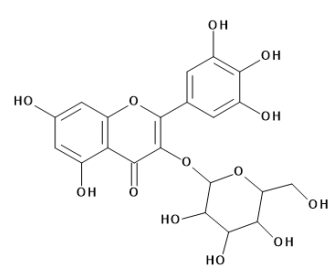

myricetin hexoside (**8** and **9**)

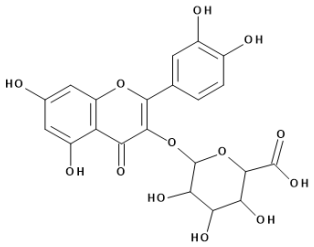

quercetin glucuronide (**12**)

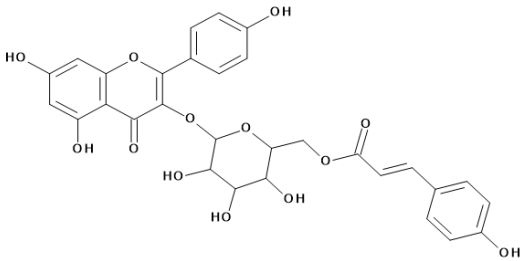

kaempferol *p*-coumaroylhexoside (**21**, **28**, and **30**)

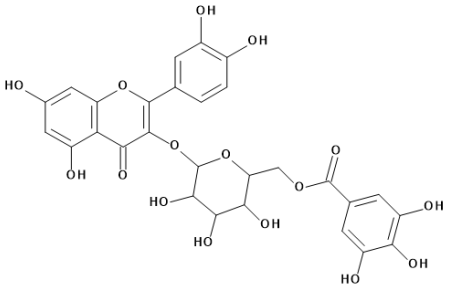

quercetin galloylhexoside (**10**)

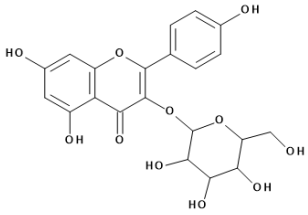

kaempferol hexoside (**15**)

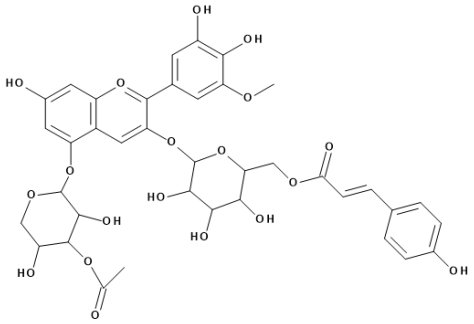

petunidin *p*-coumaroylhexoside acetylpentoside (**22**)

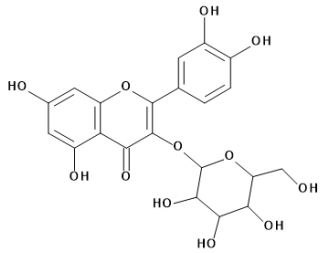

quercetin hexoside (**11**)

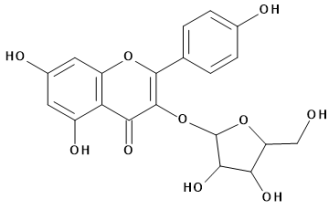

kaempferol pentoside (**18** and **20**)

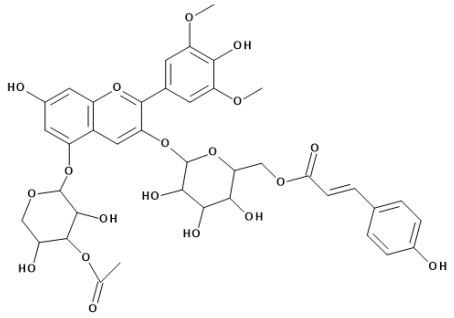

malvidin *p*-coumaroylhexoside acetylpentoside (**24**)

Figure 2.9. Compounds of *T. pulchra* flowers identified by UV-visible absorption and mass spectra.

From the twenty-four flavonoids detected, twenty-one were identified by MS and UV-Vis analyses (Figure 2.9), and eight of these compounds were isolated for the accurate identification by NMR analysis. The most abundant flavonol found was kaempferol (*m/z* 287.0549, constituents **13**, **15** to **21**, **23**, and **27** to **30**) with different substituents, besides three isomers of kaempferol galloylhexoside (constituents **13**, **16,** and **19**). Quercetin (*m/z* 303.0498, constituents **10**, **11**, **12**, and **25**) was the second most abundant flavonol found, followed by myricetin (*m/z* 319.0445, constituents **8** and **9**). Flavonols as kaempferol, myricetin, and quercetin derivatives were previously described in leaves of *T. pulchra* corroborating the present study (Furlan 2004, Motta *et al*. 2005).

The fragment *m/z* 153.0181 was observed in many constituents (**7**, **10**, **13**, **14**, **16**, **19**, **21**, and **26**). It is a typical ion signal from a fragment of A-ring, generated by Retro Diels–Alder cleavage of the C–ring bonds, resulting in structurally informative $^{i,j}A^+$ and $^{i,j}B^+$ ions. This reaction is the most diagnostic fragmentation for flavonoid aglycone identification, because it provides information on the number and type of substituents in the A- and B-rings (Cuyckens & Claeys 2004). The major routes of fragmentation result in cleavage of the C—C bonds at positions (i/j) 1/3, 0/2, 0/3, 0/4 or 2/4 of the C-ring (Figure 2.10). The fragmentation pathways strongly depend on the substitution pattern and the class of flavonoids, $^{1,3}A^+$ (*m/z* 153), $^{1,3}B^+$ + 2H, $^{1,4}A^+$ + 2H, $^{0,2}A^+$, and $^{0,2}A^+$ - CO are typically observed for flavonols, while $^{1,3}B^+$, $^{0,4}B^+$ and $^{0,4}B^+$ -H_2O are found for flavones (Ma *et al*. 1997, Kyekyeku *et al*. 2017).

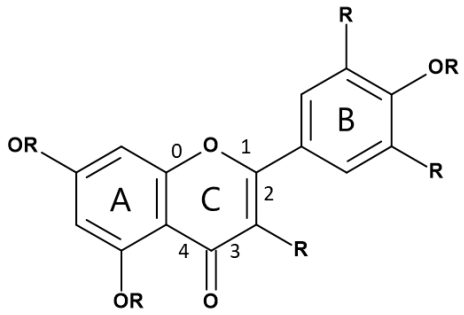

Figure 2.10. Schematic Retro Dies-Alder positions of cleavage in flavonols.

Compounds **8**, **9**, **11**, **15**, and **17** showed the loss of 162 amu indicating the presence of a hexose, probably a galactosyl or a glucosyl group. Pentoses, as arabinose, apiose or xylose, were also found as substituents, as in the case of compounds **18** and **20**, which exhibited a mass loss of 132 amu. Compounds **12** and **23** showed the presence of glucuronic acid as substituent, detected by the mass loss of 176 amu in compound **12** and 190 amu in compound

23. This difference is due to a methyl group in the later compound (**23**) as consequence of an extraction artifact. Glucose is the sugar most commonly identified, while galactose, rhamnose, xylose, and arabinose are less frequent. On the contrary, mannose, fructose, glucuronic and galacturonic acids are rare (Markham 1982, Iwashina 2000).

Mass loss of 314 amu indicates the presence of galloylhexose. This is the case for compound **10**, a quercetin galloylhexoside, as well as, constituents **13**, **16,** and **19**, which are predicted as isomers of kaempferol galloylhexoside. The mass spectrum of compound **19** showed the fragment *m/z* 449.1071 that indicates a loss of 152 amu in relation to *m/z* 601.117 $[M+H]^+$, corroborating the galloyl substitution (Ducrey *et al*. 1995, Mahmoud *et al*. 2001). Moreover, the mass loss of 162 amu $[449- 287]^+$ confirmed the hexose residue.

In relation to *p*-coumaroyl group, were identified eight compounds with this acylation pattern: **21**, **22**, **24**, **25**, **26**, **27**, **28,** and **30**. The mass loss of 308 amu is indicative of *p*-coumaroylhexose substituent, but it can also be a rutinosyl group (rhamnose-glucose). The fragment of *m/z* 147.0439 found in compounds **25**, **27**, **28**, and **30** ensure the presence of *p*-coumaroyl or rhamnosyl group. However, acylation with hydroxycynamic acids, as *p*-coumaric acid, shifts Band I of the flavonol spectrum to lower wavelength, resulting in a peak or shoulder at 305-310 nm. Furhtermore, acylation on the sugar moiety also increases retention time characterizing this type of residue (Tamura *et al*. 1994, Wang *et al*. 2003, Atoui *et al*. 2005). Thus, the absorption in UV (310 nm) and the retention time of constituents **25**, **27**, **28**, and **30** were decisive to propose the acylated identification. Excluding anthocyanins (**22** and **24**) these compounds were identified as kaempferol *p*-coumaroylhexoside. Regarding anthocyanins, compound **22** showed a fragment of *m/z* 799.2077 $[M+H]^+$, which fragmentation resulted in *m/z* 625.1552 $[M-174]^+$, *m/z* 491.1176 $[M-308]^+$, and *m/z* 317.0665 $[M-482]^+$ corresponding to the neutral loss of acetylpentose and *p*-coumaroylhexose from a petunidin. The other anthocyanin (**24**) exhibited a fragment of *m/z* 813.2243 $[M+H]^+$, which fragmentation retrieved *m/z* 639.1716 $[M-174]^+$, *m/z* 505.1336 $[M-308]^+$, and *m/z* 331.0812 $[M-482]^+$ consistent with the loss of acetylpentose and *p*-coumaroylhexose, but in this case, from a malvidin as the anthocyanidin. So, these compounds were identified as Petunidin *p*-coumaroyl-hexoside acetylpentoside (**22**) and Malvidin *p*-coumaroyl-hexoside acetylpentoside (**24**), respectively. This pattern of substituents of anthocyanins was previously reported in *T. lepdota* and *T urvilleana* (Hendra & Keller 2016, Terahara *et al*. 1993 - Table 2.1). Acylated anthocyanins are characteristic of Melastomatoideae (APG 2016).

3.2. Isolation by preparative HPLC and identification by Nuclear Magnetic Resonance (NMR)

Compounds were isolated by preparative HPLC, and their purity was analyzed by UPLC-MS, being eight of them analyzed by NMR (Table 2.3 to 2.10). Isolated substances were: kaempferol 3-*O*-(6''-*O*-galloyl)-β-D-glucopyranoside (**13**, **16** or **19**), kaempferol 3-*O*-(2''-*O*-galloyl)-β-D-glucopyranoside (**13**, **16** or **19**), kaempferol 3-*O*-glucopyranoside (**17**), kaempferol 3-*O*-glucuronide-6''-*O*-methylester (**23**), quercetin 3-*O*-(6''-*O*-*p*-coumaroyl)-β-D-glucopyranoside (**25**), kaempferol 3-*O*-(6''-*O*-*p*-coumaroyl)-β-D-glucopyranoside (**27**), kaempferol (**29**) and quercetin (**31**). Even though the later was not detected by the UPLC-DAD-ESI-HRMS analysis, it was isolated by preparative HPLC and identified by UPLC-MS and NMR (Table 2.10). All the structures are shown in figure 2.11 and their NMR spectra in Supplemental Figure 2.3 to 2.47.

Kaempferol 3-*O*-(6''-*O*-galloyl)-β-D-glucopyranoside (**13**, **16** or **19**) exhibited U.V. λ_{max}=266, 290, 350 and $[M+H]^+$ *m/z* 601.1183. ^{1}H NMR spectrum showed five aromatic hydrogen signals: two doublet signals were observed at δ 6.21 (1H, d, *J*= 2.0 Hz) and δ 6.45 (1H, d, *J*= 2.0 Hz), corresponding to a *meta*-coupling of these atoms, which were attributed to the H6 and the H8 of the flavonoid A-ring, respectively. Two other doublet signals with *ortho*-coupling constants were found at δ 6.77 (2H, d, *J*= 8.8 Hz) and δ 7.94 (2H, d, *J*= 8.8 Hz), and were assigned to H3',5' and H2',6', respectively, suggesting that the B-ring of the compound was *para*-substituted. The last aromatic signal was a singlet at δ 6.92 (2H, s) attributed to H2''' and H6''' from the galloyl group. Additionally, a doublet at δ 5.45 (1H, d, *J*= 7.6 Hz) and two double-doublets at δ 4.17 (1H, dd, *J*= 12.0 Hz and *J*= 3.8 Hz) and δ 4.26 (1H, dd, *J*= 12.0 Hz and *J*= 2.0 Hz) were assigned to H1'' and H6'' from the sugar moiety. The HMBC spectrum showed two relevant correlations: the anomeric hydrogen (δ 5.45) with C3 (δ 133.52) from flavonoid C-ring and the H6'' (δ 4.26) of the sugar moiety with C7''' (δ 165.36) from the galloyl group. Therefore, the sugar and galloyl group positions were confirmed in the structure. HSQC and HMBC spectra confirmed the assignment of the carbon signals presented in Table 2.3, in agreement with previously reported data (Markham 1982, Braca *et al*. 2003).

Kaempferol 3-*O*-(2''-*O*-galloyl)-β-D-glucopyranoside (**13**, **16** or **19**) displayed U.V. λ_{max}= 266, 290, 350 and $[M+H]^+$ *m/z* 601.1183. ^{1}H NMR spectrum also showed five aromatic hydrogen signals: two from the flavonoid A-ring at δ 6.21 (1H, d, *J*= 2.0 Hz, H6) and δ 6.45 (1H, d, *J*= 2.0 Hz, H8), two from the B-ring, δ 6.83/ 6.93 (2H, d, *J*= 8.8 Hz, H3' and 5') and δ 8.04 (2H,

d, *J*= 8.8 Hz, H2′ and 6′), and one from the galloyl group at δ 6.90 (2H, s, H2‴ and 6‴). Anomeric carbon appeared as a doublet at δ 5.47 (1H, d, *J*= 7.6 Hz, H1″). Signals at δ 3.62 and δ 3.38 were evidences of 2″ substitution. The HMBC spectrum showed one relevant correlation: the anomeric hydrogen (δ 5.47) with C3 (δ 133.22) from the flavonoid C-ring. None hydrogen of the sugar moiety coupled with C7‴ to confirm the galloyl group position, but literature data corroborates this substitution in C2″. HSQC and HMBC spectra reinforced the assignment of the carbon signals presented in Table 2.4, which is also in accordance to previously published data (Isobe *et al*. 1980, Markham 1982, Braca *et al*. 2003).

Compound **17** was confirmed by NMR as a mixture of both compounds: kaempferol 3-*O*-β-D-glucopyranoside and kaempferol-(2''-*O*-methyl)-4'-*O*-α-D-glucopyranoside (Table 2.5).

Kaempferol 3-*O*-β-D-glucopyranoside (**17**) showed U.V. λ_{max}= 266, 348 nm and $[M+H]^+$ *m/z* 449.1079. ^{1}H NMR spectrum showed four aromatic hydrogen signals: two from the flavonoid A-ring at δ 6.22 (1H, d, *J*= 2.0 Hz, H6) and δ 6.46 (1H, s, H8), two from the B-ring, δ 6.89 (2H, d, *J*= 8.4 Hz, H3′ and 5′) and δ 8.04 (2H, d, *J*= 8.4 Hz, H2′ and 6′). Anomeric carbon appeared as a doublet at δ 5.46 (1H, d, *J*= 7.6 Hz, H1″). Signals among δ 3.09 and δ 3.58 were attributed to the sugar moiety. The HMBC spectrum showed one relevant correlation: the anomeric hydrogen (δ 5.46) with C3 (δ 133.63) from the flavonoid C-ring, confirming the position of the sugar moiety. ^{13}C NMR spectrum showed nineteen carbon signals: C2 (156.61), C3 (133.63), C4 (177.92), C5 (161.65), C6 (99.16), C7 (164.62), C8 (94.12), C9 (156.82), C10 (104.45), C1′ (122.33), C2′ and 6′ (131.33), C3′ and 5′ (115.58), C4′ (160.44), C1″ (101.81), C2″ (74.67), C3″ (76.88), C4″ (70.33), C5″ (77.96), and C6″ (61.28) (Table 2.5). Signal attributions were performed according to similar data from the literature (Markham 1982, Wei *et al*. 2011).

Kaempferol-(2''-*O*-methyl)-4'-*O*-α-D-glucopyranoside (**17**) showed the same U.V (λ_{max}= 266, 348) of compound described above, but the $[M+H]^+$ was *m/z* 463.0865, suggesting the presence of an additional methyl group in the structure, which was confirmed by the signals at δ 3.26 (s, 3H) and δ 54.74. ^{1}H NMR spectrum also showed four aromatic hydrogen signals: two from the flavonoid A-ring at δ 6.21 (1H, d, *J*= 2.0 Hz, H6) and δ 6.46 (1H, s, H8), two from the flavonoid B-ring, δ 6.93 (2H, d, *J*= 8.5 Hz, H3′ and 5′) and δ 8.04 (2H, d, *J*= 8.5 Hz, H2′ and 6′). Anomeric carbon appeared as a doublet at δ 4.51 (1H, d, *J*= 3.6 Hz, H1″) and this small coupling constant suggests an α-sugar series. The HMBC spectrum showed one relevant correlation: the anomeric hydrogen (δ 4.51) with 2″*O*Me (δ 54.74) from the methyl group, confirming this group at C2″ position on the sugar moiety. Although the correlation among

the anomeric hydrogen with carbon C4' of the flavonoid has not been observed, the sugar unity was bonded in that position because the ^{13}C NMR chemical shifts at C2 (δ 147.27) and C3 (δ 136.10) positions of the flavonoid ensure the presence of a free hydroxyl group at C3. ^{13}C NMR spectrum showed twenty carbon signals: C2 (147.27), C3 (136.10), C4 (176.35), C5 (161.13), C6 (98.68), C7 (164.40), C8 (93.95), C9 (156.71), C10 (103.48), C1′ (122.10), C2′ and 6′ (129.95), C3′ and 5′ (115.91), C4′ (159.68), C1′′ (100.12), C2′′ (73.84), C3′′ (72.44), C4′′ (73.04), C5′′ (70.79), C6′′ (61.42), and *O*Me-C2′′ (54.74) (Table 2.5). Signal attributions of flavonoid were performed through HSQC and HMBC correlations. Indeed, the methyl group could be an artefact due to the use of acidified methanol in extraction procedure, further analyses are necessary to confirm this substitution. Moreover, only kaempferol 4'-*O*-β-D-glucopyranoside was described (Scheer & Wichtl 1987), being the kaempferol-(2''-*O*-methyl)-4'-*O*-α-D-glucopyranoside or kaempferol 4'-*O*-α-D-glucopyranoside an inedited substance.

Table 2.3. NMR data of ^{1}H, ^{13}C and HMBC for Kaempferol 3-*O*-(6''-*O*-galloyl)-β-D-glucopyranoside (**13**, **16** or **19**) comparing to the literature.

Carbon number	^{1}H	^{13}C*	HMBC	^{1}H (CD_3OD) (Braca *et al.* 2003)	^{13}C (CD_3OD) (Braca *et al.* 2003)
2	-	157.15	-	-	158.5
3	-	133.52	-	-	136.0
4	-	-	-	-	179.4
5	-	161.9	-	-	163.0
6	6.21 d (*J*= 2.0 Hz)	99.58	C8, C10, C7, C5	6.19 d (*J*= 2.0 Hz)	100.0
7	-	164.5	-	-	166.0
8	6.45 d (*J*= 2.0 Hz)	94.91	C10, C9, C7, C6	6.35 d (*J*= 2.0 Hz)	95.0
9	-	157.26	-	-	159.0
10	-	104.66	-	-	105.7
1'	-	121.04	-	-	122.0
2',6'	7.94 d (*J*= 8.8 Hz)	131.19	C2, C4', C6'or 2'	7.94 d (*J*= 8.0 Hz)	132.2
3',5'	6.77 d (*J*= 8.8 Hz)	116.46	C4', C1', C5' or 3'	6.73 d (*J*= 8.0 Hz)	116.1
4'	-	150.58	-	-	161.5
1''	5.45 d (*J*= 7.6 Hz)	102.17	C3	5.21 d (*J*= 7.7 Hz)	104.4
2''	3.24 - 3.50*	74.52	C1'', C3''	-	75.9
3''		76.51	C2'', C4''	-	78.1
4''		69.89	C2'', C6''	-	71.5
5''		74.60	-	-	75.8
6''	4.17 dd (*J*= 12 and 3.8 Hz), 4.26 dd (*J*= 12 and 2.0 Hz)	63.15	C5'', C4'', C7'''	-	64.3
1'''	-	120	-	-	121.3
2''',6'''	6.92 s	109.70	C7''', C2'''or 6''', C3'''or 5''', C4''', C1'''	6.94 s	110.3
3''',5'''	-	146.11	-	-	146.4
4'''	-	138.94	-	-	139.3
7'''	-	165.36	-	-	168.2
OH-C5	12.52 s	-	-	-	-
OH-C7	10.87 s	-	-	-	-
OH-C4'	10.06 s	-	-	-	-

*Chemical shifts of ^{13}C NMR were obtained by correlations in HSQC and HMBC.

Table 2.4. NMR data of ^{1}H, ^{13}C and HMBC for Kaempferol 3-*O*-(2''-*O*-galloyl)-β-D-glucopyranoside (**13**, **16** or **19**) comparing to the literature.

Carbon number	^{1}H	^{13}C*	HMBC	^{1}H (CD_3OD) (Braca *et al.* 2003)	^{13}C (DMSO-d6) (Isobe *et al.* 1980)
2	-	155.46	-	-	156.6
3	-	133.22	-	-	132.8
4	-	-	-	-	177.4
5	-	160.00	-	-	161.4
6	6.21 d (*J*= 2.0 Hz)	98.02	C8, C10, C7, C5	6.19 d (*J*= 2.0 Hz)	98.6
7	-	163.30	-	-	165.6
8	6.45 d (*J*= 2.0 Hz)	93.05	C10, C6, C7, C9	6.35 d (*J*= 2.0 Hz)	94.1
9	-	155.50	-	-	156.6
10	-	102.70	-	-	104.3
1'	-	120.90	-	-	121.1
2',6'	8.04 d (*J*= 8.8 Hz)	129.54	C2'or 6', C4', C2, C3'''or 5'''	7.94 d (*J*= 8.0 Hz)	131.2
3',5'	6.89/6.93 d (*J*= 8.8 Hz)	114.66	C3'''or 5''', C4', C1'	6.73 d (*J*= 8.0 Hz)	115.6
4'	-	158.40	-	-	160.3
1''	5.47 d (*J*= 7.6 Hz)	100.38	C3	5.21 d (*J*= 7.7 Hz)	99.1
2''	3.09 - 3.22*	73.68	C1, C3	-	74.6
3''		75.87	C2, C4	-	78.0
4''		69.48	C5	-	70.5
5''		76.74	C3, C4	-	74.6
6''	3.62 and 3.38*	60.68	C5, C4	-	61.1
1'''	-	124.00	-	-	119.9
2''',6'''	6.90 s	108.45	C7''', C4''', C3'''ou 5''', C1''', C2''' or 6'''	6.94 s	109.4
3''',5'''	-	145.96	-	-	145.7
4'''	-	138.86	-	-	138.7
7'''	-	162.11	-	-	164.4

*Chemical shifts of ^{13}C NMR were obtained by correlations in HSQC and HMBC.

Table 2.5. NMR data of ^{1}H, ^{13}C and HMBC for a mixture of both compounds: kaempferol 3-*O*-β-D-glucopyranoside and kaempferol-(2''-*O*-methyl)-4'-*O*-α-D-glucopyranoside (**17**) comparing to the literature.

Kaempferol 3-O-β-D-glucopyranoside (Astragalin)						Kaempferol-(2''-O-methyl)-4'-O-α-D-glucopyranoside				
Carbon number	^{1}H	^{13}C	HMBC	^{1}H (DMSO-d6) (Wei *et al* 2011)	^{13}C (DMSO-d6) (Wei *et al* 2011)	^{1}H	^{13}C	HMBC	^{1}H (DMSO-d6) (Scheer & Wichtl, 1987)	^{13}C (DMSO-d6) (Scheer & Wichtl, 1987)
2	-	156.62	-	-	156.72	-	147.27	-	-	145.91
3	-	133.63	-	-	133.66	-	136.10	-	-	136.30
4	-	177.92	-	-	177.94	-	176.35	-	-	176.05
5	-	161.65	-	-	161.69	-	161.13	-	-	160.69
6	6.22 d (*J*= 2.0 Hz)	99.16	C5, C7, C8, C10	6.31 d (*J*= 2.4 Hz)	99.15	6.21 d (*J*= 2.0 Hz)	98.68	C5, C7, C8, C10	6.19 d (*J*= 2.0 Hz)	98.33
7	-	164.62	-	-	164.59	-	164.40	-	-	164.32
8	6.46 sl	94.12	C4, C6, C7, C9, C10	6.55 d (*J*=2.4 Hz)	94.11	6.46 sl	93.95	C6, C7, C9	6.45 d (*J*= 2.0 Hz)	93.60
9	-	156.82	-	-	156.84	-	156.71	-	-	156.27
10	-	104.45	-	-	104.48	-	103.48	-	-	103.02
1'	-	122.33	-	-	121.36	-	122.10	-	-	124.41
2',6'	8.04 d (*J*= 8.4 Hz)	131.33	C2, C4', C3' or 5', C2' or 6'	8.16 d (*J*= 9.0 Hz)	131.34	8.04 d (*J*= 8.5 Hz)	129.95	C2, C3' or 5', C4'	8.13 d (*J*= 9.0 Hz)	129.13
3',5'	6.89 d (*J*= 8.4 Hz)	115.58	C1, C3' or 5', C4'	6.84 d (*J*= 9.0 Hz)	115.56	6.93 d (*J*= 8.5 Hz)	115.91	C1', C3' or 5', C4'	7.18 d (*J*= 9.0 Hz)	116.11
4'	-	160.44	-	-	160.41	-	159.68	-	-	158.44
1''	5.46 d (*J*=7.6 Hz)	101.81	C3, C5''	5.29 d (*J*=7.8 Hz)	101.35	4.51 d (*J*=3.6 Hz)	100.12	C2'', OMe	4.98 d (J=7.2 Hz)	99.93
2''	3.18	74.67	C1'', C3'', C4''	3.27 - 3.67	74.68	3.37	73.84	C3''	-	73.17
3''	3.22	76.88	C2'', C4''		76.89	3.18	72.44	C2''	-	76.6
4''	3.09	70.33	C6'', C5''		70.37	3.29	73.04	C1''	-	69.61
5''	3.09	77.96	C6'', C4''		77.95	3.04	70.79	C6'', C4''	-	77.12
6''	3.58 and 3.33	61.28	C5'', C4''		61.31	3.62 and 3.44	61.42	C5'', C4''	-	60.60
2''OMe	-	-	-	-	-	3.26 s	54.74	C1''	-	-

.

Kaempferol 3-*O*-glucuronide-6''-*O*-methylester (**23**) exhibited U.V. λ_{max}= 268, 320 and $[M+H]^+$ *m/z* 477.1031. ^{1}H NMR spectrum also showed four aromatic hydrogen signals: two from the flavonoid A-ring at δ 6.23 (1H, d, *J*= 2 Hz, H6) and δ 6.45 (1H, d, *J*= 2 Hz, H8), and two from the B-ring, δ 6.89 (2H, d, *J*= 8.9 Hz, H3′ and 5′) and δ 8.02 (2H, d, *J*= 8.9 Hz, H2′ and 6′). Anomeric carbon appears as a doublet at δ 5.47 (1H, d, *J*= 7.7 Hz, H1''). A singlet signal at δ 3.57 reveals the presence of a methyl group. The HMBC spectrum showed three relevant correlations: the anomeric hydrogen (δ 5.47) with C3 (δ 133.58) from the flavonoid C-ring, the H5'' (δ 3.73) from the sugar moiety with C6'' (δ 169.52) and the methoxyl group (δ 3.57) with C6'' from the carboxyl group in the glucuronic acid. Therefore, the sugar and the methyl group positions were confirmed in the structure. HSQC and HMBC spectra confirmed the assignment of the carbon signals presented in Table 2.6 in accordance with previously reported data (Markham 1982, Jung *et al*. 2003).

Quercetin 3-*O*-(6''-*O*-*p*-coumaroyl)-β-D-glucopyranoside (**25**) exhibited U.V. λ_{max}=271, 312, and $[M+H]^+$ *m/z* 611.1393. ^{1}H NMR spectrum showed seven aromatic hydrogen signals: two doublet signals were observed at δ 6.14 (1H, d, *J*= 2.1 Hz) and δ 6.38 (1H, d, *J*= 2.1 Hz), corresponding to the *meta*-coupling of H6 and H8 from the flavonoid A-ring, respectively, two other doublet signals were found at δ 6.78 (1H, d, *J*= 8.4 Hz) and δ 7.52 (1H, d, *J*= 2.3 Hz) assigned to H5′ and H2′, respectively, a double doublet was detected at δ 7.66 (1H, dd, *J*= 8.5 Hz and *J*= 2.3 Hz) corresponding to H6′, suggesting that the B-ring of the compound was substituted with two hydroxyl groups at C3′ and C4′. The last two aromatic signals were doublets at δ 6.83 (2H, d, *J*= 8.4 Hz, H3''' and 5''') and δ 7.37 (2H, d, *J*= 8.4 Hz, H2''' and 6''') attributed to a *trans*-double bond, were assigned to a *p*-coumaroyl group. Two signals from the double bond were also detected at δ 6.13 (2H, d, *J*= 15.7 Hz, H8''') and δ 7.36 (2H, d, *J*= 15.7 Hz, H7'''). Additionally, a doublet at δ 5.42 (1H, d, *J*= 7.8 Hz) and a double-doublet at δ 4.12 (1H, dd, *J*= 11.5 Hz and *J*= 4.6 Hz) were assigned to H1'' and H6'' from the sugar moiety. The HMBC spectrum was not done and the group positions were suggested by comparing signals to literature. HSQC spectra allowed assignment of carbon signals presented in Table 2.7 in agreement with data from the literature (Markham 1982, Lavault & Richomme *et al*. 2004).

Table 2.6. NMR data of ^{1}H, ^{13}C and HMBC for Kaempferol 3-*O*-glucuronide-6''-*O*-methylester (**23**) comparing to the literature.

Carbon number	^{1}H	^{13}C*	HMBC	^{1}H (DMSO- d6) (Jung *et al.* 2003)	^{13}C (DMSO- d6) (Jung *et al.* 2003)
2	-	157.17	-	-	156.4
3	-	133.58	-	-	133.0
4	-	-	-	-	177.2
5	-	161.58	-	-	161.2
6	6.23 d (*J*= 2.0 Hz)	99.53	C8, C10, C7	6.21 d (*J*= 2.0 Hz)	98.9
7	-	164.78	-	-	164.3
8	6.45 d (*J*= 2.0 Hz)	94.1	C6, C10, C7, C9	6.43 d (*J*= 2.0 Hz)	93.8
9	-	156.94	-	-	156.6
10	-	104.46	-	-	104.0
1'	-	121.05	-	-	120.6
2',6'	8.02 d (*J*= 8.9 Hz)	131.73	C3, C2' or 6', C4'	8.02 d (*J*= 8.0 Hz)	130.9
3',5'	6.89 d (*J*= 8.9 Hz)	115.5	C1', C3' or 5', C4'	6.89 d (*J*= 8.0 Hz)	115.1
4'	-	160.62	-	-	160.2
1''	5.47 d (*J*= 7.7 Hz)	101.74	C3	5.47 d (*J*= 7.4 Hz)	101.4
2''	3.24-3.36*	74.6	C1'', C3'',	-	73.9
3''		75.92	C2'', C4''	-	75.5
4''		71.95	C5'', C6''	-	71.5
5''	3.73 d (*J*= 9.7 Hz)	76.13	C1'', C6'', C4''	-	75.6
6''	-	169.52	-	-	169.0
MeO-C6''	3.57 s	52.32	C6''	3.57 s	-
OH-C5	12.51 s	-	-	12.51 s	-
OH-C7	10.97 s	-	-	-	-
OH-C4'	10.22 s	-	-	-	-

*Chemical shifts of ^{13}C NMR were obtained by correlations in HSQC and HMBC.

Table 2.7. NMR data of ^{1}H, ^{13}C and HMBC for Quercetin 3-*O*-(6''-*O*-*p*-coumaroyl)-β-D-glucopyranoside (**25**) comparing to literature.

Carbon number	^{1}H	^{13}C*	^{1}H (CD_3OD) (Lavault & Richomme *et al.* 2004)	^{13}C (CD_3OD) (Lavault & Richomme *et al.* 2004)
2	-	-	-	158.8
3	-	-	-	135.5
4	-	-	-	179.6
5	-	-	-	163.2
6	6.14 d (*J*= 2.1 Hz)	99.19	6.21 d (*J*= 1.9 Hz)	100.6
7	-	-	-	167.3
8	6.38 d (*J*= 2.1 Hz)	93.90	6.38 d (*J*= 1.9 Hz)	95.3
9	-	-	-	158.8
10	-	-	-	105.6
1'	-	-	-	123.4
2'	7.52 d (*J*= 2.3 Hz)	116.42	7.68 d (*J*= 1.7 Hz)	115.0
3'	-	-	-	146.2
4'	-	-	-	146.9
5'	6.78 d (*J*= 8.4 Hz)	116.01	6.90 d (*J*= 8.4 Hz)	116.2
6'	7.66 dd (*J*= 8.4 Hz and 2.3 Hz)	122.38	7.66 dd (*J*= 8.3 Hz and 2.0 Hz)	123.4
1''	5.42 d (*J*= 7.8 Hz)	102.03	5.32 d (*J*= 7.0 Hz)	104.2
2''	-	-	-	76.1
3''	-	-	-	78.3
4''	-	-	-	72.0
5''	-	-	-	75.9
6''	4.12 dd (*J*= 11.5 Hz and 4.6Hz)	63.62	4.29 m, 4.37 m	64.6
1'''	-	-	-	131.5
2''',6'''	7.37 d (*J*= 8.4 Hz)	130.62	7.40 d (*J*= 8.5 Hz)	117.6
3''',5'''	6.83 d (*J*= 8.4 Hz)	115.61	6.87 d (*J*= 8.8 Hz)	131.5
4'''	-	-	-	161.5
7'''	7.36 d (*J*= 15.7 Hz)	145.31	7.48 d (*J*= 15.7 Hz)	140.2
8'''	6.13 d (*J*= 15.7 Hz)	114.10	6.16 d (*J*= 15.7 Hz)	115.0
9'''	-	-	-	169.3
OH-C5	12.64 s	-	-	-
OH-C7	10.84 s	-	-	-
OH-C3'	9.16 s	-	-	-
OH-C4'	9.73 s	-	-	-
OH-C4'''	10.01 s	-	-	-

*Chemical shifts of ^{13}C NMR were obtained by correlations in HSQC.

Kaempferol 3-*O*-(6''-*O*-*p*-coumaroyl)-β-D-glucopyranoside (**27**) displayed U.V. λ_{max}=268, 314, and $[M+H]^+$ *m/z* 595.1418. ^{1}H NMR spectrum showed six aromatic hydrogen signals: two from the flavonoid A-ring at δ 6.14 (1H, d, *J*= 2.1 Hz, H6) and δ 6.40 (1H, d, *J*= 2.1 Hz, H8), two from *para*-substituted B-ring, δ 6.78 (2H, d, *J*= 8.4 Hz, H3′ and 5′) and δ 8.05 (2H, d, *J*= 8.4 Hz, H2′ and 6′), and two from *p*-coumaroyl group at δ 6.86 (2H, d, *J*= 8.7 Hz, H2''' and 6'''). Two signals from the double bond were also detected at δ 6.11 (2H, d, *J*= 15.9 Hz, H8''') and δ 7.34 (2H, d, *J*= 15.9 Hz, H7'''). Anomeric carbon appears as a doublet at δ 5.41 (1H, d, *J*= 7.7 Hz, H1''). The signal at δ 4.10 (1H, d, *J*=6.2 Hz) is an evidence of 6'' substitution. The HMBC spectrum showed one relevant correlation confirming the *p*-coumaroyl position: the H6'' (δ 4.10) from the sugar moiety with the C9''' from the *p*-coumaroyl group. None of the hydrogens of the flavonoid moiety showed correlation with carbons from the sugar moiety, however, literature data corroborate the substitution in C3 (Nikaido *et al.* 1986). HSQC and HMBC spectra reinforced the assignment of the carbon signals presented in Table 2.8 in accordance to the literature (Markham 1982, Nikaido *et al.* 1986).

Kaempferol (**29**) showed U.V. λ_{max}= 270, 368, and $[M+H]^+$ *m/z* 287.0545. ^{1}H NMR spectrum displayed four aromatic hydrogen signals. Two doublet signals were observed at δ 6.21 (1H, d, *J*= 2.0 Hz) and δ 6.46 (1H, d, *J*= 2.0 Hz), attributed to a *meta*-coupling of H6 and H8 from the flavonoid A-ring, respectively. Two other doublet signals, with *ortho*-coupling constants were found at δ 6.94 (2H, d, *J*= 8.9 Hz) and δ 8.05 (2H, d, *J*= 8.9 Hz), and were assigned to H3′,5′ and H2′,6′, respectively, suggesting that the B-ring of the compound was *para*-substituted. ^{13}C NMR spectrum showed thirteen carbon signals: C2 (147.27), C3 (136.11), C4 (176.36), C5 (161.15), C6 (96.68), C7 (64.38), C8 (93.95), C9 (156.63), C10(103.49), C1′ (122.12), C2′ and 6′ (129.95), C3′ and 5′ (115.91), C4′ (159.67) (Table 2.9). Attribution was performed according to similar data from the literature (Markham 1982, Wahab *et al*. 2014, Guo *et al.* 2016).

Quercetin (**31**) showed $[M+H]^+$ *m/z* 302.94. HSQC spectrum allowed the assignment of the hydrogen and carbon signals presented in Table 2.10, which were in accordance to previously published data (Markham 1982, Joshi *et al*. 2009). The signals at δ 6.18 and 6.42, corresponding to the flavonoid A-ring C6 and C8, respectively, and at δ 6.88, 7.52 and 7.65 from the B-ring were enough to confirm the presence of quercetin.

Table 2.8. NMR data of ^{1}H, ^{13}C and HMBC for Kaempferol 3-*O*-(6''-*O*-*p*-coumaroyl)-β-D-glucopyranoside (**27**) comparing to literature.

Carbon number	^{1}H	^{13}C*	HMBC	^{1}H (DMSO- d6) (Nikaido *et al.* 1986)	^{13}C (DMSO-d6) (Nikaido *et a.l* 1986)
2	-	156.96	-	-	155.7
3	-	-	-	-	132.5
4	-	-	-	-	176.5
5	-	161.69	-	-	155.7
6	6.14 d (*J*= 2.1 Hz)	99.30	C8, C10, C5	6.41 d (*J*= 1.8 Hz)	93.2
7	-	164.56	-	-	163.6
8	6.40 d (*J*= 2.1 Hz)	94.19	C10, C9, C7, C6	6.18 d (*J*= 1.8 Hz)	98.3
9	-	156.55	-	-	160.4
10	-	104.20	-	-	103.3
1'	-	125.58	-	-	120.2
2',6'	8.05 d (*J*= 8.4 Hz)	131.47	C2, C4', C6'or 2'	6.90 d (*J*= 8.8 Hz)	130.1
3',5'	6.78 d (*J*= 8.4 Hz)	116.35	C1', C5' or 3'	8.02 d (*J*= 8.8 Hz)	114.5
4'	-	160.38	-	-	159.2
1''	5.41 d (*J*= 7.7 Hz)	102.04	-	5.48 d (*J*= 8 Hz)	100.6
2''	3.51 - 3.7	71.47	C1	-	73.9
3''		70.32	-	-	76.0
4''		73.40	C5''ou C3'', C1'', C6''or C2''	-	69.7
5''		69.05	-	-	73.9
6''	4.10 d (*J*= 6.2 Hz)	63.71	C9''', C4'', C5''or C3''	4.08 dd (*J*= 2 e 12 Hz)	62.7
1'''	-	121.33 or 125.05	-	-	124.3
2''',6'''	7.35 d (*J*= 8.7 Hz)	130.66	C7''', C4'''	6.83 d (*J*= 8.8 Hz)	139.4
3''',5'''	6.86 d (*J*= 8.7 Hz)	115.52	C1''', C5''or C3'', C4'''	7.39 d (*J*= 8.8 Hz)	115.2
4'''	-	160.53	-	-	158.8
7'''	7.34 d (*J*= 15.9 Hz)	145.24	C9''', C2'''or C6'''	7.38 d (*J*= 16.1 Hz)	143.4
8'''	6.11 d (*J*= 15.9 Hz)	114.29	-	6.14 d (*J*= 16.1 Hz)	114.8
9'''	-	166.85	-	-	167.1
OH-C5	12.59 s	-	-	-	-
OH-C7	10.87 s	-	C7, C6, C8	-	-
OH-C4'	10.03 s	-	-	-	-
OH-C4'''	10.20 s	-	-	-	-

*Chemical shifts of ^{13}C NMR were obtained by correlations in HSQC and HMBC.

Table 2.9. NMR data of ^{1}H, ^{13}C e HMBC for Kaempferol (**29**) comparing to literature.

Carbon number	^{1}H	^{13}C	^{1}H (DMSO-d6) (Guo *et al.* 2016)	^{13}C (DMSO-d6) (Wahab *et al.* 2014)
2	-	147.27	-	146.3
3	-	136.11	-	135.2
4	-	176.36	-	175.2
5	-	161.15	-	160.4
6	6.21 d (*J*= 2.0 Hz)	96.68	6.19 d (*J*= 1.7 Hz)	98.4
7	-	164.38	-	163.7
8	6.46 d (*J*= 2.0 Hz)	93.95	6.44 d (*J*= 1.7 Hz)	93.8
9	-	156.63	-	156.7
10	-	103.49	-	103.1
1'	-	122.12	-	122.1
2',6'	8.05 d (*J*= 8.9 Hz)	129.95	8.04 d (*J*= 8.8 Hz)	129.4
4'		159.67		158.7
3',5'	6.94 d (*J*= 8.9 Hz)	115.91	6.93 d (*J*= 8.8 Hz)	115.3
OH-C3	9.38 s		9.37 s	
OH-C5	12.48 s	-	12.48 s	-
OH-C7	10.83 s	-	10.78 s	-
OH-C4'	10.13 s	-	10.10 s	-

Table 2.10. NMR data of ^{1}H, ^{13}C e HMBC for Quercetin comparing to literature.

Carbon number	^{1}H	^{13}C*	^{1}H (DMSO-d6) (Joshi *et al.*, 2009)	^{13}C (DMSO-d6) (Joshi *et al.*, 2009)
2	-	-	-	145.05
3	-	-	-	135.72
4	-	-	-	175.83
5	-	-	-	160.70
6	6.18*	98.75	6.16 d (J= 2.0 Hz)	98.34
7	-	-	-	163.80
8	6.42*	93.93	6.40 d (J= 2.0 Hz)	93.34
9	-	-	-	156.13
10	-	-	-	103.01
1'	-	-	-	121.96
2'	7.65*	115.47	7.47 d (J= 2.0 Hz)	115.00
3'	-	-	-	145.05
4'	-	-	-	147.69
5'	6.88*	116.13	6.85 d (J= 9.0 Hz)	115.60
6'	7.52*	120.52	7.62 dd (J= 2.0 e 9.0 Hz)	119.90
OH-C3	9.60 s	-	9.60 s	-
OH-C5	12.46 s	-	12.48 s	-
OH-C7	10.86 s	-	-	-
OH-C3'	9.36 s	-	-	-
OH-C4'	9.31 s	-	-	-

*Chemical shifts of ^{13}C NMR were obtained by correlations in HSQC.

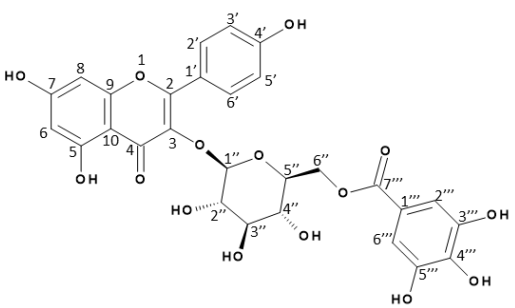

kaempferol 3-*O*-(6''-*O*-galloyl)-β-D-glucopyranoside (**13**, **16** or **19**)

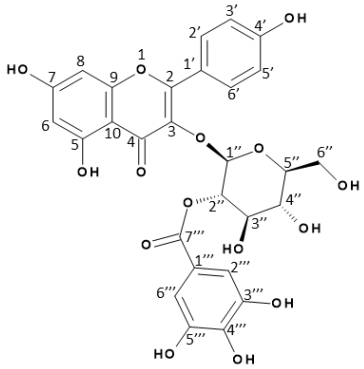

kaempferol 3-*O*-(2''-*O*-galloyl)-β-D-glucopyranoside (**13**, **16** or **19**)

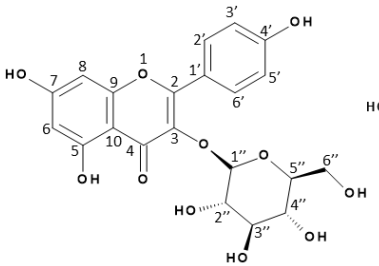

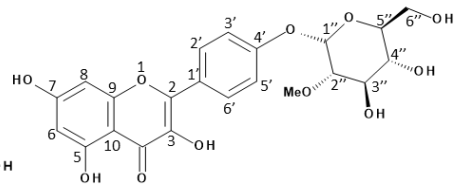

Mixture: kaempferol 3-*O*-β-D-glucopyranoside and kaempferol 4'-*O*-(2''-*O*Me)-α-D-glucopyranoside(**17**)

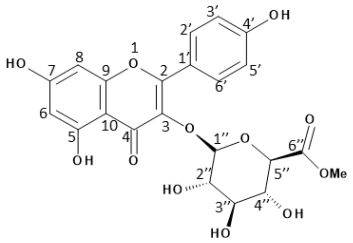

kaempferol 3-*O*-glucuronide-6''-*O*-methylester (**23**)

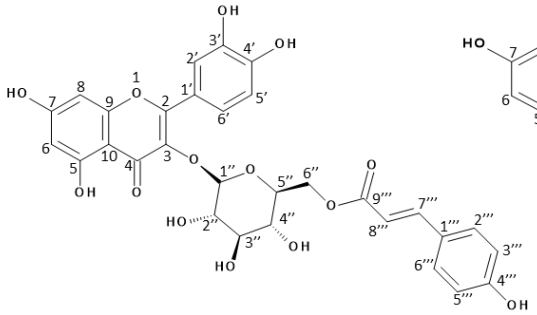

quercetin 3-*O*-(6''-*O*-*p*-coumaroyl)-β-D-glucopyranoside (**25**)

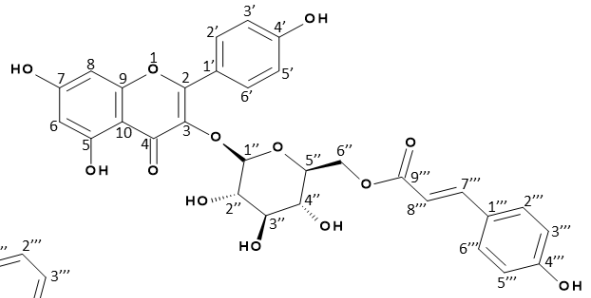

kaempferol 3-*O*-(6''-*O*-*p*-coumaroyl)-β-D-glucopyranoside (**27**)

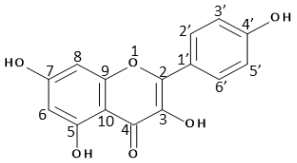

kaempferol (**29**)

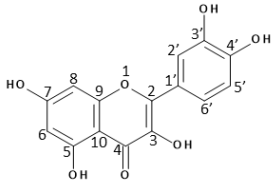

quercetin (**31**)

Figure 2.11. Compounds of *T. pulchra* flowers identified by UV-visible absorption, mass and NMR spectra.

Considering aerial parts of *T. pulchra*, sixteen compounds are described for the first time: quercetin galloylhexoside (**10**), quercetin hexoside (**11**), quercetin glucuronide (**12**), kaempferol 3-*O*-(2''-*O*-galloyl)-β-D-glucopyranoside (**13**, **16** or **19**), kaempferol 3-*O*-(6''-*O*-galloyl)-β-D-glucopyranoside (**13**, **16** or **19**), kaempferol-(2''-*O*-methyl)-4'-*O*-α-D-glucopyranoside (**17**), kaempferol pentoside (**18** and **20**), kaempferol *p*-coumaroylglucoside (**21**, **28**, and **30**), petunidin *p*-coumaroylhexoside acetylpentoside (**22**), kaempferol 3-*O*-glucuronide-6''-*O*-methylester (**23**), malvidin *p*-coumaroylhexoside acetylpentoside (**24**), quercetin 3-*O*-(6''-*O*-*p*-coumaroyl)-β-D-glucopyranoside (**25**), and kaempferol 3-*O*-(6''-*O*-*p*-coumaroyl)-β-D-glucopyranoside (**27**).

Fourteen compounds are described for the first time for the genus: myricetin hexoside (**8** and **9**), kaempferol 3-*O*-(6''-*O*-galloyl)-β-D-glucopyranoside (**13**, **16** or **19**), kaempferol 3-*O*-(2''-*O*-galloyl)-β-D-glucopyranoside (**13**, **16** or **19**), kaempferol-(2''-*O*-methyl)-4'-*O*-α-D-glucopyranoside (**17**), kaempferol pentoside (**18** and **20**), kaempferol *p*-coumaroyl-glucoside (**21**, **28**, and **30**), petunidin *p*-coumaroyl-hexoside acetylpentoside (**22**), kaempferol 3-*O*-glucuronide-6''-*O*-methylester (**23**), and kaempferol 3-*O*-(6''-*O*-*p*-coumaroyl)-β-D-glucopyranoside (**27**). Flavonols, mainly myricetins are characteristic of Mytales (APG, 2016). Although the chemical characterization of *Tibouchina* is extremely scarse, quercetin and isorhamnetin have been the most commonly found flavonols in aerial parts and already identified in *T. ciliaris*, *T. grandiflora*, *T. granulosa, T. lepidota*, *T. paratropica, T. pereirae*, *T. pulchra T. semidecantra*, and *T. urvelleana*. On the other hand, kaempferol has only been found in *T. ciliaris*, *T. pereirae*, and *T. pulchra*. Regarding anthocyanins, malvidin has already been identified in *T. lepidota*, *T. grandiflora*, *T. semidecantra*, and *T. urvelleana*, while petunidin has exclusively been described in *T. granulosa* (Table 2.2). Here, we report for the first time anthocyanins (*i.e.* malvidin and petunidin) in *T. pulchra*.

The most common acyl groups generally found as flavonoid substituents are hydroxycinnamic acids (*e.g.* caffeic, ferulic and *p*-coumaric acids) (Willians 2004). Flavonoids with *p*-coumaroyl group have already been found in *Tibouchina* species, such as *T. ciliaris* (kaempferol 7-*O*-*p*-coumaroyl), *T. grandiflora* (malvidin 3-(*p*-coumaroyl)-sambubioside-5-glucoside), malvidin 3-(*p*-coumaroyl-glucoside)-5-glucoside), and *T. urvilleana* (malvidin 3-*O*-(6-*O*-*p*-coumaryl-β-D-glucopyranoside)-5-*O*-(2-*O*-acetyl-β-D-xylopyranosyl)) (Colorado *et al*. 2007, Lowry *et al*. 1995, Bobbio *et al*. 1985, Terahara *et al*. 1993), this is in agreement with results found in *T. pulchra*.

Acylation with hydroxybenzoic acids, such as gallic acid, is rare in angiosperms because the active production of hydrolysable tannins is restricted to certain orders: Hammamelidales, Fagales, Dilleniales, Theales, Ericales, Rosales, Myrtales, Cornales, Proteales, Sapindales, Geraniales, and Juglandales (Haslam 2007). Tannin occurrence has been described in *Tibouchina* genus (Table 2.1) in at least three species: *T. semidecantra*, *T. pulchra* and *T. multiflora* (Yoshida *et al*. 1991, Furlan 2004, Motta *et al*. 2005, Santos & Furlan 2013, Yoshida *et al*. 1999). Although hydrolysable tannins were not identified neither in *T. ciliaris* nor in *T. granulosa,* the presence of quercetin 6''-*O*-gallate and quercetin 3-(*O*-galloyl)-hexoside (Colorado *et al*. 2007, Sobrinho *et al*. 2017), respectively, is indicative of the existence of this class of metabolites. Here, we found quercetin galloylhexoside and three isomers of kaempferol galloylhexoside (kaempferol-3-*O*-(6''-*O*-galloyl)-β-D-glucopyranoside, kaempferol-3-*O*-(2''-*O*-galloyl)-β-D-glucopyranoside, and one not determined the galloyl position), in agreement with the finding of tannins in *T. pulchra* (Furlan 2004, Motta *et al*. 2005, Santos & Furlan 2013).

Although in Melastomataceae many compounds have been isolated and identified by extensive spectral analyses, considering the size of the family, the number of studied species is still small. Only three of the nine tribes have been chemical investigated (Melastomeae, Miconieae and Sonerileae). The most commonly found natural products in this family belong to terpenoids, simple phenolics, quinones, lignans and their glycosides, flavonoids, as well as a vast range of tannins, mainly hydrolyzable tannins (Serna & Martínez 2015).

Below, according to Serna & Martinéz (2015), we discuss the presence of *T. pulchra* constituents identified by NMR in the context of the natural products fully structural elucidated from Melastomataceae.

The results obtained describe, for the first time, the presence of kaempferol 3-*O*-(6''-*O*-galloyl)-β-D-glucopyranoside (**13**, **16** or **19**), kaempferol 3-*O*-(2''-*O*-galloyl)-β-D-glucopyranoside (**13**, **16** or **19**), kaempferol-(2''-*O*-methyl)-4'-*O*-α-D-glucopyranoside (**17**), kaempferol 3-*O*-glucuronide-6''-*O*-methylester (**23**), and kaempferol 3-*O*-(6''-*O*-*p*-coumaroyl)-β-D-glucopyranoside (**27**) in Melastomataceae. Kaempferol 3-*O*-β-D-(2'',6''-di-*O*-*trans*-coumaroyl)-glucopyranoside was found in *Miconia cabucu* Hoehne and *M. rubiginosa* (Bonpl.) DC. (Rodrigues *et al*. 2007), but usually kaempferol is 7-*O* substituted in this family (Serna & Martinéz 2015). Kaempferol aglycone (**29**) was also found in *Medinilla magnifica* Lindley and *Centradenia floribunda* Planch (Serna & Martinéz 2015).

Regarding anthocyanins, this was the first description of petunidin *p*-coumaroylhexoside acetylpentoside (**22**) in *T. pulchra*, but further studies on this anthocyanin are necessary for its precisely identification, since it was identified by MS and UV analysis. The anthocyanins previously described in Melastomataceae include pelargonidin, cyanidin, peonidin, delphinidin, and malvidin glycosides or acylglycosides. In this work malvidin *p*-coumaroylhexoside acetylpentoside (**24**) was the major anthocyanin in *T. pulchra*, which is in agreement with the proposition of malvidin as the most common anthocyanidin moiety in Melastomataceae (Serna & Martinéz 2015).

4. CONCLUSION

Melastomataceae and, in particular, *Tibouchina* are chemically poorly characterized taxons. Here, out of the sixteen compounds described for the first time in *T. pulchra*, five of them described for the first time in Melastomataceae, moreover an unpublished compound was identified as kaempferol 4′-*O*-(2′′-methyl)-α-D-glucopyranoside. The advances in spectrometric techniques offer a unique opportunity to improve our knowledge about the chemical structure of natural products. Studies about flower anthocyanins are scarce and the understanding of their structure, biosynthesis and the regulatory mechanisms involved in their accumulation pattern can improve our knowledge about plant secondary metabolism, the relationship between flower and pollinators, and bring new insights for future biotechnological applications.

5. REFERENCES

Atoui, A.K., Mansouri, A., Boskou, G. & Kefalas, P. Tea and herbal infusions: Their antioxidant activity and phenolic profile. Food Chemistry. 2005, 89, p. 27–36. DOI:10.1016/j.foodchem.2004.01.075.

BFG [The Brazilian Flora Group]. Growing knowledge: an overview of Seed Plant diversity in Brazil. Rodriguésia. 2015, 66(4): 1085–1113.

Bobbio, F.O., Bobbio, P.A. & Degáspari, C.H. Anthocyanins from *Tibouchina grandiflora*. Food Chem. 1985, 18, 153-159. DOI: 10.1016/0308-8146(85)90138-4.

Braca, A., Politi, M., Sanogo, R., Sanou, H., Morelli, I., Pizza, C. & De Tommasi, N. Chemical composition and antioxidant activity of phenolic compounds from wild and cultivated *Sclerocarya birrea* (Anacardiaceae) leaves. Journal of agricultural and food chemistry. 2003, 51(23), 6689-6695 p. DOI: 10.1021/jf030374m.

Brito, V.L.G., Maia, F.R., Silveira, F.A.O. & Fracasso, C.M. Reproductive phenology of Melastomataceae species with contrasting reproductive systems: contemporary and historical drivers. 2017, 19:806–817. DOI: 10.1111/plb.12591,

Clausing G, Renner S.S. Molecular phylogenetics of Melastomataceae and Memecylaceae: implications for character evolution. American Journal of Botany. 2001, 88(3):486–498. DOI: 10.2307/2657114.

Colorado, A., Maya, D.C., Díaz, G.S.J., Isaza, M.J.H., Tapias, I.L.J., Veloza, L. A., Ramírez, A. L. S. Flavonoides del extracto isopropanol- agua de *Tibouchina ciliaris*. Scientia et Técnica. Universidad Tecnológica de Pereira, Pereira, Colombia, 2007, 3(33): 355-357.

Cunha W.R., dos Santos, F.M., Peixoto, J., Veneziani, E.C.S., Crotti, A.E. M., Silva, M.L.A., da Silva Filho, A.A., Albuquerque, S., Turatti, I.C.C. & Nastos, J.K. 2009. Screening of plant extracts from the Brazilian Cerrado for their in vitro trypanocidal activity. Pharmaceutical Biology. 2009, 47(8): 744–749 p. DOI: 10.1080/13880200902951361.

Cuyckens, F. & Claeys, M. Mass spectrometry in the structural analysis of flavonoids. Journal of Mass Spectrometry. 2004, 39(1), 1–15 p. DOI:10.1002/jms.585

Dos Santos, A.C., & Furlan, C.M. Levels of phenolic compounds in *Tibouchina pulchra* after fumigation with ozone. Atmospheric Pollution Research. 2013, *4*:250–256 p. DOI: 10.5094/APR.2013.027

Dias, Ê.R., Dias, T. de L.M.F., Alexandre-Moreira, M.S., & Branco, A. Antinociceptive activity of *Tibouchina pereirae*, an endemic plant from the Brazilian semiarid region. Zeitschrift Für Naturforschung C. 2016, *71*(7-8):261–265 p. DOI: 10.1515/znc-2015-0155.

Dias, E.R. Estudo fitoquímico e avaliação da atividade biológica de *Tibouchina pereirae* Aubl. (Melastomataceae). Master Dissertation, Universidade Estadual de Feira de Santana. 2013, 80p.

dos Santos, F.M., de Souza, M.G., Miller Crotti, A.E., Martins, C.H. G., Ambrósio, S.R., Veneziani, R.C.S., Andrade e Silva, M. L. & Cunha, W. R. Evaluation of antimicrobial activity of extracts of *Tibouchina candolleana* (melastomataceae), isolated compounds and semi-synthetic derivatives against endodontic bacteria. Brazilian Journal of Microbiology. 2012, *43*(2), 793–799 p. DOI: 10.1590/S1517-83822012000200045.

Ducrey, B., Wolfender, J.L., Marston, A.& Hostettmann, K. Analysis of flavonol glycosides of thirteen *Epilobium* species (Onagraceae) by LC–UV and thermospray LC-MS. Phytochemistry. 1995, 38(1): 129-137 p. DOI: 10.1016/0031-9422(94)00629-8.

Ellison, A.M., Denslow, J.S., Loiselle B.A. & Brénes D.M. Seed and seedling ecology of Neotropical Melastomataceae. Ecology. 1993, 6: 1733–1749 p. DOI: 10.2307/1939932.

Esposito, M.P., Pedroso, A.N.V. & Domingos, M. Assessing redox potential of a native tree from the Brazilian Atlantic Rainforest: A successful evaluation of oxidative stress associated to a new power generation source of an oil refinery. Science of the Total Environment. 2016, 550: 861–870 p. DOI: 10.1016/j.scitotenv.2016.01.196.

Esposito, M.P. & Domingos, M. Establishing the redox potential of *Tibouchina pulchra* (Cham.) Cogn., a native tree species from the Atlantic Rainforest in the vicinity of an oil refinery in SE Brazil. Environmental Science and Pollution Research. 2014, 21: 5484–5495 p. DOI: 10.1007/s11356-013-2453-8.

Furlan, C.M., Moraes, R.M., Bulbovas, P., Sanz, M.J., Domingos, M. & Salatino, A. *Tibouchina pulchra* (Cham.) Cogn., a native Atlantic Forest species, as a bioindicator of ozone: visible injury. Environmental Pollution. 2008, 152: 361–365 p. DOI: 10.1016/j.envpol.2007.06.042.

Furlan, C.M., Salatino, A. & Domingos, M. Influence of air pollution on leaf chemistry, herbivore feeding and gall frequency on *Tibouchina pulchra* leaves in Cubatão (Brazil). Biochemical Systematics and Ecology. 2004, 32(3): 253–263 p. DOI: 10.1016/S0305-1978(03)00176-5.

Furlan, C.M. Efeito de poluentes atmosféricos na composição química de indivíduos jovens de *Tibouchina pulchra* (Cham.) Cong. e *Psidium guajava* L. PhD thesis, Universidade de São Paulo, 2004, 117 p.

Guimarães, P.J.F. Two New Species of *Tibouchina* (Melastomataceae) from Brazil. Novon: A Journal for Botanical Nomenclature. 2014, *23*(1): 42–46 p. DOI: 10.3417/2012029.

Guimarães, P.J.F. *Tibouchina*. Lista de Espécies da Flora do Brasil. Jardim Botânico do Rio de Janeiro. 2016. Available from: http:// floradobrasil.jbrj.gov.br/jabot/floradobrasil/FB19731 (accessed: October 29th 2016).

Guo, D., Xue, W. J., Zou, G.A. & Aisa, H.A. Chemical Composition of *Alhagi sparsifolia* Flowers. Chemistry of Natural Compounds. 2016, 52(6): 1095-1097 p. DOI: 10.1007/s10600-016-1871-5.

Harbone, J.B. Plant Polyphenols- XI. The structure of acilated anthocyanins. Phytochemistry. 1964, 3:151–160 p. DOI: 10.1016/S0031-9422(00)88035-8.

Haslam, E. Vegetable tannins - lessons of a phytochemical lifetime. Phytochemistry. 2007, *68*(22-24), 2713–21 p. DOI: 10.1016/j.phytochem.2007.09.009.

Hendra, R. & Keller, P.A. Flowers in Australia: Phytochemical Studies on the Illawarra Flame Tree and Alstonville. Australian Journal of Chemistry. 2016, 69(8): 925–927 p. DOI: 10.1071/CH16058.

Isobe, T., Ito, N. & Noda, Y. Minor flavonoids of *Polygonum nodosum*. Phytochemistry. 1980, 19(8):1877.

Iwashina T. The structure and distribution of the flavonoids in plants. Journal of Plant Research. 2000, 113(3): 287-299 p. DOI: 10.1007/PL00013940.

Janna, O., Khairul, A. & Maziah, M. Anthocyanin stability studies in *Tibouchina semidecandra* L. Food Chemistry. 2007, 101(4): 1640–1646. DOI: 10.1016/j.foodchem.2006.04.034.

Jiménez, N., Carrillo-Hormaza, L., Pujol, A., Álzate, F., Osorio, E., & Lara-Guzman, O. Antioxidant capacity and phenolic content of commonly used anti-inflammatory medicinal plants in Colombia. Industrial Crops and Products. 2015, *70*, 272–279 p. DOI: 10.1016/j.indcrop.2015.03.050.

Jones, E., Ekundayo, O. & Kingston, D.G.I. Plant anticancer agents. XI. 2, 6-Dimethoxybenzoquinone as a cytotoxic constituent of *Tibouchina pulchra*. Journal of Natural Products. 1981, 44: 493–494 p. DOI: 10.1021/np50016a019.

Joshi, H., Joshi, A.B., Gururaj, M.P. & Sati, H. (2009). Flavonoids of *Memecylon umbellatum* (Burm.). Asian Journal of Chemistry. 2009, 21(2): 1639.

Jung, H.A., Kim, J.E., Chung, H.Y. & Choi, J.S. Antioxidant principles of *Nelumbo nucifera* stamens. Archives of pharmacal research. 2003, 26(4): 279-285. DOI: 10.1007/BF02976956.

Klumpp, G., Furlan, C.M., Domingos, M. & Klumpp, A. Response of stress indicators and growth parameters of *Tibouchina pulchra* Cogn. exposed to air and soil pollution near the industrial complex of Cubatão, Brazil. Science of The Total Environment. 2000, 246: 79–91 p. DOI: 10.1016/S0048-9697(99)00453-2.

Kuster, R.M., Arnold, N. & Wessjohann, L. Anti-fungal flavonoids from *Tibouchina grandifolia*. Biochemical Systematics and Ecology. 2009, *37*(1): 63–65 p. DOI: 10.1016/j.bse.2009.01.005.

Kyekyeku, J., Adosraku, R. & Asare–Nkansah, S. LC–HRESI–MS/MS Profiling of Flavonoids from *Chlorophora regia* (Moraceae). British Journal of Pharmaceutical Research. 2017, 16(1):1–9 p. DOI: 10.9734/BJPR/2017/32893.

Lavault, M. & Richomme, P. Constituents of *Helichrysum stoechas* variety *olonnense*. Chemistry of natural compounds. 2004, 40(2): 118-121 p.DOI: 10.1023/B:CONC.0000033925.00693.7b.

Ma, Y.L., Li, Q.M., Van den Heuvel, H.& Claeys, M. Characterization of flavone and flavonol aglycones by collision-induced dissociation tandem mass spectrometry. Rapid Communications Mass Spectrometry. 1997, 11(12): 1357-1364 p. DOI: 10.1002/(SICI)1097-0231(199708)11:12<1357:AID-RCM983>3.0.CO,2-9.

Mahmoud, I.I., Marzouk, M.S.A., Moharram, F.A., El-Gindi, M.R. & Hassan, A.M.K. Acylated flavonol glycosides from *Eugenia jambolana* leaves. Phytochemistry. 2001, 58(8): 1239-1244. DOI: 10.1016/S0031-9422(01)00365-X.

Markham, K.R. Techniques of Flavonoid Identification. Academic Press: London, 1982.

Michelangeli, F.A., Guimaraes, P.J.F., Penneys, D.S., Almeda, F., Kriebel, R. Phylogenetic relationships and distribution of New World Melastomeae (Melastomataceae). Botanical Journal of the Linnean Society. 2013, 171(1): 38–60. DOI: 10.1111/j.1095-8339.2012.01295.x.

Motta, L.B., Kraus, J.E., Salatino, A. & Salatino, M.L.F. (2005). Distribution of metabolites in galled and non-galled foliar tissues of *Tibouchina pulchra*. Biochemical Systematics and Ecology. 2012, 33(10): 971–981. DOI: 10.1016/j.bse.2005.02.004.

Mpalantinos, M.A., Pereira, N.A., Parente, J.P. & Kuste, R.M. Hispidulina-7-*O*-B-glucoside, the main constituent of the aqueous extract of *Tibouchina granulosa*. Abstract 8th Brazilian Meeting of Organic Synthesis, Sao Pedro, Brazil. 1988.

Nikaido, T., Ohmoto, T. & Sankawa, U. Inhibitors of adenosine 3', 5'-cyclic monophosphate phosphodiesterase in Daphne genkwa Sieb. et Zucc. Chemical and pharmaceutical bulletin. 1987, 35(2), 675-681. DOI: 10.1248/cpb.35.675.

Niño, J., Espinal, C.M., Mosquera, O.M. & Correa, Y.M. Antimycotic activity of 20 plants from Colombian flora. Pharmaceutical Biology. 2003, 41(7): 491–496. DOI: 10.1080/13880200308951341.

Okumura, F., Soares, M., Barbosa H.F., Cavalheiro & Gomes, E.T. Identificação de pigmentos naturais de espécies vegetais utilizando-se cromatografia em papel. Química Nova. 2002, *25*(4): 680-683. DOI: 10.1590/S0100-40422002000400025.

Pedroso, A.N.V., Bussotti, F., Papini, A., Tani, C. & Domingos, M. Pollution emissions from a petrochemical complex and other environmental stressors induce structural and ultrastructural damage in leaves of a biosensor tree species from the Atlantic Rain Forest. Ecological Indicators. 2016, *67*: 215–226. DOI: 10.1016/j.ecolind.2016.02.054.

Pérez-Castorena, A.L. Triterpenes and other metabolites from *Tibouchina urvilleana*. Journal of the Mexican Chemical Society. 2014, *58*(2), 218–222.

Renner, S. S. Phylogeny and classification of the Melastomataceae and memecylaceae. Nordic Journal of Botany. 1993, 13(5): 519–593. DOI: 10.1111/j.1756-1051.1993.tb00096.x.

Rodrigues, J., Rinaldo, D., dos Santos, L.C. & Vilegas, W. An unusual linked flavonoid from *Miconia cabucu* (Melastomataceae). Phytochemistry. 2007, 68: 1781–1784. DOI: 10.1016/j.phytochem.2007.04.020.

Scheer, T. & Wichtl, M. Zum Vorkommen von Kämpferol-4'-*O*-β-D-glucopyranosid in *Filipendula ulmaria* und *Allium* cepa1. Planta medica. 1987, 53(06):573-574. DOI: 10.1055/s-2006-962817.

Serna, D.M. O. & Martínez, J.H.I. Phenolics and polyphenolics from melastomataceae species. Molecules. 2015, 20(10): 17818–17847. DOI: 10.3390/molecules201017818.

Singha, U.K., Guru, P.Y., Sen, A.B.& Tandon J. S. Antileishmanial activity of traditional plants against *Leishmania donovani* in Golden hamsters. International Journal of Pharmacognosy. 1992, 30: 289–295. DOI: 10.3109/13880209209054015.

Sirat, H.M., Rezali, M.F. & Ujang, Z. Isolation and identification of radical scavenging and tyrosinase inhibition of polyphenols from *Tibouchina semidecandra* L. Journal of Agricultural and Food Chemistry. 2010, 58(19): 10404–10409. DOI: 10.1021/jf102231h.

Sobrinho, A.P., Minho, A. S., Ferreira, L.L., Martins, G.R., Boylan, F. & Fernandes, P.D. Characterization of anti-inflammatory effect and possible mechanism of action of *Tibouchina granulosa*. Journal of Pharmacy and Pharmacology. 2017, 69(6): 706-713. DOI: 10.1111/jphp.12712.

Tamura, H., Hayashi, Y., Sugisawa, H. & Kondo, T. Structure determination of acylated anthocyanins in muscat baily A grapes by homonuclear Hartmann–Hahn (HOHAHA) spectroscopy and liquid chromatography–mass spectrometry. Phytochemical Analysis. 1994, 5: 190-196. DOI: 10.1002/pca.2800050404.

Terahara, N., Suzuki, H., Toki, K., Kuwano, H., Saito, N., Honda, T. J. A diacylated anthocyanin from *Tibouchina urvilleana* flowers. Journal of Natural Products. 1993, 56: 335-340.DOI: 10.1021/np50093a004.

Tracanna, M.I., Fortuna, A.M., Contreras Cárdenas, A.V., Marr, A.K., McMaster, W.R., Gõmez-Velasco, A., Sánchez Arreola, E., Hernández, L.R. & Bach, H. Anti-Leishmanial, anti-inflammatory and antimicrobial activities of phenolic derivatives from *tibouchina paratropica*. Phytotherapy Research. 2015, 29(3), 393–397. DOI: 10.1002/ptr.5263.

Tropicos.org. Missouri Botanical Garden, St. Louis, Missouri. 2013. Available from: http://www.tropicos.org. Accessed in: August 27th 2017.

Wang, H., Race, E. J. & Shrikhande, J. Characterization of anthocyanins in grape juices by ion trap liquid chromatography–Mass Spectrometry. Journal of Agricultural and Food Chemistry. 2003, 51(7):1839-1844. DOI: 10.1021/jf0260747.

Wahab, A., Begum, S., Ayub, A., Mahmood, I., Mahmood, T., Ahmad, A. & Fayyaz, N. Luteolin and kaempferol from *Cassia alata*, antimicrobial and antioxidant activity of its methanolic extracts. FUUAST Journal of Biology. 2014, 4(1):1.

Wei, Y., Xie, Q., Fisher, D. & Sutherland, I.A. Separation of patuletin-3-*O*-glucoside, astragalin, quercetin, kaempferol and isorhamnetin from *Flaveria bidentis* (L.) Kuntze by elution-pump-out high-performance counter-current chromatography. Journal of Chromatography A. 2011, 1218(36): 6206-6211. DOI: 10.1016/j.chroma.2011.01.058.

Yoshida, T., et al. Tannins and related polyphenols of Melastomataceous plants I. Hydrolyzable tannins from *Tibouchina semidecandra* Cogn. Chemical and Pharm aceutical Bulletin 1991, 39: 2233–2240. DOI: 10.1248/cpb.39.2233.

Yoshida, T., Amakura, Y., Yokura, N., Ito, H., Isaza, J. H., Ramírez, S., Pelaez, D. P. & Renner, S. S. Oligomeric hydrolyzable tannins from *Tibouchina multiflora*. Phytochemistry. 1999, 52: 1661–1666. DOI: 10.1016/S0031-9422(99)00329-5.

Zampieri, M.C.T., Sarkis, J.E.S., Pestana, R.C.B., Tavares, A.R. & Melo-de-Pinna, G.F.A. Characterization of *Tibouchina granulosa* (Desr.) Cong. (Melastomataceae) as a biomonitor of air pollution and quantification of particulate matter adsorbed by leaves. Ecological Engineering. 2013, 61: 316–327. DOI: 10.1016/j.ecoleng.2013.09.050.

6. SUPPLEMENTAL MATERIAL

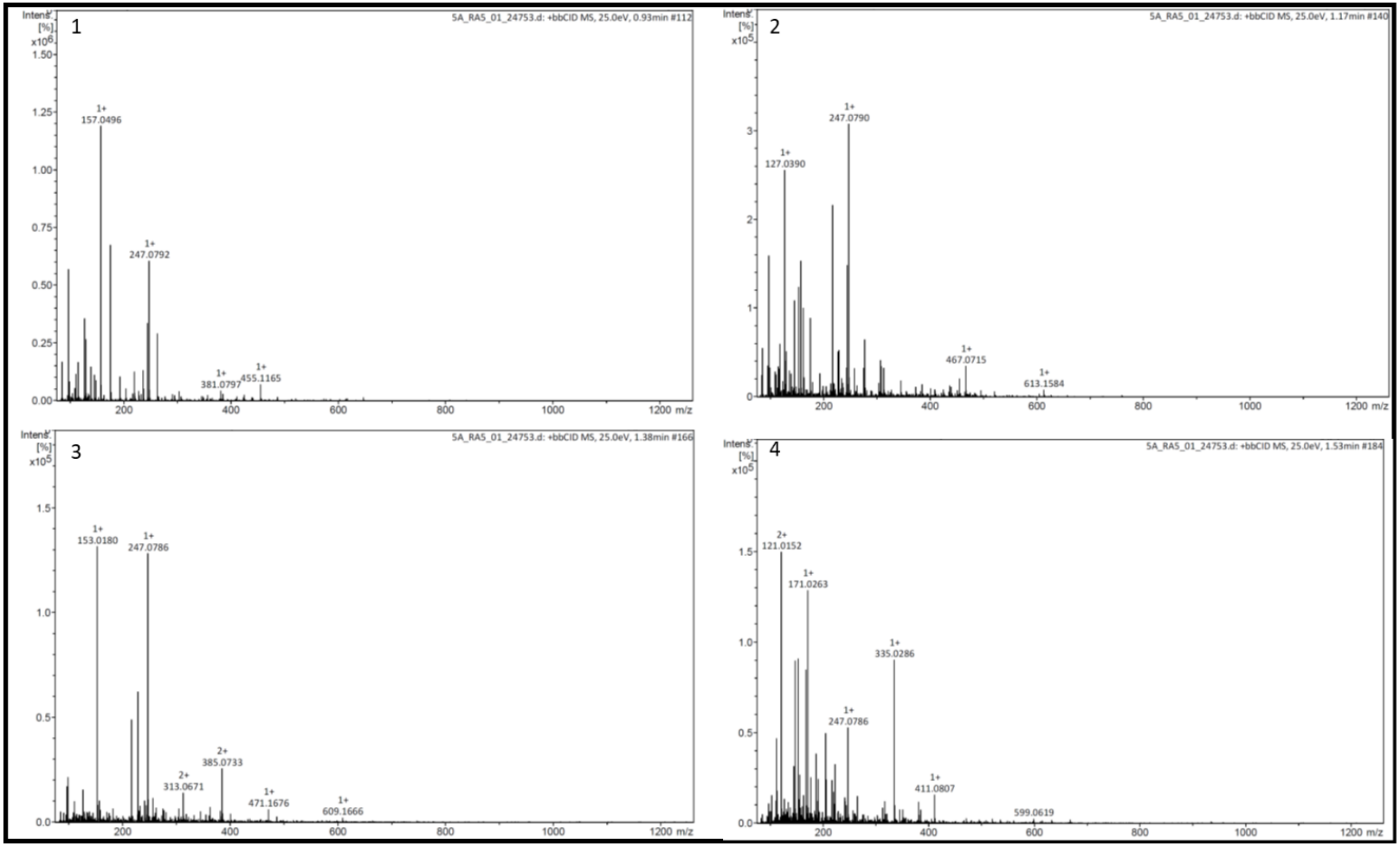

Supplemental Figure 2.1. MS^+ spectra of compounds **1**, **2**, **3**, and **4**.

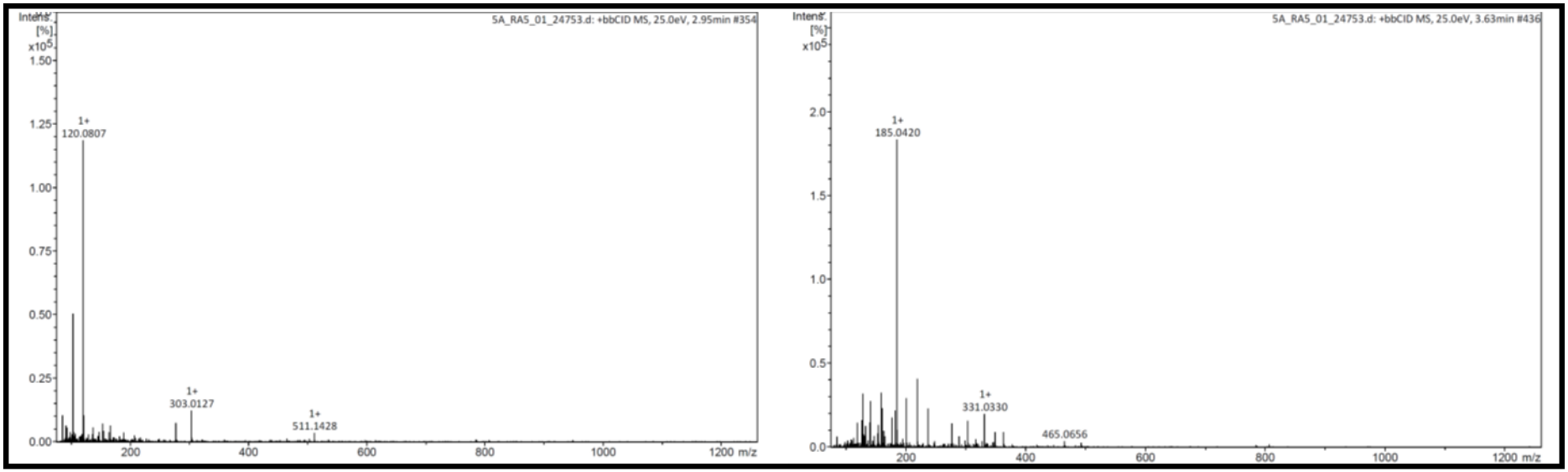

Supplemental Figure 2.2. MS^+ spectra of compounds **5** and **6**.

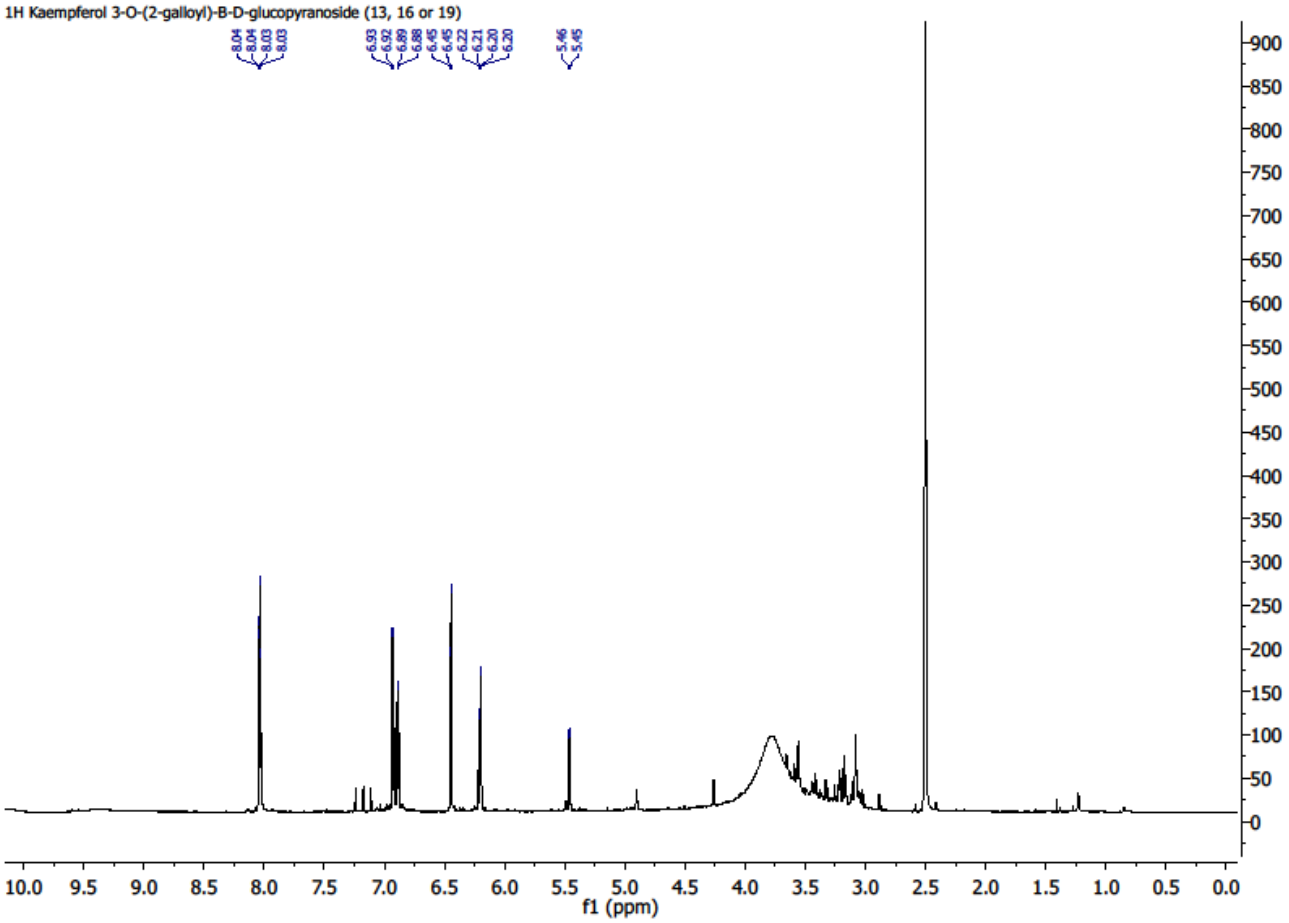

Supplemental Figure 2.3. ^{1}H spectra (DMSO-*d*6) of kaempferol 3-*O*-(2′′-galloyl)-β-D-glucopyranoside (**13**, **16** or **19**).

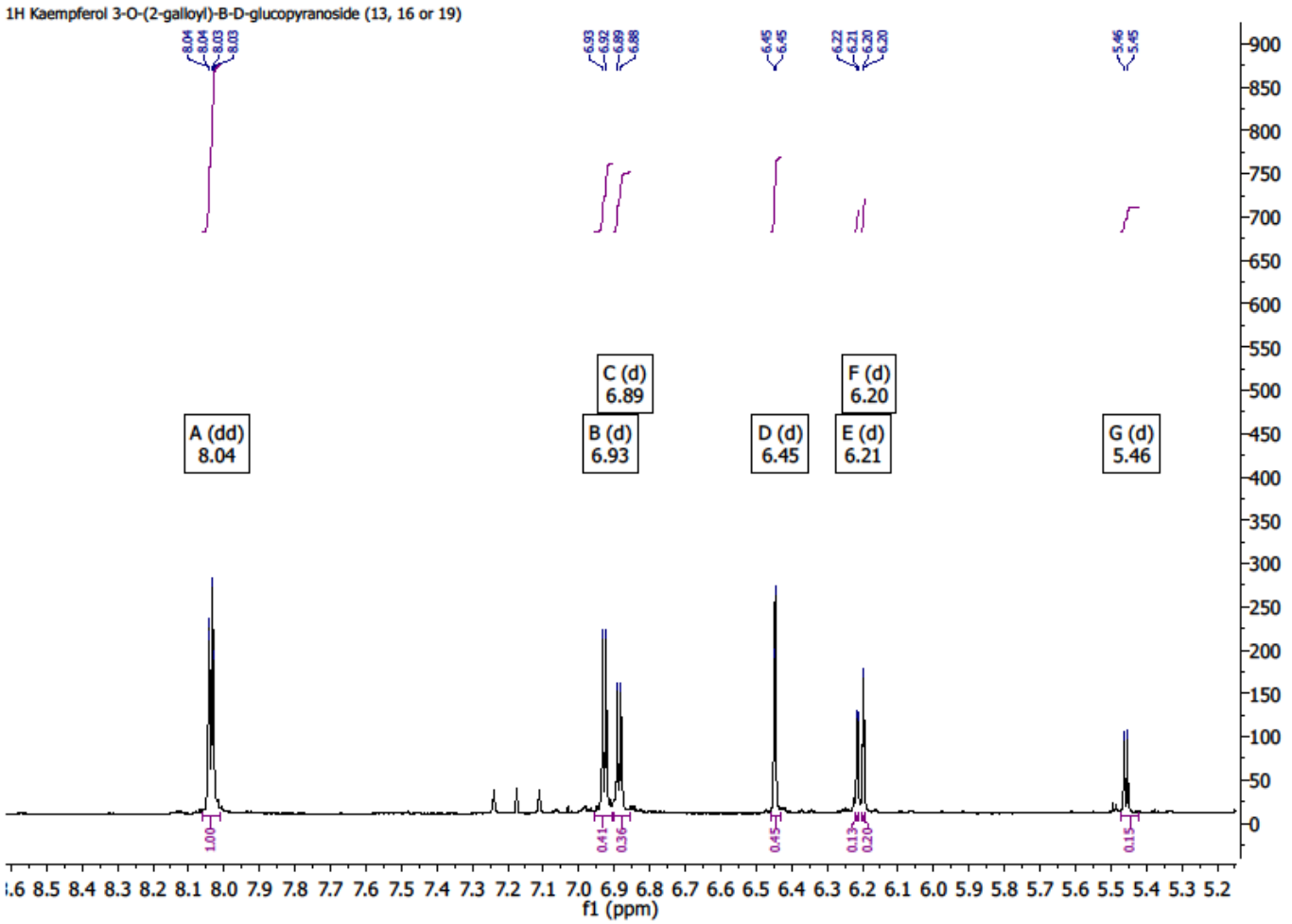

Supplemental Figure 2.4. Zoom from 5.2 to 8.5 ppm, ^{1}H spectra (DMSO-*d*6) of kaempferol 3-*O*-(2′′-galloyl)-β-D-glucopyranoside (**13**, **16** or **19**).

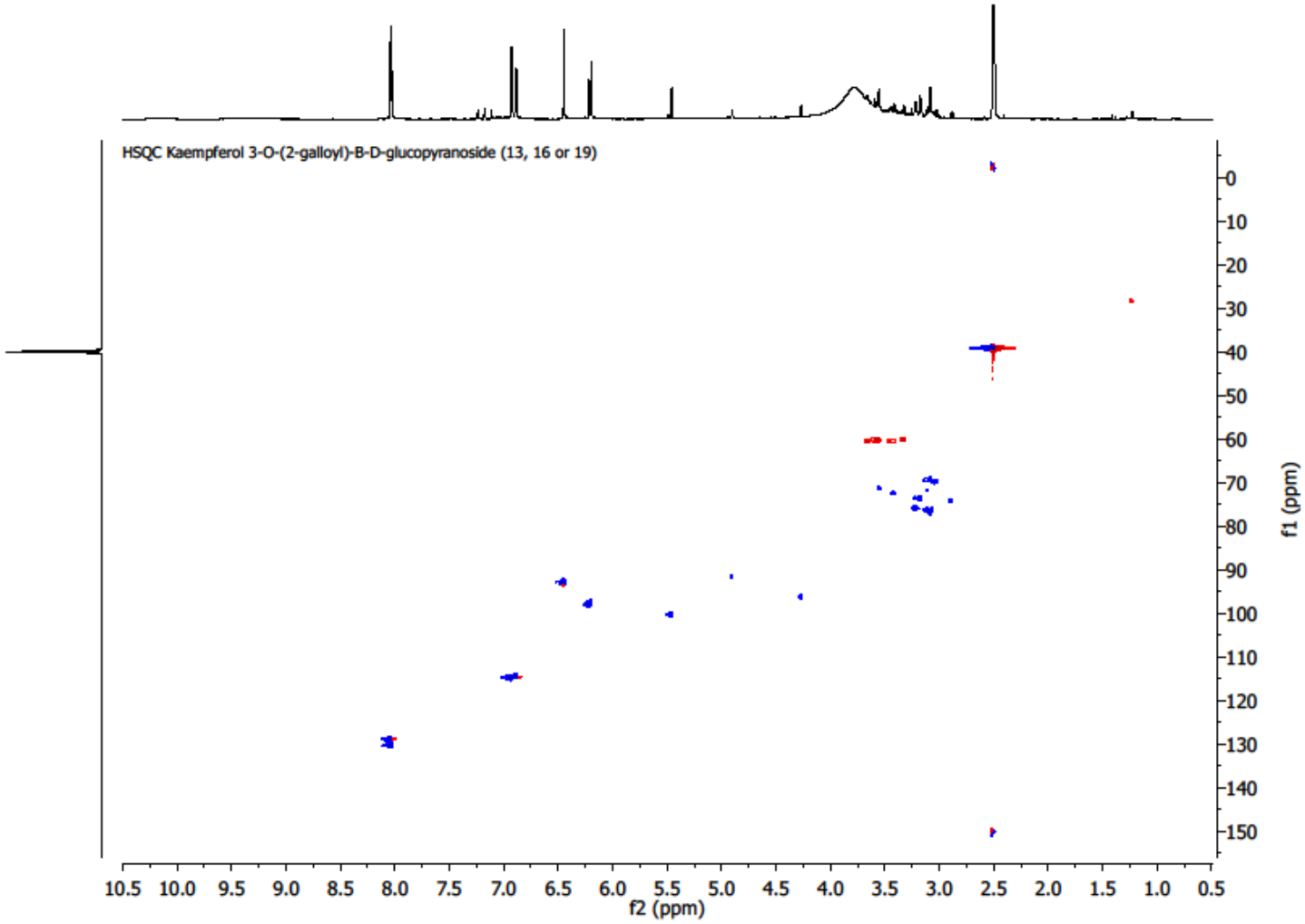

Supplemental Figure 2.5. HSQC spectra (DMSO-*d*6) of kaempferol 3-*O*-(2′′-galloyl)-β-D-glucopyranoside (**13**, **16** or **19**).

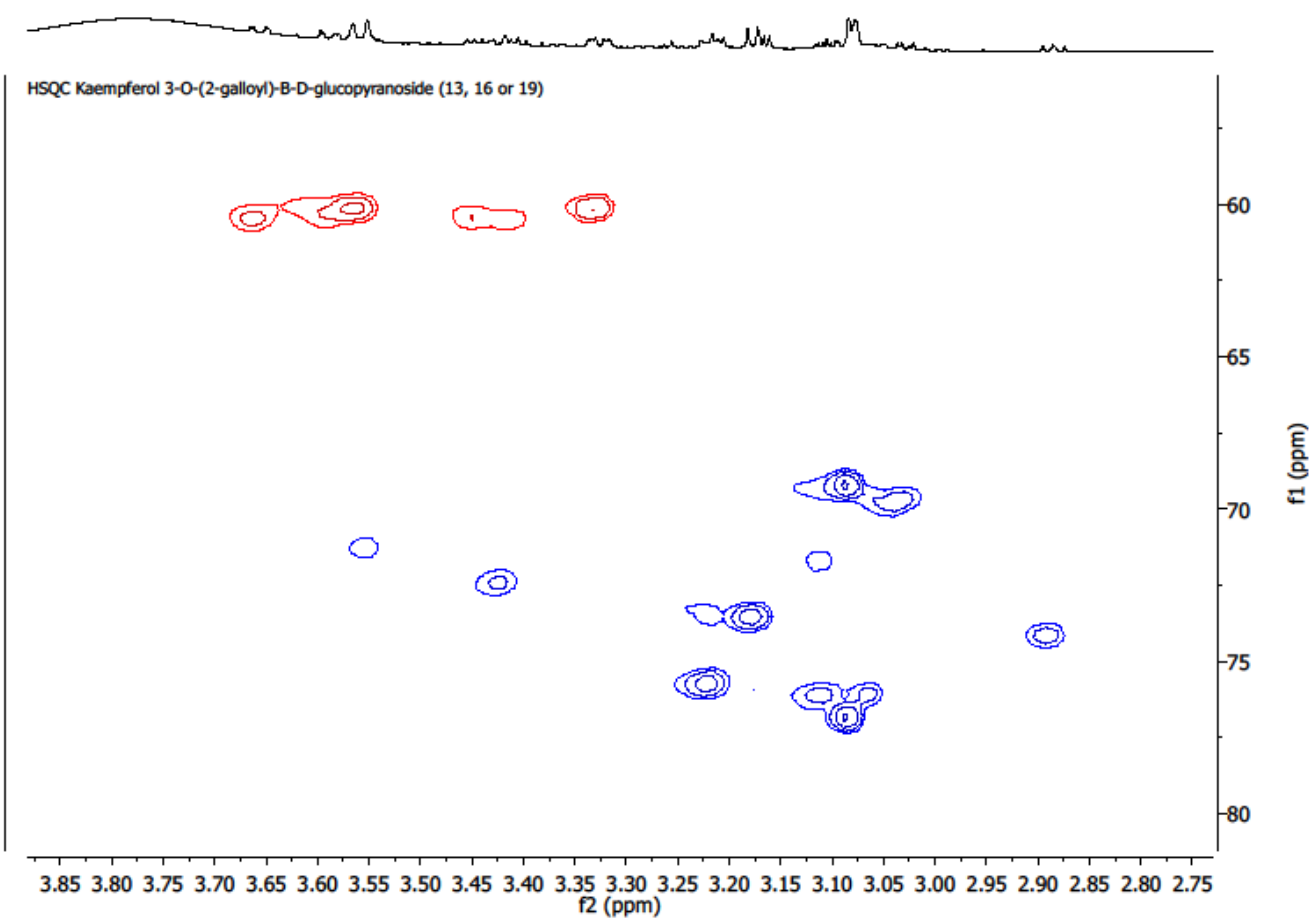

Supplemental Figure 2.6. Zoom from 2.7 to 3.8 ppm, HSQC spectra (DMSO-*d*6) of kaempferol 3-*O*-(2''-galloyl)-β-D-glucopyranoside (**13**, **16** or **19**).

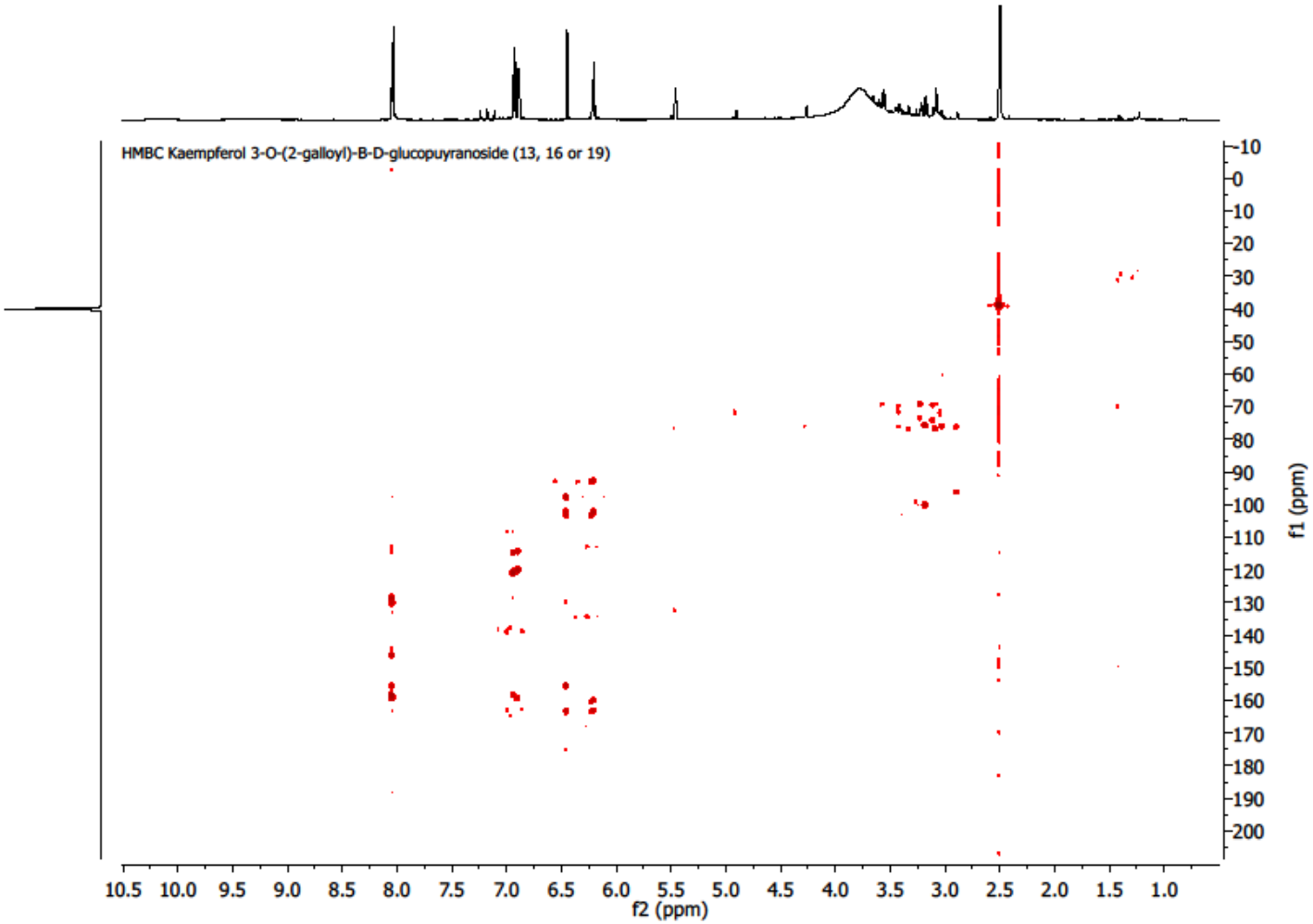

Supplemental Figure 2.7. HMBC spectra (DMSO-*d*6) of kaempferol 3-*O*-(2''-galloyl)-β-D-glucopyranoside (**13**, **16** or **19**).

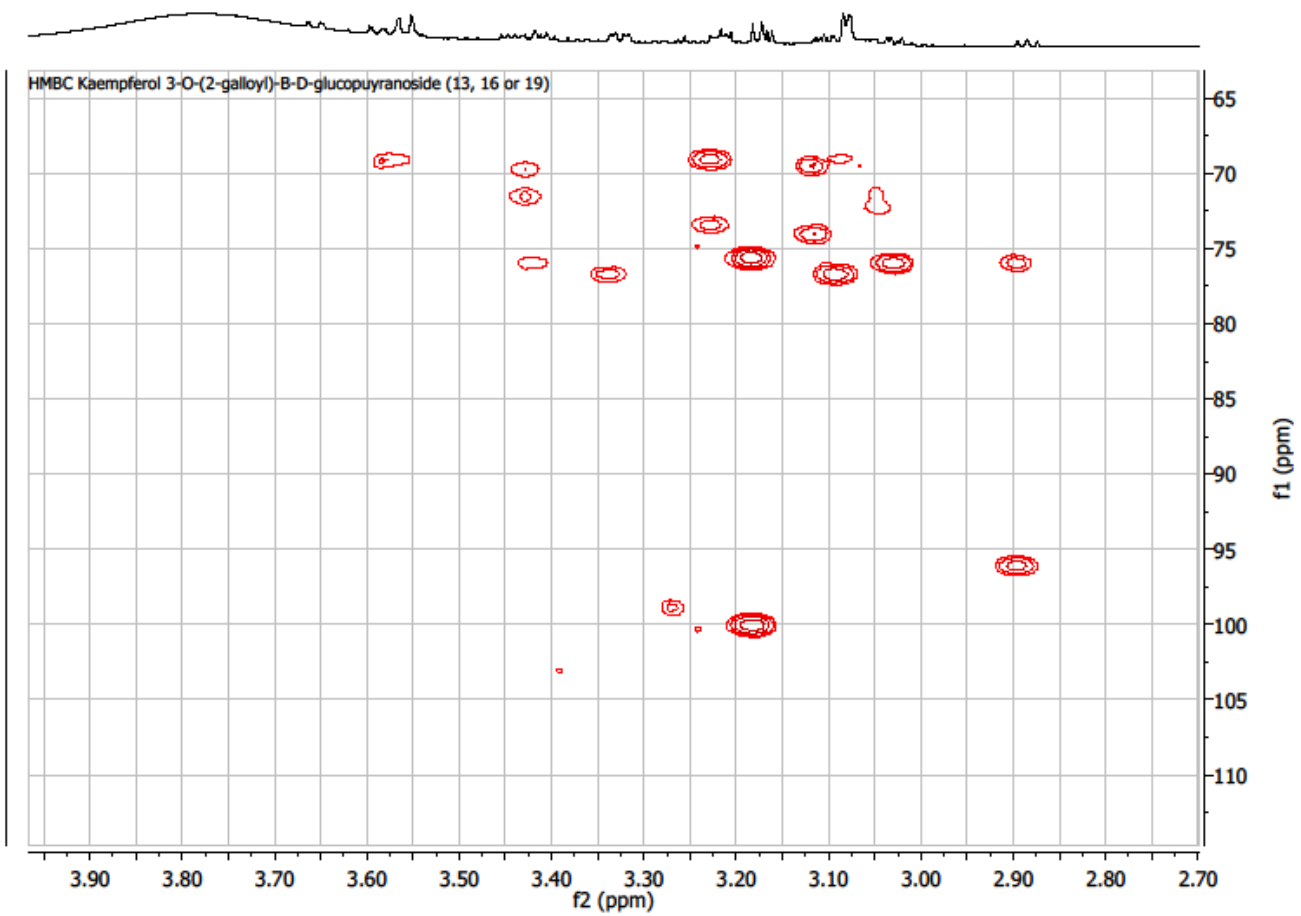

Supplemental Figure 2.8. Zoom from 2.7 to 3.9 ppm, HMBC spectra (DMSO-*d*6) of kaempferol 3-*O*-(2''-galloyl)-β-D-glucopyranoside (**13**, **16** or **19**).

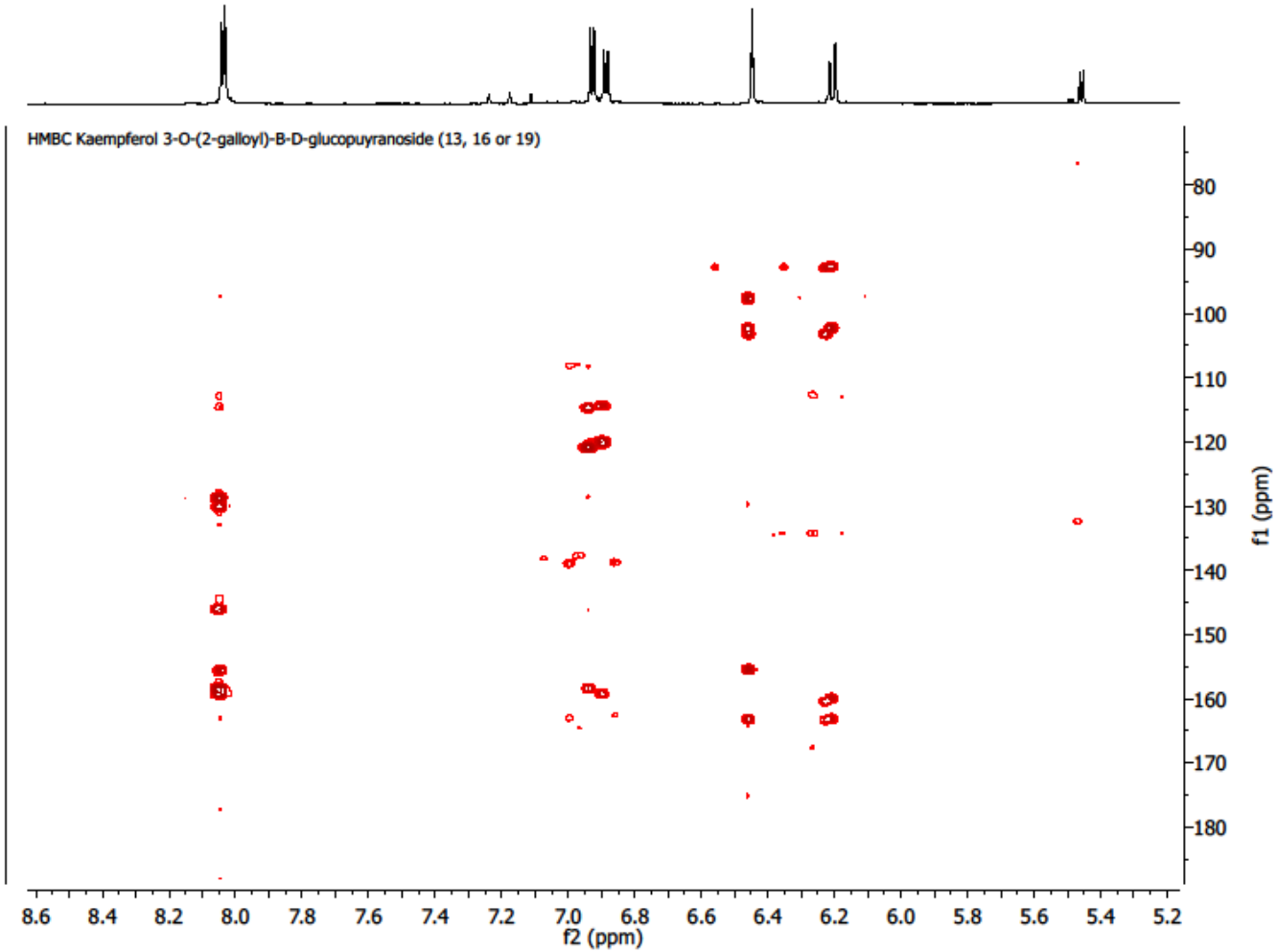

Supplemental Figure 2.9. Zoom from 5.2 to 8.6 ppm, HMBC spectra (DMSO-*d*6) of kaempferol 3-*O*-(2''-galloyl)-β-D-glucopyranoside (**13**, **16** or **19**).

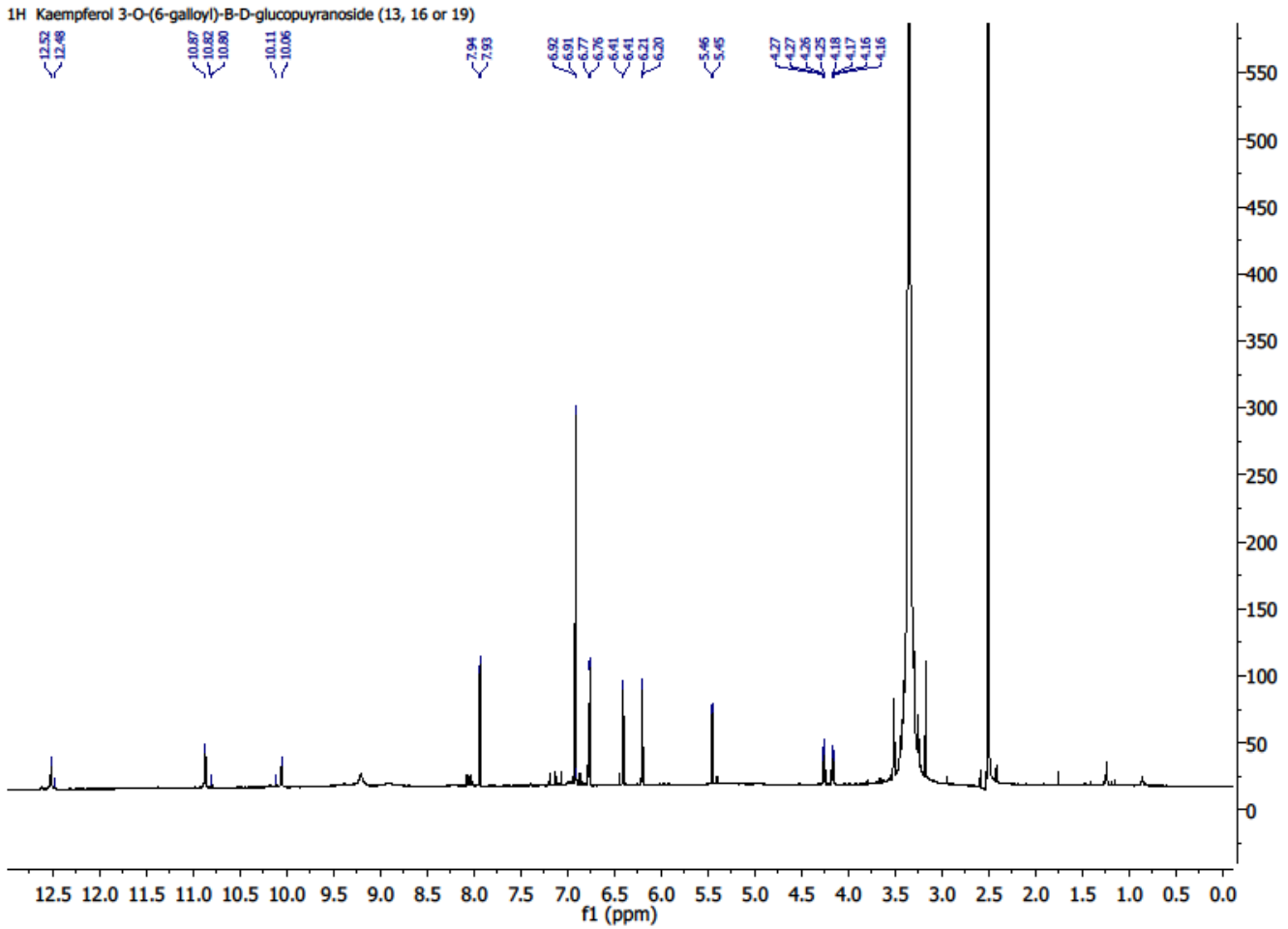

Supplemental Figure 2.10. ^{1}H spectra (DMSO-*d*6) of kaempferol 3-*O*-(6′′-galloyl)-β-D-glucopyranoside (**13**, **16** or **19**).

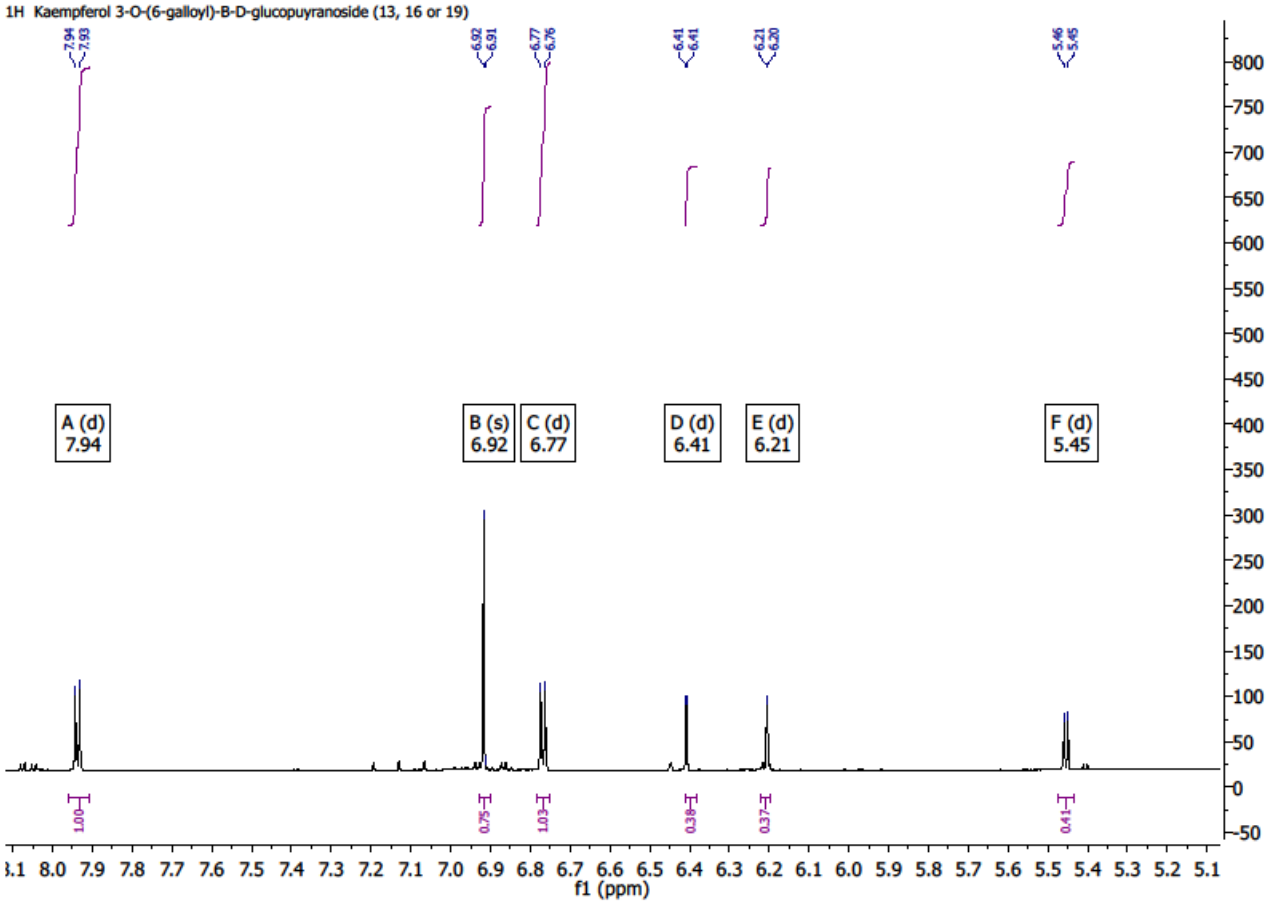

Supplemental Figure 2.11. Zoom from 5.1 to 8.1 ppm, ^{1}H spectra (DMSO-*d*6) of kaempferol 3-*O*-(6''-galloyl)-β-D-glucopyranoside (**13**, **16** or **19**).

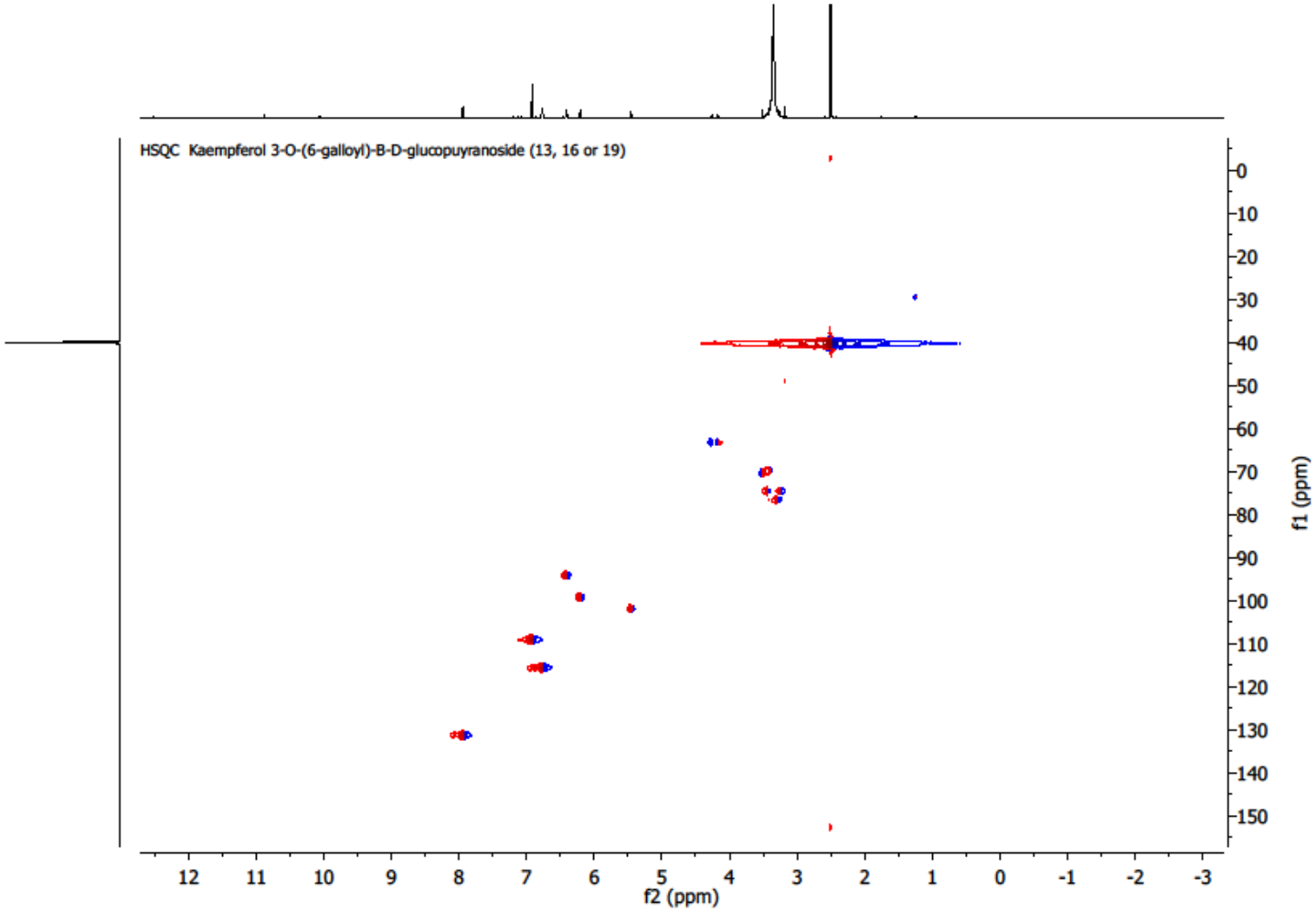

Supplemental Figure 2.12. HSQC spectra (DMSO-*d*6) of kaempferol 3-*O*-(6′′-galloyl)-β-D-glucopyranoside (**13**, **16** or **19**).

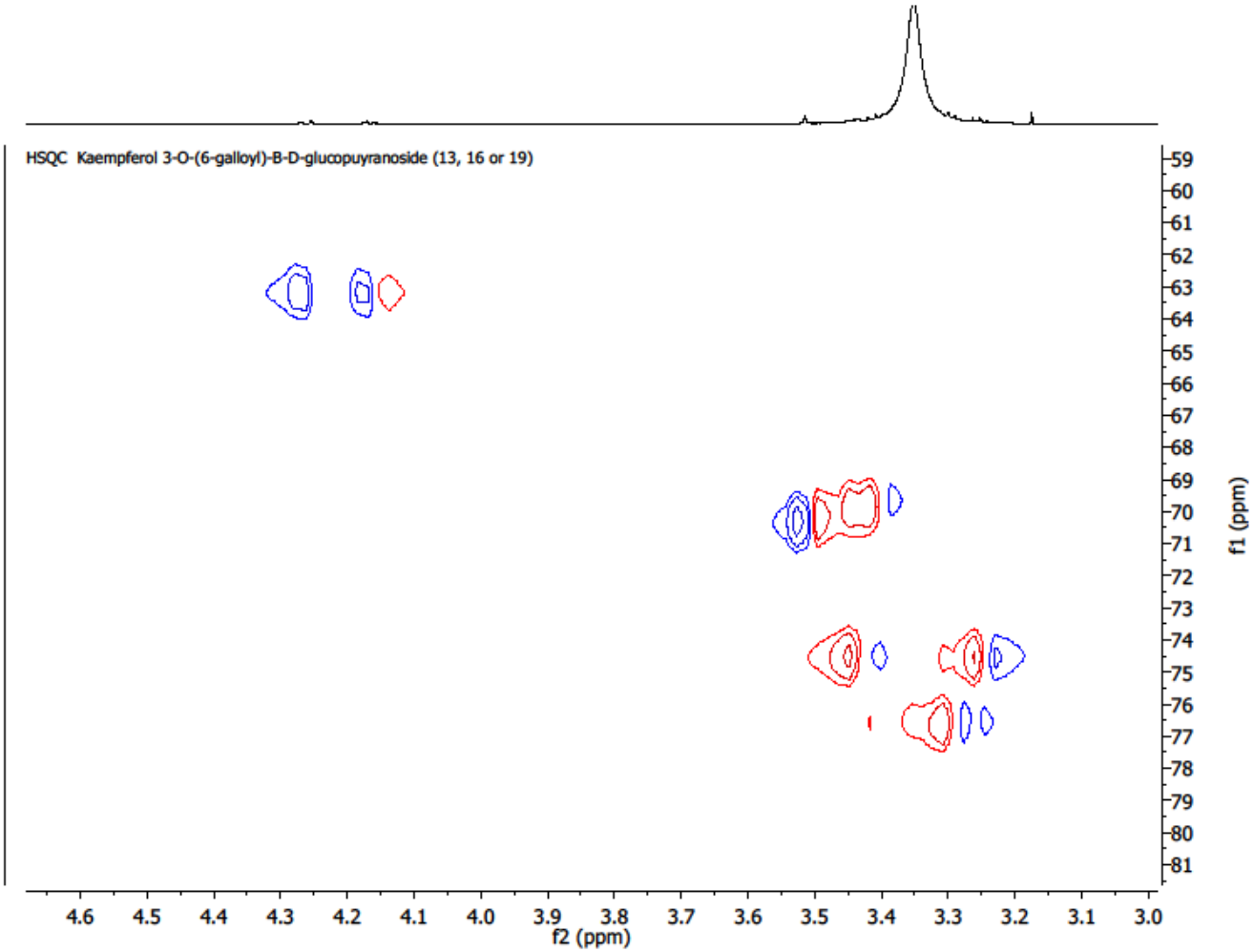

Supplemental Figure 2.13. Zoom from 3.0 to 4.6 ppm, HSQC spectra (DMSO-*d*6) of kaempferol 3-*O*-(6''-galloyl)-β-D-glucopyranoside (**13**, **16** or **19**).

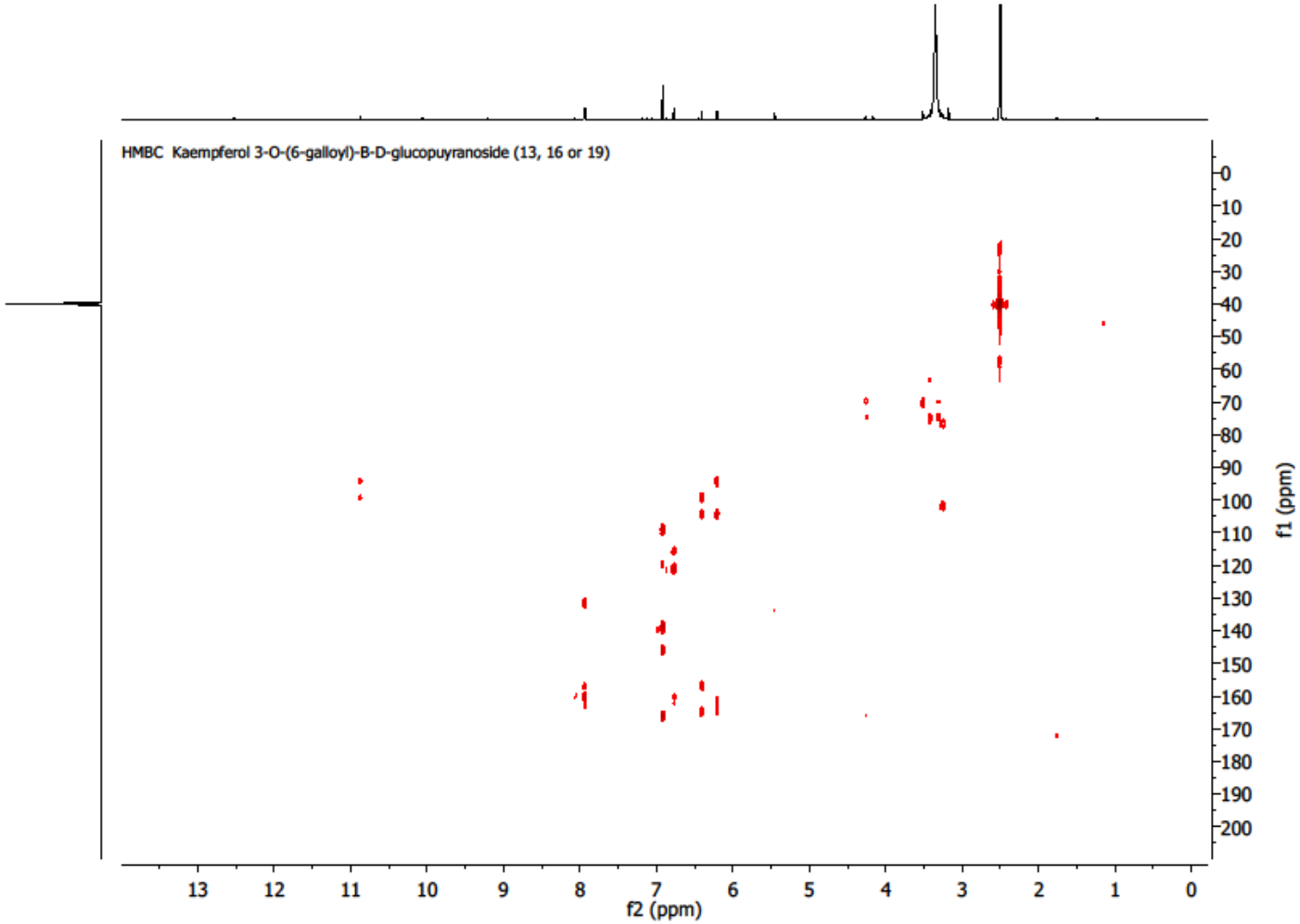

Supplemental Figure 2.14. HMBC spectra (DMSO-*d*6) of kaempferol 3-*O*-(6''-galloyl)-β-D-glucopyranoside (**13**, **16** or **19**).

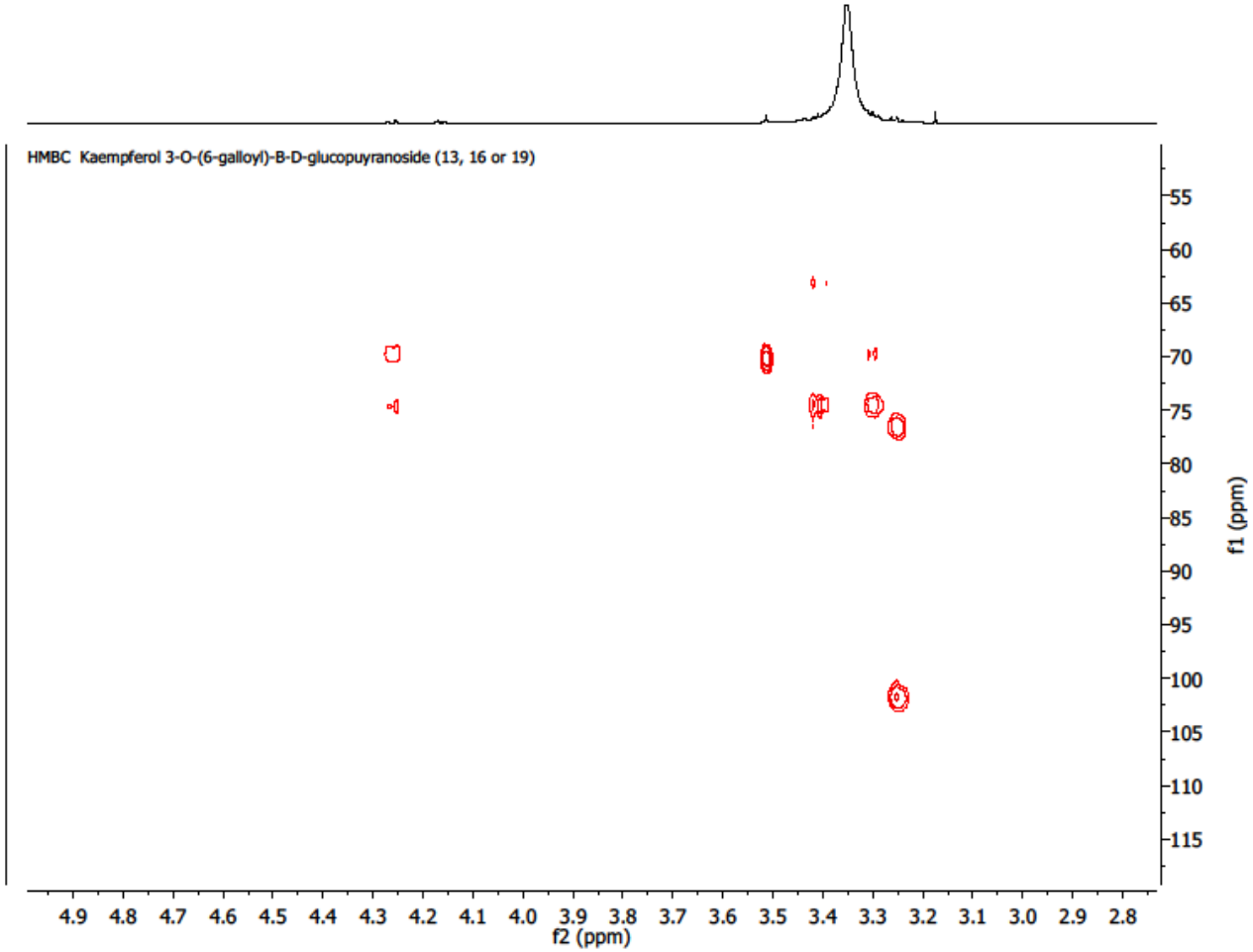

Supplemental Figure 2.15. Zoom from 2.8 to 4.9 ppm, HMBC spectra (DMSO-*d*6) of kaempferol 3-*O*-(6''-galloyl)-β-D-glucopyranoside (**13**, **16** or **19**).

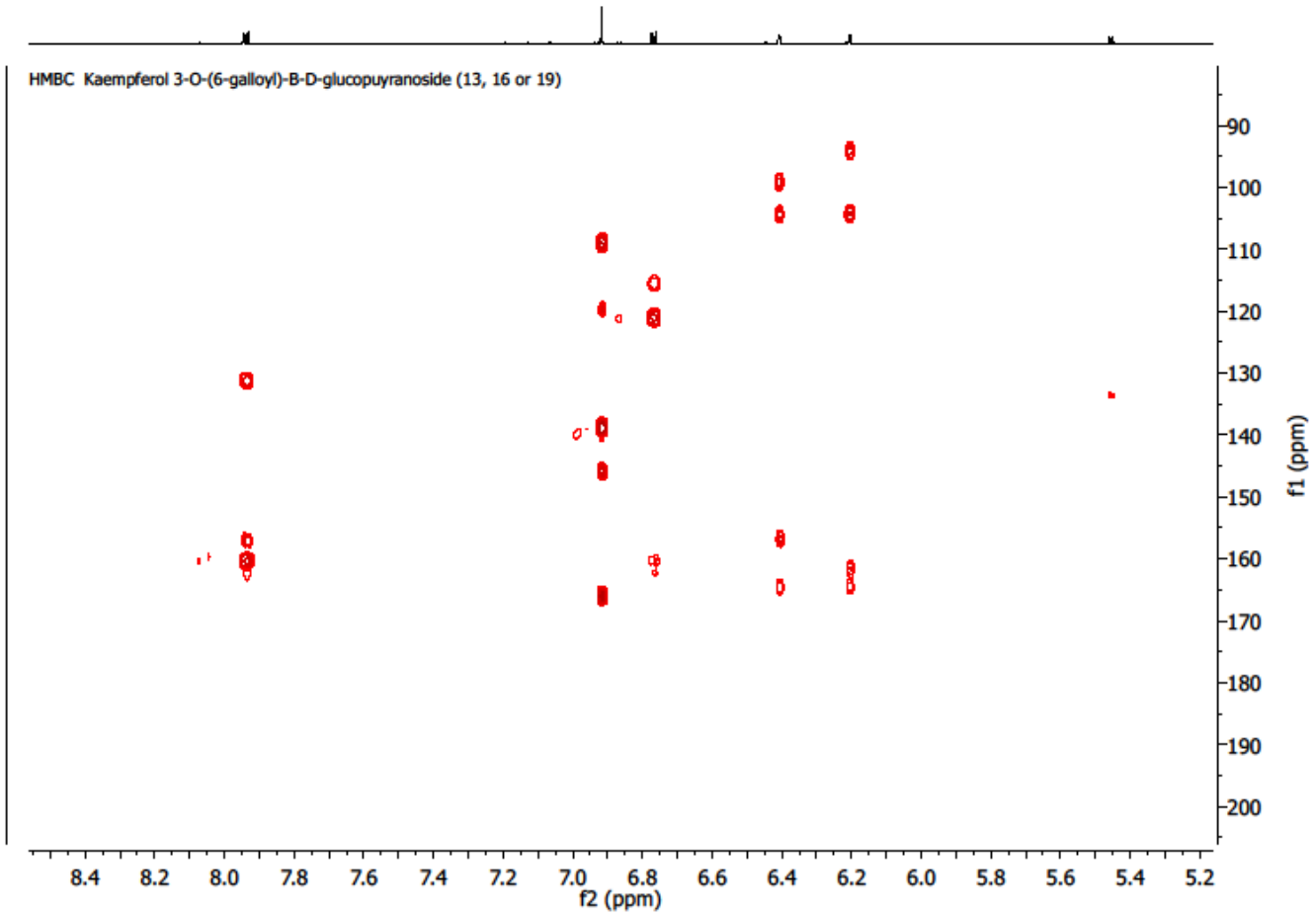

Supplemental Figure 2.16. Zoom from 5.2 to 8.4 ppm, HMBC spectra (DMSO-*d*6) of kaempferol 3-*O*-(6''-galloyl)-β-D-glucopyranoside (**13**, **16** or **19**).

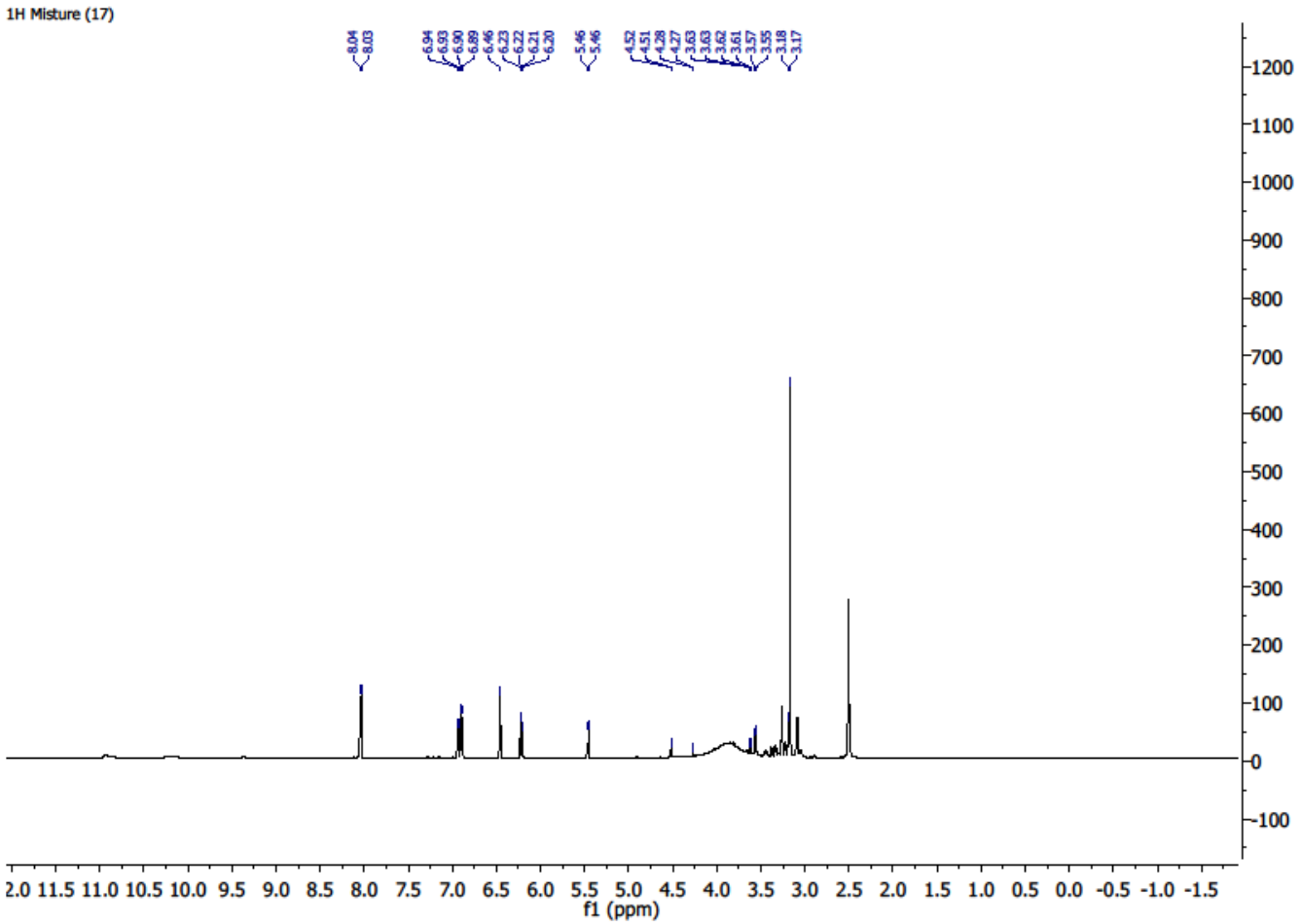

Supplemental Figure 2.17. ^{1}H spectra (DMSO-*d*6) of mixture (**17**).

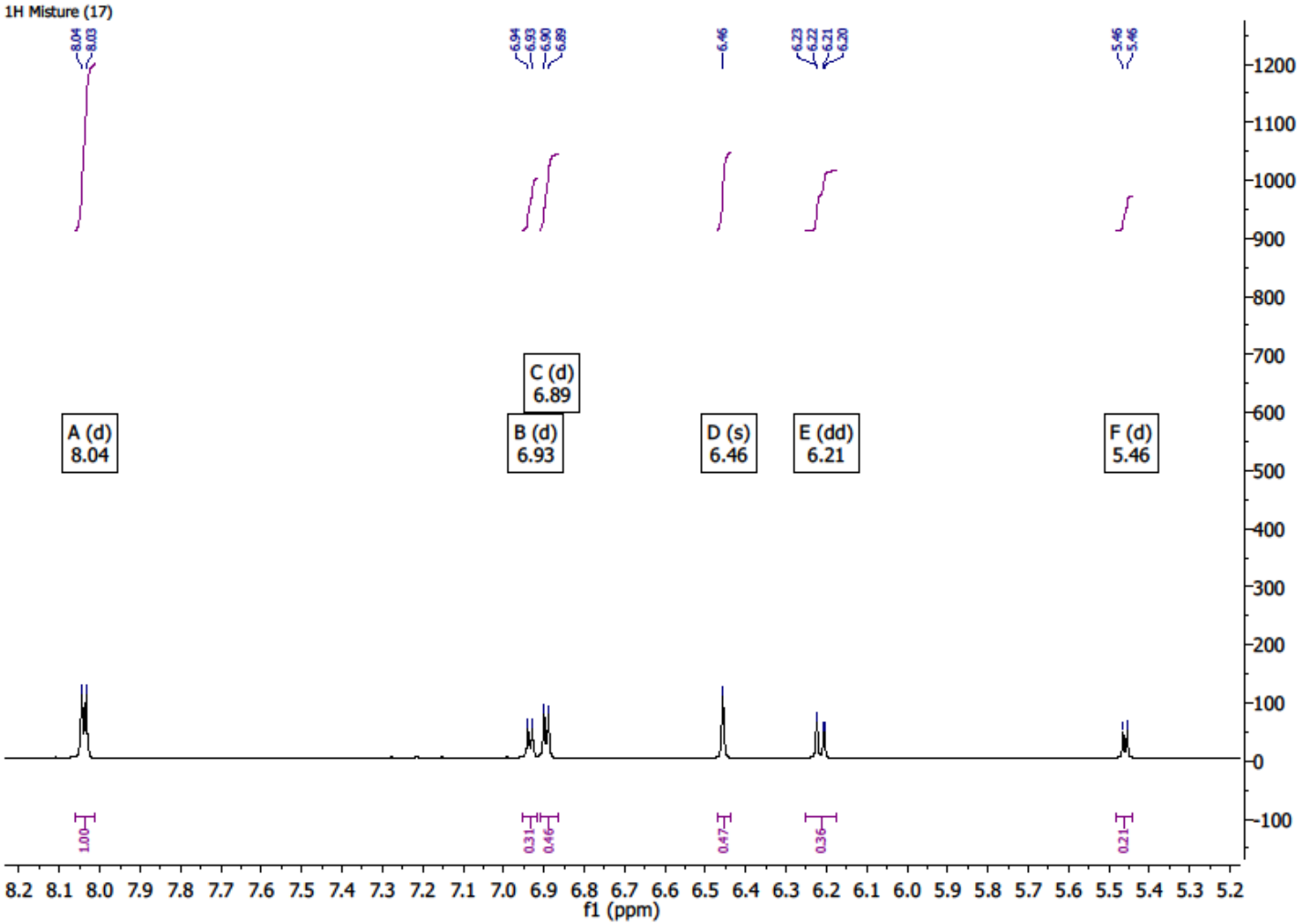

Supplemental Figure 2.18. Zoom from 5.2 to 8.2 ppm, ^{1}H spectra (DMSO-*d*6) of mixture (**17**).

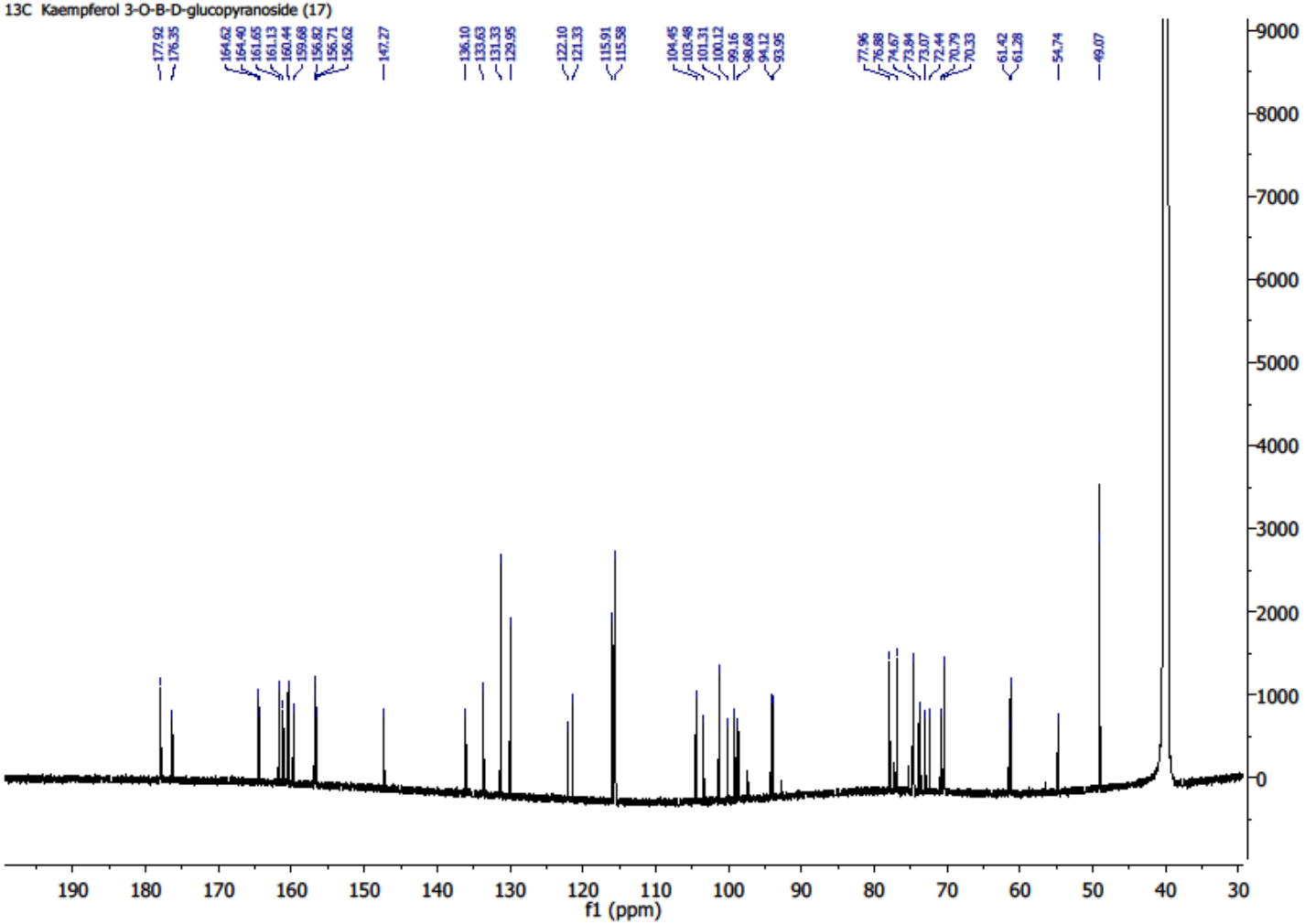

Supplemental Figure 2.19. ^{13}C spectra (DMSO-*d*6) of mixture (**17**).

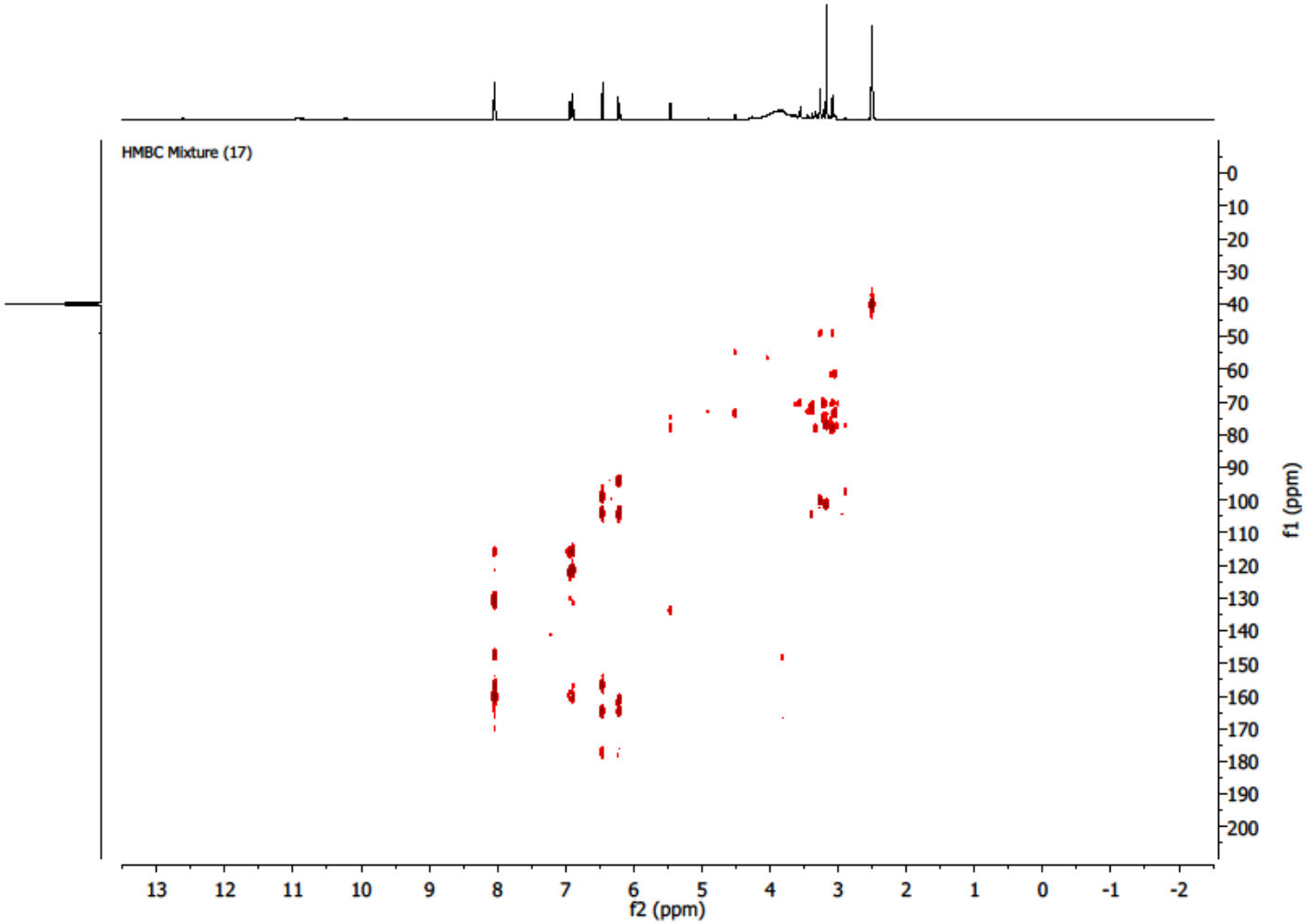

Supplemental Figure 2.20. HMBC spectra (DMSO-*d*6) of mixture (**17**).

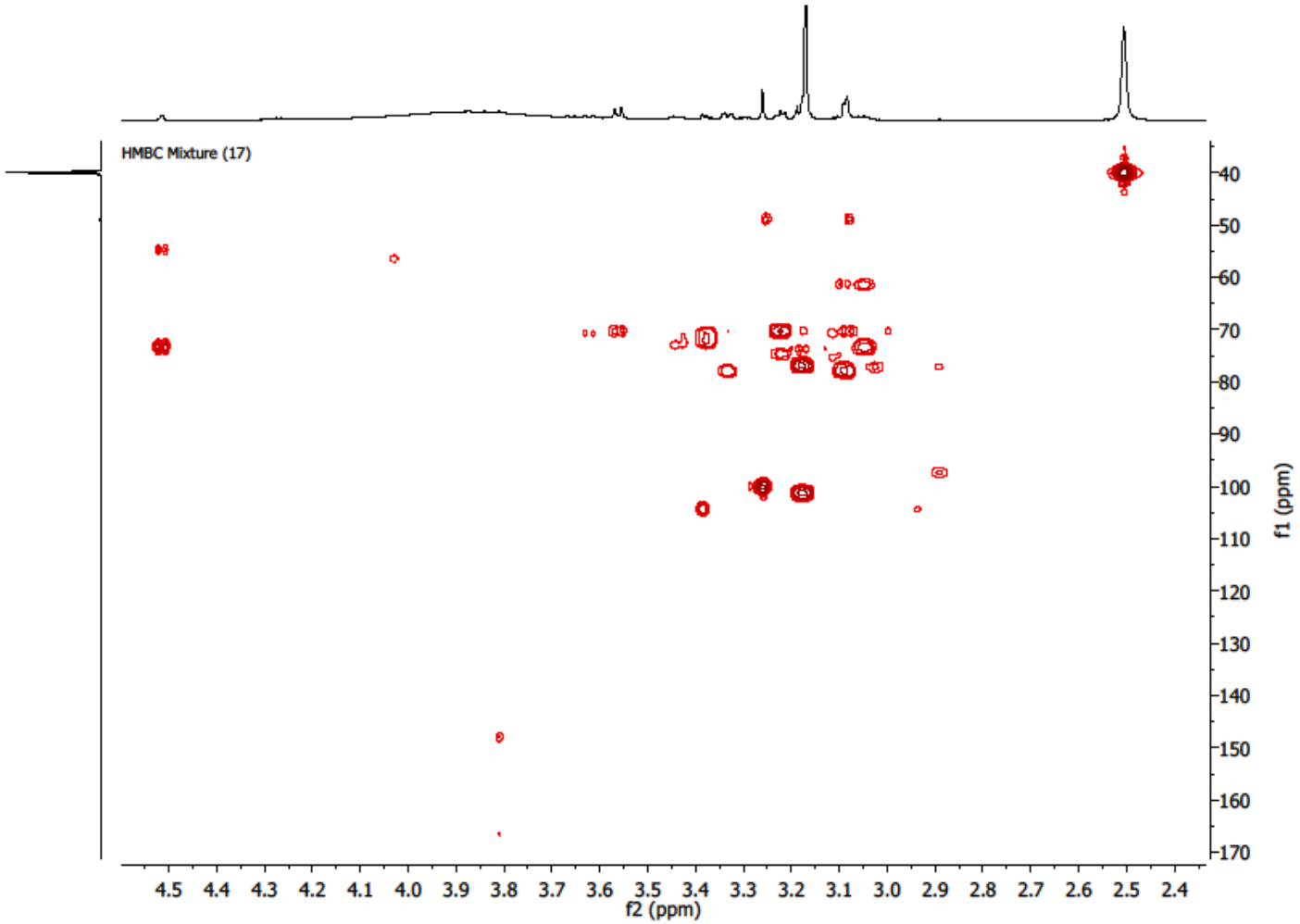

Supplemental Figure 2.21. Zoom from 2.4 to 4.5 ppm, HMBC spectra (DMSO-*d*6) of mixture (**17**).

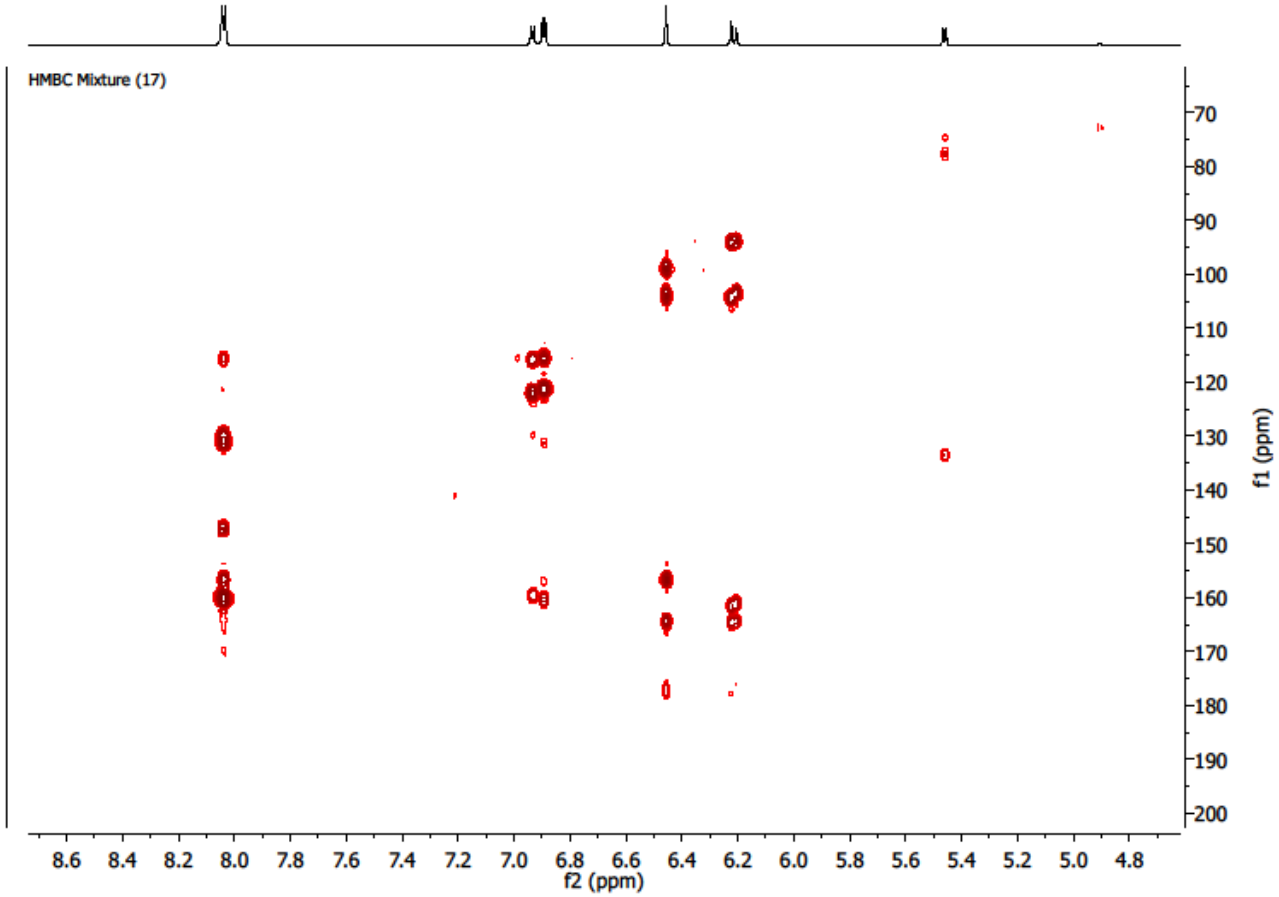

Supplemental Figure 2.22. Zoom from 4.8 to 8.6 ppm, HMBC spectra (DMSO-*d*6) of mixture (**17**).

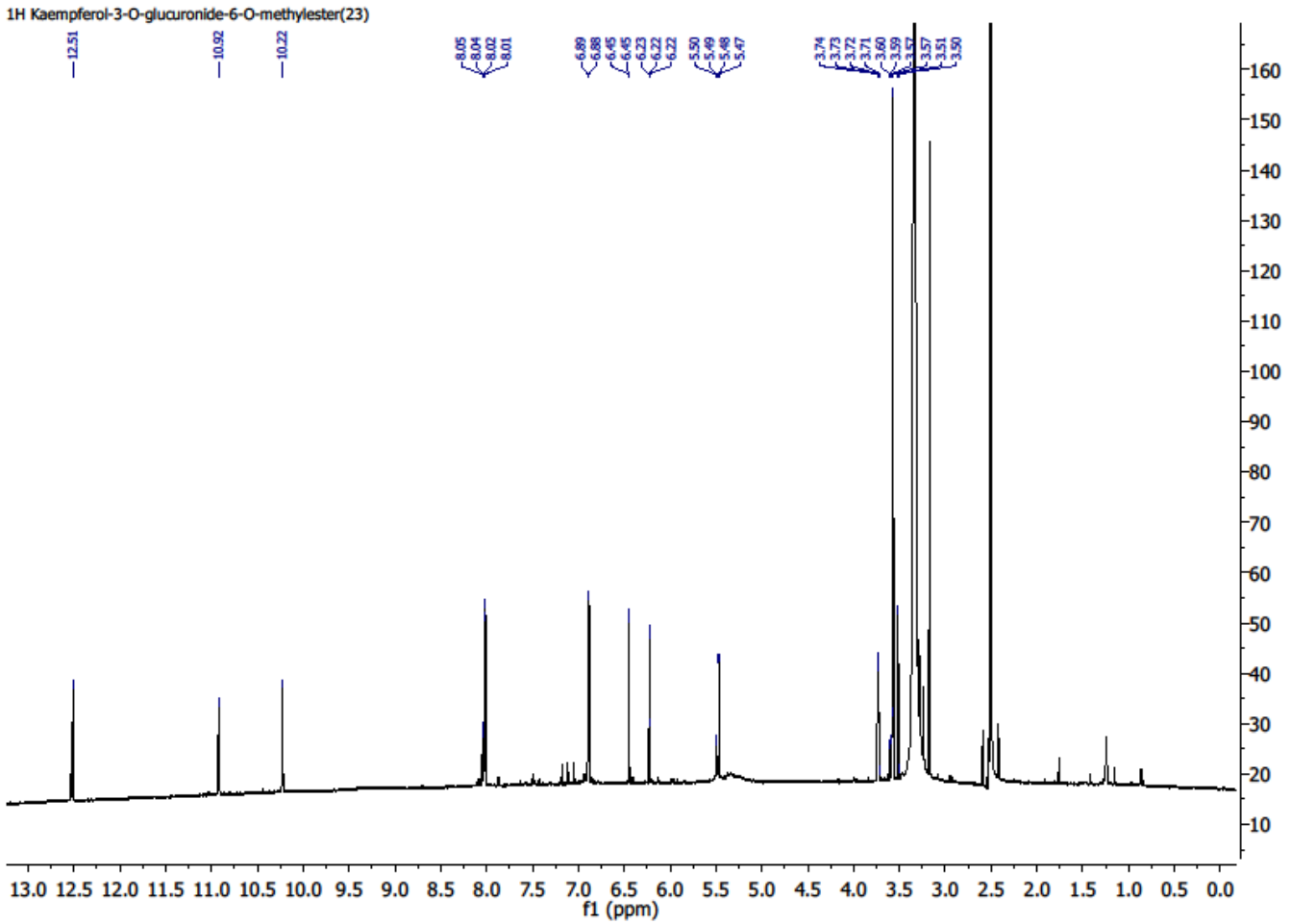

Supplemental Figure 2.23. ^{1}H spectra (DMSO-*d*6) of kaempferol 3-*O*-glucoronide-6''-*O*-methylester (**23**).

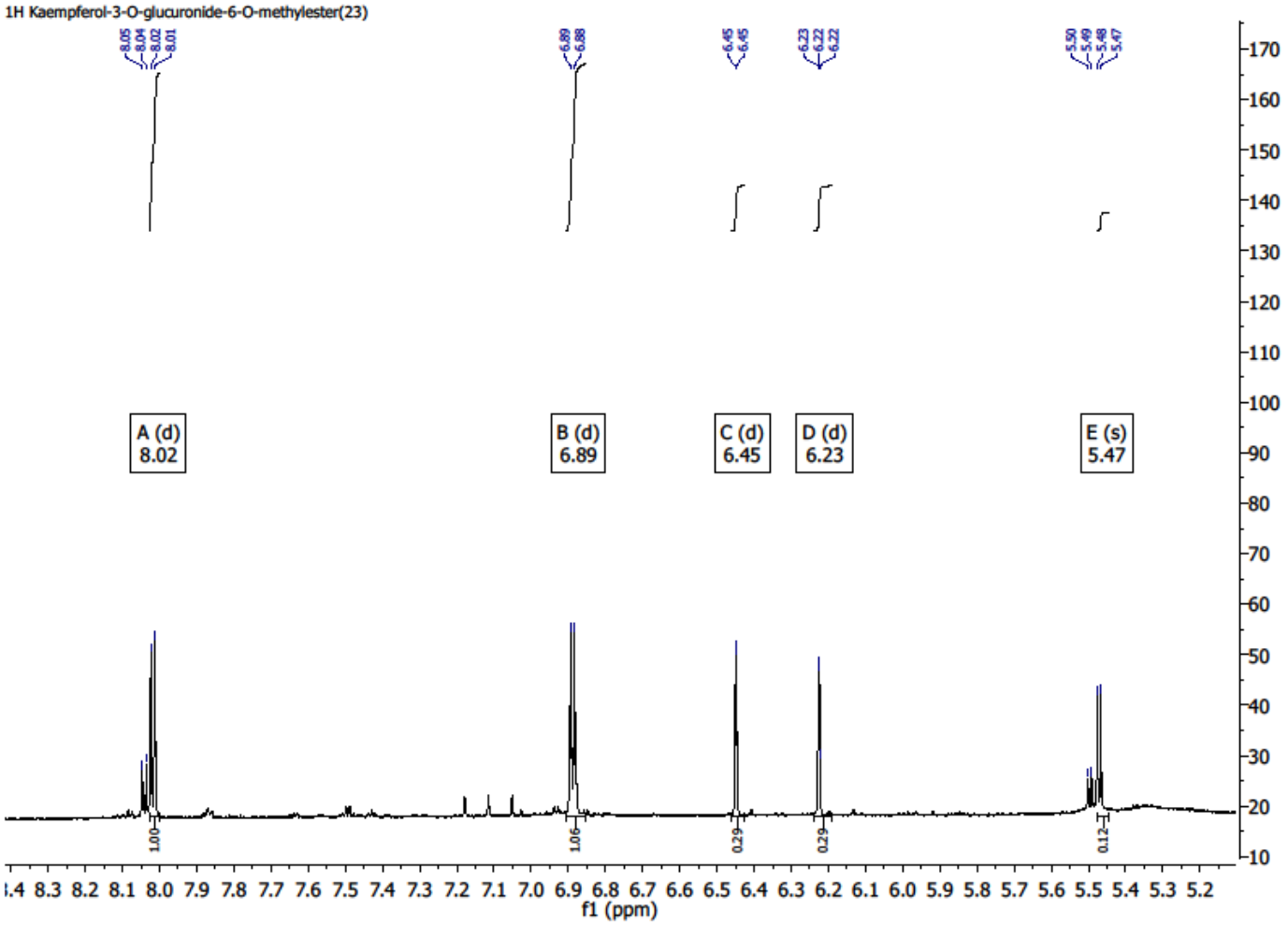

Supplemental Figure 2.24. Zoom from 5.1 to 8.1 ppm, ^{1}H spectra (DMSO-*d*6) of kaempferol 3-*O*-glucoronide-6''-*O*-methylester (**23**).

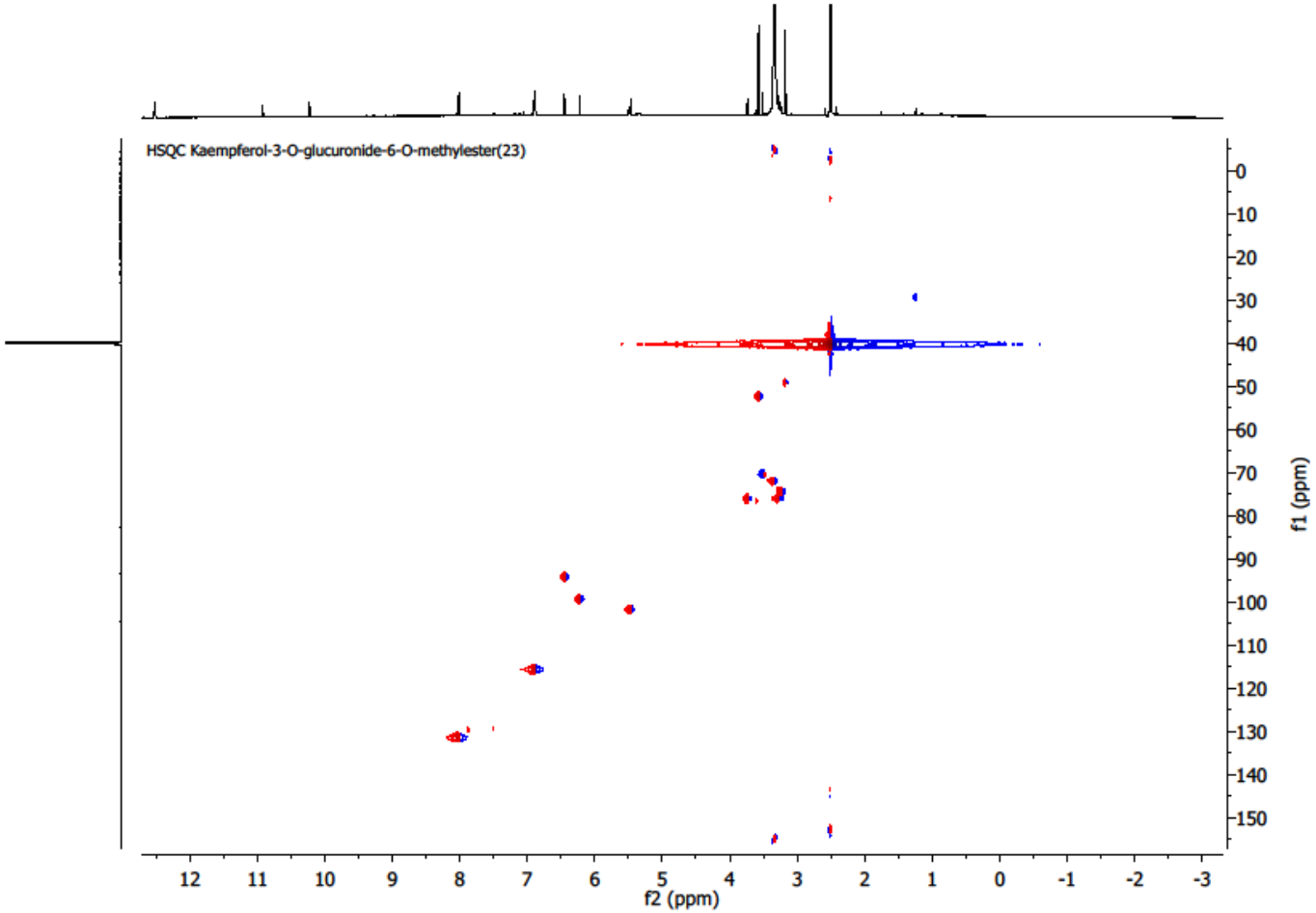

Supplemental Figure 2.25. HSQC spectra (DMSO-*d*6) of kaempferol 3-*O*-glucoronide-6''-*O*-methylester (**23**).

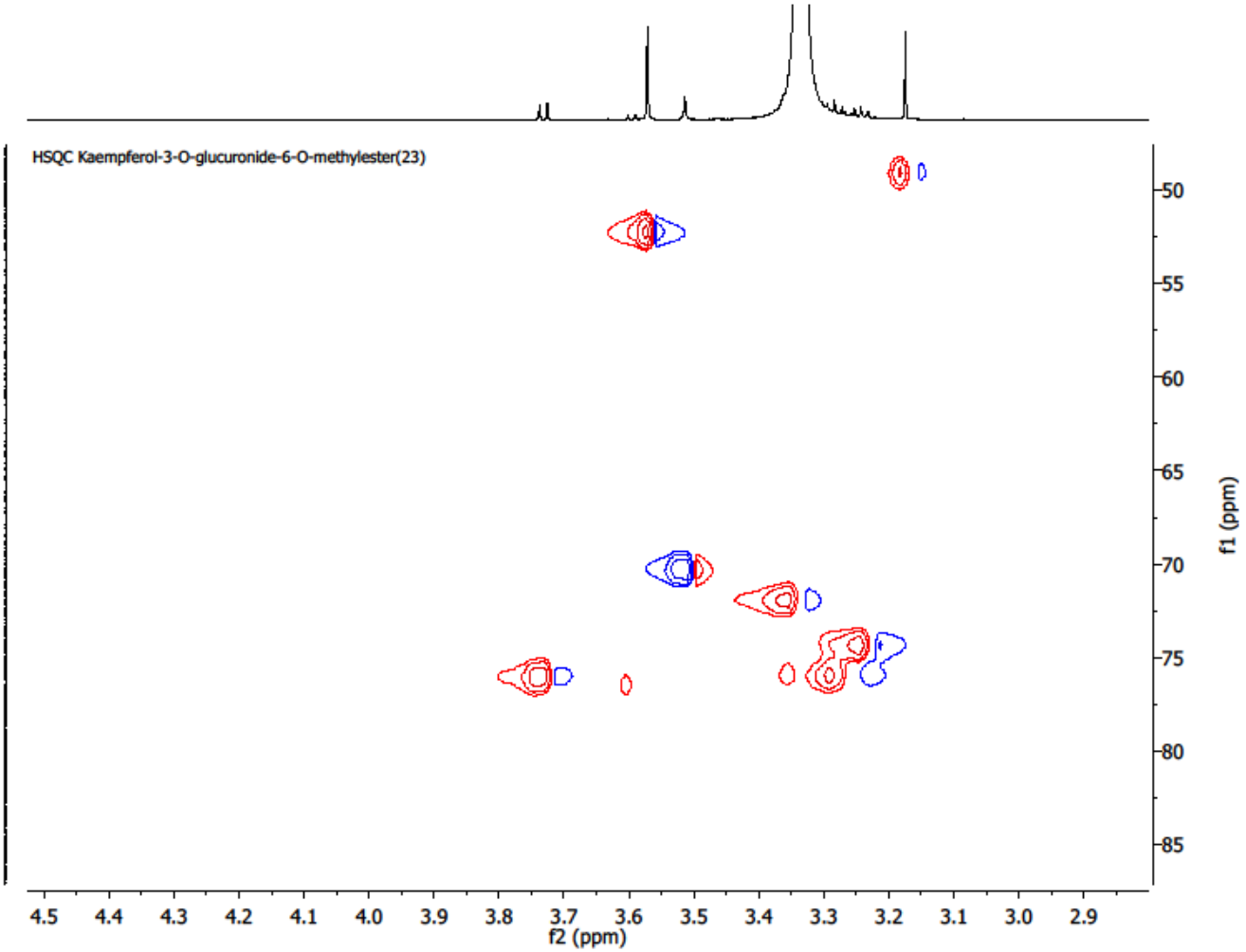

Supplemental Figure 2.26. Zoom from 2.9 to 4.5 ppm, HSQC spectra (DMSO-*d*6) of kaempferol 3-*O*-glucoronide-6''-*O*-methylester (**23**).

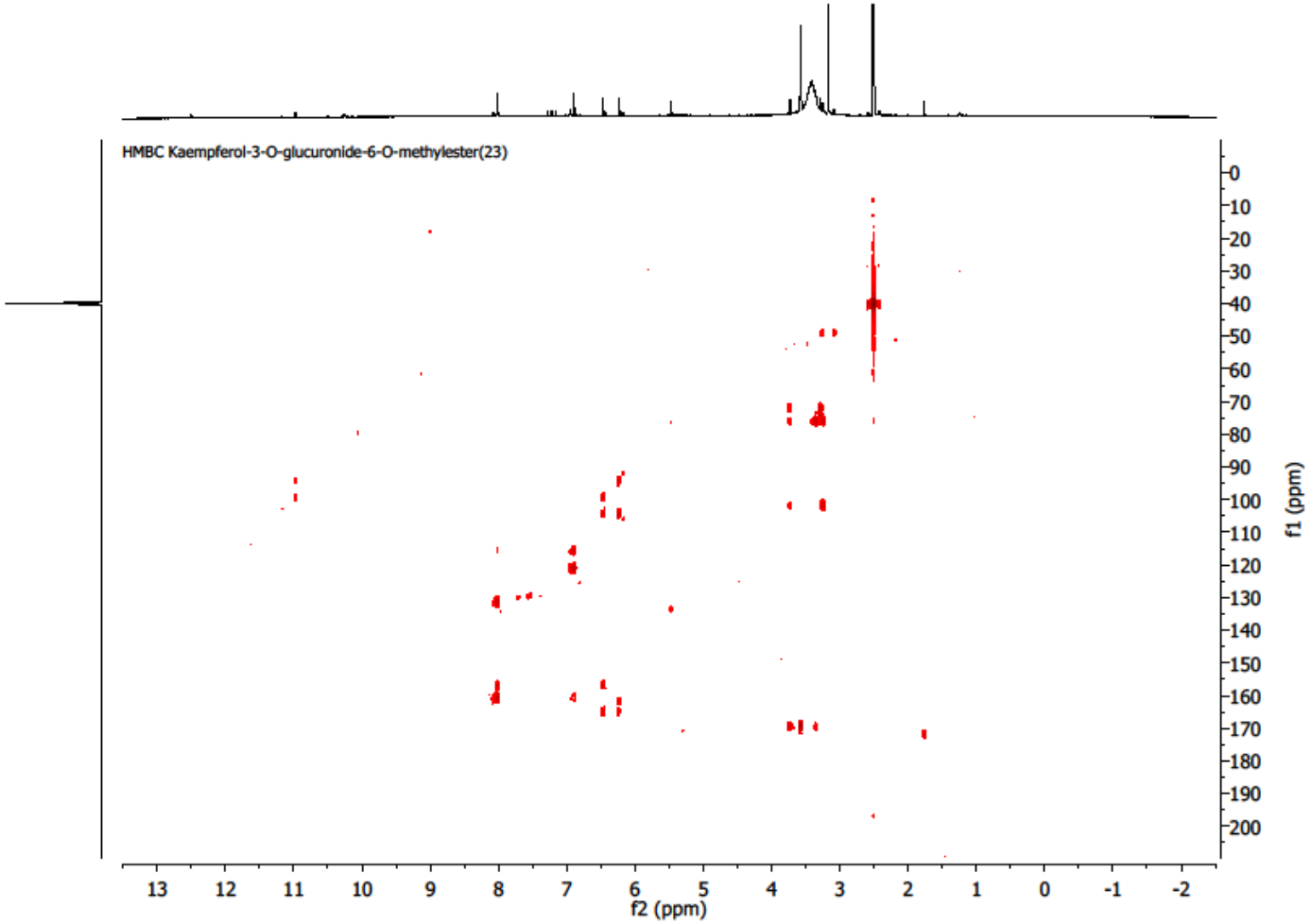

Supplemental Figure 2.27. HMBC spectra (DMSO-*d*6) of kaempferol 3-*O*-glucoronide-6′′-*O*-methylester (**23**).

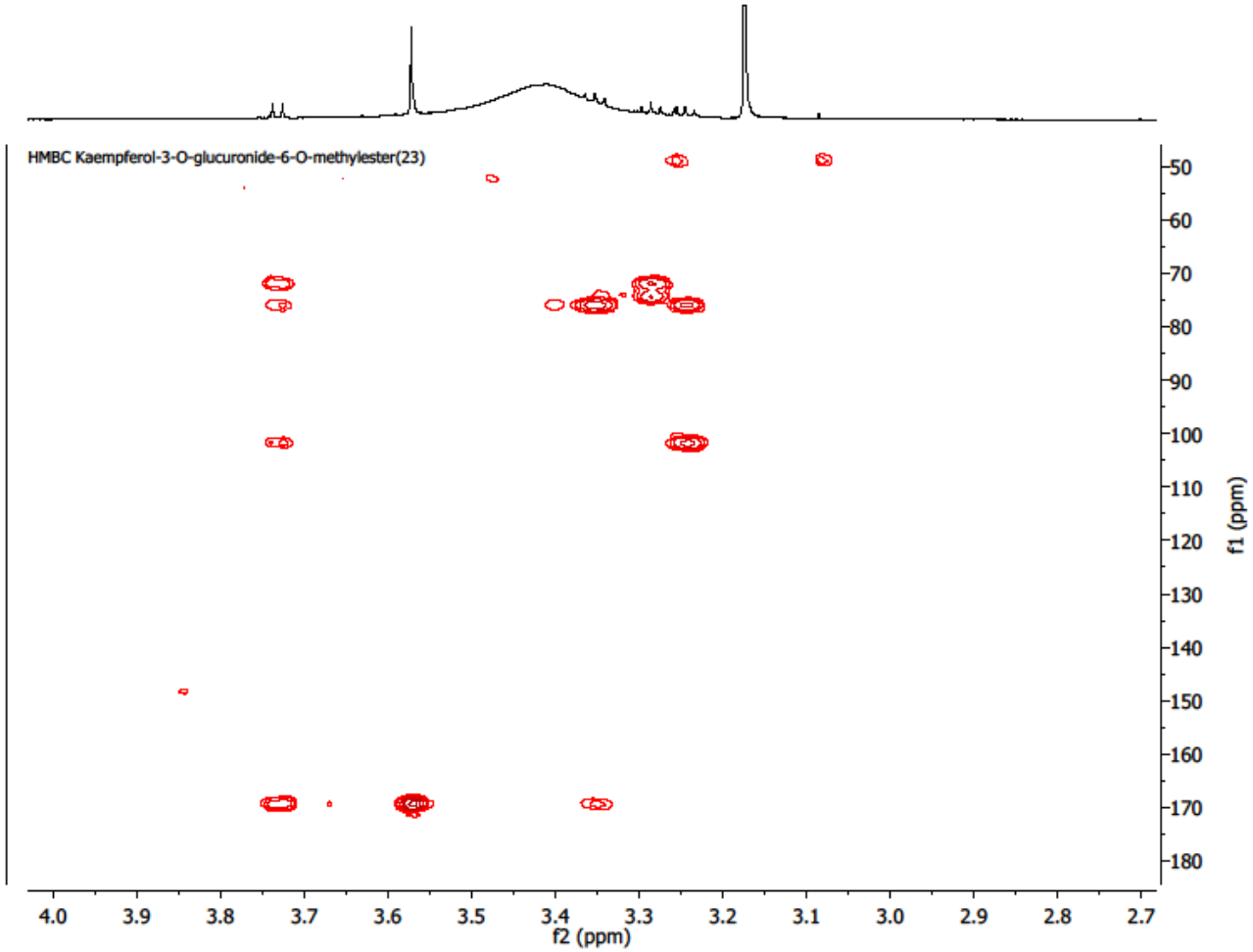

Supplemental Figure 2.28. Zoom from 2.7 to 4.0 ppm, HMBC spectra (DMSO-*d*6) of kaempferol 3-*O*-glucoronide-6''-*O*-methylester (**23**).

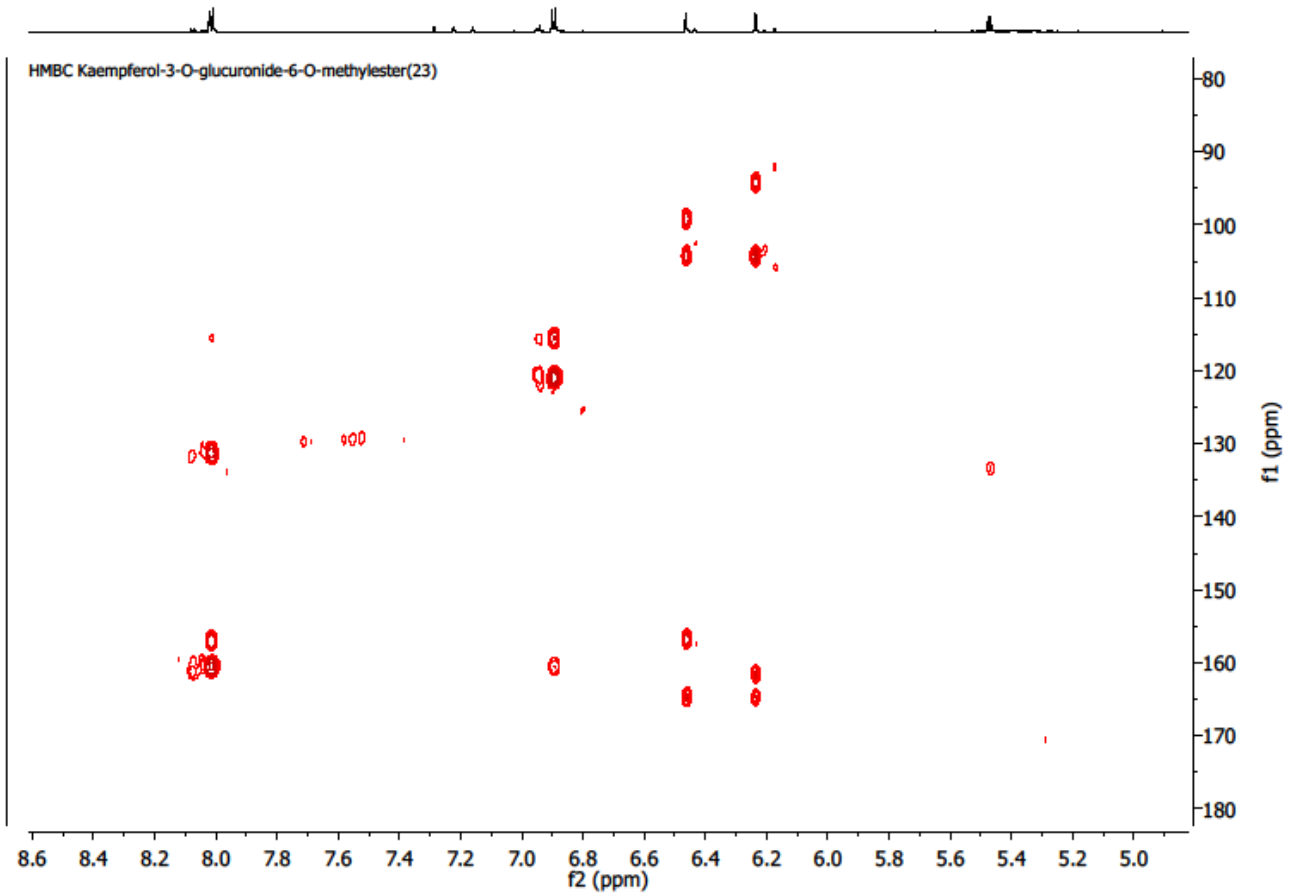

Supplemental Figure 2.29. Zoom from 5.0 to 8.6 ppm, HMBC spectra (DMSO-*d*6) of kaempferol 3-*O*-glucoronide-6''-*O*-methylester (**23**).

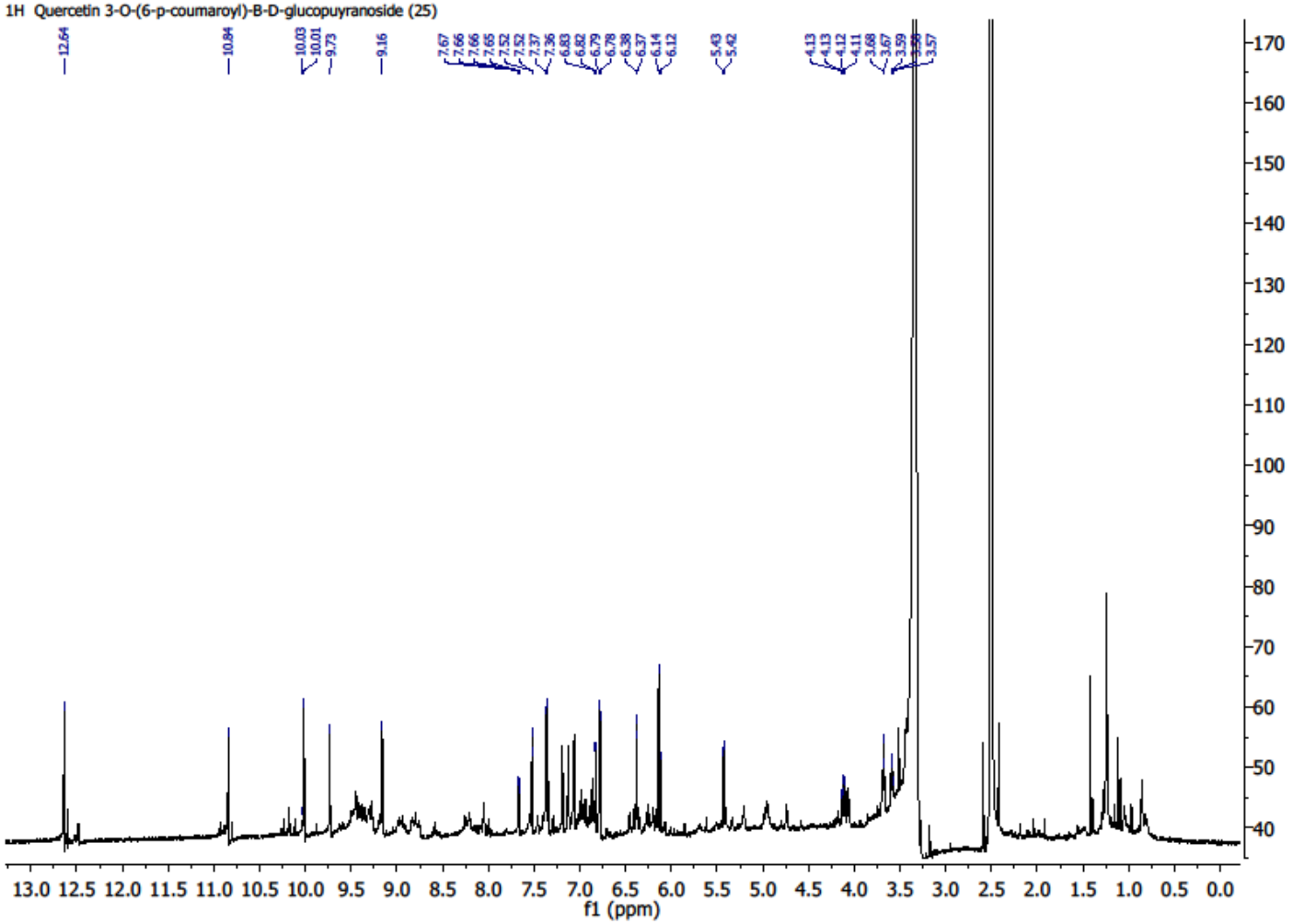

Supplemental Figure 2.30. ^{1}H spectra (DMSO-*d*6) of Quercetin 3-*O*-(6''-*p*-coumaroyl)-β-D-glucopyranoside (**25**).

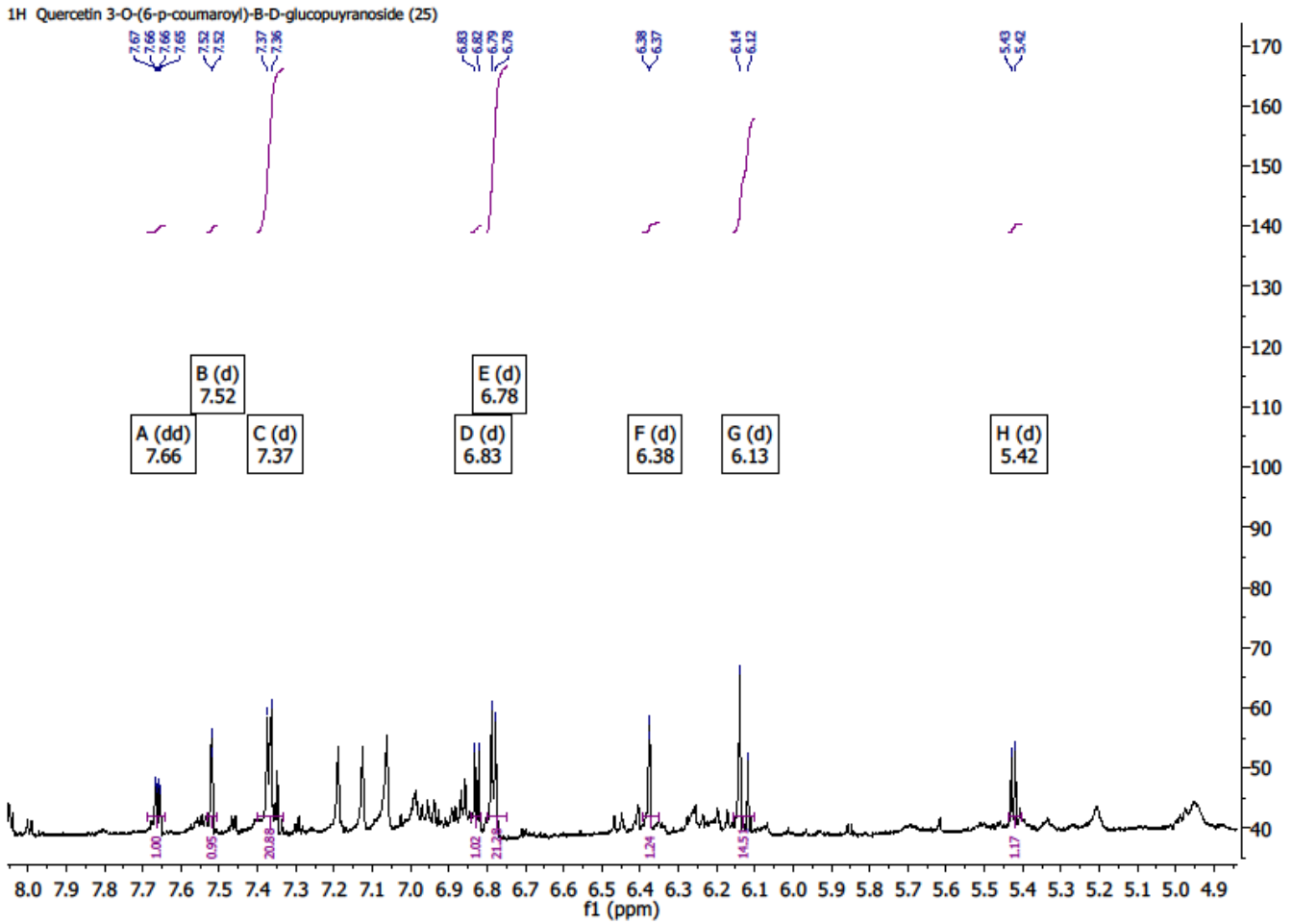

Supplemental Figure 2.31. Zoom from 5.1 to 8.1 ppm, ^{1}H spectra (DMSO-*d*6) of Quercetin 3-*O*-(6''-*p*-coumaroyl)-β-D-glucopyranoside (**25**).

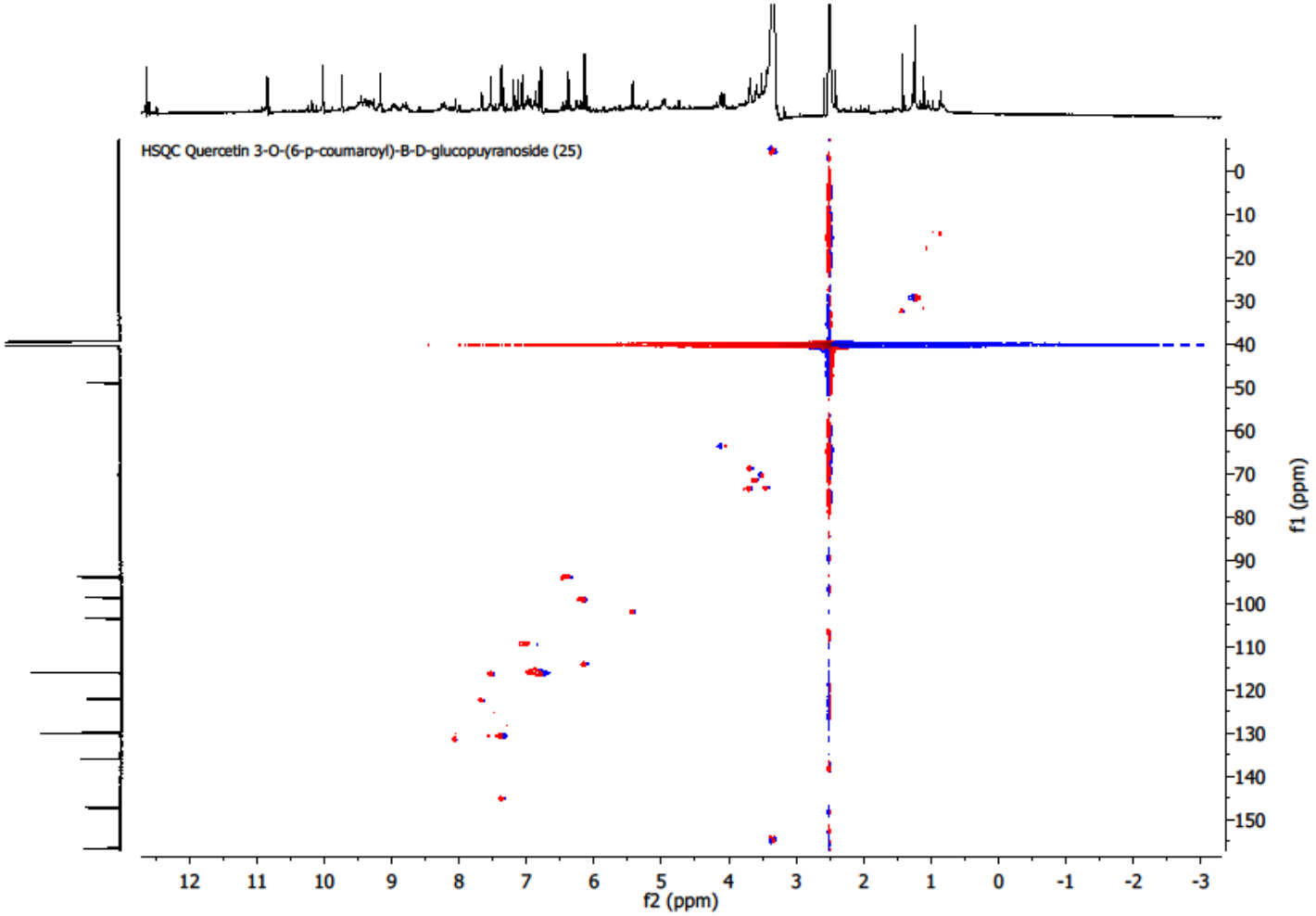

Supplemental Figure 2.32. HSQC spectra (DMSO-*d*6) of Quercetin 3-*O*-(6''-*p*-coumaroyl)-β-D-glucopyranoside (**25**).

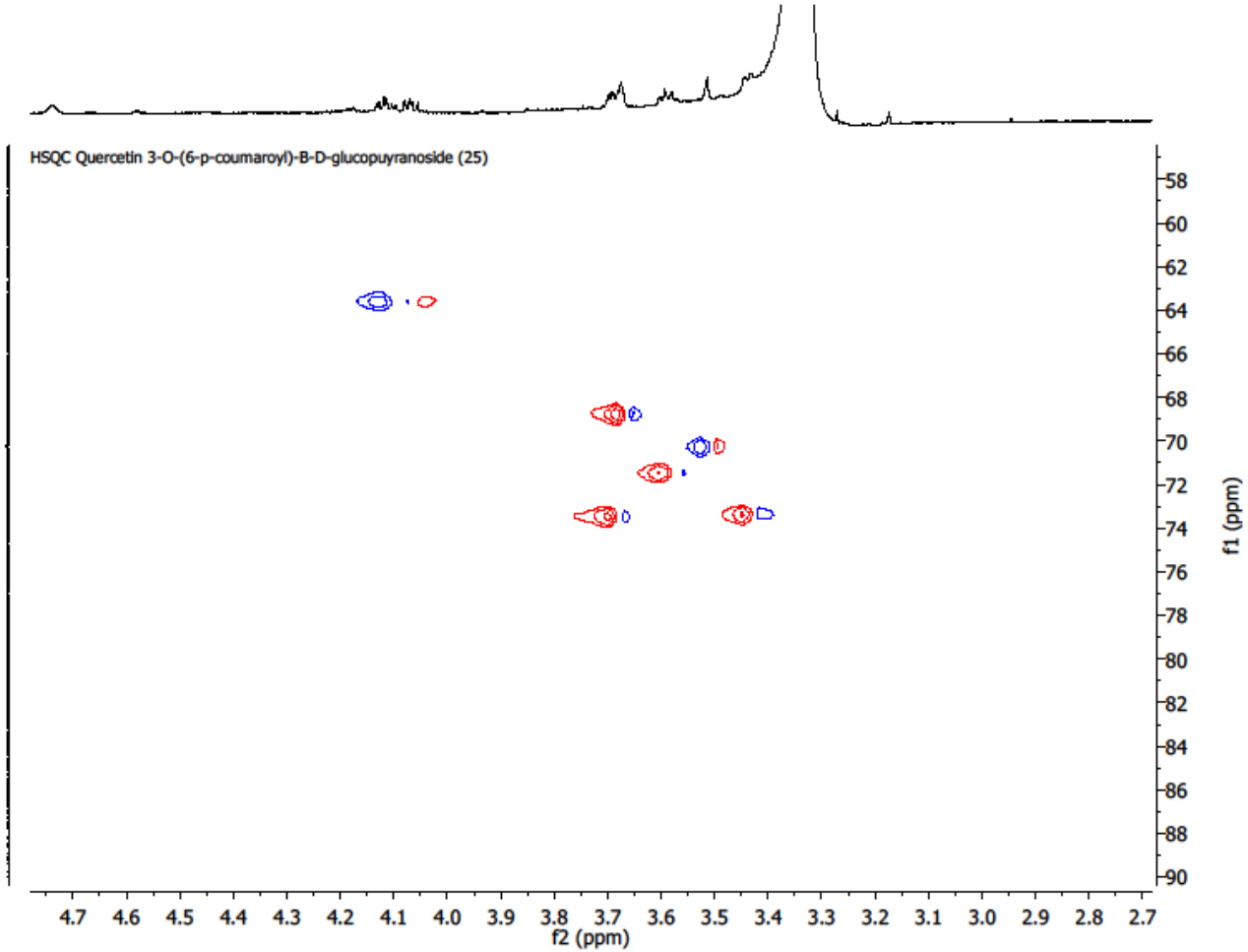

Supplemental Figure 2.33. Zoom from 2.7 to 4.7 ppm, HSQC spectra (DMSO-*d*6) of Quercetin 3-*O*-(6''-*p*-coumaroyl)-β-D-glucopyranoside (**25**).

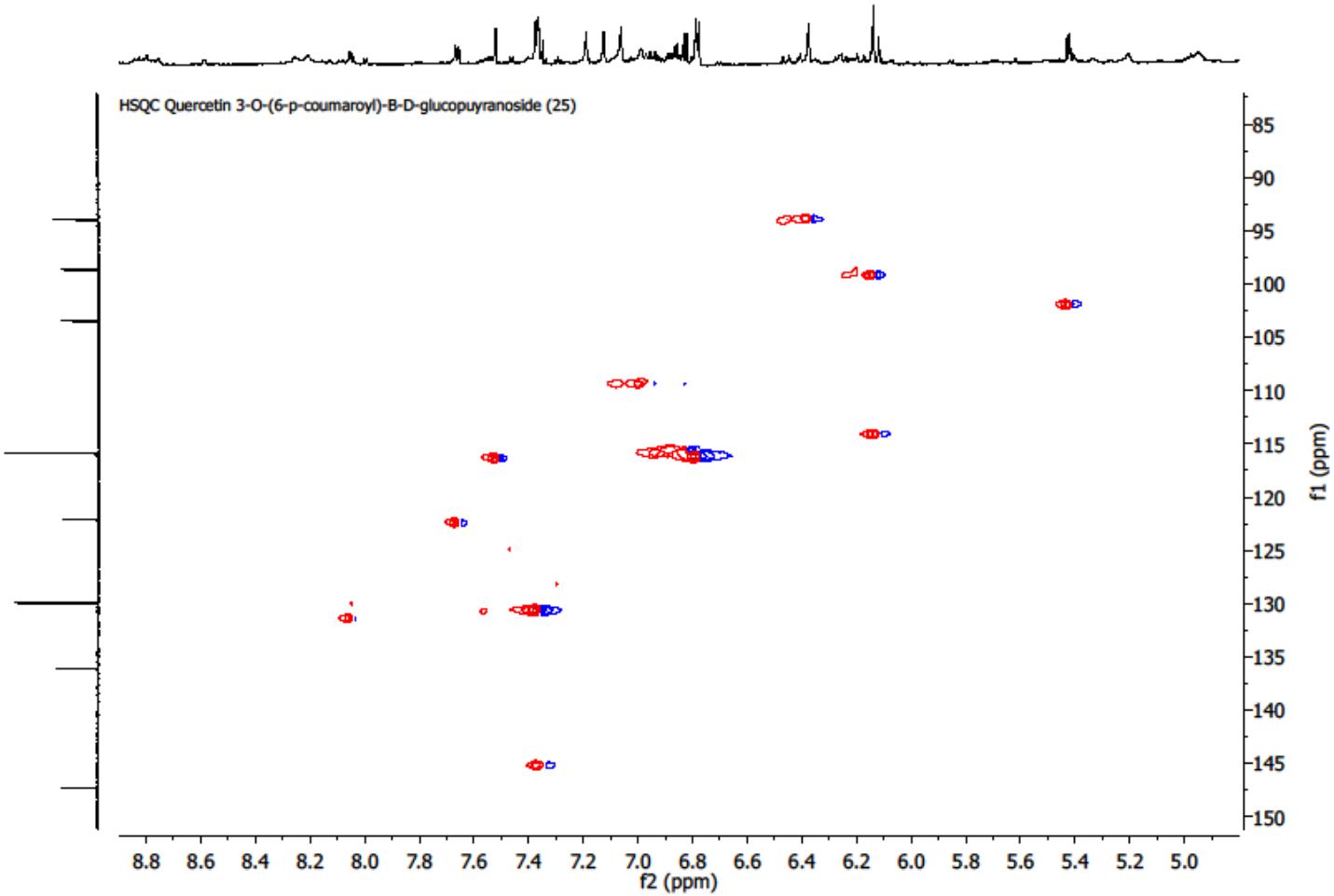

upplemental Figure 2.34. Zoom from 5.0 to 8.8 ppm, HSQC spectra (DMSO-*d*6) of Quercetin 3-*O*-(6''-*p*-coumaroyl)-β-D-glucopyranoside (**25**).

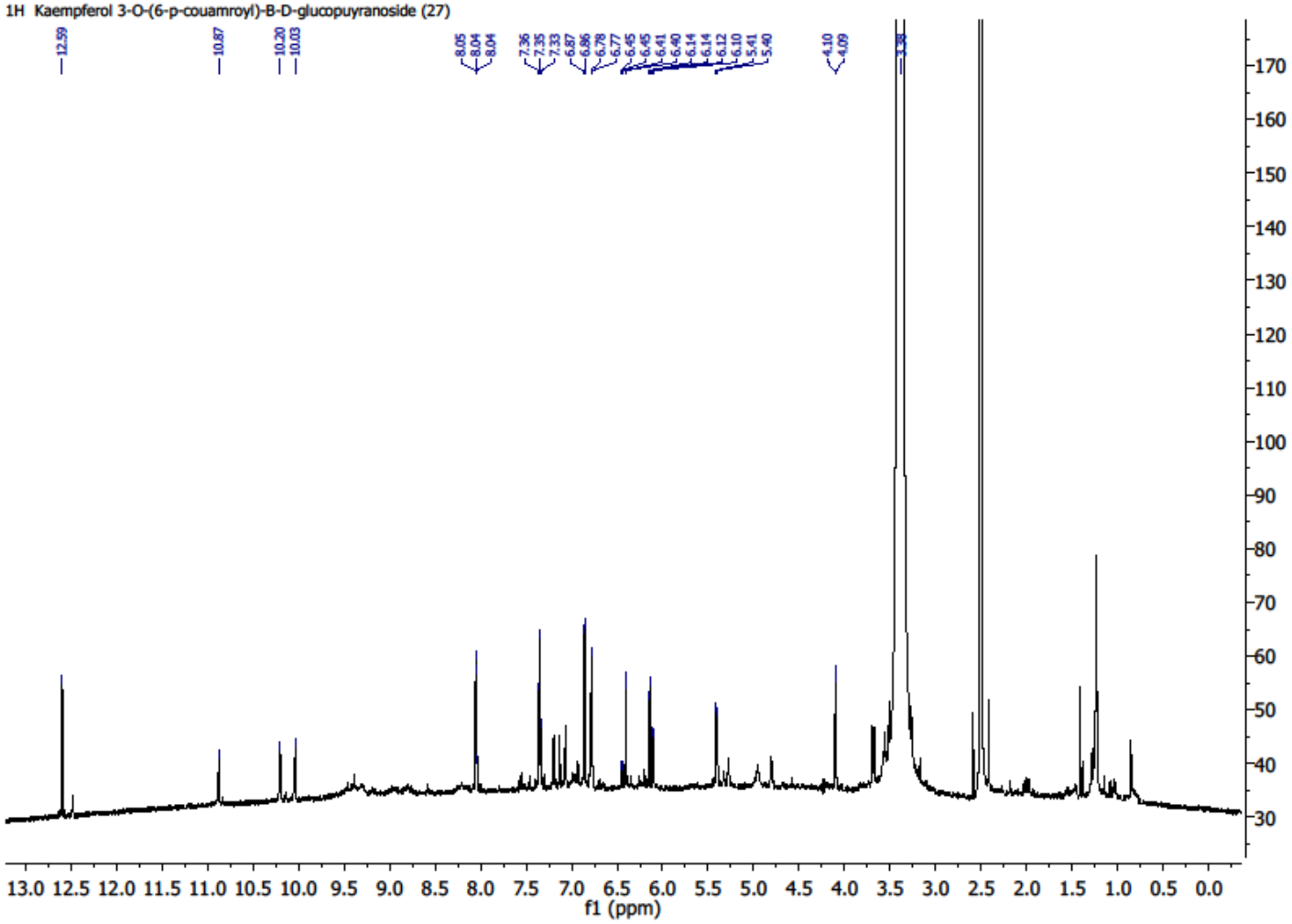

Supplemental Figure 2.35. [1]H spectra (DMSO-*d*6) of Kaempferol 3-*O*-(6′′-*p*-coumaroyl)-β-D-glucopyranoside (**27**).

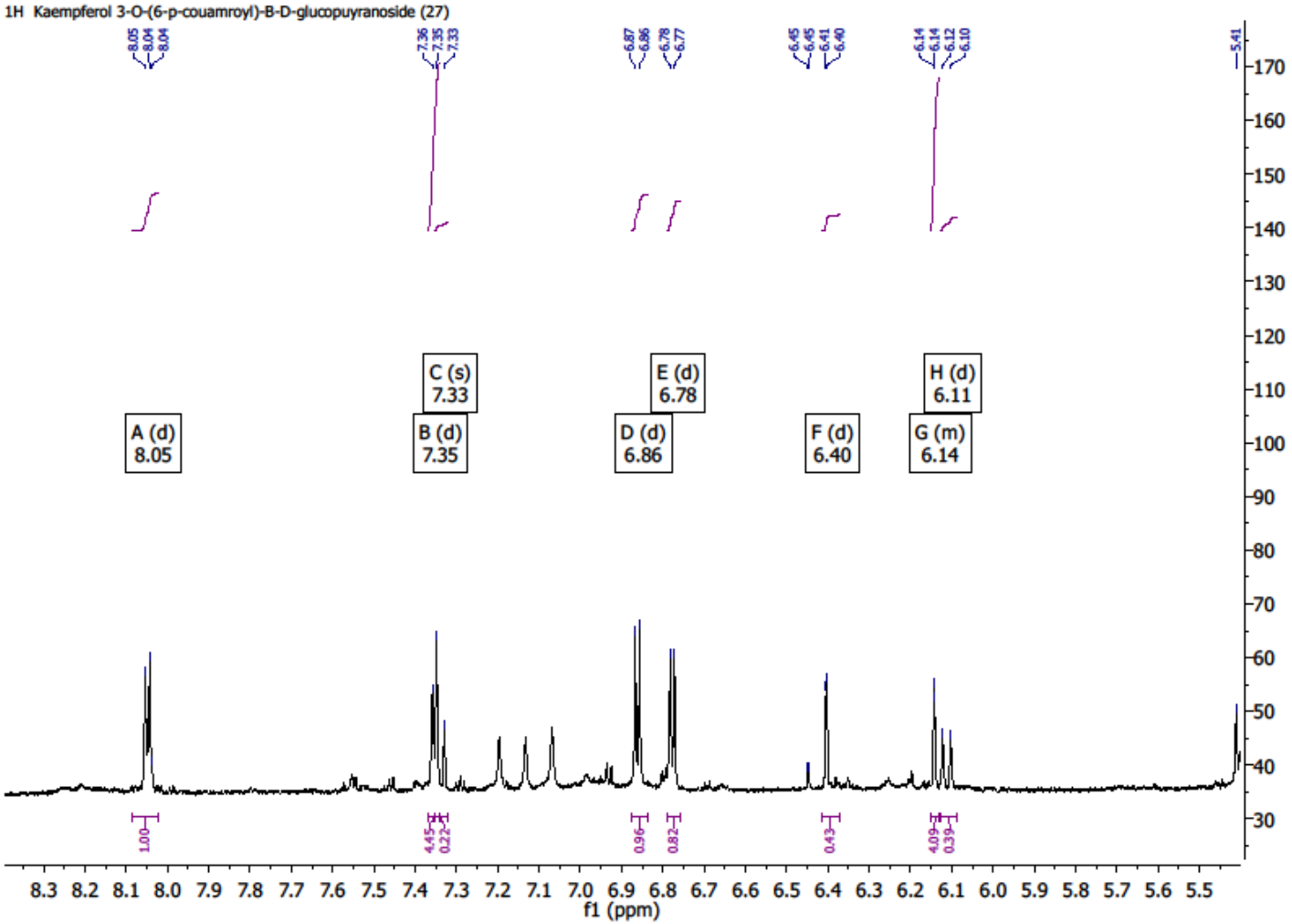

Supplemental Figure 2.36. Zoom from 5.1 to 8.1 ppm, ^{1}H spectra (DMSO-*d*6) of Kaempferol 3-*O*-(6''-*p*-coumaroyl)-β-D-glucopyranoside (**27**).

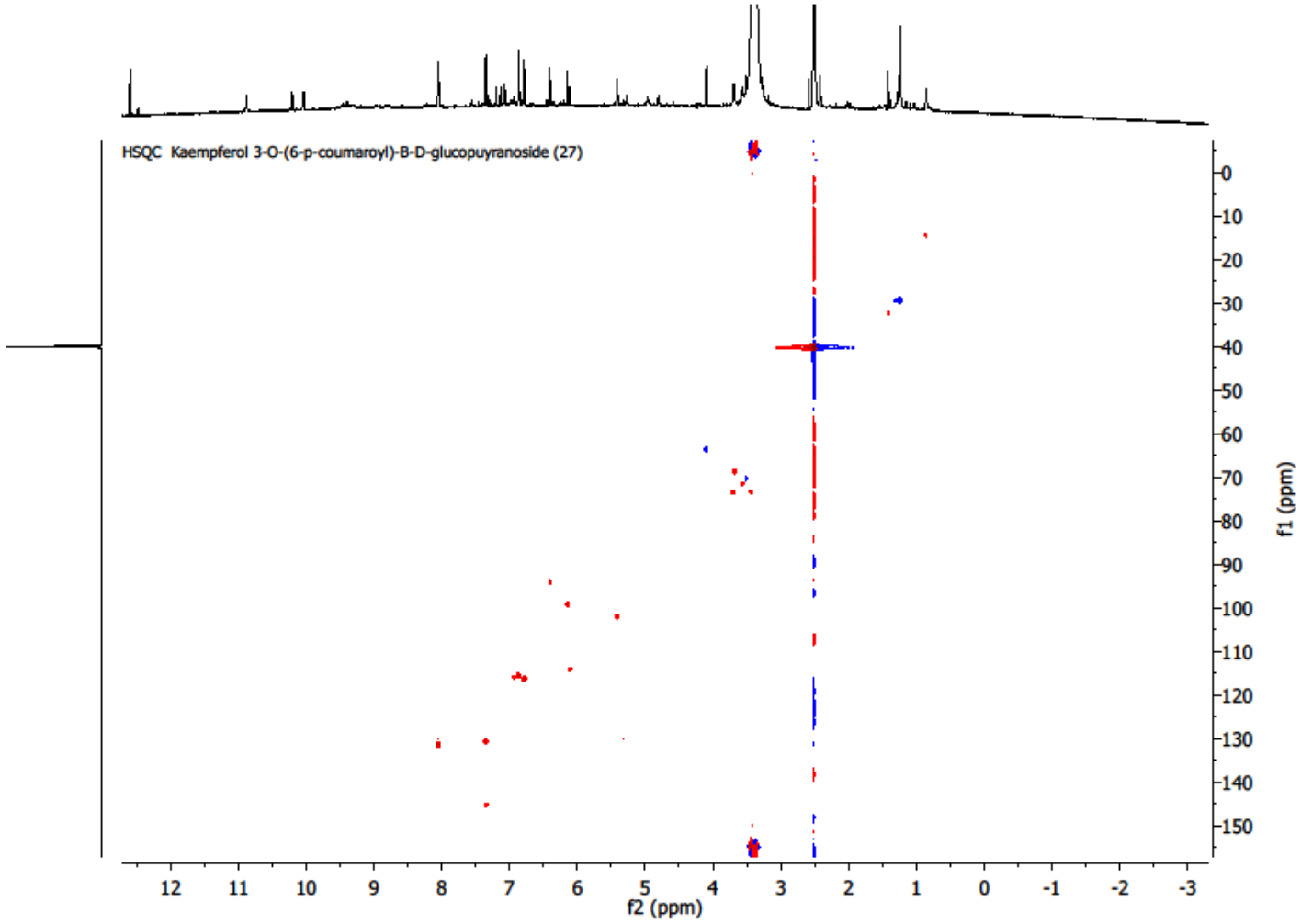

Supplemental Figure 2.37. HSQC spectra (DMSO-*d*6) of Kaempferol 3-*O*-(6''-*p*-coumaroyl)-β-D-glucopyranoside (**27**).

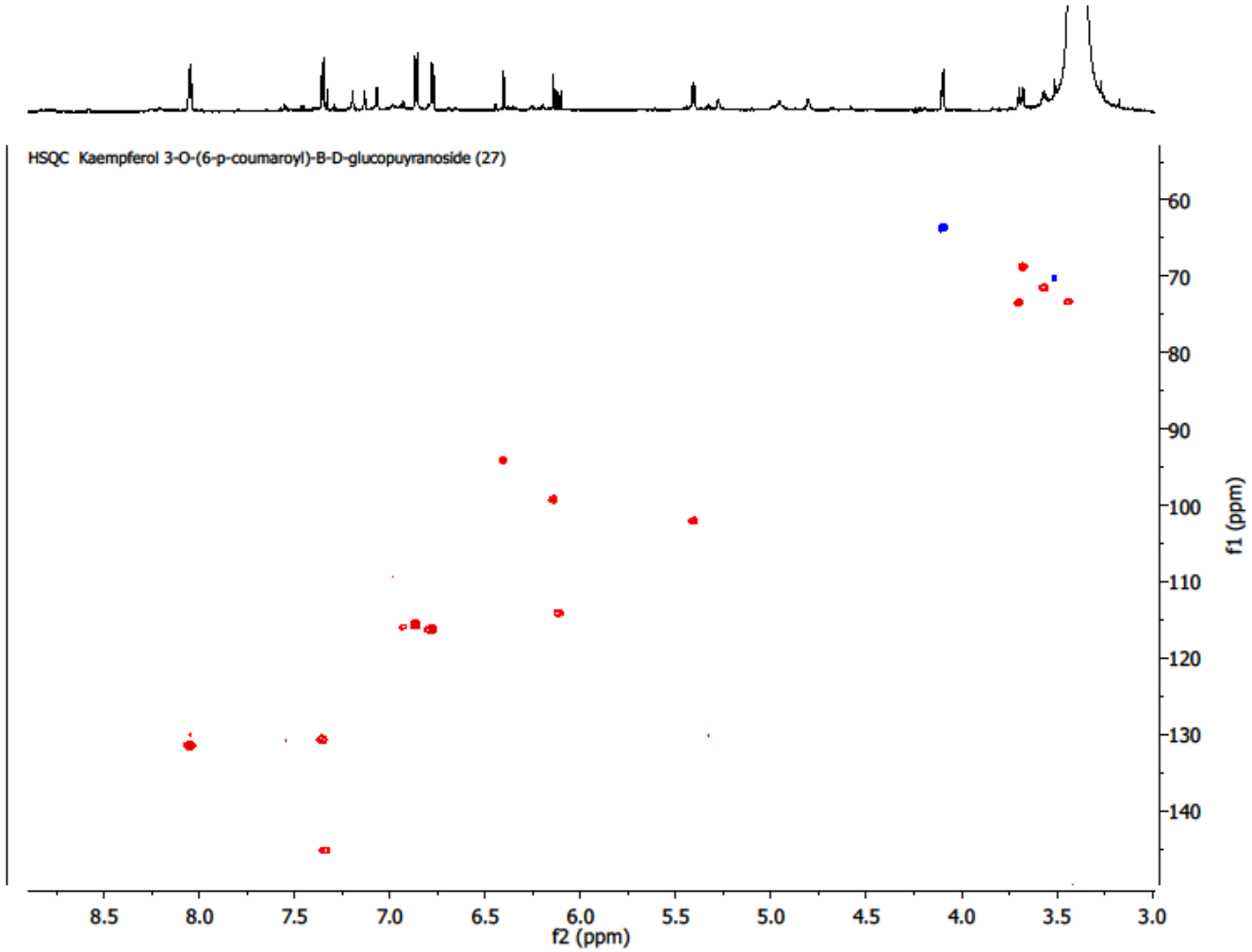

Supplemental Figure 2.38. Zoom from 3.0 to 4.6 ppm, HSQC spectra (DMSO-*d*6) of Kaempferol 3-*O*-(6''-*p*-coumaroyl)-β-D-glucopyranoside (**27**).

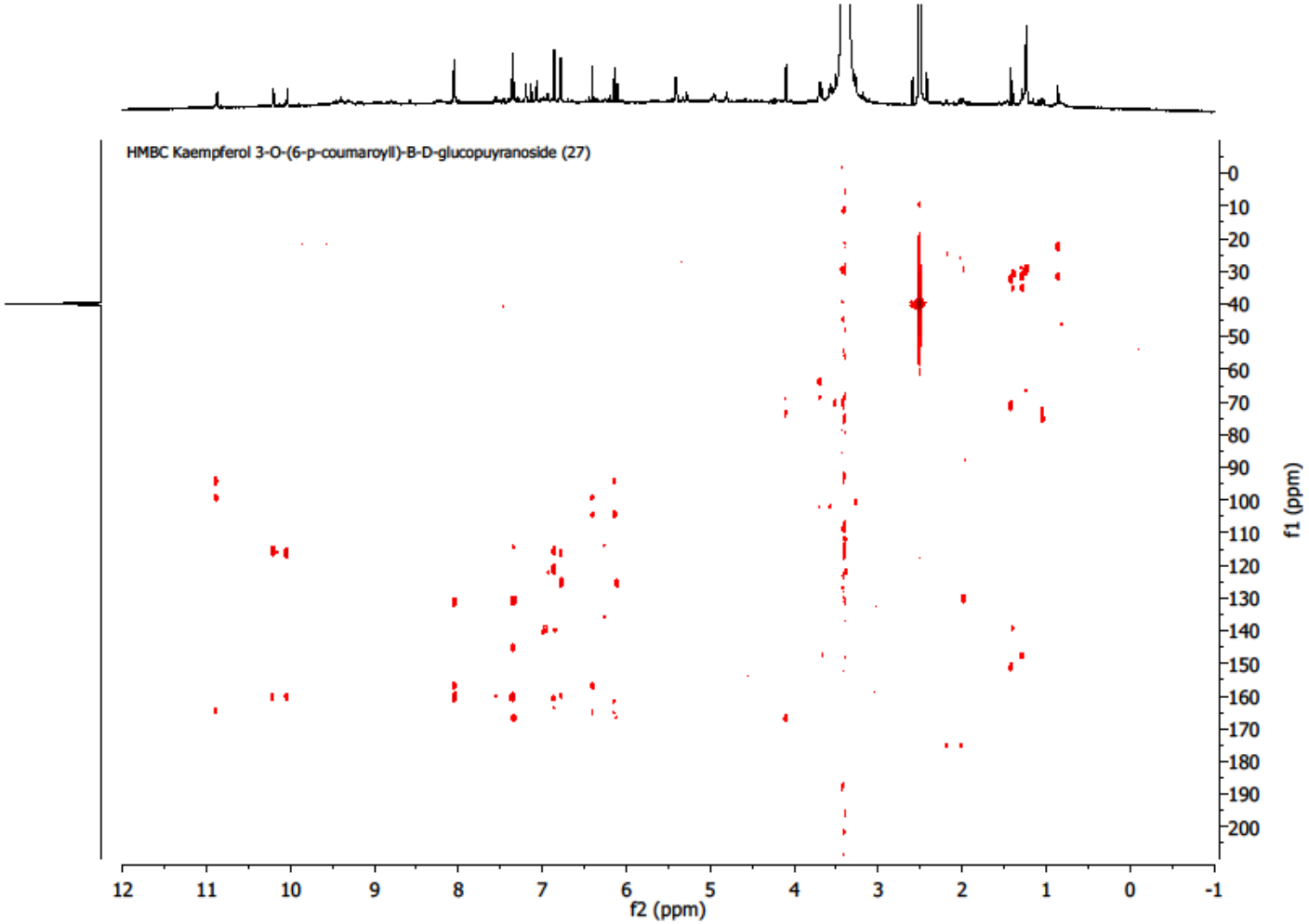

Supplemental Figure 2.39. HMBC spectra (DMSO-*d*6) of Kaempferol 3-*O*-(6′′-*p*-coumaroyl)-β-D-glucopyranoside (**27**).

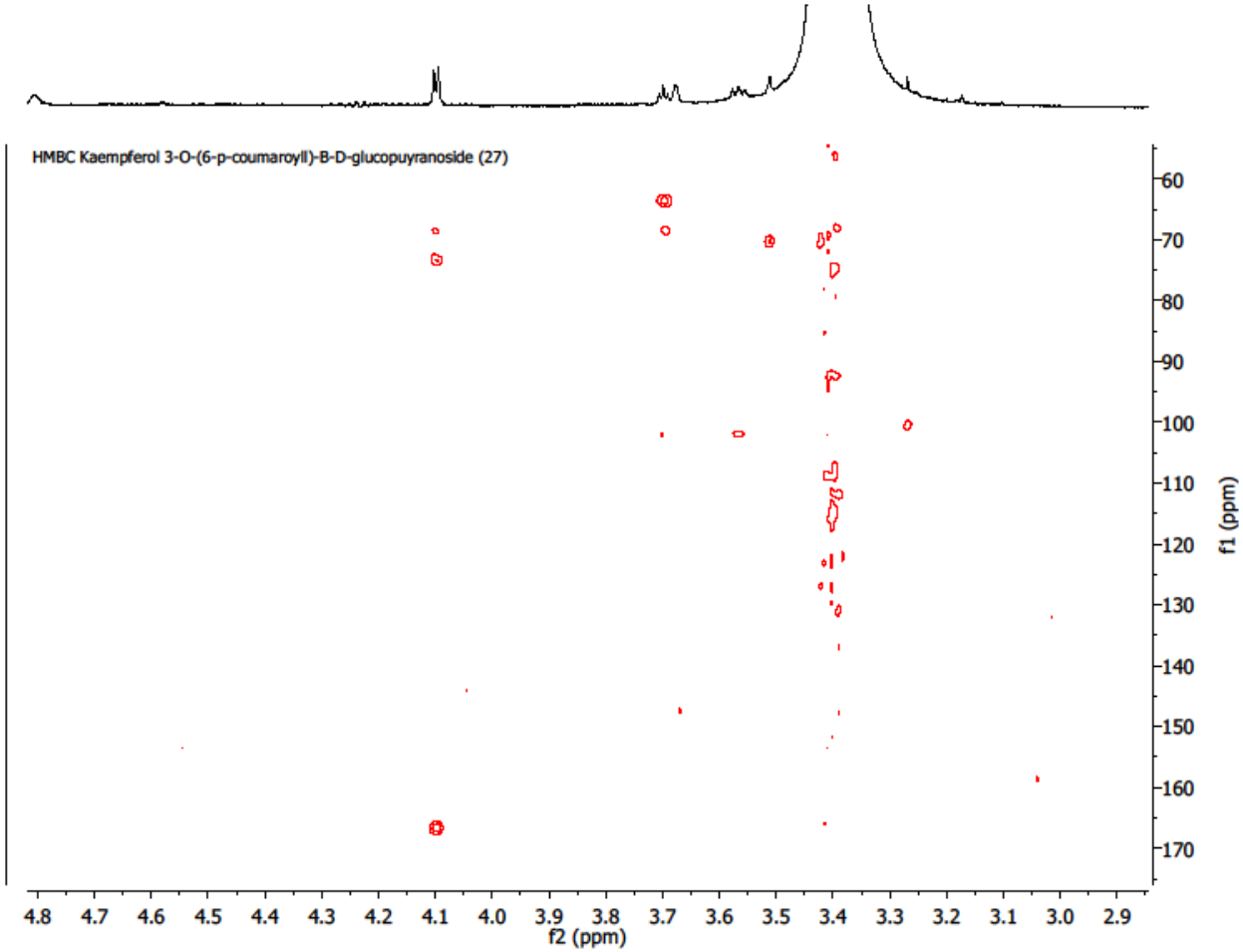

Supplemental Figure 2.40. Zoom from 2.9 to 4.8 ppm, HMBC spectra (DMSO-*d*6) of Kaempferol 3-*O*-(6''-*p*-coumaroyl)-β-D-glucopyranoside (**27**).

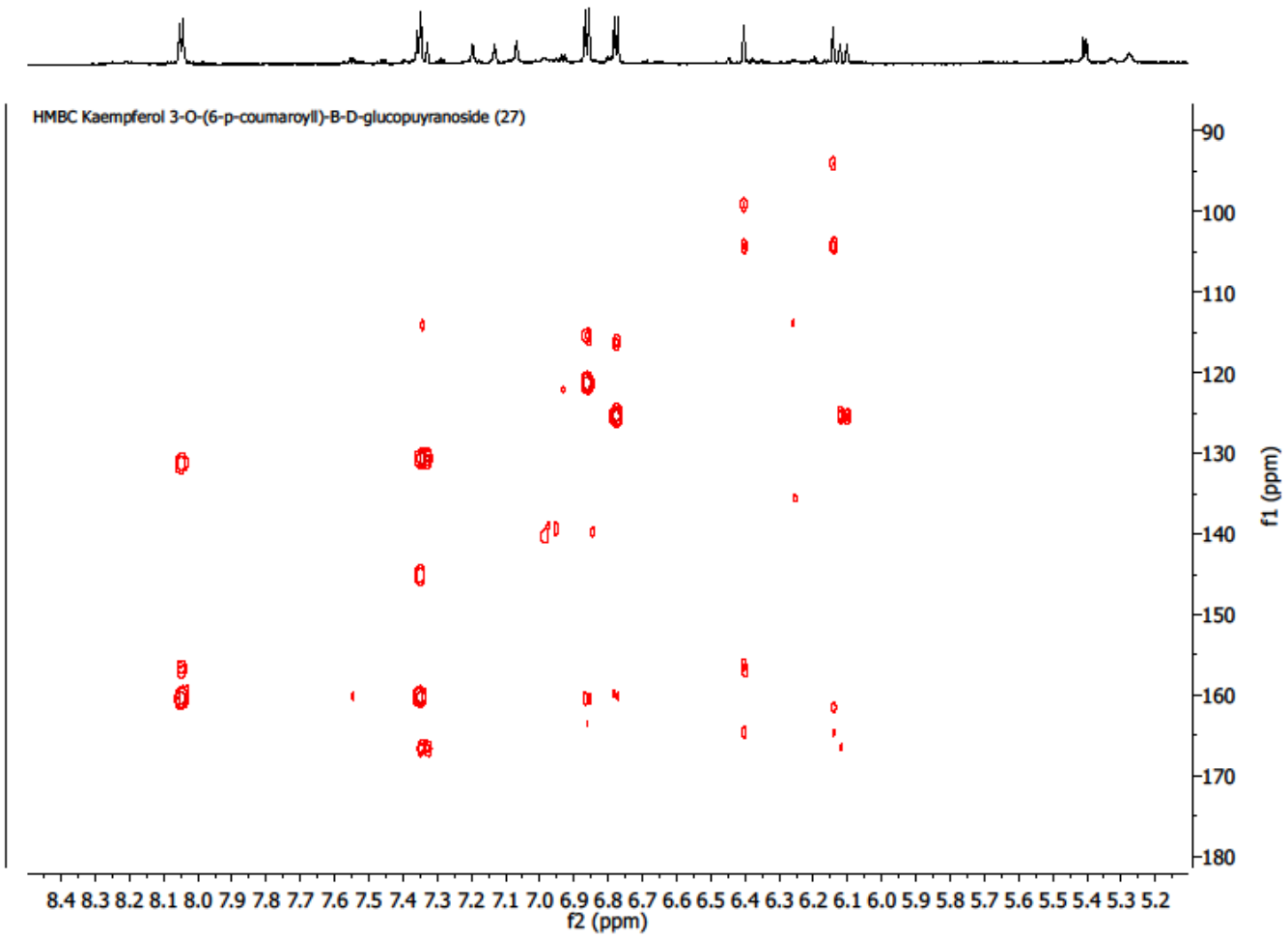

Supplemental Figure 2.41. Zoom from 5.2 to 8.4 ppm, HMBC spectra (DMSO-*d*6) of Kaempferol 3-*O*-(6''-*p*-coumaroyl)-β-D-glucopyranoside (**27**).

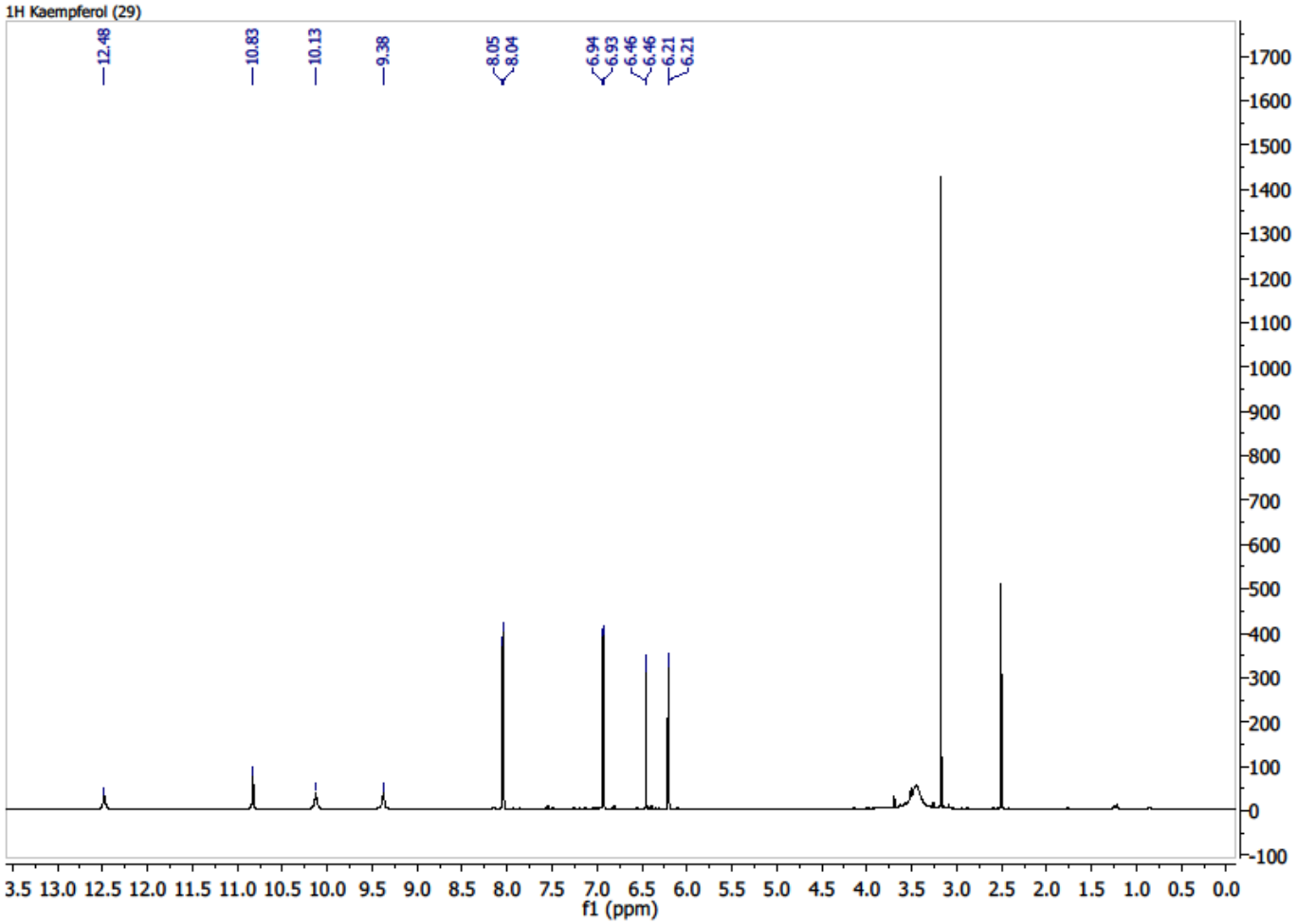

Supplemental Figure 2.42. ^{1}H spectra (DMSO-*d*6) of kaempferol (2**9**).

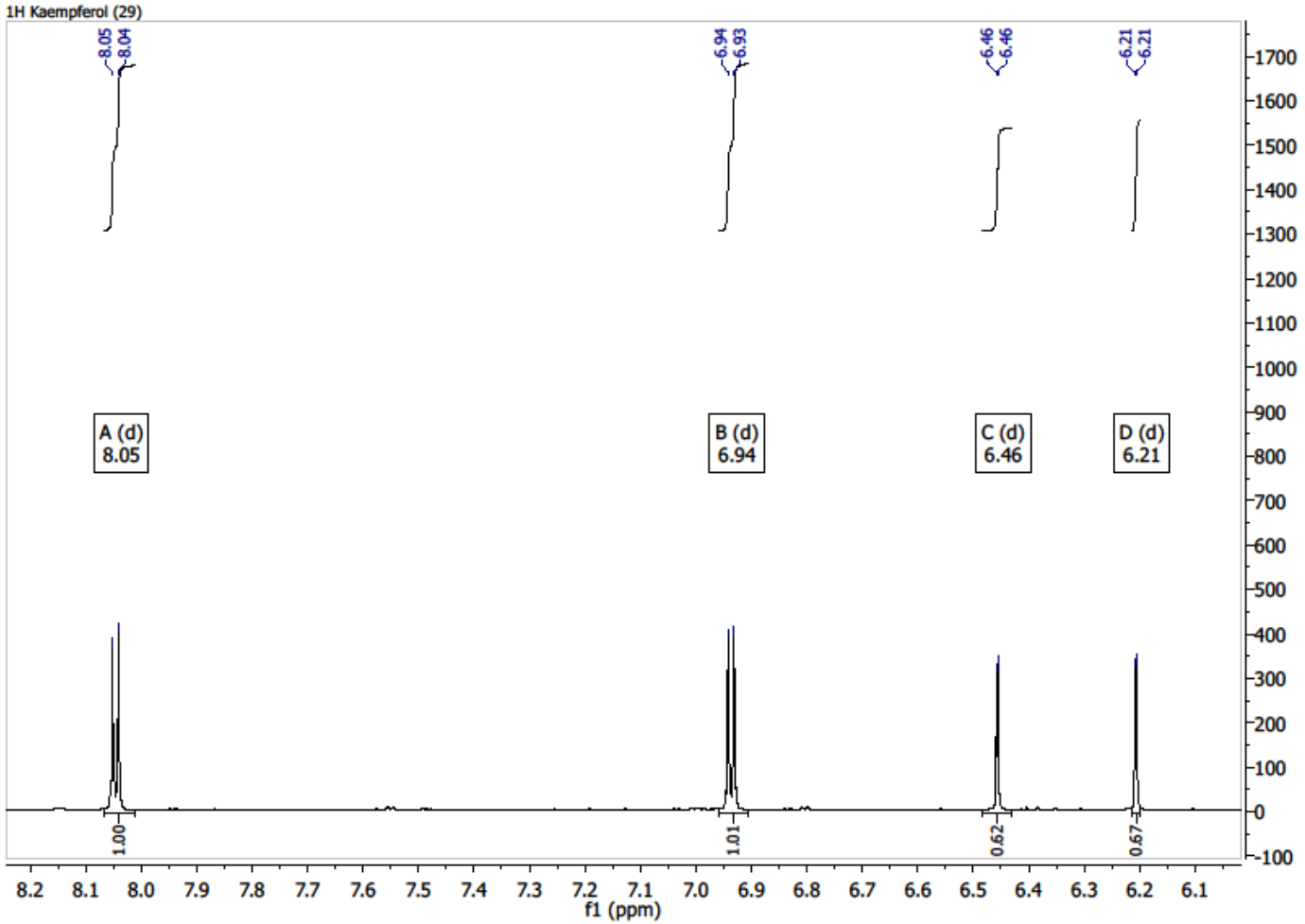

Supplemental Figure 2.43. Zoom from 6.1 to 8.2 ppm, ^{1}H spectra (DMSO-*d*6) of kaempferol (2**9**).

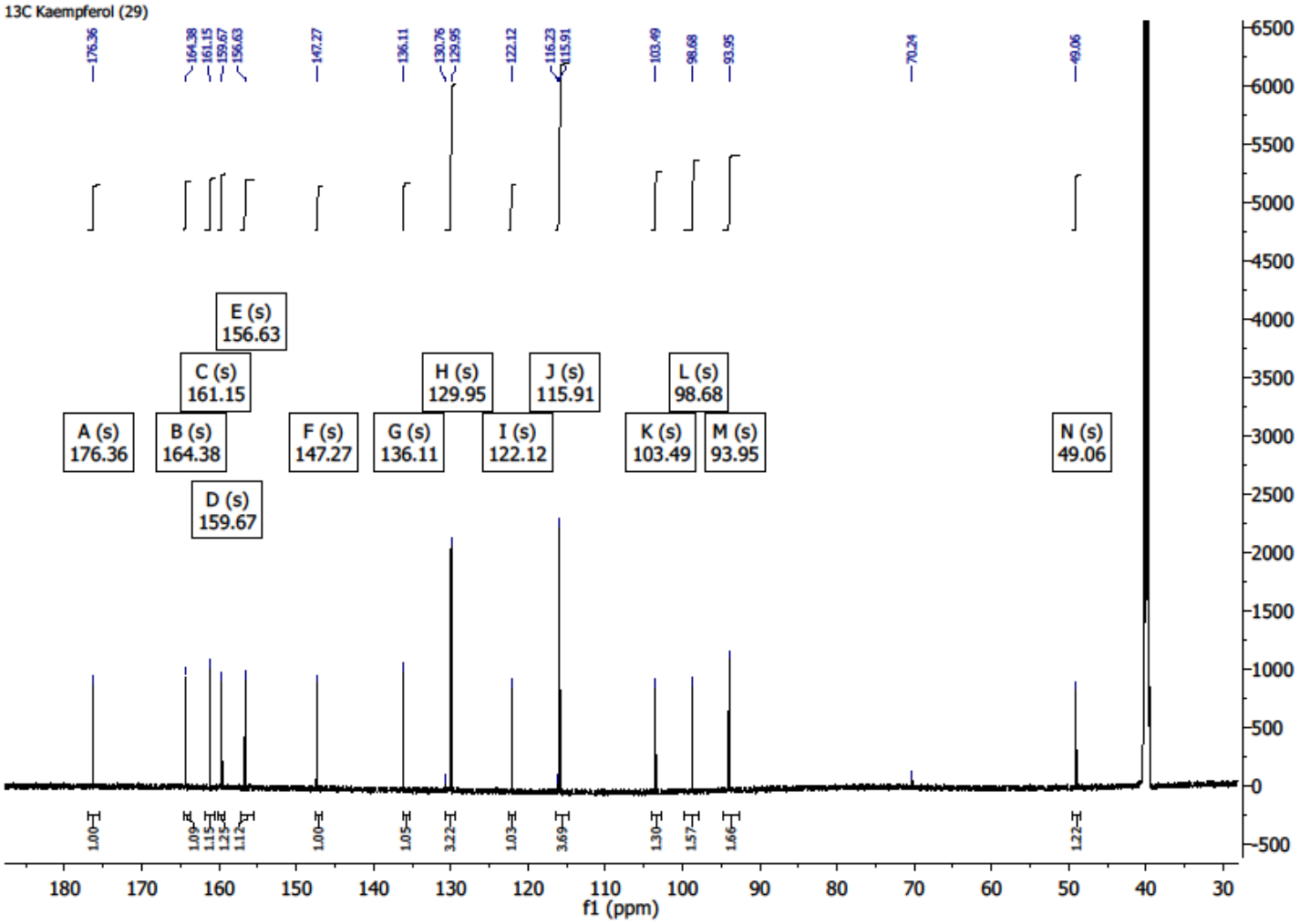

Supplemental Figure 2.44. ^{13}C spectra (DMSO-*d*6) of kaempferol (**29**).

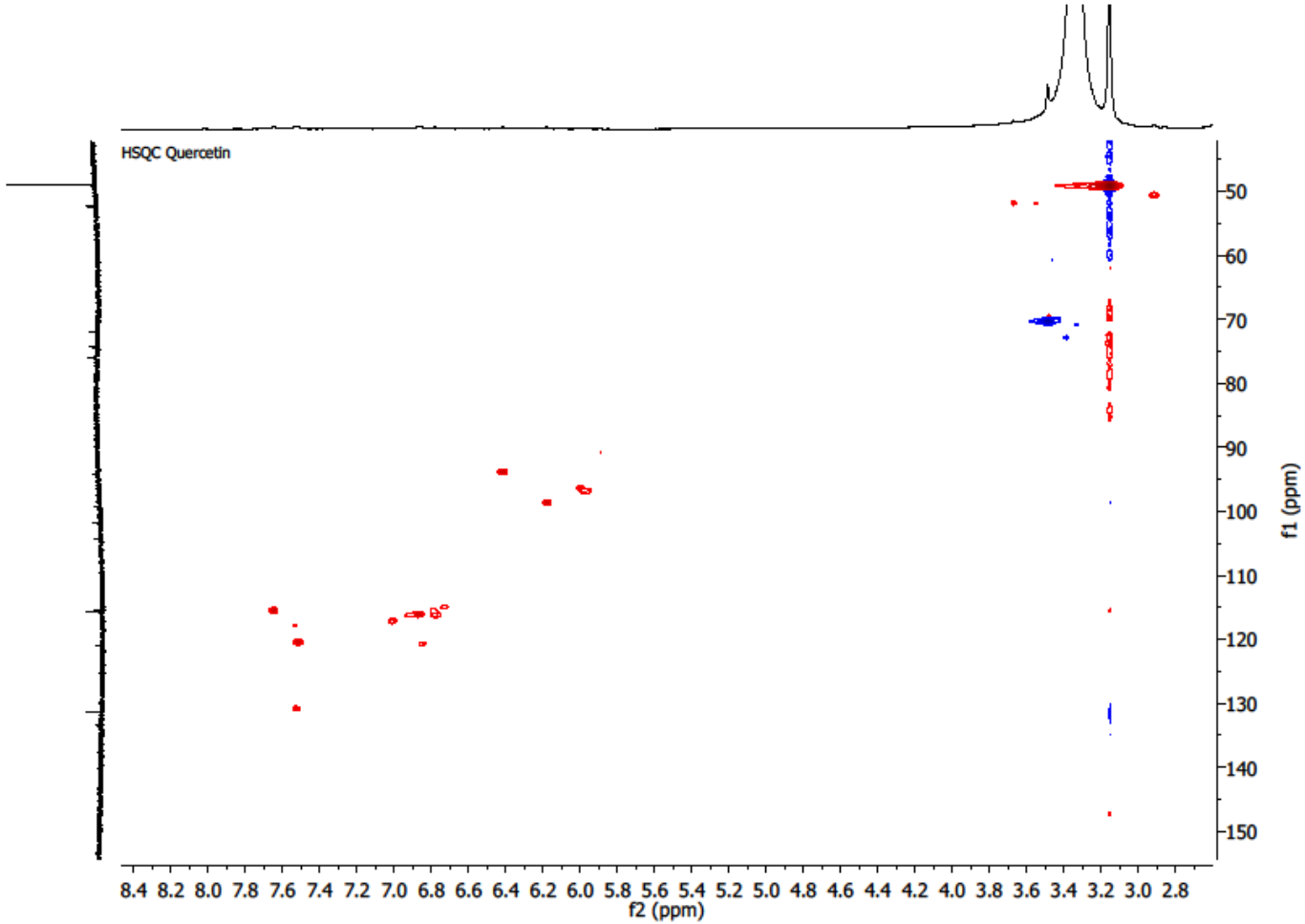

Supplemental Figure 2.45. HSQC spectra (DMSO-*d*6) of quercetin.

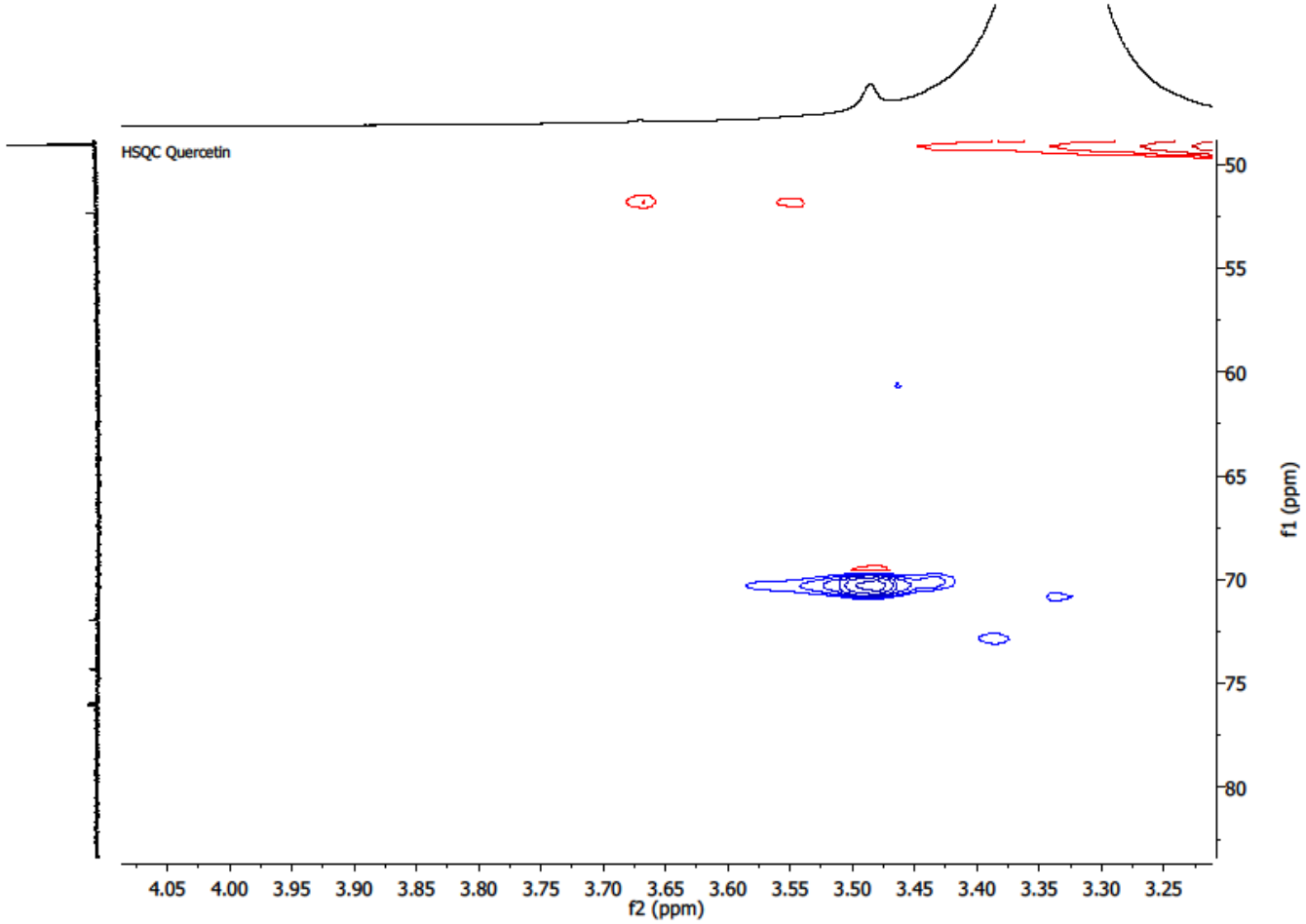

Supplemental Figure 2.46. Zoom from 3.2 to 4.0 ppm, HSQC spectra (DMSO-*d*6) of quercetin.

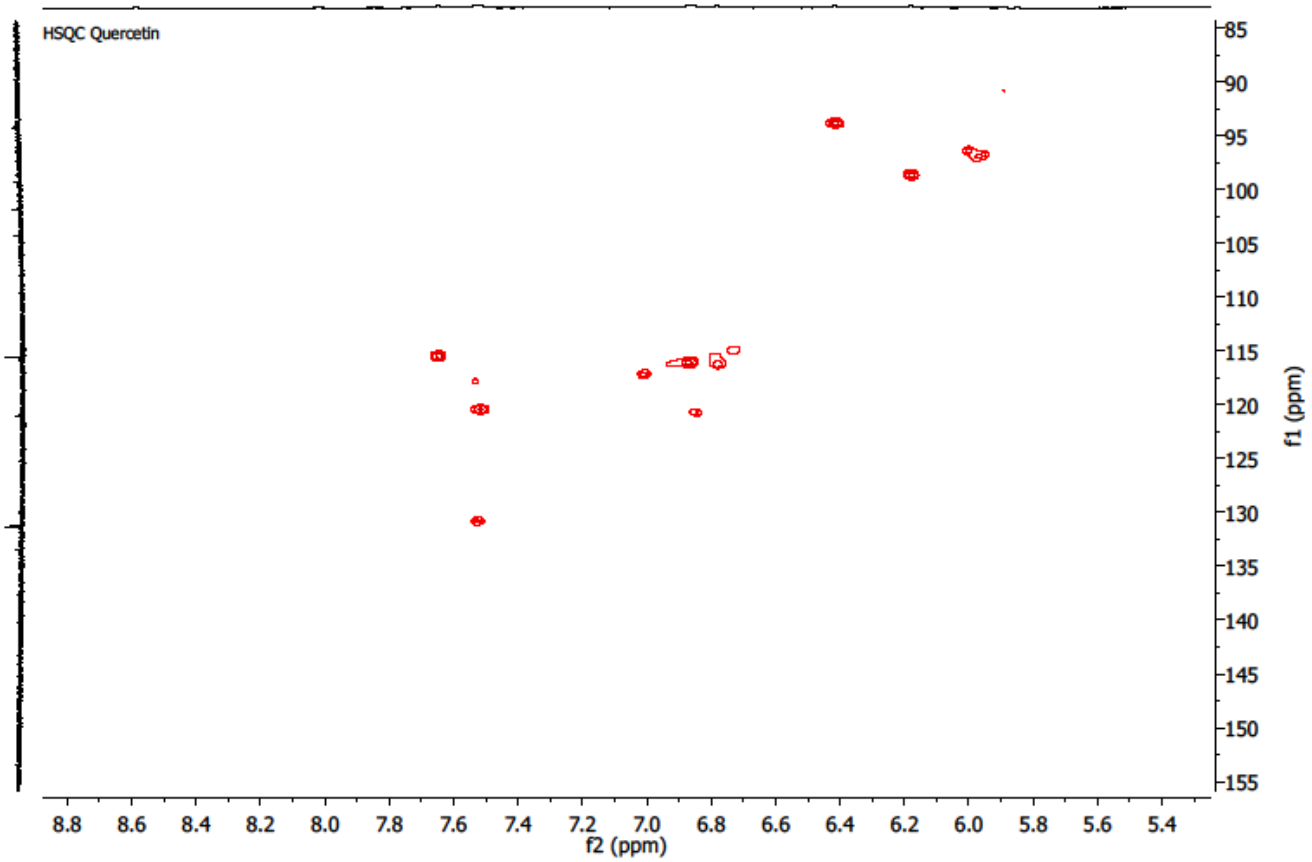

Supplemental Figure 2.47. Zoom from 5.4 to 8.8 ppm, HSQC spectra (DMSO-*d*6) of quercetin.

Chapter 3 – The regulation of floral color change in *Tibouchina pulchra*.

1. INTRODUCTION

Tibouchina pulchra (Cham.) Cogn. (Melastomataceae, Myrtales), named as "manacá da serra", is a native species from the Atlantic Forest. Its use for urban ornamentation is increasing due to its beautiful flowers. In this sense, the ornamental dwarf cultivar of *T. pulchra* ("manacá-anão") blooms with the same temporal pattern of floral color as the wild parental: buds, first stage (S1), open as white flowers (S2) that, one day after, become light pink (S3), further, flowers are deep pink (S4), from the third day towards senescence (Figure 3.1). As reviewed in chapter 1, the temporal alteration of flower color can be regulated by pollination, gene expression regulation, the presence of copigments and flavonoid-metal complexation, resulting in the differential accumulation of phenolic acids, flavonols, and anthocyanins extensively characterized in chapter 2.

Figure 3.1. Stages of floral color change of *T. pulchra*. S1- buds (day 0), S2- white flowers (day 1), S3- light pink (day 2), S4- dark pink (day 3).

T. pulchra flowers are nectarless, with poricidal anthers, hermaphrodite, heterantherous, herkogamous and self-compatible (Renner 1989, Brito & Sazima 2012). Concerning pollinators, Pereira *et al*. (2011) observed fifteen species of floral visitors in *T. pulchra,* being only four described as effective pollinators (*Bombus morio*, *B. pauloensis*, *Xylocopa frontalis* and *X. brasilianorum*). These large bees interact with poricidal anthers transferring the pollen to the stigmas by vibration. *Xylocopa* species collected pollen exclusively from white flowers, while *Bombus* visited pink flowers only at the end of the flowering season, when white flowers are scarce. Moreover, by performing controlled pollination experiments, it was demonstrated that the pollen viability, stigma receptivity and fruit setting were similar in white and pink flowers. This data together with the bee color preference described above suggest that flower color

change is not associated to pollination but, according to Da Silva (2006), may enlarge the visitor diversity.

As aforementioned, the pigments responsible for the color of *T. pulchra* flowers are phenolic acids and flavonoids (flavonols and anthocyanins). These phenolic compounds are produced by the combination of products from shikimic (SKM) and malonate (MAL) pathways, whose building blocks are derived from primary metabolism (Figure 3.2). Many simple benzoic acid derivatives (*e.g.* gallic acid, C_6C_1) and phenylpropanoids (*e.g. p*-coumaric, C_6C_3) are produced by SKM pathway, while flavonoids ($C_6C_3C_6$) are biosynthesized by intermediates from both, SKM and MAL pathways (Davies *et al*. 2009).

PHENYLALANINE AMMONIA LYASE (PAL) is the first enzyme in the phenylpropanoid and flavonoid pathway, it catalyzes the nonoxidative deamination of phenylalanine yielding *trans*-cinnamic acid. CINNAMATE 4-HYDROXYLASE (C4H) is a CYTOCHROME P450 MONOOXYGENASE (P450) enzyme involved in the hydroxylation of *trans*-cinnamic acid at C4 position to produce *p*-coumaric acid. This is a branching point that can channel the metabolic flux towards phenylpropanoids or flavonoids. By the action of COUMARATE 3-HYDROXYLASE (C3H), cinnamic acid derivatives as caffeic, ferulic, and sinapic acids are synthetized. On the other hand, *p*-coumaric acid is activated to the corresponding Co-A thioester facilitating further conversion to flavonoids, this reaction is catalyzed by 4-COUMARATE:CO-A LIGASE (4CL) (Dewick 2009, Saito *et al*. 2013).

The first produced flavonoid class comprises the chalcones, which are formed by the action of CHALCONE SYNTHASE (CHS). This enzyme belongs to a family of type III polyketide synthases and is the first committed enzyme in biosynthesis of flavonoids. Three sequential additions of the extender molecule malonyl-CoA in a *p*-coumaroyl-CoA is the reaction catalyzed by CHS (Dewick 2009, Saito *et al*. 2013). Chalcones are the first colored flavonoid, and provide yellow coloration to petals of a few plant species (*e.g. Dianthus caryophyllus* L., Caryophyllaceae, Caryophyllales) (Ono *et al*. 2006a, 2006b). CHALCONE ISOMERASE (CHI) acts in the stereospecific cyclization of naringenin chalcone to flavanone. FLAVANONE 3-HYDROXYLASE (F3H) is responsible for the oxygenation at C3 position of flavanone to form dihydroflavonol (dihydrokaempferol). FLAVONOID 3′-HYDROXYLASE (F3′H) and FLAVONOID 3′-5′-HYDROXYLASE (F3′5′H) are P450 that catalyze the hydroxylation at C3′and C3′-C5′-positions of the B-ring of flavonoid, respectively, rendering dihydroflavonols.

FLAVONOL SYNTHASE (FLS) and DIHYDROFLAVONOL REDUCTASE (DFR) are competitors for the same substrate, dihydroflavonol, a branching point for flavonols and anthocyanins formation (Pelletier *et al*. 1997). FLS catalyzes the double bond formation between C2 and C3, while DFR reduces the C4-keto group of dihydroflavonol to the corresponding leucoanthocyanidin. FLS, F3H and ANTHOCYANIDIN SYNTHASE (ANS) are the three 2-OXOGLUTARATE/FE(II)-DEPENDENT DIOXYGENASE (2-ODD) enzymes in the flavonoid biosynthesis pathway. The enzyme ANS catalyzes the formation of anthocyanidin from leucoanthocyanidin. Anthocyanidins exhibit a conjugated double bond system encompassing A, B and C rings, the later with two double bonds carrying a positive charge. Anthocyanidins are the chromophore moiety of anthocyanins, which are formed after glycosylation, acylation and/or methylation by the action of specific enzymes as FLAVONOID GLUCOSYLTRANSFERASE (FGT), ANTHOCYANIDIN ACYLTRANSFERASE (ACT) and/or *O*-METHYLTRANSFERASE (OMT) (Figure 3.2). In *Arabdopsis thaliana* (L.) Heynh. (Brassicaceae, Brassicales), FGT can transfer glucose to the C3 position of both, flavonol and anthocyanin aglycones (Yonekura *et al*. 2012).

Due to anthocyanins appeal as natural food colorant, nutraceutic and bioactive compounds (Norberto *et al*. 2013, De Ferrars *et al*. 2014, Xiaonan *et al*. 2016, Gowd *et al*. 2017), the regulation of anthocyanin biosynthetic pathway has been extensively explored. Most of the structural genes have been isolated (Winkel-Shirley 2001) and several regulatory genes have been characterized. Petunia (*Petunia hybrid* Vilm., Solanaceae, Solanales) and snapdragon (*Antirrhinum majus* L., Plantaginaceae, Lamiales) are the major model species for the study of anthocyanin biosynthesis, especially in floral tissues, however, maize (*Zea mays* L., Poaceae, Poales) and *Arabdopsis thaliana* have been extensively studied as well (Cone *et al*. 1986, Goodrich *et al*. 1992, Quattrocchio *et al*. 1998, 1999, Broun 2005, Dixon *et al*. 2005, Koes *et al*. 2005, Grotewold 2006).

Regarding the position in the pathway, structural genes can be grouped into two classes: early biosynthetic genes (*e.g. PAL*, *C4H*, *CHS*, and *FLS*) and late biosynthetic genes (*e.g*. *DFR* and *ANS*) (Tornielli *et al*. 2009). The early genes of anthocyanin pathway were functionally characterized in many plant species such as *A. thaliana*, *Solanum lycopersicum* L. (Solanaceae, Solanales), *Vitis vinifera* L. (Vitaceae, Vitales), *P. hybrida*, and *A. majus* (Sparvolli *et al.* 1994, Brugliera *et al*. 1999, Mol *et al.* 1983, Guo *et al.* 2009, Huang *et al.* 2010), while late genes (*DFR* and *ANS*) have been characterized mostly in *P. hybrid* and *A. thaliana*. (Pelletier *et al*. 1997, Devic *etal.* 1999). However, much less is known about the subsequent modifications

(substituents), such as glycosylation, acylation, and methylation (Grotewold 2006). In fact, there are several types of substituents that guarantee the chemical diversity in flower color. For example, *P*. *hybrida* synthesizes methylated anthocyanins with an acylated rutinose moiety, while *A*. *thaliana* accumulates more complex anthocyanins with seven sugar and acyl moieties but no methyl groups (Brouillard *et al*. 2003, Saito *et al*. 2013).

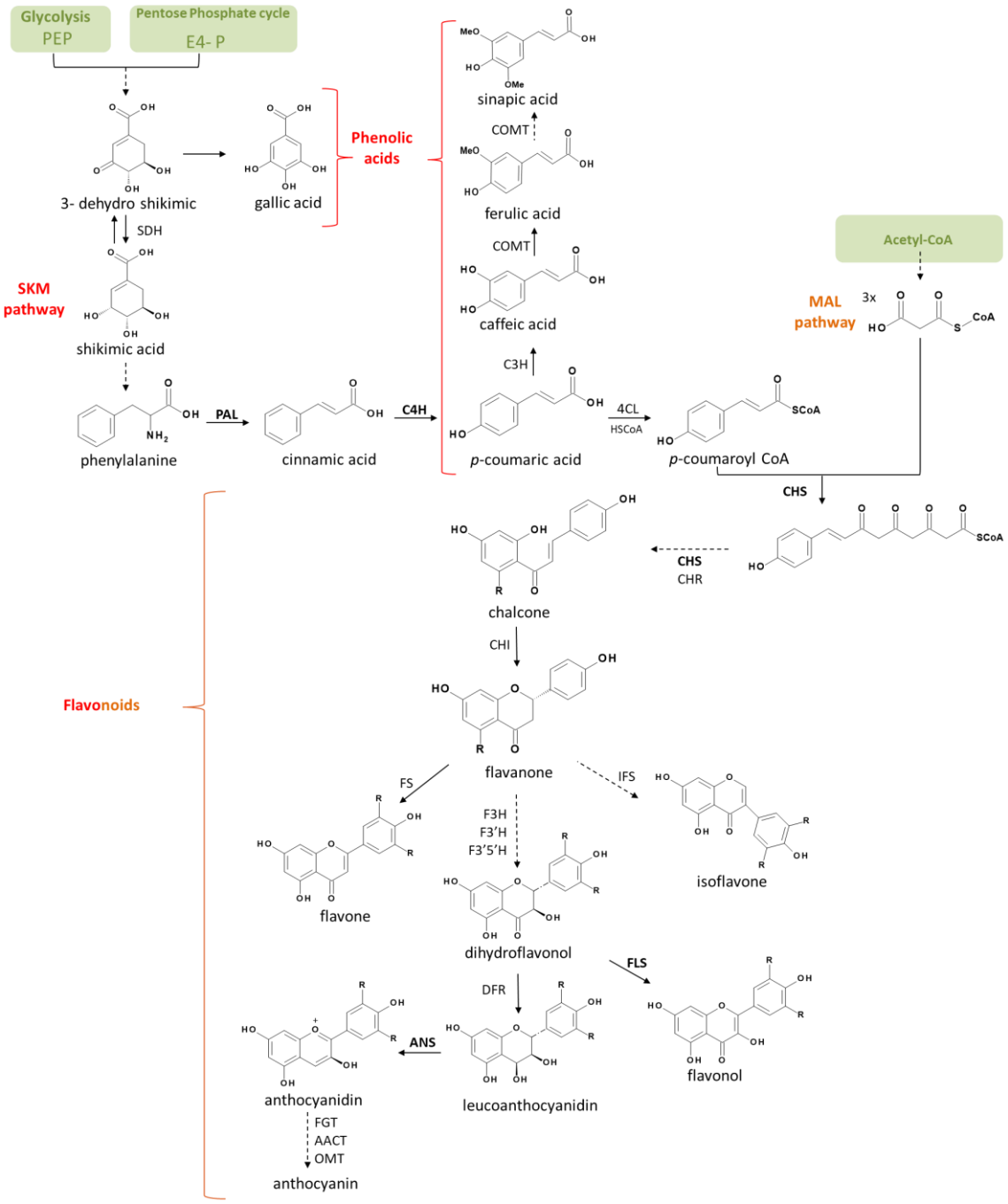

Figure 3.2. Simplified schematic representation of flavonoid biosynthetic pathway. Primary metabolism is highlighted in green. Abbreviations indicate the following enzymes: 4-COUMARATE:CO-A LIGASE (4CL), ANTHOCYANIDIN ACYL TRANSFERASE (AACT), **ANTHOCYANIDIN SYNTHASE (ANS),** CAFFEIC ACID *O*-METHYLTRANSFERASE (COMT), **CINNAMATE 4-HYDROXYLASE (C4H),** CHALCONE ISOMERASE (CHI), CHALCONE REDUCTASE (CHR), **CHALCONE SYNTHASE (CHS),** Coenzyma A (CoA), COUMARATE 3-HYDROXYLASE (C3H), DIHYDROFLAVONOL 4-REDUCTASE (DFR), erythrose 4-phosphate (E4P), FLAVANONE 3-HYDROXYLASE (F3H), FLAVONE SYNTHASE (FS), FLAVONOID 3'-HYDROXYLASE (F3'H), FLAVONOID 3'5'-HYDROXYLASE (F3'5'H), FLAVONOID GLYCOSYL TRANSFERASE (FGT), **FLAVONOL SYNTHASE (FLS),** HSCoA: coenzyme A, ISOFLAVONE SYNTHASE (IFS), malonate (MAL), *O*-METHYLTRANSFERASE (OMT), **PHENYLALANINE AMMONIA LYASE (PAL),** phosphoenolpyruvate (PEP), SHIKIMATE DEHYDROGENASE (SDH), and shikimate (SKM). The enzymes studied in the present work are highlighted in bold. Dotted lines represent more than one enzymatic reaction. Adapted from Dewick *et al.* (2009).

Numerous studies have demonstrated the transcriptional regulation of anthocyanin biosynthesis. A transcription factor complex (MBW complex) composed by a MYELOBLASTOSIS (MYB), a BASIC HELIX-LOOP-HELIX (bHLH), and a BETA-TRANSDUCIN REPEAT (WD40) protein, has shown to regulate the expression of the structural genes (Koes *et al*. 2005, Hichri *et al*. 2011, Xu *et al*. 2014, 2015). In vegetative tissues of *A. thaliana*, an eudicot, anthocyanin early biosynthetic genes are co-activated by bHLH and WD40 transcription factors in a MYB-independent manner, while the late biosynthetic genes require all three proteins to form the active MBW complex. Interestingly, in maize, a monocot, early and late biosynthetic genes are transcriptionally activated exclusively by MYB and bHLH proteins (Petroni & Tonelli 2011). By the characterization of mutant genotypes and transgenic lines, the transcriptional induction of anthocyanin biosynthesis in flowers has been addressed in several species, where distinct combinations of the aforementioned transcriptional factors have shown to be needed to determine floral pigmentation. MYB transcription factors induce early and late biosynthetic genes in *Nicotiana tabacum* L. (Solanaceae, Solanales), *Brassica oleracea* L. (Brassicaceae, Brassicales), *Anthurium andraeanum* Linden ex André (Araceae, Alismatales), *Mimulus lewisii* Pursh (Scrophulariaceae, Lamiales), and *M. cardinalis* Douglas ex Benth. flowers (Chiu *et al*. 2010, Pattanaik *et al*. 2010, Li *et al*. 2016, Yuan *et al*. 2016). In *Ipomea purpurea* (L.) Roth (Convolvulaceae, Solanales) transposon-insertion double mutants for *bHLH* and *MYB* genes resulted in snow-white flowers where the expression of the late biosynthetic genes was completely abolished (Park *et al.* 2007).

Additionally, the existence of post-transcriptional regulatory mechanisms has also been verified to control anthocyanin biosynthesis. In *A. thaliana*, it has been reported that the expression of the anthocyanin-associated MYB transcription factors is regulated by miRNAs and tasiRNAs-mediated hetero-silencing (Rajagopalan *et al*. 2006, Hsieh *et al*. 2009). In particular, the miR156 targets SQUAMOSA PROMOTER BINDING PROTEIN-LIKE (SPL) mRNA, whose product destabilizes the MBW transcriptional activation complex. Thus, increased miR156 activity promotes the accumulation of anthocyanins by the MBW complex-mediated transcriptional induction of the late biosynthetic genes (Gou *et al*. 2011). Moreover, in *Petunia*, *CHS* has also shown to be post-transcriptionally regulated by siRNA (Koseki *et al*. 2005). Interestingly, anthocyanin accumulation in maize kernels is controlled by the regulation of the splicing patter of *Bz2* gene, a GLUTATHIONE S-TRANSFERASE (GST) that mediates transfer of cytoplasmic anthocyanin into the vacuole (Pairoba & Walbot 2003).

Finally, post-translational regulation has also been reported for anthocyanin biosynthesis. In *A. thaliana*, KELCH REPEAT F-BOX proteins have shown to physically interact with four PAL isozymes inducing their 26S proteasome- mediated ubiquitination, resulting in the downregulation of phenylpropanoid biosynthesis (Zhang *et al*. 2013).

Although for some biological systems the regulation of anthocyanin biosynthesis has been elucidated, including the identification of master transcription factors (Butelli *et al.* 2008), many gaps remain unsolved for the complete understanding of the mechanisms underneath the accumulation of these pigments. Improving the knowledge about the multilevel regulation of gene expression will favor the development of new biotechnological tools for the generation of new varieties with enhanced health-promoting properties and visual appeal (Hichri 2011).

Some studies showed that metals can influence the color by establishing a flavonoid-metal complex. In cornflowers (*Centaurea sp.*, Asteraceae, Asterales), the bright blue color is the result of a supramolecular structure with stacking between copigments, pigments and metals: six molecules of apigenin, six molecules of cyanidin and four metal ions (Fe^{3+}, Mg^{2+} and two Ca^{2+}) (Shiono *et al*. 2005). Hortensia flowers (*Hydrangea macrophylla* (Thumb.) Ser., Hydrangeaceae, Cornales) are the best-known example of flavonoid-metal complexation influencing the corolla color. Under high aluminum content and acidity of the soil, the flowers are blue due to a nonstoichiometric complex with Al^{3+}, delphinidin 3-glucosides, quinic acid derivatives, while upon low aluminum concentrations, the same metal-pigment-copigment complex became light pink, as the result of soil pH change (Yoshida *et al.* 2003, Kondo *et al*. 2005, Oyama *et al*. 2015, Trouillas *et al*. 2016).

The pH affects the final color of flower petals by determining the conformation and absorption spectrum of anthocyanins. The light blue petals of morning glory (*Ipomoea tricolor* Cav.*,* Convolvulaceae, Solanales) owe their color to the effect of the alkaline pH on the accumulated anthocyanins. The closed buds of these flowers are purplish red and their cells have a pH of 6.6. However, when the flowers open, the petal cell pH increases up to 7.7, and the pigment changes color to sky blue (Yoshida *et al.* 1995). Recently, studying the genetic determinants of *P. hybrida* flower pigmentation, Verweij *et al*. (2016) have identified PH3 protein, a WRKY-type transcriptional factor that regulates the expression of the proteins responsible for the vacuolar acidification.

The well-determined stages of flower coloring in *T. pulchra*, raise interesting questions about the genetic and chemical mechanisms involved in the regulation of this phenomenon,

which has been unexplored up to now. Here, we addressed this issue by cloning key flavonoid biosynthetic genes and profiling mRNA levels, pigment composition and metal content along flower development.

2. MATERIAL AND METHODS

2.1. Plant material

Petals at S1 to S4 stages (Figure 3.1) were sampled from five *Tibouchina pulchra* (cv. "manacá-anão") plants located in Praça Carlos José Gíglio (Latitude: -23.57998, Longitude: -46.73403) in the most vigorous flowering period (May and June/2016) between 8 and 9 a.m. For each developmental stage a pool of petals (~ 5 g) from each plant was considered a biological replicate (n = 5). Samples were collected with gloves, in a sterile tube and immediately frozen in liquid nitrogen. Petals were stored at -80°C for mRNA extraction, or freeze dried in a lyophilizer (K202, Liobras) for chemical analysis. All material was crushed in a ball mill (TissueLyser, Qiagen) for further analyses. For gene cloning a pool of all stages collected in May and June/2014 was used. An exsiccate was deposited on herbarium of Institute of Bioscience (SPF) of University of São Paulo (ID: Furlan73).

2.2. Pigment profile

Phenolic profile was assessed analyzing petal extracts by Ultra Performance Liquid Chromatography (UPLC) system with Diode Array Detector (DAD) (Dionex Ultimate 3000) and Electrospray Ionization Quadrupole Time-of-Flight High-Resolution Mass Spectrometry (ESI-QTOF-HRMS) detector (Bruker Maxis). The extraction was performed as described in chapter 2 (item 2.2). To quantify the compounds, the areas of MS^+ chromatograms were compared with standard curves of *p*-coumaric acid, kaempferol and cyanidin. This analysis was performed in the Department of Chemistry at Denmark Technical University under the supervision of Ph.D. Mads H. Clausen.

2.3. Gene cloning and expression

2.3.1. Sequence analysis for primers design

The sequences of the functionally characterized genes *PAL* (AT2G37040.1), *C4H* (AT2G30490.1), *CHS* (AT5G13930.1), *FLS* (AT5G08640.1) and *ANS* (AT4G22880.1) from *Arabdopsis thaliana* (Wanner *et al*. 1995, Bell-Lelong *et al.* 1997, Pelletier *et al*. 1997, Feinbaum & Ausubel 1998) were used as query to identified, by tBLASTx program (Altschul *et al.* 1997), the orthologous sequences from *Vitis vinifera*, *Eucalyptus grandis* W.Hill (Myrtaceae, Myrtales), and *Solanum lycopersicum* fully sequenced genomes available in the Phytozome v 9.0 database

(http://www.phytozome.net/). The amino acid coding sequences were aligned using the MUSCLE program following the standard configurations of the MEGA 6 package (Tamura *et al*. 2011). After the identification of conserved domains, the alignments were converted to nucleotides for degenerated primer design based on *Eucalyptus grandis* sequences, which is the *T. pulchra* closest related species with completely sequenced genome (Supplemental Figure 3.1 and Supplemental Table 3.2). The quality of the designed primers was verified using the software Oligo Analyzer 3.1 (http://www.idtdna.com).

Additionally, using the same strategy described above, primers were designed for the cloning of two reference genes for Reverse Transcriptase Quantitative Polymerase Chain Reaction (RT-qPCR) normalization. The chosen genes were those previously described for gene expression analyses in *Petunia hybrida* flowers, *ELONGATION FACTOR 1α* (*EF1*) and *RIBOSOMAL PROTEIN S13* (*RPS*) (Mallona *et al*. 2010).

2.3.2. RNA extraction and cDNA synthesis

Total RNA from 3 g of petal samples was extracted with CTAB (Cetyl trimethylammonium bromide- Chang *et al*. 1993) (Supplemental Figure 3.2). DNA was removed with 100 U of amplification-grade DNase (Invitrogen) following the recommended protocol. cDNA was synthesized from 1 µg of RNA using oligo dT (for gene cloning) or random primers (for RT-qPCR) and the SuperScript III kit (Invitrogen). cDNA quality was confirmed by PCR using *RPS* constitutive gene primers.

2.3.3. Cloning

Gene fragments were amplified by PCR in a total volume of 50 µL containing 0.2 mM each dNTPs, 0.2 µM each primer (Supplemental Table 3.2), 1X reaction buffer, 1.5 mM $MgCl_2$, 50 ng of cDNA, and 2 U of Taq DNA polymerase (Invitrogen). The amplification conditions were: 94°C for 3 min, 35 cycles of 94°C for 30 s, 50°C for 30 s, and 72°C for 1 min, and then 72°C for 10 min. Amplification products were purified (Kit GFX Amersham Biosciences) and cloned into a TOPO-TA vector (Dual promoter Kit Invitrogen) following the recommended protocols. Transformation was carried by using 50 µL of *Escherichia coli* DH10B competent cells with 2 µL of the ligation product. The mixture was kept on ice for 30 min, and subjected to a thermal shock of 45 sec at 65°C and 2 min on ice. 500 µL of SOC (Super Optimal Broth) medium (Hanahan 1983) was added for a shaking incubation (45 min at 37°C). Samples were centrifuged (3 min, 3,000 rpm at room temperature) and cells resuspended and plated on Luria-Bertani (LB)

agar (Bertani *et al.* 1951) with kanamycin, X-Gal (5-bromo-4-chloro-3-indoxyl-β-D-galactopyranoside) and IPTG (isopropil β-D-1-tiogalactopiranosida). Five positive colonies for each gene were grown in liquid LB and plastidial DNA was purified and sequenced with vector universal primers.

2.3.4. Sequence analyses

To verify the identity of the cloned *T. pulchra* gene fragments, phenetic analyses were performed. Orthologous sequences from *Arabdopsis thaliana* (AT) and *Brassica rapa* L. (Brara)- Brassicaceae, Brassicales, *Eucalyptus grandis* (Eucgr)- Myrtaceae, Myrtales, *Mendicago trunculata* (Medtr) and *Trifolium pratense* L. (Tp) – Fabaceae, Fabales, and *Solanum lycopersicum* (Soly) – Solanaceae, Solanales, were retrieved from Phytozome v 12.1 database (http://www.phytozome.net /) by tBLASTx program (Altschul *et al.* 1997). The species were selected according to the following criteria: i) fully sequenced genome, ii) genes belonging to gene families whose functional annotation was associated to phenolic compound biosynthesis (gene family 94476114 for *PAL*, 94469571 for *C4H*, 94475332 for *CHS*, 94475392 for *FLS*, 94470119 for *ANS*, 94475526 for *RPS* and 94476231 for *EF1*), and iii) species placed in Rosids clade in APG IV classification (AT, Brara, Eucgr, Medtr and Tp, and Soly as outgroup). The coding sequences were aligned using the Clustal program following the standard configurations of the MEGA 6 package (Tamura *et al*. 2011), with manual verification of each codon according to the amino acid sequence. The phenograms were constructed with the following parameters: *Neighbor-joining*, *Bootstrap* of 1,000 replicates and the best model test for each analysis.

2.3.5. RT-qPCR

Based on *T. pulchra* sequences, gene specific primers for expression analysis were designed to amplify fragments of approximately 160 bp (Supplemental Table 3.2). To quantify mRNA levels by RT-qPCR, reactions were carried out in a QuantStudio 6 Flex Real-Time PCR system (Applied Biosystems) using 2X Power SYBR Green Master Mix reagent (Life Technologies) in 14 µL final volume. Absolute fluorescence data were analyzed using the LinRegPCR software package (Ruijter *et al*. 2009) to obtain quantitation cycle (Cq) values and calculate primer efficiencies (the primer efficiency values ranged from 1.85 to 1.98). Expression values were normalized against the geometric mean of the two reference genes (*EF1* and *RPS*), according to Quadrana *et al*. (2013). A permutation test lacking sample distribution assumption

(Pfaffl *et al*. 2002) was applied (formula below) to detect statistical differences ($P<0.05$) in expression ratios using the algorithms in the fgStatistics software package (Di Rienzo 2009).

$$RE = \frac{Pe_{goi}^{\wedge (\text{control Ct mean} - \text{sample Ct mean})}}{Pe_{ref}^{\wedge (\text{control Ct mean} - \text{sample Ct mean})}}$$

RE: relative expression, Pe: primer efficiency, goi: gene of interest, Ct: treshold cycle, control Ct: Ct mean of control biological replicates, sample Ct: Ct mean of sample biological replicates, ref: reference gene.

2.4. Metal content

To analyze the content of metals 500 mg of freeze-dried powder petals were sent to Laboratory of Vegetal Tissue (ESALQ, USP). After a nitro-perchloric digestion, contents of Mg, K, Na, Ca, Cu, Mn, Zn and Fe^{3+} were determined by Atomic Absorption Spectroscopy (AAS).

2.5. Data analyses

Statistical analysis for pigment and metal profiles were performed using Infostat package (Di Rienzo *et al*. 2011). When the data set showed normality, ANOVA followed by Tukey test ($P<0.05$) were performed to compare differences between groups. In the absence of normality, a non-parametric comparison was performed by applying the Kruskal-Wallis test ($P<0.05$). All values represent the mean of five biological replicates.

3. RESULTS

3.1. Pigment profile

Pigment profile revealed that *T. pulchra* flowers contain a diverse mixture of six phenolic acids, twenty-two flavonols and two anthocyanin (Table 3.1)- see details about identification in chapter 2. Flavonols were the most abundant pigments ranging from 20 to 25 mg g^{-1} DW, followed by phenolic acids that varied between 10 and 18 mg g^{-1} DW and anthocyanins displaying values of 0.028 to 0.076 mg g^{-1} DW.

Pigment abundance along flower development revealed that the amount of total phenolic acids increases during the transition from S1 to S2 maintaining constant levels from S2 onwards. This increment is due to the accumulation of the non-identified compound **6**. Regarding flavonols, except for kaempferol *p*-coumaroylhexoside (compound **30**), which showed increment from S2 to S3, the other twenty-one compounds showed a decreasing trend along flower development. Both identified anthocyanins were detected from the S3 stage exhibiting a significant increment in S4.

Table 3.1- Pigment profile in each developmental stage of *T. pulchra* flowers.

Compound	S1 (mg g^{-1}DW)	S2 (mg g^{-1}DW)	S3 (mg g^{-1}DW)	S4 (mg g^{-1}DW)
1- Phenolic acid	4.43 ± 2.96	5.9 ± 2.67	3.76 ± 2.46	7.6 ± 3.08
2- Cinnamic acid derivative	3.89 ± 2.28	4.18 ± 3.85	6.16 ± 1.50	3.53 ± 3.41
3- Phenolic acid	0.84 ± 0.91	1.55 ± 0.17	1.85 ± 0.20	1.92 ± 0.21
4- Phenolic acid	0.38 ± 0.75	0.14 ± 0.22	0.14 ± 0.21	0.15 ± 0.20
5- Cinnamic acid derivative	0.23 ± 0.23	0.57 ± 0.62	0.22 ± 0.16	0.26 ± 0.27
6- Phenolic acid	**0.90^{b} ± 0.61**	**5.24^{a} ± 1.33**	**4.19^{a} ± 1.08**	**4.23^{a} ± 0.94**
Phenolic acids total	**10.69^{b} ± 3.43**	**17.58^{a} ± 2.66**	**16.39^{a} ± 2.24**	**17.69^{a} ± 0.49**
Compound	**S1 (mg g^{-1}DW)**	**S2 (mg g^{-1}DW)**	**S3 (mg g^{-1}DW)**	**S4 (mg g^{-1}DW)**
7- N.I.	0.40 ± 0.41	0.70 ± 0.13	0.49 ± 0.40	0.57 ± 0.34
8- Myricetin hexoside	0.77 ± 0.47	0.56 ± 0.19	0.56 ± 0.08	0.58 ± 0.18
9- Myricetin hexoside	0.29 ± 0.21	0.22 ± 0.13	0.23 ± 0.07	0.27 ± 0.06
10- Quercetin galloylhexoside	0.41 ± 0.30	0.22 ± 0.10	0.23 ± 0.06	0.23 ± 0.16
11- Quercetin hexoside	1.26 ± 0.65	1.02 ± 0.37	0.98 ± 0.19	0.94 ± 0.16
12- Quercetin glucuronide	0.16 ± 0.07	0.06 ± 0.03	0.07 ± 0.04	0.11 ± 0.06
13- Kaempferol galloylhexoside	1.61 ± 0.85	1.36 ± 0.61	1.34 ± 0.22	1.24 ± 0.33
14- N.I.	0.19 ± 0.12	0.14 ± 0.08	0.14 ± 0.08	0.17 ± 0.09
15- Kaempferol hexoside	3.40 ± 1.30	3.20 ± 0.91	3.12 ± 0.55	2.92 ± 0.42
16- Kaempferol galloylhexoside	2.16 ± 0.94	1.78 ± 0.72	1.78 ± 0.46	1.70 ± 0.23
17- Kaempferol 3-*O*-β-D-glucopyranoside	6.48 ± 1.51	6.32 ± 0.85	6.44 ± 0.50	6.21 ± 0.47
18- Kaempferol pentoside	2.75 ± 1.43	2.41 ± 1.07	2.23 ± 0.63	1.96 ± 0.30
19- Kaempferol galloylhexoside	0.24 ± 0.14	0.22 ± 0.11	0.18 ± 0.07	0.16 ± 0.04
20- Kaempferol pentoside	0.23 ± 0.15	0.15 ± 0.10	0.14 ± 0.07	0.11 ± 0.05
21- Kaempferol *p*-coumaroylhexoside	0.53 ± 0.29	0.46 ± 0.26	0.40 ± 0.18	0.29 ± 0.07
23- Mixture- Kaempferol 3-*O*-glucuronide-6''-*O*-methylester / Petunidin derivative	0.28 ± 0.15	0.29 ± 0.09	0.21 ± 0.01	0.17 ± 0.05

Table 3.1. (*Continued)*

Compound	**S1 (mg g^{-1}DW)**	**S2 (mg g^{-1}DW)**	**S3 (mg g^{-1}DW)**	**S4 (mg g^{-1}DW)**
25- Quercetin 3-*O*-(6''-*O*-*p*-coumaroyl)-β-D-glucopyranoside	0.68 ± 0.38	0.52 ± 0.19	0.44 ± 0.08	0.40 ± 0.05
26- N.I.	0.43 ± 0.21	0.35 ± 0.20	0.31 ± 0.13	0.26 ± 0.04
27- Kaempferol 3-*O*-(6''-*O*-*p*-coumaroyl)-β-D-glucopyranoside	1.44 ± 0.65	1.20 ± 0.46	1.05 ± 0.00	0.94 ± 0.12
28- Kaempferol *p*-coumaroylhexoside	0.19 ± 0.09	0.16 ± 0.06	0.10 ± 0.03	0.08 ± 0.02
29- Kaempferol	0.94 ± 0.48	1.05 ± 0.44	0.83 ± 0.20	0.71 ± 0.08
30- Kaempferol *p*-coumaroylhexoside	**0.00^{b} ± 0.00**	**0.08^{b} ± 0,00**	**0.13^{a} ± 0.03**	**0.13^{a} ± 0.03**
Flavonol total	24.99 ± 10.31	22.17 ± 6.66	21.25 ± 3.13	19.94 ± 2.64
Compound	**S1 (µg g^{-1}DW)**	**S2 (µg g^{-1}DW)**	**S3 (µg g^{-1}DW)**	**S4 (µg g^{-1}DW)**
22- Petunidin *p*-coumaroylhexoside acetylpentoside	**0.00^{c} ± 0.00**	**0.00^{c} ± 0.00**	**8.43^{b} ± 2.21**	**22.42^{a} ± 8.00**
24- Malvidin *p*-coumaroylhexoside acetylpentoside	**0.00^{c} ± 0.00**	**0.00^{c} ± 0.00**	**19.87^{b} ± 5.28**	**53.72^{a} ± 20.18**
Anthocyanin total	**0.00^{c} ± 0.00**	**0.00^{c} ± 0.00**	**28.29^{b} ± 7.47**	**76.14^{a} ± 28.11**

* S1- buds (day 0), S2- white flowers (day 1), S3- light pink (day 2), S4- dark pink (day 3). DW- Dry weight. NI- not identified. Compounds highlighted in bold showed statistically significant differences between stages. Letters indicate statistically significant different values.

3.2. Gene cloning and expression analysis

In order to analyze the transcriptional profile of flavonoid biosynthetic genes and since no information about genome sequence is available for *T. pulchra*, the first aim proposed was the cloning of partial gene sequences for some key enzymes. The genes encoding for PAL, C4H, CHS, FLS, and ANS enzymes were chosen because they have been reported to be transcriptional regulated in other species. Additionally, two constitutive genes previously used for expression analyses in *Petunia hybrida* were also selected to be used as reference genes in RT-qPCR experiments. The gene fragment cloning was based on the identification of conserved protein domains and degenerated primers were designed based on the *E. grandis* paralog sequences, the *T. pulchra* most closely related species with complete sequenced genome (see item 2.3.1 in Material and Methods). Gene fragments with approximately the predicted size were amplified (Supplemental Figure 3.3), cloned and sequenced (Supplemental Figure 3.4).

The identity of the obtained gene fragments was corroborated by a phenetic analysis. Although the topology did not strictly follow the species phylogenetic relationship, species belonging to the same order grouped together: *B. rapa* and *A. thaliana* (Brassicales), *M. trunculata* and *T. pratense* (Fabales), and *T. pulchra* and *E. grandis* (Myrtales) (Figure 3.3). It is worth mentioning that the aim of this analysis was exclusively to confirm the identity of the cloned sequences corroborating its homology to sequences predicted as the corresponding genes. All five *T. pulchra* sequences grouped together to the corresponding putative homologous from *E. grandis* demonstrating that the strategy was successful to clone partial sequences of flavonoid biosynthetic genes.

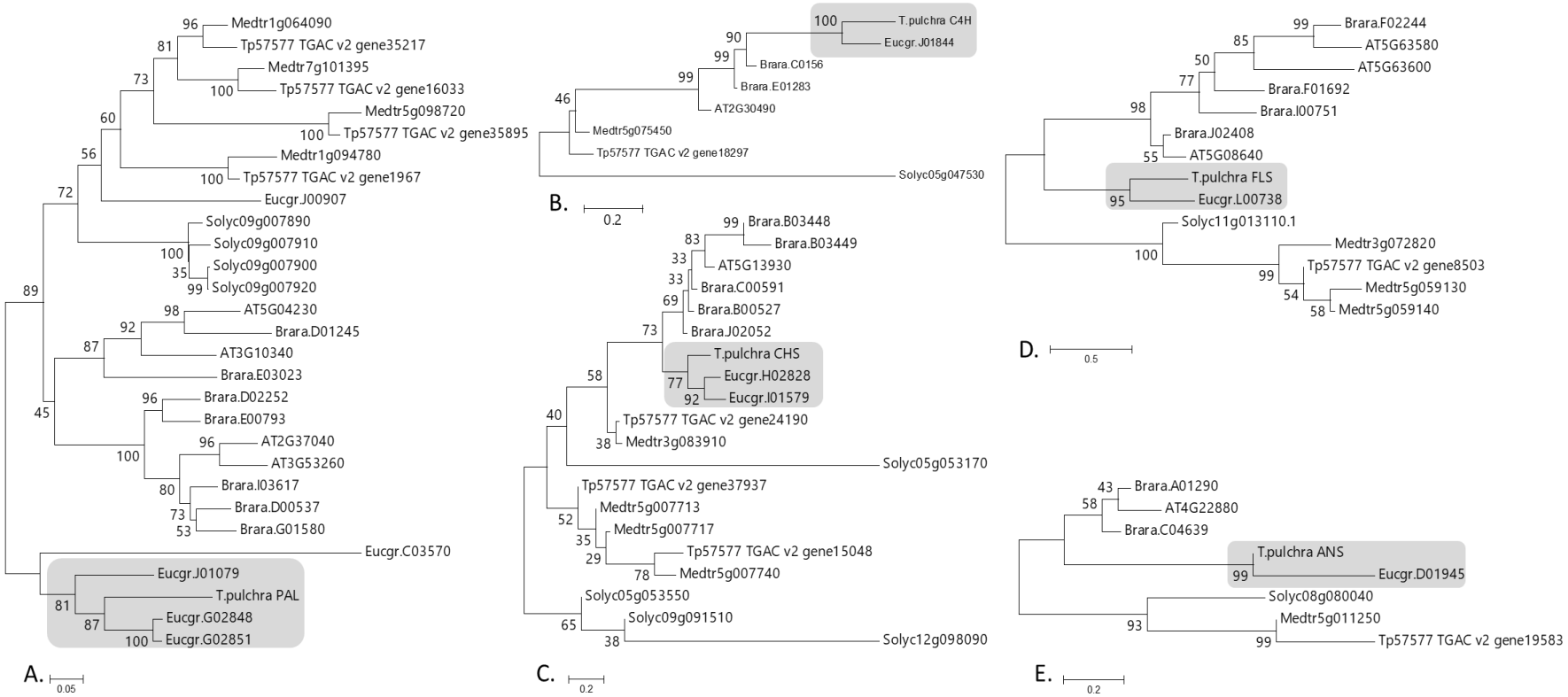

Figure 3.3. Phenograms for *PHENYLALANINE AMMONIUM LYASE* (*PAL)* (A)*, CINAMMATE 4-HYDROXYLASE (C4H)* (B), *CHALCONE SYNTHASE* (*CHS)* (C), *FLAVONOL SYNTHASE* (*FLS)* (D), and *ANTHOCYANIDIN SYNTHASE* (*ANS)* (E) genes. Sequences from species with full sequenced genomes were included in the analyses: *Eucalypstus grandis* (Eucgr), *Arabdopsis thaliana* (AT), *Brasica rapa* (Brara), *Mendicago trunculata* (Medtr), *Trifolium pratense* (Tp) and *Solanum lycopersicum* (Soly). Trees were constructed using the following parameters: *Neighbor-joining*, *Bootstrap* of 1,000 replicates and the best model test for each analysis. Grey boxes show the clusters for *T. pulchra* (T.pulchra) and *E. grandis* sequences.

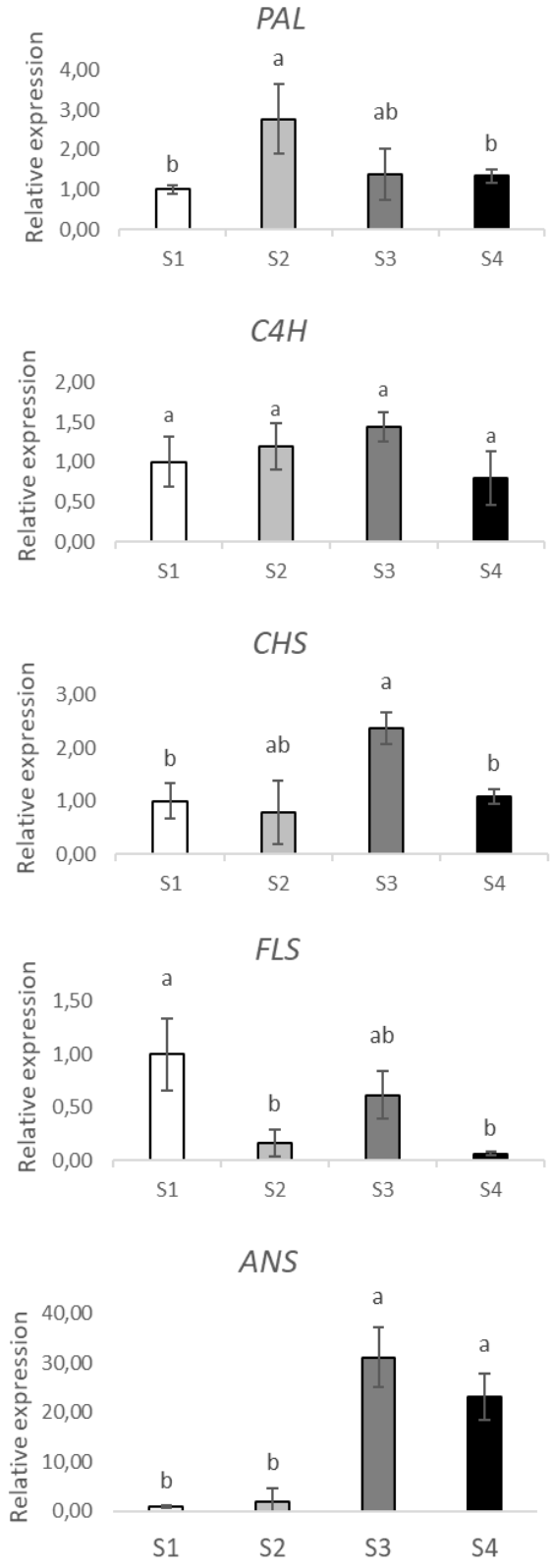

Figure 3.4. Expression profile of *PHENYLALANINE AMMONIUM LYASE* (*PAL), CINAMMATE 4-HYDROXYLASE (C4H)*, *CHALCONE SYNTHASE* (*CHS)*, *FLAVONOL SYNTHASE* (*FLS),* and *ANTHOCYANIDIN SYNTHASE* (*ANS*) genes along flower development. Different letters indicate statistically different relative expression ratios. S1- buds (day 0), S2- white flowers (day 1), S3- light pink (day 2), S4- dark pink (day 3).

To address whether the transcriptional regulation of gene expression is involved in *T. pulchra* flower color change, the mRNA accumulation of the cloned enzyme-encoding genes was profiled in four flower stages (S1 to S4) analyzed (Figure 3.4). As expected, since the gene fragments were cloned from petal cDNA, the presence of mRNA from all five genes was identified. With the exception of *C4H* that maintained constant levels of mRNA, the other four genes analyzed showed to be transcriptionally regulated along flower development.

The expression of the first committed gene in the phenolic compound biosynthetic pathway, *PAL*, peaked in the white opened flower (S2), while *CHS* mRNA reached its highest level at the first pink stage (S3). *FLS*, whose product diverges the route towards flavonols synthesis, showed maximum expression level in buds (S1), decreasing onwards. Finally, the *ANS* enzyme encoding gene, responsible for the synthesis of the anthocyanin chromophores, is 30-fold upregulated from white to pink stages (S2 to S3) and remains highly expressed until dark pink stage (S4).

3.3. Metal content

Due to the eventual impact of metal concentration on pigment color, the metal content was also profiled along flower development. Among the analyzed metals, Fe^{3+} and K were the most abundant macro and micronutrients, respectively (Figure 3.5). The only metal that showed fluctuation between flower stages was Fe^{3+}, which increased from S3 to S4.

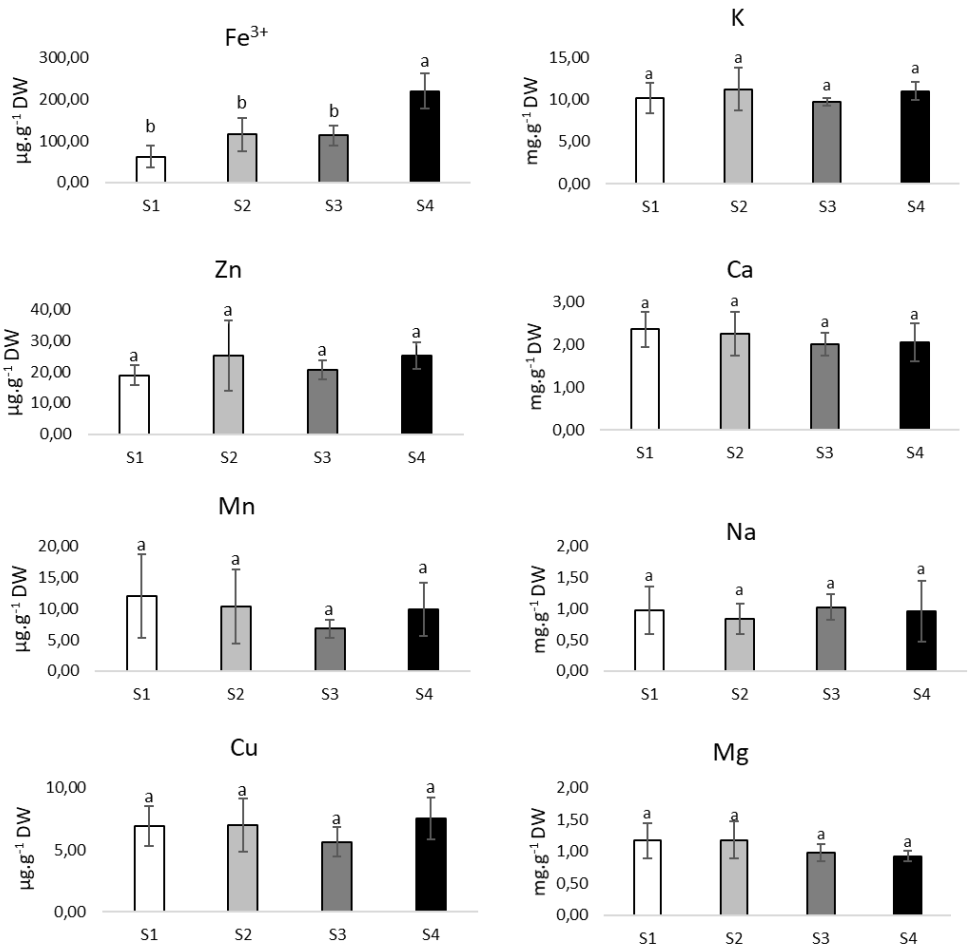

Figure 3.5. Metal quantification along *T. pulchra* flower development. Different letters indicate statistically different values. S1- buds (day 0), S2- white flowers (day 1), S3- light pink (day 2), S4- dark pink (day 3).

4. DISCUSSION

Flower color change is a widespread phenomenon in angiosperms and poorly studied from the chemical and molecular point of view. In this work, the phenomenon of *T. pulchra* floral color change was addressed by a comprehensive analysis of pigments, gene expression and metal profiling along flower development.

In general, phenolic acids and, especially, flavonols are associated to white flowers (*e.g. Petunia hybrid* (Saito *et al*. 2006), *Trifolium repens* L., Fabaceae, Fabales (Abeynayake *et al*. 2012), and *Cymbidium hybrid*, Orchidaceae, Asparagales (Wang *et al*. 2014)). These copigments are also found in pink, purple and red flowers, although the color is attributed to the presence of anthocyanins, *e.g. I. tricolor* (Park *et al*. 2014), *P. hybrida* (Saito *et al*. 2006), *Trifolium repens* (Abeynayake *et al*. 2012), *Cymbidium hybrid* (Wang *et al*. 2014), *Dendrobium* sp, Orchidaceae, Asparagales (Willians *et al*. 2002), *Rosa rugosa* Thunb*., R. multiflora* Thunb., and *Prunus persica* (L.) Batsch Rosaceae, Rosales, *Dianthus caryophyllus* L., Caryophyllaceae, Caryophyllales, *Camellia japonica* L., Theaceae, Ericales (Luo *et al*. 2016), *Rhododendron* sp, Ericaceae, Ericales (Du *et al*. 2017).

Ferulic, caffeic and *p*-coumaric acids derivatives are the phenolic acids commonly found in flower tissues, while, kaempferol (acylated glycoside, diglycoside, glycoside, glucuronide), quercetin (acylated glycoside, diglycoside, glycoside, glucuronide), myricetin (acylated glycoside, diglycoside, glycoside), and isorhamnetin derivatives (glycoside) are the most abundant flavonols (Mulinacci *et al*. 2000, Saito *et al.* 2006, Abeynayake *et al*. 2012, Carocho *et al*. 2014, Wang *et al.* 2014, Snoussi *et al*. 2016). In pink flowers, the anthocyanins that have been identified are cyanidin (acylated glycoside, diglycoside, glycoside), perlargonidin (diglucoside), peonidin (acylated triglycoside, acylated glycoside, diglycoside, glycoside), petunidin (acylated diglycoside) and malvidin (acylated diglycoside) (Bobbio *et al*. 1985, Terahara *et al*. 1993, Willians 2004, Saito *et al*. 2006, Schmitzer *et al.* 2010, Wang *et al*. 2014, Gao *et al*. 2016, Hendra & Keller 2016). Pigments identified in *T. pulchra* were mainly the same as those mentioned above, moreover, an inedited substance, kaempferol 4'-*O*-(2''methyl)-α-D-glucoside was characterized for the first time. The kaempferol *p*-coumaroylhexoside (**30**) accumulation profile accompanied that observed for both identified anthocyanins that exhibited significant increment from white to pink floral stages, suggesting that this flavonol may act as an important copigment in pink flowers.

Gene expression analysis in *T. pulchra* flowers was a challenging enterprise because not only the genome is not sequenced, but there is no genomic sequence available for phylogenetic related species, being the most closely related species, *E. grandis*, from a different family, Myrtaceae. However, the approach used here was successful and allowed the transcriptional profiling of five key genes of flavonoid biosynthesis. Although five clones were sequenced for each gene, unique sequences were obtained. However, we cannot rule out that paralog genes, or even allelic variants, are missing, keeping in mind that we didn`t use systematically bred germplasm and *T. pulchra* genomic complement is unknown.

Despite of the mentioned reservations, our results showed robustness and clear correlations between pigment and gene expression profiles from both, early and late biosynthetic genes (Figure 3.6). *PAL* expression increases in S2 stage, providing precursors for the increment in phenolic acids (S2) and the further accumulation of anthocyanins (S3 and S4). Downstream, the *CHS* is upregulated in S3 stage, directly related with anthocyanin detection. Interestingly, *FLS* was the only enzyme-encoding gene that showed reduction in the expression profile from S1 onwards in accordance with the decreasing trend observed in flavonol contents, which was the most abundant pigment along all flower development. The late biosynthetic gene *ANS* showed a pronounced increment in mRNA level from white (S1 and S2) to pink (S3 and S4) stages confirming that the expression of this gene is responsible for the anthocyanin accumulation in *T. pulchra* flowers.

The obtained results are in clear agreement with those reported for *Viola cornuta* L. (Violaceae, Malpighiales), whose flowers open white turning to lavender and further to purple (Farzad *et al*. 2003). By using a similar approach to that adopted in the present work, the authors have found that the expression of *CHS* and *DFR* increase along flower development. Moreover, *ANS* is strongly upregulated in colored stages (Farzad *et al*. 2003). Furthermore, a study in *Nicotiana mutabilis* flowers has found that the color change from white to red, passing through different shades of pink, is determined by anthocyanin accumulation (*i.e.* malvidin) and correlated with *CHS* expression (Macnish *et al*. 2010).

Recently, a transcriptomic analysis in *Paeonia ostii* T.Hong & J.X.Zhang (Paeoniaceae, Saxifragales) aimed to understand the mechanism underneath the flower color change from white to pink and demonstrated a positive correlation between the concentration of anthocyanins and the expression of biosynthestic genes. *CHI*, *F3H*, *F3'H*, *DFR* and *ANS* exhibited higher levels of mRNA in pink flowers than in white ones. Interestingly, the genes encoding the

MBW transcription factor complex did not showed differential expression during flower color change, instead, the expression of a MYB transcriptional factor encoding gene (*PoMYB2*) showed an inverse pattern compared to that observed for anthocyanin accumulation (Gao *et al*. 2016). Transcriptional repressors of anthocyanin accumulation have also been suggested in *P. hybrida*, *Z. mays*, *A. thaliana*, and *Fragaria ananassa* Duchesne ex Rozier (Rosaceae, Rosales) (Aharoni *et al*. 2001, Albert *et al*. 2011, Petroni & Tonelli 2011). Additionally, other metabolic pathways have shown to influence flower color change in *P. ostii*, such as carbohydrate and fatty acid metabolism, as well as ethylene signaling (Gao *et al*. 2016).

In vegetative tissues, the regulation of flavonoid biosynthesis is intimately associated with environmental changes to enhance plant survival under stressful environmental conditions. Various factors, such as UV, visible light, cold, osmotic stress, pollution and pathogen infection, can induce flavonoid biosynthesis. In particular, the role of phytochrome-mediated signaling transduction pathway, associated to temperature and light perception, has been abundantly explored (Guo *et al*. 2008, Maier *et al*. 2013, Maier & Hoecker 2015, Li *et al*. 2016, Kim *et al*. 2017). In this sense, various phytochrome signaling components in *A. thaliana*, such as the PHYTOCROME INTERACTING FACTORS (PIFs) and PROTEIN LONG HYPOCOTYL 5 (HY5), have shown to act as positive regulators of anthocyanin biosynthesis (Shin *et al*. 2007, Liu *et* al. 2015, Kim *et al*. 2017). In other plants this relationship between light perception and anthocyanin accumulation has also been addressed (Czemmel *et al*. 2012, Zhang *et al*. 2016, Zong *et al*. 2017). In *T. pulchra* we performed a pilot experiment to evaluate the role of light in flower pigment accumulation. When the plants were maintained indoor under low light irradiance, the flowers did not homogenously turn from white to pink and fell down in 24 hours (Supplemental Figure 3.5). This was indicative that, at least, the transcriptional regulation demonstrated for *ANS* might be light-dependent. Similarly, in cotton flowers (*Gossypium* sp., Malvaceae, Malvales), which turn from white to pink, gene expression analysis has shown that light and shade regulate anthocyanin biosynthesis, in particular *ANS* (Tan *et al*. 2013). Likewise, *V. cornuta* flowers did not undergo color change in the darkness (Farzad *et al*. 2003).

Finally, as discussed in the introduction, flavonoid-metal complexing and pH alterations influence flower color. Here, we have identified an increment in Fe^{3+} concentration accompanying the transition from pink to dark pink stage (Figure 3.6), thus an effect of this ion in the color change seems likely. Whether Fe^{3+} is involved in color change by pigment complexation or pH alteration remains to be further investigated.

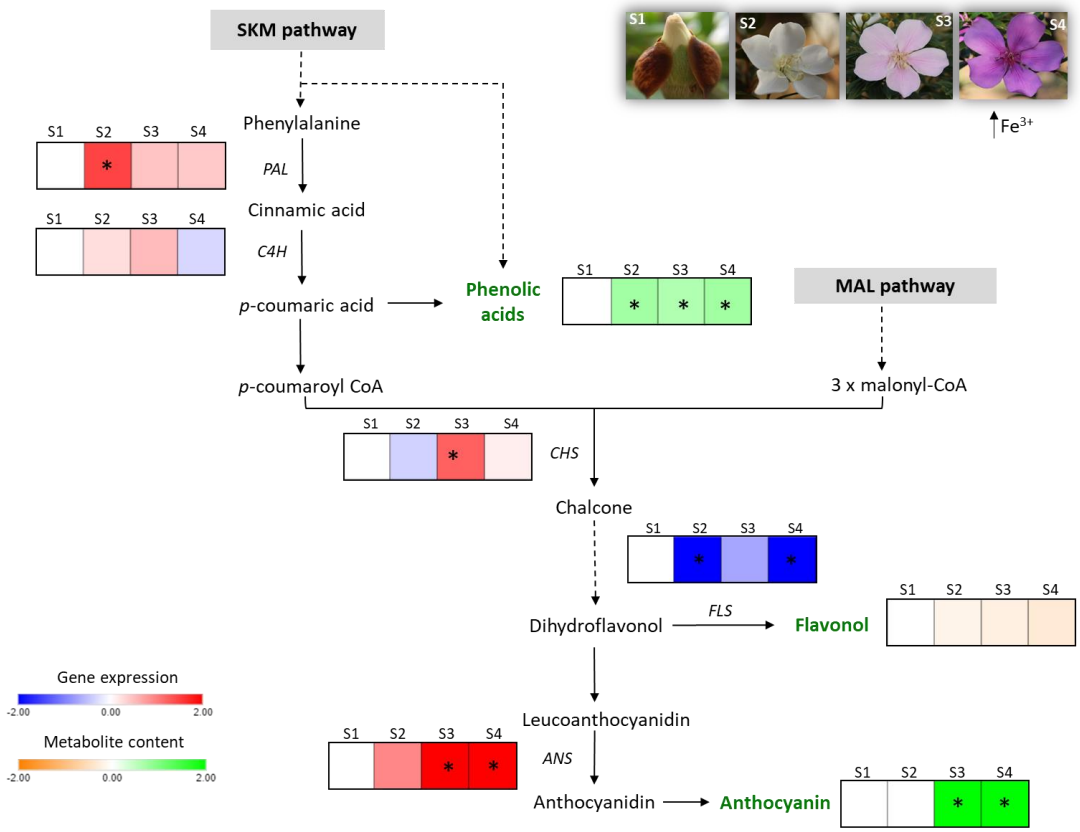

Figure 3.6. Comprehensive schematic representation of the obtained results. Flavonoid biosynthetic pathway showing heatmaps representing pigment content (orange to green) and mRNA expression profile (blue to red). Dotted lines represent more than one enzymatic reaction. Quantified compounds are highlighted in green. Asterisks indicate statistically significant different values compare to S1 stage. Abreviations: *PHENYLALANINE AMMONIUM LYASE* (*PAL*), *CINAMMATE 4-HYDROXYLASE (C4H)*, *CHALCONE SYNTHASE* (*CHS*), *FLAVONOL SYNTHASE* (*FLS*) and *ANTHOCYANIDIN SYNTHASE (ANS*) genes, S1- buds (day 0), S2- white flowers (day 1), S3- light pink (day 2), S4- dark pink (day 3).

5. CONCLUSION

In this work, by applying a combined approach of detailed biochemical and molecular genetic techniques, we characterized the pigment profile and investigated the mechanism that determines *T. pulchra* flower color change. The thirty phenolic compounds identified in chapter 2 were quantified showing variations in pigment and copigment contents along flower development. The partial cloning of five key genes of flavonoid biosynthetic pathway allowed to profile mRNA levels that explained, at least in part, the pigment accumulation pattern. Collectively these data indicate that the flower color change in *T. pulchra* is regulated by the transcriptional control of the structural genes of the flavonoid biosynthetic pathway that determine the accumulation of petunidin and malvidin, as well as, the copigment kaempferol *p*-coumaroylhexoside. Additionally, the quantification of metal contents suggested that Fe^{3+} might influence the saturation of the color at dark pink stage.

6. REFERENCES

Abeynayake, S.W., Panter, S., Chapman, R., Webster, T., Rochfort, S., Mouradov, A., & Spangenberg, G. Biosynthesis of proanthocyanidins in white clover flowers: cross talk within the flavonoid pathway. Plant Physiology. 2012, 158(2): 666–78. DOI: 10.1104/pp.111.189258

Aharoni, A., De Vos, C.H., Wein, M., Sun, Z., Greco, R., Kroon, A., Mol, J.N., O'Connell, A.P. The strawberry FaMYB1 transcription factor suppresses anthocyanin and flavonol accumulation in transgenic tobacco. Plant Journal. 2001, 28: 319–332.

Altschul, S.F., Madden, T.L., Schaffer, A.A., Zhang, J., Zhang, Z., Miller, W., Lipman, D. Gapped & J. BLAST and PSLBLAST: a new generation of protein database search programs. Nucleic acids research. 1997, 25: 3389-3402. DOI: 10.1093/nar/25.17.3389.

Bell-Lelong, D.A., Cusumano, J.C., Meyer, K., & Chapple, C. Cinnamate-4-hydroxylase expression in *Arabidopsis* (regulation in response to development and the environment). Plant Physiology. 1997, 113(3): 729-738.

Bertani, G. Studies on lysogenesis: The Mode of Phage Liberation by Lysogenic *Escherichia coli*1. Journal of bacteriology. 1951, 62(3): 293. DOI: 10.1016/j.tifs.2017.07.015.

Bobbio, F.O., Bobbio, P.A. & Degáspari, C.H. Anthocyanins from *Tibouchina grandiflora* Food Chem. 1985, 18: 153-159.

Brito, L.G., & Sazima, M. *Tibouchina pulchra* (Melastomataceae): reproductive biology of a tree species at two sites of an elevational gradient in the Atlantic rainforest in Brazil. Plant Systematics and Evolution. 2012, 7: 1271–1279. DOI: 10.1007/s00606-012-0633-5.

Brouillard, R. & Dangles, O. Flavonoids and flower colour. In: Harborne, J.B. (ed.) The Flavonoids: Advances in Research Since 1986. Chapman & Hall. 1993: 565–587.

Broun P. Transcriptional control of flavonoid biosynthesis: a complex network of conserved regulators involved in multiple aspects of differentiation in *Arabidopsis*. Current Opinion Plant Biology. 2005, 8: 272–279.

Brugliera, F., Barri-Rewell, G., Holton, T.A., & Mason, J.G. Isolation and characterization of a flavonoid 3'-hydroxylase cDNA clone corresponding to the Ht1 locus of *Petunia hybrida*. The Plant Journal. 1999, 19(4): 441-451. DOI: 10.1046/j.1365-313X.1999.00539.x.

Carocho, M., Barros, L., Bento, A., Santos-Buelga, C., Morales, P., & Ferreira, I.C. *Castanea sativa* Mill. flowers amongst the most powerful antioxidant matrices: A phytochemical approach in decoctions and infusions. BioMededical research international. 2014. DOI: 10.1155/2014/232956.

Chang, S., Puryear, J. & Cairney, J.A simple and Efficient Method for Isolating RNA from Pine Trees. Plant Molecular Biology Reporter, 1993, 11(2): 113-116.

Chiu, L.W., Zhou, X., Burke, S., Wu, X., Prior, R.L., & Li, L. The purple cauliflower arises from activation of a MYB transcription factor. Plant Physiology. 2010, 154(3): 1470-1480.

Cone, K.C., Cocciolone, S.M., Burr, F.A. and Burr, B. (Maize anthocyanin regulatory gene pl is a duplicate of c1 that functions in the plant. Plant Cell. 1993, 5: 1795–1805.

Czemmel, S., Heppel, S.C., & Bogs, J. R2R3 MYB transcription factors: key regulators of the flavonoid biosynthetic pathway in grapevine. Protoplasma, 2012, 249: 109–118. DOI: 10.1007/s00709-012-0380-z.

Da silva, J. Biologia das interações entre os visitantes florais (Hymenoptera, Apidae) em *Tibouchina pulchra* cogn. (Melastomataceae). Master dissertation, Universidade Federal do Paraná. 200661p.

De Ferrars, R.M., Czank, C., Zhang, Q., Botting, N.P., Kroon, P.A., Cassidy, A. & Kay, C.D. The pharmacokinetics of anthocyanins and their metabolites in humans. British Journal of Pharmacology. 2014, 171: 3268–3282. doi:10.1111/bph.12676.

Devic, M., Guilleminot, J., Debeaujon, I., Bechtold, N., Bensaude, E., Koornneef, M., ... & Delseny, M. The BANYULS gene encodes a DFR-like protein and is a marker of early seed coat development. The Plant Journal. 1999, 19(4): 387-398. DOI:10.1046/j.1365-313X.1999.00529.x.

Dewick, P.M. Medicinal Natural Products – A biosynthetic approach. Third edition. John Wiley and Sons. West Sussex. UK. 2009, 546 p.

Di Rienzo, J.A. (2009). InfoStat versión 2009. Grupo InfoStat, FCA, Universidad Nacional de Córdoba, Argentina. http://www. infostat. com. ar.

Di Rienzo, J.A., Casanoves, F., Balzarini, M. G., Gonzalez, L., Tablada, M., & Robledo, Y. C. InfoStat versión 2011. Grupo InfoStat, FCA, Universidad Nacional de Córdoba, Argentina. URL http://www. infostat. com. Ar. 2011, 8: 195-199.

Dixon R.A., Xie, D.Y., Sharma, S.B. Proanthocyanidins— a final frontier in flavonoid research? New Phytologist. 2005,165: 9–28.

Du, H., Lai, L., Wang, F., Sun, W., Zhang, L., Li, X., … Zheng, Y. Characterisation of flower colouration in 30 *Rhododendron* species via anthocyanin and flavonol identification and quantitative traits. Plant Biology. 2018, 20(1): 121–129. DOI: 10.1111/plb.12649.

Farzad, M., Griesbach, R., Hammond, J., Weiss, M.R., & Elmendorf, H.G. Differential expression of three key anthocyanin biosynthetic genes in a color-changing flower, *Viola cornuta* cv. Yesterday, Today and Tomorrow. Plant Science. 2003, 165(6): 1333–1342. DOI: 10.1016 DOI:/j.plantsci.2003.08.001

Feinbaum, R.L. & Ausubel, F.M. Transcriptional Regulation of the *Arabidopsis thaliana* Chalcone Synthase Gene. Molecular and cellular biology., 1988, 8(5): 1985-1992.

Gao, L., Yang, H., Liu, H., Yang, J., & Hu, Y. Extensive Transcriptome Changes Underlying the Flower Color Intensity Variation in *Paeonia ostii*. Frontiers in Plant Science. 2016, 6: 1–16. DOI: 10.3389/fpls.2015.01205.

Gou, J.-Y., Felippes, F.F., Liu, C.-J., Weigel, D., & Wang, J.-W. (2011). Negative Regulation of Anthocyanin Biosynthesis in Arabidopsis by a miR156-Targeted SPL Transcription Factor. The Plant Cell. 2011, 23(4): 1512–1522. DOI: 10.1105/tpc.111.084525.

Gowd, Vemana, Jia, Zhenquan, Chen, Wei (2017). Anthocyanins as promising molecules and dietary bioactive components against diabetes – A review of recent advances. Trends in Food Science & Technology. 2017, 68: 1-13 2017.

Grotewold, E. The genetics and biochemistry of floral pigments. Annu Rev Plant Biol. 2006, 57: 761–780.

Guo, J. & Wang, M. H. Characterization of the phenylalanine ammonia-lyase gene (SlPAL5) from tomato (*Solanum lycopersicum* L.). Molecular biology reports. 2009, 36(6): 1579. DOI: 10.1007/s11033-008-9354-9

Guo, J., Han, W. & Wang, M. H. Ultraviolet and environmental stresses involved in the induction and regulation of anthocyanin biosynthesis: a review. African Journal of Biotechnology, 2008, 7(25).

Hanahan, D. Studies on transformation of *Escherichia coli* with plasmids. Journal of Molecular Biology. 1983, 166: 557 – 580.

Hendra, R., & Keller, P.A. Flowers in Australia: Phytochemical Studies on the Illawarra Flame Tree and Alstonville. Australian Journal of Chemistry. 2016, 69(8), 925–927. DOI: 10.1071/CH16058.

Hichri, I., Barrieu, F., Bogs, J., Kappel, C., Delrot, S. & Lauvergeat, V. Recent advances in the transcriptional regulation of the flavonoid biosynthetic pathway. Journal of Experimental Botany. 2011, 62(8): 2465–2483. DOI: 10.1093/jxb/erq442.

Hsieh, L.C., Lin, S.I., Shih, A.C.C., Chen, J.W., Lin, W.Y., Tseng, C.Y., Li, W.H. & Chiou, T.J. Uncovering small RNA-mediated responses to phosphate deficiency in Arabidopsis by deep sequencing. Plant physiology. 2009, 151(4): 2120-2132. DOI: 10.1104/pp.109.147280.

Huang, J., Gu, M., Lai, Z., Fan, B., Shi, K., Zhou, Y.-H., Yu, J. Q. & Chen, Z. Functional Analysis of the *Arabidopsis* PAL Gene Family in Plant Growth, Development, and Response to Environmental Stress. Plant Physiology. 2010, 153(4): 1526–1538. DOI: 10.1104/pp.110.157370.

Kim, S., Hwang, G., Lee, S., Zhu, J. Y., Paik, I., Nguyen, T. T., & Oh, E. High ambient temperature represses anthocyanin biosynthesis through degradation of HY5. Frontiers in plant science. 2017, 8: 1787. DOI: 10.3389/fpls.2017.01787.

Koes, R., Verweij, W. & Quattrocchio, F. Flavonoids: a colorful model for the regulation and evolution of biochemical pathways. Trends in Plant Science. 2005, 10(5): 236–242. DOI: 10.1016/j.tplants.2005.03.002.

Kondo, T., Toyama-Kato, Y. & Yoshida, K. Essential structure of co-pigment for blue sepal-color development of hydrangea. Tetrahedron letters. 2005, 46(39), 6645-6649.

Koseki, M., Goto, K., Masuta, C. & Kanazawa, A. The star-type color pattern in Petunia hybrida "Red Star" flowers is induced by sequence-specific degradation of chalcone synthase RNA. Plant and Cell Physiology. 2005, 46(11): 1879–1883. DOI: 10.1093/pcp/pci192.

Li, S., Gao, J., Yin, K., Wang, R., Wang, C., Petersen, M., Mundy, J. & Qiu, J.L. MYB75 Phosphorylation by MPK4 Is Required for Light-Induced Anthocyanin Accumulation in *Arabidopsis*. The Plant Cell. 2016, tpc-00130. DOI: 10.1105/tpc.16.00130.

Liu, Z., Zhang, Y., Wang, J., Li, P., Zhao, C., Chen, Y. & Bi, Y. Phytochrome-interacting factors PIF4 and PIF5 negatively regulate anthocyanin biosynthesis under red light in *Arabidopsis* seedlings. Plant Science. 2015, 238: 64–72. DOI: 10.1016/j.plantsci.2015.06.001.

Luo, P., Ning, G., Wang, Z., Shen, Y., Jin, H., Li, P., Huang, S., Zhao, J. & Bao, M. Disequilibrium of Flavonol Synthase and Dihydroflavonol-4-Reductase Expression Associated Tightly to White vs. Red Color Flower Formation in Plants. Frontiers in Plant Science. 2016, 6:1257. DOI: 10.3389/fpls.2015.01257.

Macnish, A.J., Jiang, C.Z., Zakharov-Negre, F. & Reid, M. Physiological and molecular changes during opening and senescence of *Nicotiana mutabilis* flowers. Plant Science. 2010, 179: 267-272. DOI: 10.1016/j.plantsci.2010.05.011.

Maier, A., & Hoecker, U. COP1/SPA ubiquitin ligase complexes repress anthocyanin accumulation under low light and high light conditions. Plant signaling & behavior. 2015, 10(1), e970440. DOI: 10.4161/15592316.2014.970440.

Maier, A., Schrader, A., Kokkelink, L., Falke, C., Welter, B., Iniesto, E., Rubio, V., Uhrig, J.F., Hülskamp & Hoecker, U. Light and the E3 ubiquitin ligase COP1/SPA control the protein stability of the MYB transcription factors PAP1 and PAP2 involved in anthocyanin accumulation in *Arabidopsis*. The Plant Journal. 2013, 74(4): 638-651. DOI: 10.1111/tpj.12153.

Mallona, I., Lischewski, S., Weiss, J., Hause, B. & Egea-Cortines, M. Validation of reference genes for quantitative real-time PCR during leaf and flower development in *Petunia hybrida*. BMC Plant Biology, 2010, 10(4): 1-11. DOI: 10.1186/1471-2229-10-4.

Mol, J.N.M., Schram, A.W., De Vlaming, P., Gerats, A.G.M., Kreuzaler, F., Hahlbrock, K., ... & Veltkamp, E. Regulation of flavonoid gene expression in *Petunia hybrida*: description and partial characterization of a conditional mutant in chalcone synthase gene expression. Molecular and General Genetics MGG. 1983, 192(3): 424-429. DOI: 10.1007/BF00392185.

Mulinacci, N., Romani, A., Pinelli, P., Vincieri, F.F., & Prucher, D. Characterization of *Matricaria recutita* L. Flower extracts by HPLC-MS and HPLC-DAD analysis. Chromatographia. 2000, 51(5-6): 301–307. DOI: 10.1007/BF02490607.

Norberto, S., Silva, S., Meireles, M., Faria, A., Pintado, M. & Calhau, C. Blueberry anthocyanins in health promotion: A metabolic overview. Journal of Functional Foods. 2013, 5:1518–1528. DOI: 10.1016/j.jff.2013.08.015.

Ono, E., Fukuchi-Mizutani, M., Nakamura, N., Fukui, Y., Yonekura-Sakakibara, K., Yamaguchi, M., Nakayama, T., Tanaka, T., Kusumi, T. & Tanaka, Y. Yellow flowers generated by expression of the aurone biosynthetic pathway. Proceedings of the National Academy of Sciences. 2006A, 103: 11075–11080. DOI: 10.1073/pnas.0604246103.

Ono, E., Hatayama, M., Isono, Y., Sato, T., Watanabe, R., Yonekura-Sakakibara, K., Fukuchi- Mizutani, F., Tanaka, Y., Kusumi, T., Nishino T. & Nakayama, T. Localization of a flavonoid biosynthetic polyphenol oxidase in vacuoles. Plant Journal. 2006b, 45: 133–143. DOI: 10.1111/j.1365-313X.2005.02625.x.

Oyama, K.I., Yamada, T., Ito, D., Kondo, T., & Yoshida, K. Metal Complex Pigment Involved in the Blue Sepal Color Development of *Hydrangea*. Journal of Agricultural and Food Chemistry. 2015, 63(35): 7630–7635. DOI: 10.1021/acs.jafc.5b02368.

Pairoba, C.F. & Walbot, V. Post-transcriptional regulation of expression of the Bronze2 gene of *Zea mays* L. Plant Molecular Biology. 2003, 53: 75. DOI: 10.1023/B:PLAN.0000009267.76482.ce.

Park, K.I., Hoshino, A., Saito, N. & Tatsuzawa, F. Anthocyanins in the flowers of *Ipomoea tricolor* Cav.(Convolvulaceae). Biochemical Systematics and Ecology. 2014, 54: 15-18. DOI: 10.1016/j.bse.2013.12.034

Park, K I., Ishikawa, N., Morita, Y., Choi, J.D., Hoshino, A. & Iida, S. A bHLH regulatory gene in the common morning glory, *Ipomoea purpurea*, controls anthocyanin biosynthesis in flowers, proanthocyanidin

and phytomelanin pigmentation in seeds, and seed trichome formation. The Plant Journal. 2007,49(4): 641-654. DOI: 10.1111/j.1365-313X.2006.02988.x.

Pattanaik, S., Kong, Q., Zaitlin, D., Werkman, J. R., Xie, C.H., Patra, B. & Yuan, L. Isolation and functional characterization of a floral tissue-specific R2R3 MYB regulator from tobacco. Planta. 2010, 231(5): 1061-1076. DOI: 10.1007/s00425-010-1108-y.

Pelletier, M.K., Murrell, J.R. & Shirley, B. W. Characterization of flavonol synthase and leucoanthocyanidin dioxygenase genes in *Arabidopsis* (Further evidence for differential regulation of "early" and "late" genes). Plant physiology. 1997, 113(4): 1437-1445. PMC158268.

Pereira, A.C., da Silva, J.B., Goldenberg, R., Melo, G. A. R. & Varassin, I.G. Flower color change accelerated by bee pollination in *Tibouchina* (Melastomataceae). Flora - Morphology, Distribution, Functional Ecology of Plants. 2011, 206(5): 491–497. DOI: 10.1016/j.flora.2011.01.004.

Petroni, K. & Tonelli, C. Recent advances on the regulation of anthocyanin synthesis in reproductive organs. Plant Science. 2011, 181(3): 219-229. DOI: 10.1016/j.plantsci.2011.05.009

Pfaffl, M.W., Horgan, G.W. & Dempfle, L. Relative expression software tool (REST©) for group-wise comparison and statistical analysis of relative expression results in real-time PCR. Nucleic Acids Research. 2002, 30(9): e36. DOI: 10.1093/nar/30.9.e36.

Quattrocchio, F., Wing, J.F., Va, K., Mol, J.N. & Koes, R. Analysis of bHLH and MYB domain proteins: species-specific regulatory differences are caused by divergent evolution of target anthocyanin genes. The Plant Journal. 1998, 13(4): 475-488. DOI: 10.1046/j.1365-313X.1998.00046.x.

Quattrocchio, F., Wing, J., van der Woude, K., Souer, E., de Vetten, N., Mol, J. & Koes, R. Molecular analysis of the anthocyanin2 gene of petunia and its role in the evolution of flower color. The Plant Cell. 1999, 11(8), 1433-1444. DOI: 10.1105/tpc.11.8.1433.

Rajagopalan, R., Vaucheret, H., Trejo, J. & Bartel, D.P. A diverse and evolutionarily fluid set of microRNAs in *Arabidopsis thaliana*. Genes and Development. 2006, 20(24): 3407–3425. DOI: 10.1101/gad.1476406.

Renner, S.S. A survey of reproductive biology in neotropical Melastomataceae and Memecylaceae. Ann. Mo. Bot. Gard. 1989, 76: 496–518.

Ruijter, J.M., Ramakers, C., Hoogaars, W.M., Karlen, Y., Bakker, O., van den Hoff, M.J. & Moorman, A.F. Amplification efficiency: linking baseline and bias in the analysis of quantitative PCR data. Nucleic Acids Research. 2009, 37: e45. DOI: 10.1093/nar/gkp045.

Saito, K., Yonekura-Sakakibara, K., Nakabayashi, R., Higashi, Y., Yamazaki, M., Tohge, T. & Fernie, A. R. The flavonoid biosynthetic pathway in *Arabidopsis*: Structural and genetic diversity. Plant Physiology and Biochemistry. 2013, 72: 21–34. DOI: 10.1016/j.plaphy.2013.02.001

Saito, R., Fukuta, N., Ohmiya, A., Itoh, Y., Ozeki, Y., Kuchitsu, K. & Nakayama, M. Regulation of anthocyanin biosynthesis involved in the formation of marginal picotee petals in *Petunia*. Plant Science. 2006, 170: 828–834. DOI: 10.1016/j.plantsci.2005.12.003.

Schmitzer, V., Veberic, R., Osterc, G., & Stampar, F. Color and phenolic content changes during flower development in groundcover rose. Journal of the American Society for Horticultural Science. 2010, 135(3): 195–202. ISSN: 2327-9788.

Shin, D.H., Choi, M.G., Kang, C.S., Park, C.S., Choi, S.B., & Park, Y.I. Overexpressing the wheat dihydroflavonol 4-reductase gene TaDFR increases anthocyanin accumulation in an *Arabidopsis* dfr mutant. Genes & Genomics. 2016, 38(4): 333-340.

Shiono, M., Matsugaki, N., & Takeda, K. Phytochemistry: structure of the blue cornflower pigment. Nature. 2005, 436(7052): 791-791. DOI: 10.1038/436791[a].

Snoussi, M., Trabelsi, N., Dehmeni, A., Benzekri, R., Bouslama, L., Hajlaoui, B. ... & Papetti, A. Phytochemical analysis, antimicrobial and antioxidant activities of *Allium roseum* var. odoratissimum (Desf.) Coss extracts. Industrial Crops and Products. 2016, 89: 533-542. DOI: 10.1016/j.indcrop.2016.05.048.

Sparvoli, F., Martin, C., Scienza, A., Gavazzi, G., & Tonelli, C. Cloning and molecular analysis of structural genes involved in flavonoid and stilbene biosynthesis in grape (*Vitis vinifera* L.). Plant molecular biology. 1994, 24(5), 743-755.

Tamura, K., Peterson, D., Peterson, N., Stecher, G., Nei, M. & Kumar, S. MEGA5: molecular evolutionary genetics analysis using maximum likelihood, evolutionary distance, and maximum parsimony methods. Molecular Biology and Evolution, 2011, 28: 2731-9. DOI: 10.1093/molbev/msr121.

Tan, J., Wang, M., Tu, L., Nie, Y., Lin, Y. & Zhang, X. The Flavonoid Pathway Regulates the Petal Colors of Cotton Flower. Plos One. 2013, 8(8). DOI: 10.1371/journal.pone.0072364.

Terahara, N., Suzuki, H., Toki, K., Kuwano, H., Saito, N. &Honda, T. J. Anthocyanin, A. D. A diacylated anthocyanin from. Journal of Natural Products 1993, 56(3): 3–8. DOI: 10.1271/bbb.63.1420.

Tornielli, G., Koes, R. & Quattrocchio, F. The genetics of flower color In: T. Gerats and J. Strommer (eds.). *Petunia*. Springer. 2009, 269–299.

Trouillas, P., Sancho-garc, J.C., Freitas, V. De, Gierschner, J., Otyepka, M. & Dangles, O. Stabilizing and Modulating Color by Copigmentation: Insights from Theory and Experiment. 2016, 116(9): 4937-82. DOI: 10.1021/acs.chemrev.5b00507.

Verweij, W., Spelt, C.E., Bliek, M., de Vries, M., Wit, N., Faraco, M., et al. Functionally similar WRKY proteins regulate vacuolar acidification in *Petunia* and hair development in *Arabidopsis*. Plant Cell. 2016, 28: 786– 803. DOI: 10.1105/tpc.15.00608.

Wang, L., Albert, N.W., Zhang, H., Arathoon, S., Boase, M.R., Ngo, H., … & Lewis, D.H. Temporal and spatial regulation of anthocyanin biosynthesis provide diverse flower colour intensities and patterning in *Cymbidium* orchid. Planta. 2014, 240(5): 983–1002. DOI: 10.1007/s00425-014-2152-9.

Wanner, L.A., Li, G., Ware, D., Somssich, I.E. & Davis, K.R. The phenylalanine ammonia-lyase gene family in Arabidopsis thaliana. Plant Molecular Biology. 1995, 27: 327-338.

Williams, C. A. & Grayer, R.J. Anthocyanins and other flavonoids. Natural product reports. 2004, 21(4): 539-573. DO: 10.1039/B311404J.

Williams, C.A., Greenham, J., Harborne, J. B. & Kong, J. (2002). Acylated anthocyanins and flavonols from purple flowers of *Dendrobium* cv. "Pompadour". 2002, 30: 667–675.

Winkel-shirley, B. Flavonoid Biosynthesis. A Colorful Model for Genetics, Biochemistry, Cell Biology, and Biotechnology. Plant Physiology. 2001, 126(2): 485-493. DOI: 10.1104/pp.126.2.485.

Xiaonan, S., Zhang, Y. & Weibiao, Z. Bread fortified with anthocyanin-rich extract from black rice as nutraceutical sources: Its quality attributes and in vitro digestibility. Food Chemistry. 2016, 196: 910 – 916. DOI: 10.1016/j.foodchem.2015.09.113.

Xu, W., Dubos, C., & Lepiniec, L. Transcriptional control of flavonoid biosynthesis by MYB–bHLH–WDR complexes. Trends in Plant Science. 2015, 20(3): 176-185. DOI: 10.1016/j.tplants.2014.12.001.

Xu, W., Grain, D., Bobet, S., Le Gourrierec, J., Thévenin, J., Kelemen, Z., … & Dubos, C. Complexity and robustness of the flavonoid transcriptional regulatory network revealed by comprehensive analyses of MYB-bHLH-WDR complexes and their targets in Arabidopsis seed. New Phytologist. 2014, 202 (1): 132–144. DOI: 10.1111/nph.12620.

Yonekura-Sakakibara, K., Fukushima, A., Nakabayashi, R., Hanada, K., Matsuda, F., Sugawara, S., ... & Wangwattana, B. Two glycosyltransferases involved in anthocyanin modification delineated by transcriptome independent component analysis in *Arabidopsis thaliana*. The Plant Journal. 2012, 69(1): 154-167. DOI: 10.1111/j.1365-313X.2011.04779.x.

Yoshida, K., Toyama-Kato, Y., Kameda, K., & Kondo, T. Sepal color variation of *Hydrangea macrophylla* and vacuolar pH measured with a proton-selective microelectrode. Plant and Cell Physiology. 2003, 44(3), 262–268. DOI: 10.1093/pcp/pcg033.

Yuan, Y.W., Rebocho, A.B., Sagawa, J.M., Stanley, L.E., & Bradshaw, H.D. Competition between anthocyanin and flavonol biosynthesis produces spatial pattern variation of floral pigments between Mimulus species. Proceedings of the National Academy of Sciences. 2016, 113(9), 2448-2453. DOI: 10.1073/pnas.1515294113

Zhang, H.N., Li, W.C., Wang, H.C., Shi, S.Y., Shu, B., Liu, L.Q., et al. Transcriptome profiling of light-regulated anthocyanin biosynthesis in the pericarp of *Litchi*. Frontiers in Plant Science. 2016, 7:963. DOI: 10.3389/fpls.2016.00963.

Zhang, X., Gou, M., & Liu, C.-J. *Arabidopsis* Kelch Repeat F-Box Proteins Regulate Phenylpropanoid Biosynthesis via Controlling the Turnover of Phenylalanine Ammonia-Lyase. The Plant Cell, 2013, 25(12): 4994–5010. DOI: 10.1105/tpc.113.119644.

Zong, Y., Xi, X., Li, S., Chen, W., Zhang, B., Liu, D., … & Zhang, H. Allelic Variation and Transcriptional Isoforms of Wheat TaMYC1 Gene Regulating Anthocyanin Synthesis in Pericarp. Frontiers in Plant Science. 2017, 8: 1645. DOI: 10.3389/fpls.2017.01645.

7. SUPPLEMENTAL MATERIAL

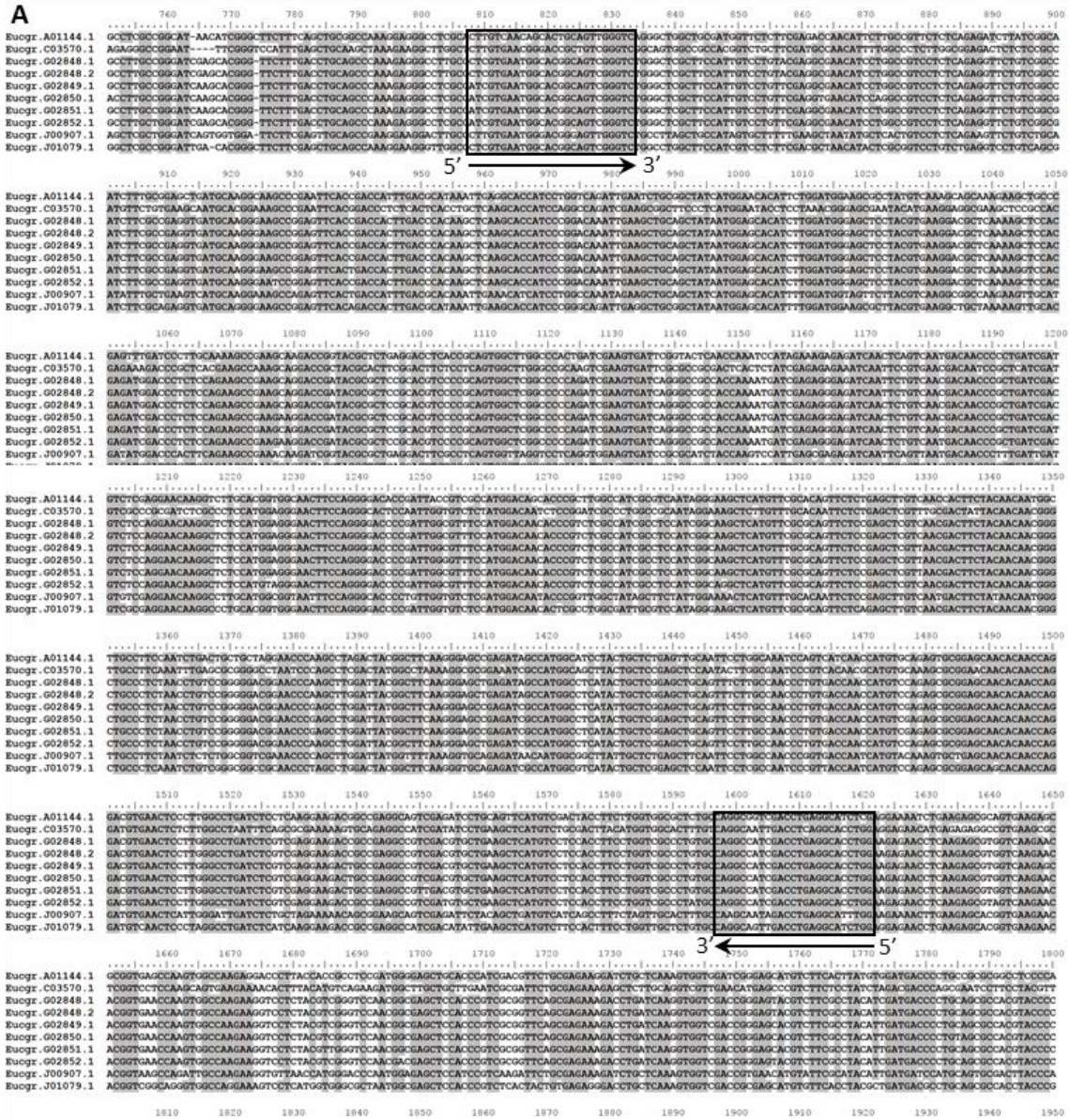

Supplemental Figure 3.1. Alignments used for primer design to clone the gene partial sequences of *PHENYLALANINE AMMONIUM LYASE* (*PAL)* (A), *CINAMMATE 4-HYDROXYLASE (C4H)* (B), *CHALCONE SYNTHASE* (*CHS)* (C), *FLAVONOL SYNTHASE* (*FLS)* (D) and *ANTHOCYANIDIN SYNTHASE (ANS*) genes. Boxes indicates the primer region.

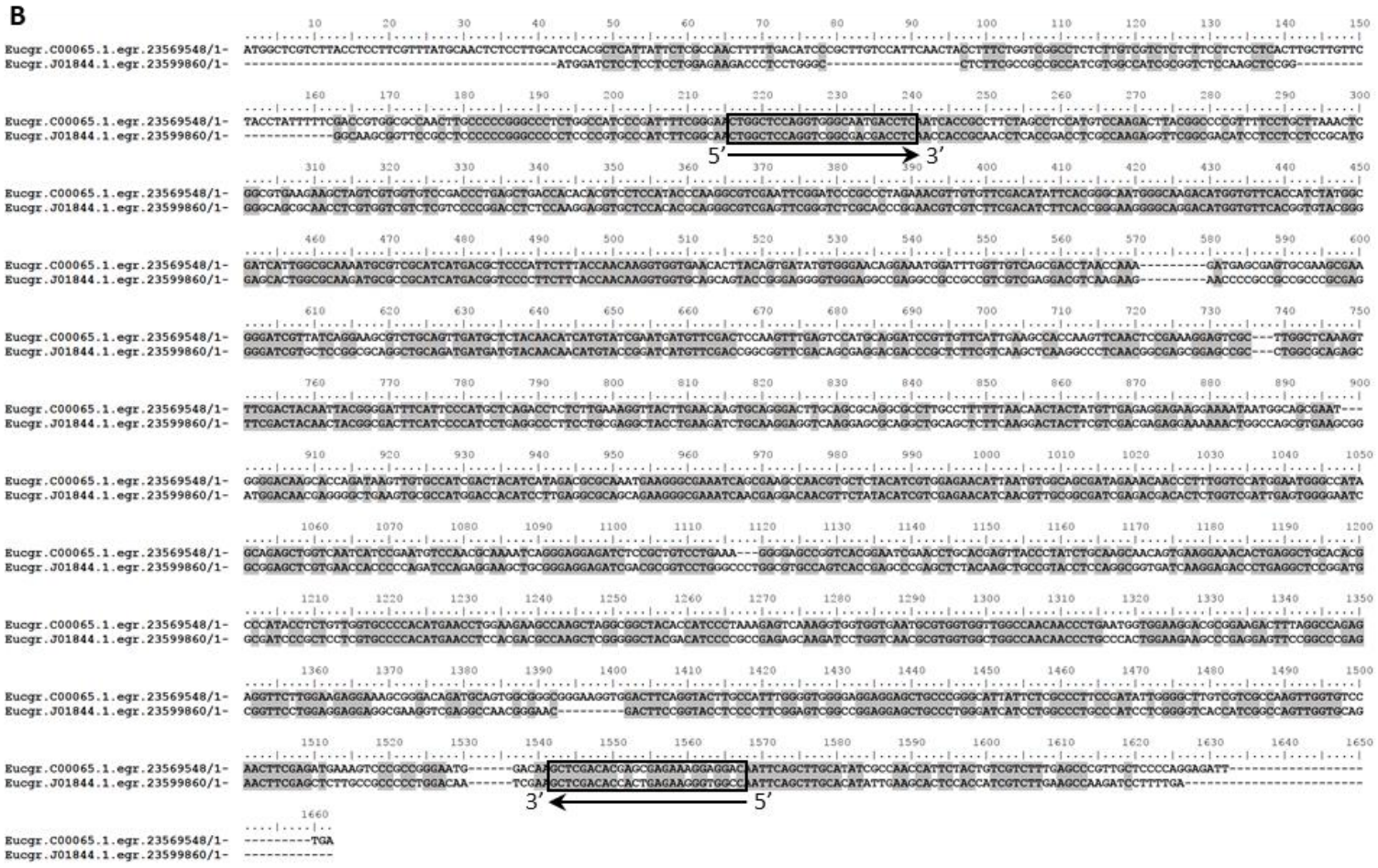

Supplemental Figure 3.1. *(Continued)*

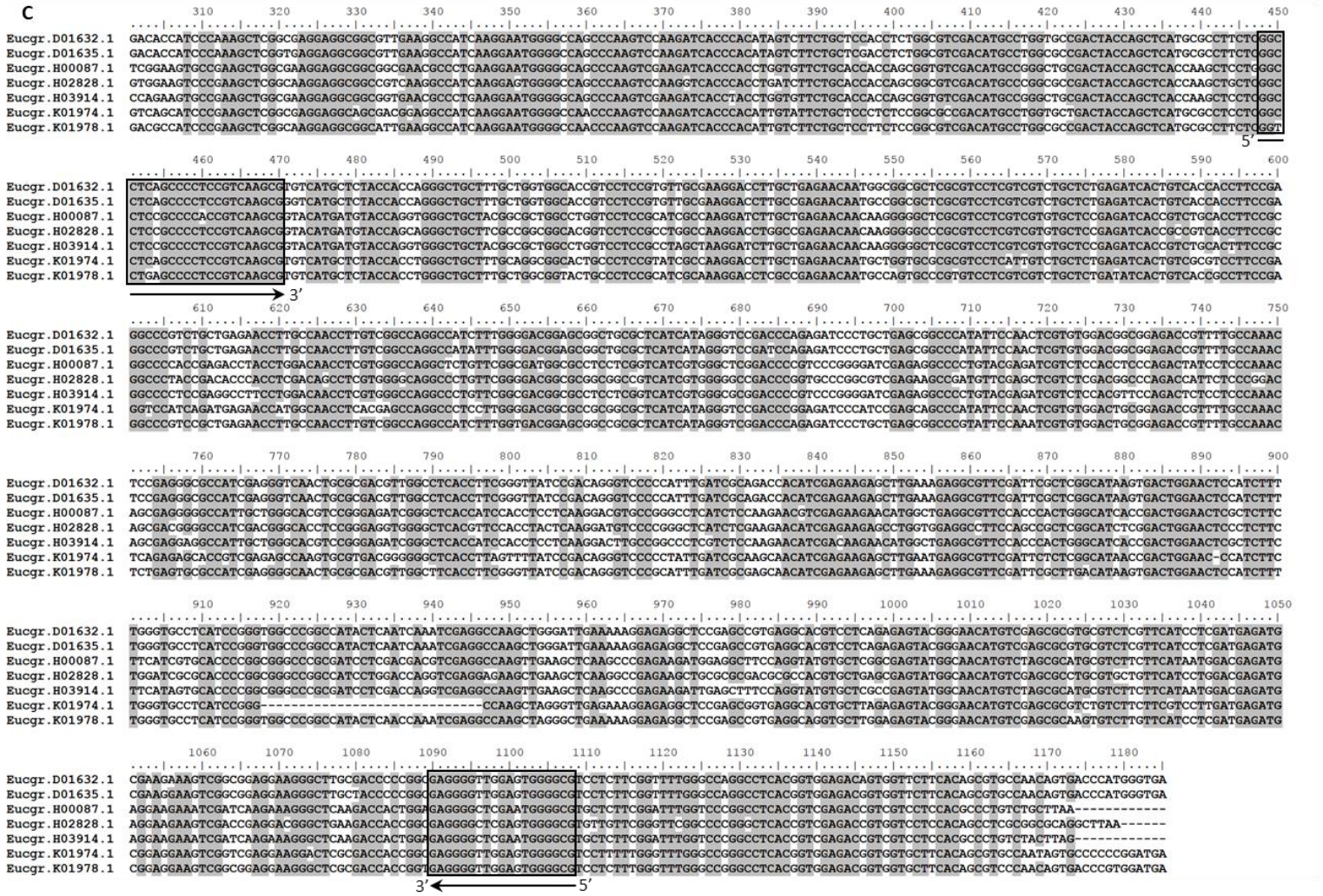

Supplemental Figure 3.1. *(Continued)*

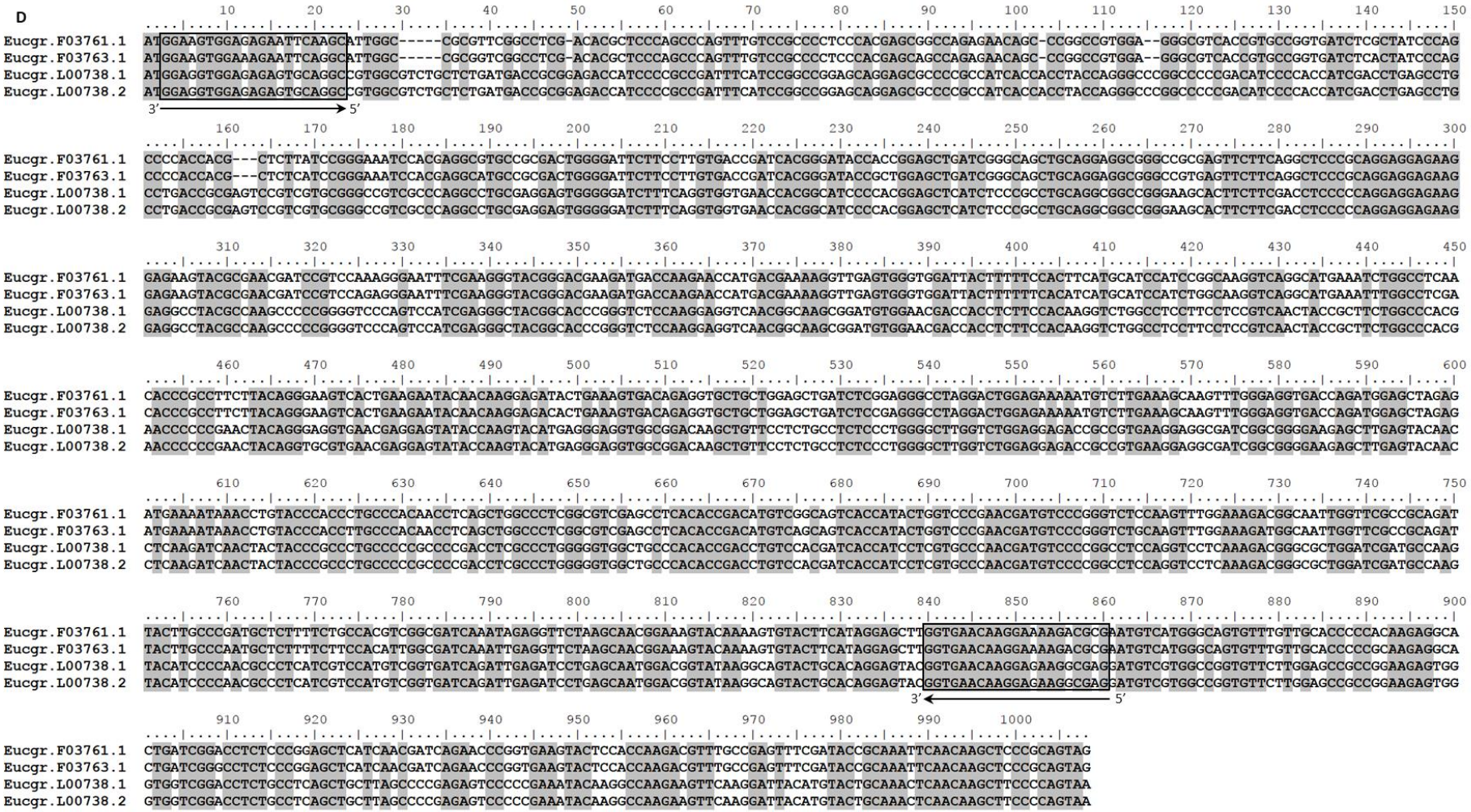

Supplemental Figure 3.1. *(Continued)*

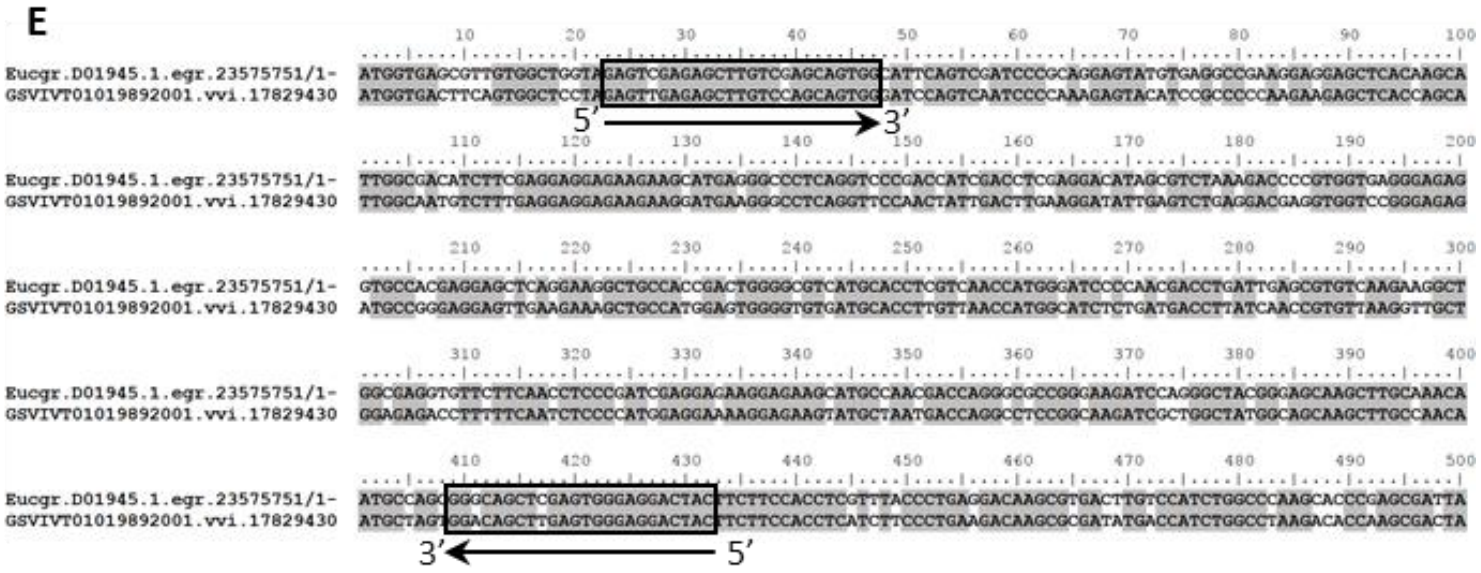

Supplemental Figure 3.1. *(Continued)*

A

Stage	Biological replicates	ng/µL	260/280	260/230
S1	1	875,70	2,11	2,30
	2	494,40	2,07	1,93
	3	629,80	2,15	1,78
	4	3.173,30	2,12	2,23
	5	418,70	2,10	2,21
S2	1	1.012,80	2,13	2,25
	2	847,70	2,10	2,01
	3	499,30	2,10	1,96
	4	1.039,80	2,13	2,32
	5	1.135,40	2,13	2,30
S3	1	888,20	2,11	2,20
	2	1.136,90	2,12	2,37
	3	890,30	2,13	2,36
	4	1.026,60	2,12	2,29
	5	702,70	2,16	2,21
S4	1	1.030,30	2,13	1,93
	2	534,20	2,15	2,08
	3	1.262,70	2,14	2,35
	4	1.565,40	2,12	2,31
	5	954,20	2,12	1,92

B

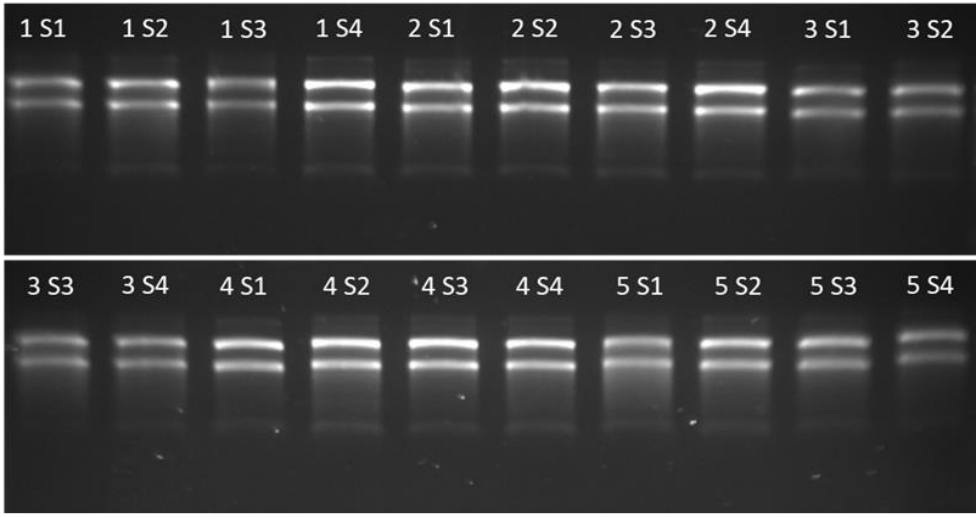

Supplemental Figure 3.2. RNA quantification (A) and integrity (B). Agarose gel (1%) for analysis of RNA integrity, approximately 500 µg of each sample was deposited. The numbers indicate the biological replicates for each stage (S1 to S4). S1- buds (day 0), S2- white flowers (day 1), S3- light pink (day 2), S4- dark pink (day 3).

Gene	Enzyme	Nucleotides number in partial sequence of *T. pulchra*	Ammino acids number in partial sequence of *T. pulchra*	Identity of ammino acids (%) with *E. grandis*
PAL	PHENYLALANINE AMMONIA-LYASE	633	206	95
C4H	CINNAMATE 4-HYDROXYLASE	1.073	357	87
CHS	CHALCONE SYNTHASE	621	207	88
FLS	FLAVONOL SYNTHASE	817	272	69
ANS	ANTHOCYANIDIN SYNTHASE	361	120	83
RPS	RIBOSOMAL PROTEIN S13	371	123	98
EF1	ELONGATION FACTOR 1α	694	231	93

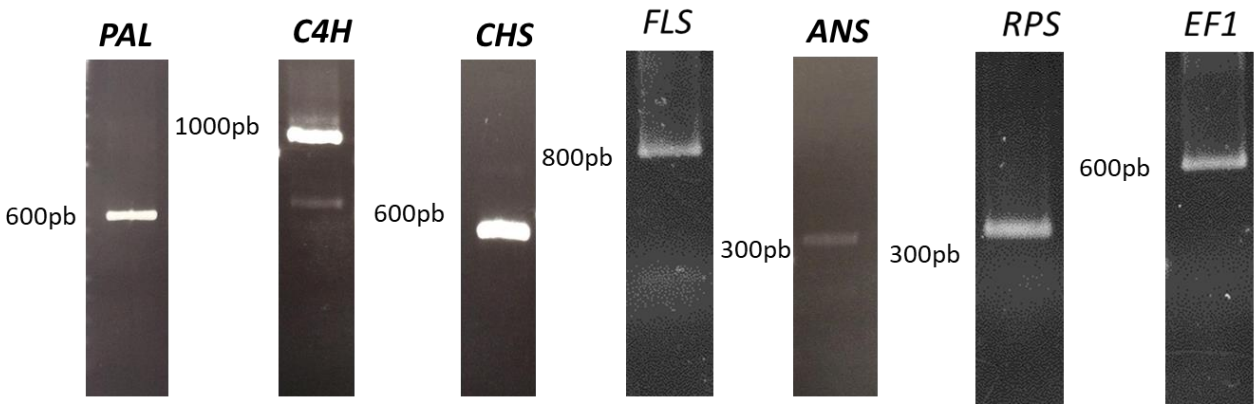

Supplemental Figure 3.3. Identity of obtained with *E. grandis* sequences (A). Agarose gel (0.8%) of the cloning sequences (B). The abbreviations indicate: *PHENYLALANINE AMMONIUM LYASE* (*PAL)*, *CINAMMATE 4-HYDROXYLASE (C4H)*, *CHALCONE SYNTHASE* (*CHS)*, *FLAVONOL SYNTHASE* (*FLS)* and *ANTHOCYANIDIN SYNTHASE (ANS*), *ELONGATION FACTOR 1-α* (*EF1*) e *RIBOSSOMOAL PROTEIN S13* (*RPS*) genes.

>T.pulchra_n_PAL

GGGATTGGCGTCCATTGTCCTGTTCGAGGCGATCATGGAGCATATCCTGGAGGGAAGCGAGATCATTAAGGCCGCGCAGAAGT
TGCACGAGATGGACCCGTTGCAGAAGCCGAAGCAGGACCGATATGCCCTTAGGACATCGCCGCAGTGGCTCGGACCCCAGATC
GAGGTCATAAGGGCCGCAACCAAGATGATCGAAAGGGAAATCAACTCGGTGAACGACAACCCTTTGATTGACGTGTCGAGAAA
CAAGGCCCTCCATGGCGGGAATTTCCAAGGCACTCCCATTGGCGTCTCGATGGACAACACCCGGCTCGCTATTGCCTCGATCG
GGAAGCTCATGTTCGCTCAGTTCCCCGAGCTCGTGAACGACTTTTACAACAATGGACTGCCCTCTAACTTGTCCGGGGGTCGG
AACCCGAGCCTAGATTACGGGTTCAAGGGCGCAGAGATCGCAATGGCCTCGTACTGCTCTGAGCTGCAGTTCCTGGCCAACCC
GGTGACTAACCACGTGCAGAGCGCAGAACAACACAACCAAGACGTCAACTCCCTCGGTCTCATCTCGTCAAGGAAGACCGCGG
AGGCCGTCGACGTGCTGAAACTGATGTCATCACCTTCCTAGTCGCACTCTGC

>T.pulchra_n_C4H

AGAAAGATGAGGAGGATCATGACTGTTCCTTTCTTCACCAACAAGGTGGTCCAGCAGTACAGGTTCGGTTGGGAGGACGAGGC
CACCAAGGTCGTAGAGGACGTGAAGAAGAACCCCGAGTCGGCCACCAATGGGATCGTCCTCCGACGCAGGCTCCAGCTCATGA
TGTACAACAACATGTTCCGGATCATGTTCGATAGGAGGTTCGAGAGTGAGGAGGATCCCCTGTTCATAAGGCTGAGGACCCTC
AACGGAGAGCGCAGCCGCCTAGCCCAGAGCTTCGAGTACAACTACGGGGACTTCATCCCCATCCTGAGGCCGTTCCTCCGTGG
CTACCTCAAGGTATGCAAGGAGGTGAAGGAGAAGAGGTTGAAGCTCTTCAAGGACTACTTCGTCGACGAGAGGAAGAAGCTGG
CGGGGACCAAGAAAGTCGAGAACGACGGCCTCAAGTGCGCGATCGACCACATCCTGGACGCCCAGCAGAAGGGCGAGATCAAC
GAGGACAACGTCCTCTACATCGTCGAGAACATCAACGTTGCCGCGATCGAGACTACCCTCTGGTCGATCGAATGGGGCATCGC
TGAGCTCGTCAACCACCCTGAGATCCAGAGGAAGCTCCGCGACGAGCTGGACACTGTGCTCGGTCCCGGCGTCCAGATCACCG
AGCCTGACACTTATAGGCTCCCCTACCTCCAGGCCGTCATCAAGGAGACCCTCCGCCTCCGGATGGCGATCCCGCTCCTCGTG
CCCCACATGAACCTCCACGATGCCAAGCTCGGAGGGCACGACATCCCCGCGGAGAGCAAGATCCTCGTCAATGCCTGGTACCT
CGCCAACAACCCTTCCCTGTGGAAGAACCCCGAAGAGTTCCGCCCCGAGAGGTTCATGGAGGAGGAGGCCAAGGTCGAGGCCA
ACGGTAACGACTTCAGGTACCTCCCCTTCGGTGTTGGTAGGAGGAGCTGCCCCGGAATCATCCTCGCGTTGCCCATCCTGGGC
ATAACGATCGGGAGGCTGGTCCAGAACTTCGAGATGCTGCCGCCTCCTGGTCAGTCCAAGTTGGCGAGGTACCAGGC

>T.pulchra_n_CHS

CGCCTCATGATGTACCAGCAGGGCTGCTTCGCCGGAGGCACTGTCCTCCGCCTTGCCAAGGATCTCGCCGAGAACAACAAGGG
GGCTCGTGTCCTTGTCGTCTGCTCTGAGATCACCGCCGTCACCTTCCGTGGCCCCAGCGAGTCGCACCTCGACAGCCTTGTCG
GGCAGGCCCTTTTCGGTGATGGCGCGGCTGCCATCATCATGGGATCCGATCCCGTCCCTGGAGTGGAGAGGCCCATGTTCGAG
CTCGTTTCTGCCGCGCAGACCATCCTGCCTGACTCGGACGGGGCCATCGATGGGCACCTGAGGGAGGTCGGGCTGACTTTCCA
CCTCCTGAAGGACGTCCCCGGGCTCATCTCCAAGAACATCGAGAAGAGCCTCGTCGAGGCCTTCACCCCAATCGGCATCTCGG
ACTGGAACTCCATCTTCTGGATCGCTCACCCAGGGGGTCCAGCCATCCTGGACCAGGTCGAGGAGAAGATGGGCCTGAAGCCC
GAGAAGATGCGGGCCACAAGGCAGGTCCTGAGCGATTACGGCAACATGTCCAGCGCCTGCGTCCTCTTCATCTTAGATGAGAT
GAGGACGAACTCCGCCCAGAACGGGATGAAGACGACCGGG

Supplemental Figure 3.4. Amino acid (aa) and nucleotide (n) partial sequences of genes cloned from *Tibouchina pulchra*. *PHENYLALANINE AMMONIUM LYASE* (*PAL*), *CINAMMATE 4-HYDROXYLASE (C4H)*, *CHALCONE SYNTHASE* (*CHS*), *FLAVONOL SYNTHASE* (*FLS*), *ANTHOCYANIDIN SYNTHASE (ANS*), *ELONGATION FACTOR 1-α* (*EF1*) e *RIBOSSOMOAL PROTEIN S13* (*RPS*) genes, S1- buds (day 0), S2- white flowers (day 1), S3- light pink (day 2), S4- dark pink (day 3).

>T.pulchra_n_FLS

CGTCGCTTCCTCGTTTATCTCCAAGGGGGTCATCCCTGCTGAGTACATCCGTCCCGAGCAGGAGCAGCCCTCTGTCACCACCT
ACCATGGCCCCGTCCCTACCATACCCACCGTTGACCTCGGAGATGCTGACCACGAGGGATTGGTGCGCGCCGTGGCGGATGCC
AGCCGGGAATGGGGAATGTTCCAGGTTTTTAACCACGGGATCCCTGCAGAGGTGATCGCGGAGCTTCAGCGTGTTGGGAAGGA
GTTCTTCGAACTGCCTGCGGAGGAGAAGGAGAAGTACGCGCGCCCGCCTGGCGCCCAGAGTTTGGAAGGTTACGGGACTCGGC
TCCAGAAGAACCTCGACGGGAAGAAGTCCTGGGTCGATCACCTCTTCCACAAGATTTGGCCGCCTTCCTCTGTCGACTACAAG
TACTGGCCCGCCAACACGCCTGCCTATAGGGAGGCTAACGAGGAGTATGCGAAACACATCCGGAAGGTGGCAGACAAGCTGTT
CGGGTGCCTGTCGGTGGGGCTAGGTCTGGAGGAGGATGCCATGAAGAAAGCCGTGGGAGGAGATGACCTGCTGTACAACCTCA
AGATAAACTATTATCCGCCCTGCCCACGTCCGGACCTCGCCCTCGGTGTTCTTCCCCACACTGATCTCTCTGCGCTGACATTG
CTGGTACCCAATGAGATCCCCGGCCTTCAGGTTTTCAAGGACGGGAAGTGGATTGATGCCGAGTACATCCCCAATGCCCTTAT
CGTACATATTGGTGACCAAGTCGAGATCCTGAGCAATGGGGAGTACAGGAGCGTGTTACACAGGACCACG

>T.pulchra_n_ANS

GATACTCTCCATCCCCAAGGAGTACATCAGGCCTCAGGAGGAGCTCAGGAGCATCGGGGACGTGTTCGAGGAGGAGAAGAAGC
ATGAGGGCCCACAGGTCCCCACCATTGATCTCCAGGATATCGATTCAGAGGATCCGGTTGTGCGTGAGACCTGCCGTGAGGAG
CTCAAGAAGGCCGCCACCCAGTGGGGGGTGATGCACCTCGTTAACCATGGTATCCCTAATGAACTCATCGAGCGTGTTAAGAA
GGCTGGTGATGAGTTCTTCACTCTCCCCGTCGAGGAGAAGGAGAAGTACGCCAATGACCAGGGGTCGGGGAAGATCCAAGGCT
ACGGCAGCAAGCTTGCTAACAACGCCAGT

>T.pulchra_n_EF1

AACATCGTGGTCATCGGCCATGTCGACTCCGGAAAGTCGACCACCACTGGGCACTTGATCTACAAGCTCGGTGGGATCGACAA
GCGTGTTATCGAGAGATTCGAGAAGGAAGCTGCTGAGATGAACAAGAGGTCTTTCAAGTATGCTTGGGTGCTCGACAAGCTGA
AGGCCGAGCGCGAGCGTGGTATCACCATTGATATTGCCCTGTGGAAGTTCGAGACCACCAAGTACTACTGCACCGTCATCGAC
GCTCCCGGACATCGCGACTTTATCAAGAACATGATCACGGGAACTTCCCAGGCTGACTGTGCTGTCCTTATCATTGACTCCAC
CACTGGTGGTTTCGAAGCTGGTATCTCCAAGGATGGACAGACCCGTGAGCACGCTCTTCTGGCTTTCACCCTTGGTGTCAGGC
AAATGATTTGCTGCTGCAACAAGATGGATGCCACCACCCCCAAGTACTCGAAGGCTAGGTACGACGAAATTGTCAAGGAAGTC
TCTTCATATATGAAGAAGGTCGGATACAACCCCGAGAAGATCCCGTTTGTCCCCATTTCCGGATTCGAGGGTGACAATATGAT
TGACAGATCCACCAACCTTGACTGGTACAAGGGCCCTACCCTGTTGGATGCTCTTGACATGATTCAGAGCCCAAGAGGCCCTC
GGACAAGCCCCTCCGTCTTCCCCTTCAGAC

>T.pulchra_n_RPS

GAAGGGTATCTCGGCGTCGGCTCTTCCCTACAAGAGGACCTCCCCCAGTTGGCTCAAGATCTCCTCCCAGGATGTCGAGGAGA
ACATCTGCAAGTTCGCAAAGAAGGGTCTGACCCCGTCTCAGATCGGCGTCATCCTTAGGGACTCGCATGGCATTGCCCAGGTG
AGGAGCGTCACGGGAAGCAAGATCCTTCGTATACTCAAGGCTCACGGCCTGGCACCCGAAATTCCCGAGGATCTGTATCACTT
GATCAAGAAGGCTGTTTCCATCAGGAAACATTTGGAAAGGAACAGGAAGGACAAGGATTCCAAGTTTAGGCTCATCCTTGTTG
AGAGTAGGATCCACAGGCTGGCTCGCTACTACAAGAAGA

Supplemental Figure 4. *(Continued)*

> T.pulchra_aa_PAL

GLASIVLFEAIMEHILEGSEIIKAAQKLHEMDPLQKPKQDRYALRTSPQWLGPQIEVIRAATKMIEREINSVNDNPLIDVSRN
KALHGGNFQGTPIGVSMDNTRLAIASIGKLMFAQFPELVNDFYNNGLPSNLSGGRNPSLDYGFKGAEIAMASYCSELQFLANP
VTNHVQSAEQHNQDVNSLGLISSRKTAEAVDVLKLMSSPS

> T.pulchra_aa_C4H

RKMRRIMTVPFFTNKVVQQYRFGWEDEATKVVEDVKKNPESATNGIVLRRRLQLMMYNNMFRIMFDRRFESEEDPLFIRLRTL
NGERSRLAQSFEYNYGDFIPILRPFLRGYLKVCKEVKEKRLKLFKDYFVDERKKLAGTKKVENDGLKCAIDHILDAQQKGEIN
EDNVLYIVENINVAAIETTLWSIEWGIAELVNHPEIQRKLRDELDTVLGPGVQITEPDTYRLPYLQAVIKETLRLRMAIPLLV
PHMNLHDAKLGGHDIPAESKILVNAWYLANNPSLWKNPEEFRPERFMEEEAKVEANGNDFRYLPFGVGRRSCPGIILALPILG
ITIGRLVQNFEMLPPPGQSKLARYQ

> T.pulchra_aa_CHS

RLMMYQQGCFAGGTVLRLAKDLAENNKGARVLVVCSEITAVTFRGPSESHLDSLVGQALFGDGAAAIIMGSDPVPGVERPMFE
LVSAAQTILPDSDGAIDGHLREVGLTFHLLKDVPGLISKNIEKSLVEAFTPIGISDWNSIFWIAHPGGPAILDQVEEKMGLKP
EKMRATRQVLSDYGNMSSACVLFILDEMRTNSAQNGMKTTG

> T.pulchra_aa_FLS

VASSFISKGVIPAEYIRPEQEQPSVTTYHGPVPTIPTVDLGDADHEGLVRAVADASREWGMFQVFNHGIPAEVIAELQRVGKE
FFELPAEEKEKYARPPGAQSLEGYGTRLQKNLDGKKSWVDHLFHKIWPPSSVDYKYWPANTPAYREANEEYAKHIRKVADKLF
GCLSVGLGLEEDAMKKAVGGDDLLYNLKINYYPPCPRPDLALGVLPHTDLSALTLLVPNEIPGLQVFKDGKWIDAEYIPNALI
VHIGDQVEILSNGEYRSVLHRTT

> T.pulchra_aa_ANS

ILSIPKEYIRPQEELRSIGDVFEEEKKHEGPQVPTIDLQDIDSEDPVVRETCREELKKAATQWGVMHLVNHGIPNELIERVKK
AGDEFFTLPVEEKEKYANDQGSGKIQGYGSKLANNAS

> T.pulchra_aa_RPS

KGISAXALPYKRTSPSWLKISSQDVEENICKFAKKGLTPSQIGVILRDSHGIAQVRSVTGSKILRILKAHGLAPEIPEDLYHL
IKKAVSIRKHLERNRKDKDSKFRLILVESRIHRLARYYKK

> T.pulchra_aa_EF1

NIVVIGHVDSGKSTTTGHLIYKLGGIDKRVIERFEKEAAEMNKRSFKYAWVLDKLKAERERGITIDIALWKFETTKYYCTVID
APGHRDFIKNMITGTSQADCAVLIIDSTTGGFEAGISKDGQTREHALLAFTLGVRQMICCCNKMDATTPKYSKARYDEIVKEV
SSYMKKVGYNPEKIPFVPISGFEGDNMIDRSTNLDWYKGPTLLDALDMIQSPRGPRTSPSVFPFR

Supplemental Figure 4. *(Continued)*

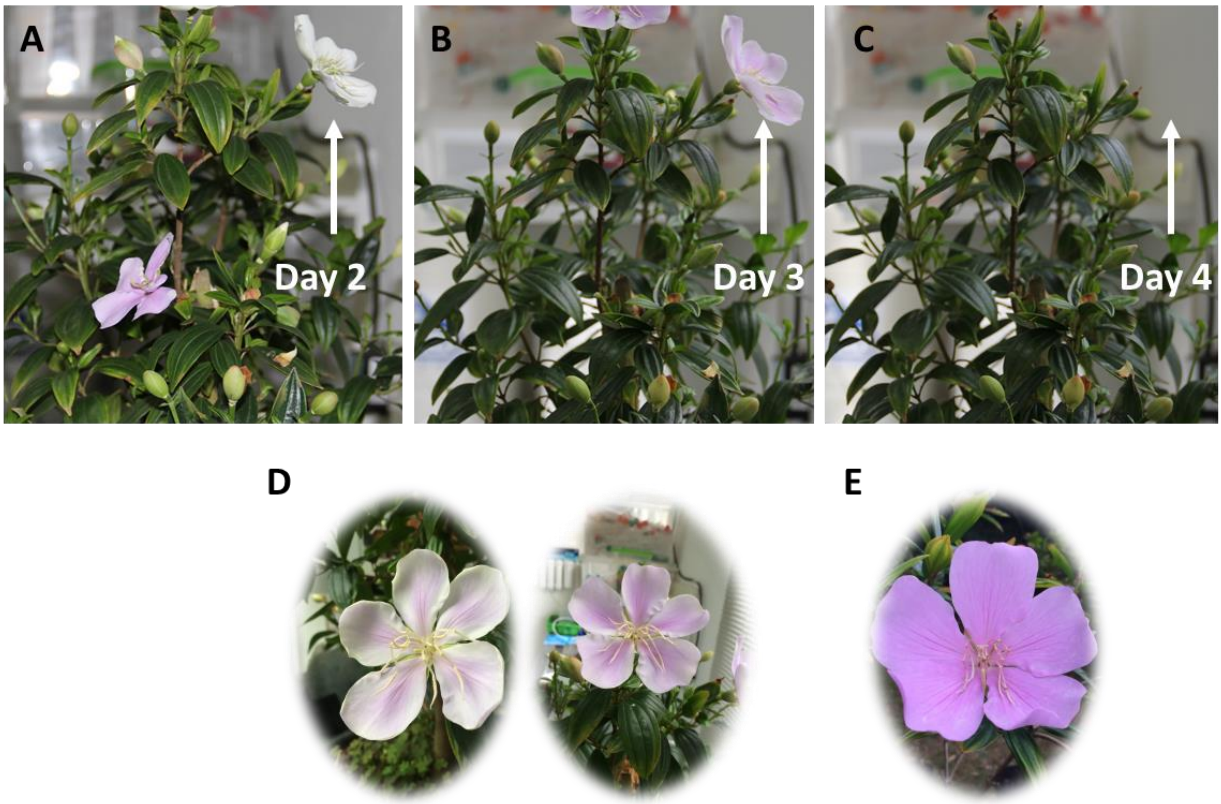

Supplemental Figure 3.5. *Tibouchina pulchra* flowers need light to turn from white to pink color. Plants were maintained indoor under low light irradiance. After 24 h (A to B) white flowers did not homogenously turn to pink (D) and fell down to following day (B to C). E. Normal pink flower.

Supplemental Table 3.1. Standard curves parameters.

Compound	R^2	equation
p-coumaric	0.99	y=12955x
kaempferol	0.97	y=49285x
cyanidin	0.99	y=364963x

Supplemental Table 3.2. Primers used for gene cloning and RT-qPCR.

Gene	Description	Forward	Melting temperature	Reverse	Melting temperature	Amplicon	Use
PAL	flavonoid biosynthesis	MTYGTSAAYRGCACBGSWGTYGGGTC	65.3°C	CSRTGCCTSAGGTCDAYBGCYTG	63.4°C	813	Cloning
C4H	flavonoid biosynthesis	CTGGCTCCAGGTSGGCRAYGACCTC	65.4°C	GKCCWCCYTTCTCRSTSGTGTCGAGC	64.3°C	1277	Cloning
CSH	flavonoid biosynthesis	GGYCTSMGCCCCWCCGTCAAG	65.0°C	CGCCCCAYTCSARCCCCTC	63.5°C	661	Cloning
FLS	flavonoid biosynthesis	GGARGTGGARAGARTKCARGC	58.1°C	GACATYCKCGYCTTKTCCTTGTTCAC	56.2°C	863	Cloning
ANS	flavonoid biosynthesis	GAGTYGAGAGCTTGTCSAGCAGTGG	62.7°C	GTAGTCCTCCCACTCRAGCTGSCC	64.7°C	385	Cloning
EF1α	reference gene	GGGTAARGARAAGGTTCACATC	54.9°C	CCRATACCACCAATCTTGASAC	53.7°C	740	Cloning
RPS13	reference gene	GTCGCATGCACAGYCGMGG	61.9°C	CCARACRGGWGGKAGCTTCTTGG	58.1°C	412	Cloning
PAL	flavonoid biosynthesis	GCACGAGATGGACCCGTTGC	61.3°C	GTGCCTTGGAAATTCCCGCC	59.6°C	158	RT-qPCR
C4H	flavonoid biosynthesis	GGCGAGATCAACGAGGACAACGTCC	63.2°C	GAGGTTCATGTGGGGCACGAGG	62.4°C	229	RT-qPCR
CSH	flavonoid biosynthesis	GAACAACAAGGGGGCTCGTGTCC	62.4°C	CCGAGTCAGGCAGGATGGTCTG	61.6°C	168	RT-qPCR
FLS	flavonoid biosynthesis	GCTGACCACGAGGGATTGGTGCG	64.5°C	CTTCTGGAGCCGAGTCCCGTAACC	64.5°C	166	RT-qPCR
ANS	flavonoid biosynthesis	CGGTTGTGCGTGAGACCTGCC	63.3°C	GCCTTGGATCTTCCCCGACCCC	64.3°C	150	RT-qPCR
EF1α	reference gene	GAGGAGCGTCACGGGAAGCAAG	62.3°C	GTAGTAGCGAGCCAGCCTGTGG	61.8°C	142	RT-qPCR
RPS13	reference gene	GGATGGACAGACCCGTGAGCACG	63.8°C	GGGACAAACGGGATCTTCTCGGGG	63.3°C	155	RT-qPCR

Final Considerations

Floral color change along flower developement is a phenomenom controlled by serveral factors. This work proposed to gain insights about the chemical and genetic mechanism that underneath *Tibouchina pulchra* (Melastomataceae) flower color change.

Among the thrirty detected compounds, five were described for the first time in Melastomataceae, fourteen in *Tibouchina* and sixteen in *T. pulchra*. Moreover, an inedited substance was described: kaempferol-(2''-*O*-methyl)-4'-*O*-α-D-glucopyranoside. Five key genes of the flavonoid biosynthetic pathway were successfully cloned, and their expression profiled. Our results exhibited a clear relation among color transition, pigmentation, copigmentation, gene expression, and metal content. The flower color change in *T. pulchra* is mostly the consequence of an increment in *ANS* expression, which in turn, results in the accumulation of petunidin and malvidin found in pink stages (S3 and S4). Only one copigment (kaempferol-*p*-coumaroylhexoside - **30**) appeared in the pink stages, while all the others were present in the white ones remaining all along flower development. Interestingly, Fe^{3+} ion increased in dark pink stage (S4), suggesting its involvement in color saturation.

Futher analyzes are necessary to fully elucidate the mechanism of color change in *T. pulchra*. Regarding gene expression, the identification of the transcriptional factors that control flavonols/anthocyanins accumulation would bring light on the differential expression pattern displayed by the distinct analyzed genes. Additionally, the genetic analysis of the late reactions, such as methylations, glycosilations and acylations of flavonoid structures has been lagged behind, probably because of the ubiquity of these reactions, which difficults the identification of the specific enzyme encoding genes (*OMT*, *FGT* and *ACT*). Due to the demonstrated post-transcriptional regulation of some flavonoid biosynthetic genes, the study of the enzymatic activity would increase the knowledge about this phenomenon. Finally, the effect of Fe^{3+} ion on flower color needs to be better understood by means addressing the subcellular localization, the formation of metal-flavonoid complexes and/or its influence on vacuolar pH.

Concluding, the generated information contributed, for the first time, to the understanding of the flower color change phenomena in a Brazilian native species and constitute a repository data for future studies with Melastomataceae.